Report to BSEE:

Three-Dimensional Mapping of Dissolved Hydrocarbons and Oil Droplets Using a REMUS-600 Autonomous Underwater Vehicle

Submitted by:
Lisa DiPinto
NOAA, National Ocean Service
Office of Response and Restoration
1305 East West Highway
N/ORRx3 Station 10218
Silver Spring, MD 20910
(240) 533-0432
Lisa.dipinto@noaa.gov

Three-Dimensional Mapping of Dissolved Hydrocarbons and Oil Droplets Using a REMUS-600 Autonomous Underwater Vehicle
Final

Submitted to:

Nancy Kinner and Kathy Mandsager
Coastal Response Research Center
Center for Spills in the Environment
236 Gregg Hall
University of New Hampshire
Durham, NH 03824

Submitted by:

Abt Associates
1881 Ninth Street, Suite 201, Boulder, CO 80302
Contacts: Heather Forth and Jamie Holmes

Woods Hole Oceanographic Institution
266 Woods Hole Road, MS #10, Woods Hole, MA 02543
Contact: Amy Kukulya

National Oceanic and Atmospheric Administration
Office of Response and Restoration
1305 East West Highway, N/ORRx3 Station 10218, Silver Spring, MD 20910
Contacts: Lisa DiPinto and George Graettinger

U.S. Environmental Protection Agency
26 West MLK Drive, Cincinnati, OH 45268
Contact: Robyn Conmy

Water Mapping, LLC
1041 Edge Water Ln, Gulf Breeze, FL 32563
Contact: Oscar Garcia

January 17, 2020

14607

Contents

Appendices

Acronyms and Abbreviations

Abt	Abt Associates
ACOMMS	acoustic communications
ADAC	Arctic Domain Awareness Center
ADCP	Acoustic Doppler Current Profiler
ARD	Assessment and Restoration Division
AUV	autonomous underwater vehicle
BTEX	benzene, toluene, ethylene, and xylenes
CHL	chlorophyll
COP	common operational picture
COTS	commercial off-the-shelf
CTD	conductivity-temperature-depth
DHS	Department of Homeland Security
DI	deionized
DIVER	Data Integration Visualization Exploration and Report
DO	dissolved oxygen
DWH	*Deepwater Horizon*
EPA	U.S. Environmental Protection Agency
ERMA	Environmental Response Management Application
FDOM	fluorescent dissolved organic matter
GPS	global positioning system
HSP	Health and Safety Plan
INS	inertial navigation system
LRAUV	long-range autonomous underwater vehicle
MBARI	Monterey Bay Aquarium Research Institute
NBOSI	Neil Brown Ocean Sensors, Inc.
NOAA	National Oceanic and Atmospheric Administration
NRDA	natural resource damage assessment
OBS	optical backscatter
ORISE	Oak Ridge Institute for Science and Education
OR&R	Office of Response and Restoration
OSL	Oceanographic Systems Laboratory

PAH	polycyclic aromatic hydrocarbon
PAR	photosynthetically active radiation
ppb	parts per billion
QSE	quinine sulfate equivalents
REMUS	remote environmental monitoring units
ROS	Robot Operating System
ROV	remotely operated vehicle
SAP	Sampling and Analysis Plan
SD	secure digital
SWL	safe working load
2D	two-dimensional
3D	three-dimensional
TPH	total petroleum hydrocarbons
UAS	unmanned aerial system
USCG	U.S. Coast Guard
UV	ultraviolet
VDC	volts direct current
VIP	Vehicle Interface Program
Water Mapping	Water Mapping LLC
WHOI	Woods Hole Oceanographic Institution

1. Introduction

The ability to rapidly characterize oil dispersed in the water column and floating on the water surface during and after an oil spill is a primary need of oil spill response teams, and is an important objective of natural resource damage assessments (NRDAs). In response to the 2010 Gulf of Mexico *Deepwater Horizon* (DWH) oil spill, scientists used numerous technologies and techniques to characterize oil in the environment, many of which were novel or new to oil spill response efforts and NRDA work (White et al., 2016). In many cases, these new technologies demonstrated utility in furthering responders' efforts to characterize oil in the water column and on the water surface. However, use of these technologies in future spill response efforts depends on developing the necessary procedures and operational guidelines that allow responders and NRDA practitioners to rapidly determine which technology is best suited for a particular situation, quickly obtain and deploy the chosen technology, and then efficiently digest the information obtained by that technology (White et al., 2016).

Due to the magnitude of the spill and the extreme depth of the well blowout, the DWH oil spill presented numerous challenges to responders and NRDA practitioners with regard to characterizing oil in the water column. One technology that demonstrated considerable utility in characterizing the nature and extent of oil in the water column, especially at depth, was the autonomous underwater vehicle (AUV) equipped with *in situ* sensors capable of characterizing oil. In developing AUV technology for future spills, the propeller-driven Remote Environmental Monitoring UnitS (REMUS) class of AUVs, is of particular interest, as they are relatively lightweight, easily deployable, and require a minimal logistical footprint and a small operational team. Furthermore, REMUS-class AUVs are modular, allowing the AUV to perform specific measurements or custom tasks by equipping it with different sensors, instruments, or tools (Farrell et al., 2003).

Fluorometry has a long history of use during oil spill responses to detect and quantify oil in the water column (White et al., 2016). It is a relatively simple, low-cost method that is capable of providing continuous measurements, which allows for the mapping of oil in the water column at fine spatial and temporal scales. Furthermore, fluorescence intensity measurements are highly sensitive and proportional to the aromatic hydrocarbon concentration in the water, making the technique semi-quantitative (or potentially quantitative with proper calibration). However, fluorometry on its own suffers from low selectivity, because many other naturally occurring compounds fluorescence at the same or similar wavelengths as aromatic hydrocarbons. This means that false positives can occur regularly, making the measurements unreliable without additional confirmatory data.

During the DWH oil spill, a number of studies included the collection of fluorometry data. However, NRDA practitioners had difficulty relying on the data to characterize oil in the water column because they did not have confirmatory supplemental data. This project aimed to address this data gap by outfitting a REMUS-class AUV with a suite of complementary sensors, including fluorometry, water quality sensors, and two new capabilities, to improve our ability to detect and quantify oil in the water column. The project also aimed to test and demonstrate synoptic sampling by an AUV and an unmanned aerial system (UAS). This provides tactical positioning and allows us to concurrently map surface oil and oil in the shallow surface mixing layer beneath an oil slick. These data improve our understanding of oil transport from the subsurface to the surface and our estimates of oil quantity. Finally, for this project the team

endeavored to develop data products compatible with existing common operational pictures (COPs) and processes to deliver these products in real-time or near real-time to help improve response efforts. Near real-time data transmission could be a matter of minutes from collection to the COP upload, for data requiring minimal processing collected on an internet-connected ship; or it could be several hours, for data collected on an AUV requiring post-processing before the COP upload.

1.1 Objectives

The overall objective of this project was to further develop our ability to utilize AUV and UAS technologies to characterize surface and subsurface oil during oil spill responses. The specific objectives include the following:

- Equip a REMUS-600 with a customized suite of oil sensing tools, including a typical suite of oil characterization sensors such as a fluorometer and a water quality sonde (see Section 2.1.1), as well as two new capabilities: a holographic camera and a water sampler (i.e., the Water Gulper). These tools are designed to improve the sensitivity, selectivity, and reliability of the detection and quantification of oil in the water column.

- Develop AUV and UAS data products that inform response operations and NRDA work.

- Develop processes to deliver these data products, including delivery of certain products in real-time or near real-time, to existing data management and visualization tools used in operations such as the National Oceanic and Atmospheric Administration's (NOAA's) COP, the Environmental Response Management Application (ERMA).

- Demonstrate the operational readiness of the REMUS-600 via deployment and testing at the natural seeps off the coast of Santa Barbara, California.

- Demonstrate synoptic sampling by AUV and UAS sensors during field testing.

Ultimately, the project deliverables aim to significantly improve spill response decision-making and enhance water column damage assessment capabilities.

1.2 Additional Science

While not a specific objective for this project, a REMUS-100 was also deployed during the field testing to help locate oil and collect complementary data; therefore, some data from this instrument are also included in this report. In addition, a long-range AUV (LRAUV) developed by the Woods Hole Oceanographic Institution (WHOI), in collaboration with the Monterey Bay Aquarium Research Institute (MBARI), was used in conjunction with this project. While we present overall mission planning LRAUV data, we do not include detailed data in this report, as deployment of the LRAUV was part of another project funded by the Center of Excellence, Arctic Domain Awareness Center (ADAC), and therefore outside of the scope of this project.

1.3   Team

The research team for this project (Figure 1) included scientists and engineers from multiple institutions, companies, and agencies, including WHOI, NOAA, the U.S. Environmental Protection Agency (EPA), the U.S. Coast Guard (USCG), Abt Associates (Abt), and Water Mapping LLC (Water Mapping). In the following sections we introduce the team members from each of these groups, and briefly describe their roles in the project.

Figure 1. The fieldwork team from WHOI, NOAA, EPA, Abt, and Water Mapping on the deck of the research vessel, the USCG Cutter George Cobb, with the REMUS-600.

Source: WHOI.

1.3.1   WHOI Team Members

The following team of engineers and scientists from WHOI led the design and development of the REMUS-600, which included equipping the AUV with two new capabilities (i.e., water sampling and a holographic camera) and developing data-transfer schema to provide data from the REMUS sensors to the research team in proper formats compatible with COPs such as ERMA, in near real-time.

- **Ms. Amy Kukulya**, a research engineer and principal investigator at WHOI in the Department of Applied Ocean Physics and Engineering, participated in all aspects of the study, including the study design. She was a co-developer of the WHOI Water Gulper; and served as the Principle Investigator, Expedition Leader, and technical lead for the REMUS-

600 development and testing. She led mission deployment of the REMUS-600 and REMUS-100 during the field test, and was responsible for reporting.

- **Dr. Erin Fischell**, a scientist at WHOI in the Department of Applied Ocean Physics and Engineering, participated in the field testing. She also was the lead in the development of holographic camera software to collect and classify holographic images. She performed all analyses of select holographic camera images.

- **Mr. Sean Whelan**, a senior engineering technician at WHOI, participated in all aspects of the study. During the field study he oversaw all deck operations during deployment and retrieval of the REMUS AUVs. He also assisted with the system integration and AUV operations.

- **Ms. Noa Yoder**, an engineer at WHOI, participated in the field testing, assisting with pre-operations checks and deck operations during deployment and retrieval of the REMUS AUVs. She also assisted with data processing.

- **Mr. Daniel Gomez-Ibanez**, a research engineer at WHOI, participated in all aspects of the study. He was the lead electrical engineer and co-developer of the WHOI Water Gulper, including the integration of the Water Gulper into the REMUS-600. He oversaw the implementation of the Water Gulper to collect water samples in the field.

- **Mr. Liam Cross**, an engineering technician at WHOI, participated in all aspects of the study, specifically assisting with the development of the Water Gulper, integrating it into the REMUS-600, and assisting with the implementation of the Water Gulper in the field.

- **Mr. Manyu Belani**, an engineer at WHOI, participated in the development of the Water Gulper and integration of the Water Gulper with the AUV.

- **Mr. Kevin Ducharme**, an engineer at WHOI, participated in the AUV development, specifically assisting with software development and integration of the sensors with the AUV.

1.3.2 NOAA Team Members

Scientists from NOAA's Ocean Service, Office of Response and Restoration (OR&R), led and participated in all phases of this project:

- **Dr. Lisa DiPinto**, a senior scientist at OR&R, participated in all aspects of the project and served as NOAA's Principle Investigator and project lead.

- **Mr. George Graettinger**, a senior environmental scientist in the Assessment and Restoration Division (ARD), Spatial Data Branch of OR&R and co-lead of the Gulf of Mexico ERMA, NOAA's COP, participated in all aspects of the project and oversaw development of the data transfer schema for delivery of AUV and UAS data to ERMA.

1.3.3 EPA Team Members

- **Dr. Robyn Conmy**, an ecologist at EPA's National Risk Management Research Laboratory, participated in all aspects of the project, including the initial study design. She served as the

EPA Principle Investigator and project lead, overseeing the collection and analysis of fluorometry and water chemistry data.

- **Dr. Devi Sundaravadivelu**, an environmental engineer at EPA's National Risk Management Research Laboratory, participated in the field testing and analyzed water samples collected during field activities.

- **Mr. Alexander Hall**, a geographer and Oak Ridge Institute for Science and Education (ORISE) research fellow at EPA, participated in the development of the data transfer schema and field testing, working with Mr. Graettinger at NOAA to process fluorometry data and deliver the data to ERMA in near real-time.

1.3.4 USCG Team Members

- **Ms. Dana S. Tulis**, Director, Emergency Management at USCG, served as the liaison between the research team and the USCG in planning the field testing and participated in field testing activities.

- **Lt. Shea Winterberger**, commanding officer on the USCG George Cobb, captained the vessel used by the team during the field testing activities.

1.3.5 Abt Team Members

- **Dr. Heather Forth**, an environmental scientist at Abt, was the lead author of the Sampling and Analysis Plan (SAP) and Health and Safety Plan (HSP), assisted with the logistical planning, and participated in the field testing activities. She was also the overall manager, co-author, and editor of this final project report.

- **Mr. Jamie Holmes**, a principal scientist at Abt, provided input on project design and was a reviewer of the SAP, HSP, and this final project report.

1.3.6 Water Mapping Team Members

- **Dr. Oscar Garcia**, Director of Water Mapping, helped with the overall project design, collected and analyzed UAS remote sensing data, and participated in review of the available satellite data.

- **Ms. Diana Garcia** assisted with the collection and analysis of UAS data in the field, and with post-processing and data delivery activities.

2. Methods

2.1 AUV Development

2.1.1 AUV Capability and Sensor Development

For the initial phase of this project, the Oceanographic Systems Laboratory (OSL) at WHOI equipped a WHOI-owned REMUS-600 AUV with a miniaturized holographic camera (SN#4 Seascan, Inc.) and a newly developed modular WHOI water gulping system (i.e., the Water Gulper) capable of collecting six 1-L bottles of water per module. The Water Gulper and the holographic camera are discussed further in Sections 2.2.5 and 2.2.6, respectively.

For the field testing, the WHOI team integrated two modular Water Gulpers into a REMUS-600, allowing for the collection of up to twelve, 1-L samples per deployment. In addition, the WHOI team transitioned the typical suite of oil characterization sensors from a REMUS-100 onto a REMUS-600. This suite of sensors included:

- A Neil Brown Ocean Sensors, Inc. (NBOSI) CTD (conductivity-temperature-depth) sensor

- An AADI dissolved oxygen (DO) probe

- A 300-m rated high-definition GoPro camera

- A Sea-Bird/Wet Labs, Inc. SeaOWL (oil-in-water locator) ultraviolet (UV)-A optical sensor configured with three wavelength pairs to simultaneously measure dissolved hydrocarbons fluorescence or fluorescent dissolved organic matter (FDOM), chlorophyll (CHL), and optical backscatter (OBS).

See Section 2.2.1 for a full description of the sensors. The rapid development of the technology for this effort was augmented by the investment made by the Department of Homeland Security (DHS) under the Center of Excellence, ADAC. The original testing and successful demonstration of the REMUS-100 oil system was conducted in fall 2016 at the WHOI-DHS-ADAC Demonstration in Woods Hole using a dye tracer as a signal proxy. In summer 2017, WHOI further tested the REMUS-100 oil characterization capabilities at the Mississippi Canyon lease block #20 oil release site (Abt Associates, 2018).

In addition to the development and integration of vehicle sensors, the OSL team integrated a secondary computer that allowed for "backseat" autonomy software, which makes it easier for engineers to write drivers for the sensors (i.e., write code that instructs REMUS to run new instruments) and develop new behaviors to respond to environmental anomalies such as dissolved hydrocarbons at water depths up to 600 m. This secondary computer saves money and time during the integration of technologies with REMUS AUVs, allowing for a more rapid development and adaptation of the technology.

2.1.2   AUV Software Development for Water Gulper

In support of the newly developed Water Gulper, WHOI developed two new AUV behaviors that dictate when and where the water sampler collects a sample. Here we provide a brief description of these behaviors. Additional detail on how these behaviors work, including the coding behind the behaviors, is provided in Appendix A.

The first AUV behavior, referred to as the "Circle/Spiral/Gulp Behavior," is an adaptive behavior that runs on the backseat "autonomy" computer at the start of the mission, and then interrupts the vehicle when it finds something of interest, which for this project is elevated fluorescence measurements. Specifically, the AUV is triggered to return to the location of the highest FDOM reading and collect a water sample using a circular search pattern at multiple depths around the location to relocate the point with the highest FDOM. This behavior is only triggered if the fluorometer onboard the AUV detects elevated FDOM readings above a specified background reading during a mission.

For this behavior, the user must define an area for the AUV to explore, using a specified search pattern, target depth(s), and set speed. This is defined in the vehicle mission plan prior to the start

of the mission. During the mission, using real-time data, the AUV adapts the specified mission to collect water samples where the FDOM level is highest. The Circle/Spiral/Gulp Behavior is best suited for exploratory missions, where operators are unsure where the oil is and what oil concentrations are in the water column.

The second AUV behavior, referred to as the "Point and Gulp Behavior," is a non-adaptive behavior that runs on the backseat "autonomy" computer throughout the mission. This behavior mode does not interrupt control of the vehicle during the mission, and therefore requires all the planning of the mission to occur prior to the start of the mission. This behavior is used when a specific latitude, longitude, and depth are desired for sampling. Only one sample is taken per transition; however, many transitions can be generated within a mission plan.

Overall, these two behaviors were developed to test and verify the functionality of the Water Gulper, and demonstrate two different ways it can be applied in the field. However, these behaviors are only a subset of what is possible, and additional behaviors can be developed to address other approaches for water sampling.

2.2   REMUS-600

2.2.1   AUV Payload and Missions

The REMUS-600 (600-m depth rating) is a commercially available AUV with over 20 years of development. The modular 12.75-in. diameter vehicle contains a standard 5.0 kWh, internal rechargeable lithium-ion battery pack, with the possibility of adding 15 kWh more batteries for missions capable of 72 hours of run time at speeds of 1.5 m/s (0.7–2.5 m/s).

The WHOI team chose the REMUS-600 vehicle as the host for the oil assessment payload because it is large enough to comfortably accommodate several 1-L bottles, along with other oil sensors, within its 32-cm diameter body and 3-m length. Weighing only 300 kg with a long battery life, the REMUS-600 is well-suited for single day or overnight search and survey operations in water depths up to 600 m, employing payloads requiring 100–200 W power.

Furthermore, the REMUS-600 is modular, allowing for easy reconfiguration depending on mission needs. Its rear-half implements core vehicle control, propulsion, navigation, and communication functions; while its forward-half is a reconfigurable payload section that can accommodate a variety of mission-specific sensor payloads such as the oil sensing payload developed for this project. Payloads are fastened to the 32-cm diameter ring joints and use one of the supported electrical payload interfaces, which include five RS-232 serial, five gigabit ethernet ports, five switchable 12 volt direct current (VDC) power supplies, and five 28 VDC power supplies.

For this project, a WHOI-owned REMUS-600 vehicle was configured to have several optical sensors specific for oil characterization in the water column. The sensors were located close to the center of the vehicle, as outlined in the Section 2.1, AUV Development. The SeaOWL, which was the primary sensor used to detect oil, had three independent optical channels for simultaneously measuring FDOM, OBS, and CHL; and a co-located Anderaa 4831F optode, which measured oxygen concentration. In front of the optical sensors were two water sampler sections, each containing six 1-L bottles. In front of the water sampler sections were two cameras, a holographic camera, and a GoPro camera, which were used to record gas bubbles

and oil droplets. The Seascan, Inc. holographic camera captured a three-dimensional (3D) holographic image of an undisturbed volume of water between two probes in front of the vehicle, which can be used to estimate oil droplet number concentrations and size distributions in the water column. An adjustable, forward-facing GoPro Hero 3 video camera captured continuous video for up to 4.5 hours, allowing for visible assessment of the water column.

In addition to oil characterization sensors and capabilities, the REMUS-600 oil detection vehicle was outfitted with the following commercial off-the-shelf (COTS) instrument capabilities: iridium, WHOI micromodem acoustic communications (ACOMMS), a 1,200-kHz up/down ADCP (Acoustic Doppler Current Profiler), a PHINS inertial navigation system (INS, model C7), a NBOSI CTD, an AADI dissolved oxygen probe, and a Licor photosynthetically active radiation (PAR) sensor. In addition, the REMUS-600 was outfitted with backseat autonomy, custom acoustic communications capabilities with oil-specific near-real-time messaging, and ROS (Robot Operating System) software.

Missions were conducted using the different AUV behaviors developed during the initial phase of the project (see Section 2.1.2). Typical search patterns included a uniform grid of tracklines, known as mow-the-lawn, a simple rectangle around an area of interest, or a circular pattern. With each of these grid shapes, the AUV could be kept at a constant depth or moved up and down through specified depths of the water column in a yo-yo pattern.

2.2.2   AUV Launch and Recovery Procedures

Both the REMUS-100 and REMUS-600 were launched and recovered using the ship's 20,000-lb SWL (safe working load) buoy crane. The vehicles were rigged with a WHOI quick-release hook while two–four people used poles and a slip line to safely keep the AUVs away from the ship (Figure 2). Once the vehicle was in the water, the slip line was released, which was followed by a quick release. The vehicle was then driven away from the ship by REMUS operators or the ship's captain using a WiFi-enabled tablet.

Since AUV launch and recovery efforts are not normally performed on buoy tenders, there was a mismatch between regular USCG protocol and what was necessary for the AUVs to be recovered smoothly. On the first day, for both the REMUS-100 and REMUS-600 launches and recoveries, there were more personnel than necessary for a standard AUV recovery, and the vehicle made contact with the side of the vessel multiple times. Fortunately, other than a slight dent to the REMUS-100 propeller, no other damage was sustained. On the following day, better fenders were constructed out of the boat hooks, and WHOI personnel were stationed on both ends of the vehicle, with only one USCG member (see Figure 2). These adjustment greatly aided in successful launch and recoveries throughout the rest of the field testing.

2.2.3   CTD

The REMUS-600 included a hull-mount type NBOSI CTD sensor for measuring salinity (i.e., conductivity), water temperature, and depth (i.e., pressure). These measurements were collected continuously throughout the mission. CTD data were retrieved from the REMUS-600 every time the AUV surfaced during or after a mission (see Section 2.2.7 for details). These data were then immediately transferred to data analysts for processing and near real-time delivery to ERMA.

Figure 2. Image shows AUV safety sticks improvised by the USCG crew (left), and deck crew preparing to recover the REMUS-600 using safety sticks (right).

Sources: USCG (left), NOAA (right).

2.2.4   Fluorometer

The REMUS-600 was also outfitted with a SeaOWL UV-A fluorometer, which is an improved version of the FDOM ECO fluorometer that was used during the DWH oil spill to characterize oil in the water column. While the FDOM ECO fluorometer has been shown to reliably detect and quantify low concentrations of dispersed oil in wave tank studies (Conmy et al., 2014), Sea-Bird Scientific reports that the SeaOWL UV-A fluorometer has five times the optical resolution of the FDOM ECO fluorometer. Furthermore, the SeaOWL UV-A fluorometer is configured with three excitation/emission wavelength pairs to simultaneously measure dissolved and particulate aromatic hydrocarbon concentrations via the FDOM sensor (excitation/emission λ 370/460 nm), particulate concentrations (i.e., oil droplets) via the OBS sensor, and CHL concentrations via the CHL sensor. Collection of these three data types simultaneously helps better discriminate a fluorescent signal due to crude oil from other naturally occurring sources of fluorescence. The SeaOWL UV-A fluorometer was produced specifically for autonomous platforms, allowing easy integration into AUVs like the REMUS-600.

In general, data from the SeaOWL UV-A fluorometer were retrieved from the REMUS-600 every time the AUV surfaced during or after a mission, as described in Section 2.2.7. Once retrieved from the AUV, data analysts merged the SeaOWL data with the CTD data and produced plots that related salinity and depth to FDOM, OBS, and CHL. In Section 3 (Results

and Discussion), we present the data products that were delivered to ERMA and describe how the data were used to characterize oil in the water column to inform response operations and NRDA work.

2.2.5 Water Gulper

As part of the scope of work for this project, WHOI developed a multi-chamber, large volume water sampler for integration with the REMUS-600. Each water sampler holds six 1-L samples arranged in two rows of three bottles each (Figure 3). The water sampler was designed around standard 1-L sample bottles, a volume that is sufficient for the testing of both volatile hydrocarbons, including benzene, toluene, ethylene, and xylenes (BTEX) and polycyclic aromatic hydrocarbons (PAHs), from the same sample without a significant reduction in detection limits. The team chose to use glass sample bottles instead of more robust plastic alternatives, because plastic bottles can introduce measurable amounts of hydrocarbons into the water sample.

Figure 3. Picture of the WHOI water gulping system used to collect water samples with the REMUS-600 AUV.
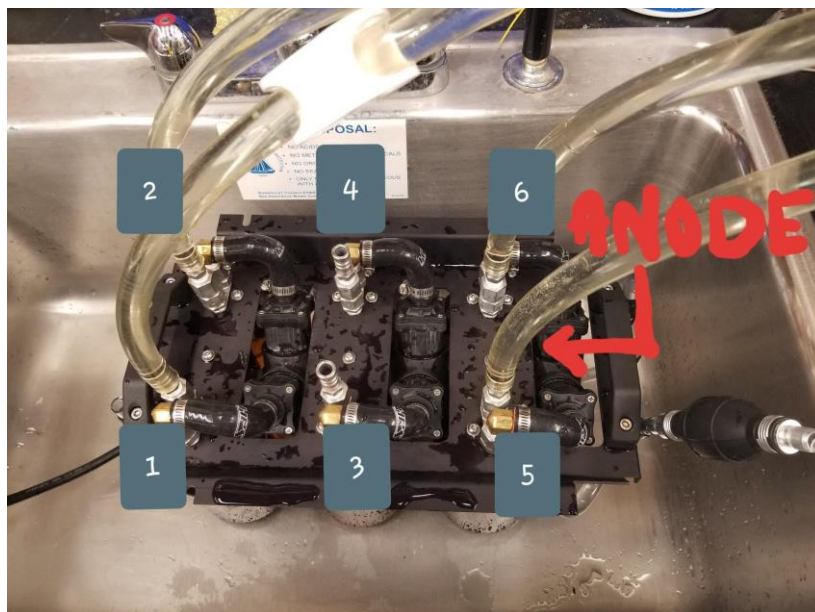
Source: WHOI.

For each bottle, the WHOI team installed a pair of check valves (Swagelock SS 4CP5-1/3) at the inlet and exhaust ports of the bottle adapter to seal the sampler bottle when not in use. The team equipped each bottle with its own water pump (ZKSJ Pump model DC-40A), which is located downstream of the sample bottle past the exhaust check valve. This prevents contact between the sample water and the pump, which is made with hydrocarbon thermoplastics. To provide communication between the sampler and the vehicle's systems, the valves and pumps were then plugged into a REMUS-600 guest port.

During the field testing, the research team tested different approaches and AUV behaviors for triggering a water sample. These included targeting the highest fluorescence signal from a mapped area by returning to a location and circling the area while collecting the water sample,

collecting a water sample every time the measured fluorescence was above a specified threshold, and manually triggering a sample. All the behaviors associated with when and what triggered the REMUS-600 to gulp or not gulp are discussed in Section 2.1.2.

The water sampler utilizes COTS 1-L, certified trace chemistry glass bottles to collect the water samples. Once filled with a sample, these bottles could be directly shipped to the analytical laboratory without transfer to another bottle. Collecting the water samples directly into laboratory-grade, single-use sample bottles minimizes sample handling and avoids the need to decontaminate sampling equipment. This capability provides numerous advantages, including eliminating potential contamination due to sample transfer and reuse of sample bottles, as well as reducing the required time for sample processing. To further reduce opportunities for contamination, each bottle collects water through a separate inlet. In addition, attached to each inlet is a 6–8 in. piece of tubing, which shifts the sampling point away from the surface of the AUV, minimizing the potential influence of AUV surface contamination on the water sample. The soft inlets are resilient against accidental impacts during launch and recovery of the vehicle.

To maintain neutral buoyancy of the AUV, each sample bottle must be pre-filled with clean, hydrocarbon-free water prior to installation into the REMUS-600. The pre-filled water sample bottles are then installed into the sampler, and any remaining air is burped out of the system, as air bubbles can impair functioning of the pump. During a mission, a sample is collected by pumping the clean water out of the sample bottle though the outlet, which then pulls in sample water through a one-way check value at the inlet. The only materials in the sample path are a 316 stainless steel check value, and fluoropolymer inlet tubing and fittings. For the field testing, the team used drinking water from the Goleta Drinking Water Company. For further details on preparation of the water samplers for deployment, see Appendix B.

Samplers were designed so they could be installed end-to-end with the AUV to increase the sampling capacity of the REMUS-600. For this project, the field team installed two samplers into the REMUS-600 for each mission. For integration into the REMUS-600, WHOI placed each module in an aluminum frame with 32-cm diameter ring joints. To offset the weight of the sampler and frame, they attached yellow-painted syntactic foam blocks to the frame. To facilitate sample processing, WHOI designed the water gulping system to allow a technician to remove each module from the vehicle individually without unsealing any pressure housing or disturbing other modules. This allowed for fast access to the water samples after or in-between missions without disassembly of other vehicle parts.

During the field test, water samples were typically processed at the end of each day, following retrieval of the REMUS-600. On the second-to-last day, the REMUS-600 was retrieved mid-day to unload water samples that were collected during the morning missions, and then the AUV was re-deployed to conduct additional missions (and water sampling) in the afternoon. Following retrieval of the REMUS-600, the water sampling trays were removed from the AUV (if used), and each sample bottle disconnected from the sampler, noting the sample bottle location. Two 40-mL subsamples were collected from each sample into 40-mL glass vials for BTEX analysis (according to modified EPA Method 524.2), while the remaining water volume in the 1-L bottle was analyzed for total petroleum hydrocarbons (TPH) according to modified EPA Method 8015b, and for PAHs according to EPA's internal method G-LMMD-SOP-1209-0. All bottles were dried, labeled, and packed on ice for overnight shipping to the EPA laboratory in Cincinnati, Ohio.

At the end of each day, the AUV operators provided the sampling team with that day's sampler log file from the AUV computer, which indicated the date, time, and position of each sample collected that day. In some cases, not all six sample bottles from a tray were sampled during deployments. Sample bottles that were not gulped during a mission were either submitted as trip blanks or discarded. All sample bottles that the log indicated had been gulped were processed and shipped to the EPA laboratory in Cincinnati, Ohio. At the laboratory, EPA staff further verified that each sample bottle was successfully gulped by measuring the salinity of each sample prior to extraction. For a few sample bottles, the salinity of the sample was close to zero, indicating the Water Gulper failed to gulp a sample. For these cases, the samples were discarded.

2.2.6 Holographic Camera

During the initial phase of this project, WHOI equipped a REMUS-600 with a miniaturized holographic camera (i.e., Holographic Imaging System) by mounting the device on a specially designed nose endcap for the AUV. The holographic camera captures 3D images of the particulates *in situ* using a laser light source and a digital camera. A holographic image is created by shining a laser beam though the volume of water that is between the light source and the camera. This light is scattered by particles suspended in the water, creating an interference pattern of scattered light, which is then captured by the digital camera. The interference pattern produces a hologram of the particles from which images of the particles are reconstructed. Once the images are created, standard image processing methods can be applied to obtain statistics about the particles found in the image, including particle shape, size distribution, total area, and total number. These statistics can be used as estimates of oil droplet and/or gas bubble concentrations in the water column, providing additional evidence and complementary data for the fluorometry data.

The holographic camera uses a 4.2-megapixel, black-and-white camera; and a 658-nm collimated laser light source separated by a known distance to capture a digital image of a fixed volume of water. The camera resolution, pixel size, and the separation distance between the light source and camera define the total image volume. The user can set the camera frame rate from 1 to 10 Hz, depending on operating conditions. The imaging system will automatically start capturing images at the user-defined frame rate when the system power is turned on. The imaging system software controls the camera and triggers the laser light. The pulse width of the laser light is 4 microseconds, operating at about 75 mA at 5 V. These values are preset by the manufacturer (Seascan) for optimal lighting over a wide temperature range.

The holographic camera uses a laptop computer for operating and accessing the imaging system, as well as for processing the holographic images. For the field testing, WHOI transferred the images from the internal solid-state hard drive in the camera to a laptop computer using a gigabyte hardwire connection at the end of each day following retrieval of the REMUS-600.

The holographic camera has a 2-Tb, solid-state hard drive for storing holographic images. The file format is .pgm, which is compatible with the post-processing software. Each image file is approximately 4.1 MB. Due to the size of the image files and the rate of imaging, a hard drive can easily be filled during a day's worth of missions, and download of these data can take up to 10 hours. Once the data are retrieved, it can then take an analyst multiple hours to sift through the images before processing can begin. These time-consuming steps currently prevent the

holographic camera from being a near real-time sensor. Future research could include development of machine-learning algorithms to automate image processing.

The REMUS-600 host platform turns the imaging system on by continuously applying 2.3 to 3.5 VDC at pin 8. The imaging system will power on, start the application program (approximately 40 seconds), and then start the image capture. The application program does not have a clock and does not timestamp the images, but will send the image number to the REMUS-600 computer over the serial line. Time stamping is then done by the REMUS computer in real-time as long as there is a working serial connection between the holographic camera central processing unit and the REMUS central processing unit during the mission. When downloading data from the REMUS, a .csv file with image number, depth, and time is also exported for the holographic image data processing. Data collected during the field test, as well as results of the image processing, are provided in the Section 3, Results and Discussion.

2.2.7   Data Retrieval Process from the REMUS-600

Except for the gigabyte-sized GoPro videos and holographic camera images, all data were retrieved from the AUV every time it surfaced post-mission. The data were retrieved via a WiFi connection with frontseat and backseat computers aboard the vessel. Once surfaced and within WiFi range (~ 1,000 m or less), operators were able to download a .csv file with CTD data, SeaOWL data, time, and position information, and within minutes the data were transferred to data analysts for processing. The processed data products were then posted to ERMA within hours of data collection. As discussed later in this report, we demonstrated this near real-time data delivery capability during our field tests at the Santa Barbara seeps.

For the larger holographic images, data were downloaded via a hardwire connection once the vehicle was recovered and aboard the vessel. Each downloaded image was stamped with the image number and time to facilitate post-processing of the data following the mission.

Likewise, the GoPro videos were retrieved at the end of each day (or once the AUV was recovered) by removing the secure digital (SD) card from the video camera, and downloading the videos from the card to a computer. The GoPro was only operable during the first 4–4.5 hours of the mission. While the GoPro videos from the field testing have not been fully reviewed, the WHOI team has rendered all the individual files into one video file, and encoded the mission time to make any future processing or review more efficient.

2.3   REMUS-100

The REMUS-100 AUV was leveraged during this project to provide a secondary autonomous sensing platform with complementary capabilities.

2.3.1   AUV Payload and Missions

The REMUS-100 AUV was outfitted with the following instrument capabilities: iridium, WHOI ACOMMS, a 1,200-kHz up/down ADCP, a PHINS INS (model C3), a NBOSI CTD, an AADI dissolved oxygen probe, a SeaOWL UV-A fluorometer (configured with three wavelength pairs to simultaneously measure FDOM, CHL, and OBS), a Suna nitrate sensor, a Simrad EK80 Splitbeam sonar, a Marinesonics sidescan sonar, and a GoPro camera.

The main function of the REMUS-100 was to provide additional support during the field testing to identify areas within the water column with dispersed oil or dissolved hydrocarbons. Its primary mission was to conduct a mow-the-lawn pattern at a set depth, using the up-facing sonar data to quickly identify locations of oil droplet and/or gas bubble plumes in the water column under the defined grid of the mission.

2.3.2   CTD and Fluorometer

Similar to the REMUS-600, a hull-mount type NBOSI CTD and a SeaOWL UV-A fluorometer were included on the REMUS-100 payload. Together, the data from these sensors were used to detect and map oil in the water column within our study area. Like the REMUS-600 data, the team processed and delivered FDOM and OBS track maps, as well as scatterplots showing the relationship among FDOM, OBS, and CHL, with depth.

2.3.3   Sonar

The Simrad EK80 provides users with scientific echosounder data in the water column. In the configuration used for this experiment, broadband scattering is measured from the AUV up to the surface, providing data on scatterers in the water column, including fish/biology, gas bubbles, and oil droplets. The great benefit of the EK80 is that as it can traverse an area at a single, set depth and provide information on the potential presence of scatterers, such as oil droplets and gas bubbles for the entire water column above or below the echosounder (depending on if the instrument is facing up or down). This is in contrast to the fluorometer that only detects oil that has come into contact with the sensor. This means the EK80 can be used as a prescreening tool, assessing for the potential presence of oil and illuminating potential hot spots over a much greater area than can be covered by the fluorometer. Once these potential hot spots have been identified, oil spill responders can target sampling by the AUV to a smaller region. The broadband frequency spectra of this sensor provides the potential to distinguish different types of biological scatter from other scattering materials, which could be exploited in future experiments. For this project, it was deployed on the REMUS-100 AUV to obtain water column profiles of scattering due to oil droplets or gas bubbles.

2.3.4   Data Retrieval Process from the REMUS-100

Retrieval and processing of CTD, SeaOWL, and position data from the REMUS-100 were similar to the REMUS-600. For the large echosounder data files, data were downloaded via a hardwire connection once the vehicle was recovered and aboard the vessel. This download often took up to 12 hours (overnight) to complete, and therefore the echosounder data were not readily available until the following day. However, data downloaded overnight were compiled the following morning during transit to our study area, allowing the data products from the EK80 to be used to inform the next day's sampling.

2.4   Additional AUV Support from LRAUV

In addition to the REMUS-100, a third AUV, the LRAUV, was deployed and in continuous operation for 6 days in support of a DHS Center of Excellence, ADAC-funded project. The LRAUV, operated by MBARI, was used to inform the research team of the potential hot spots, or locations with elevated dissolved hydrocarbon concentrations, within our study area. These data were used to direct the daily field operations during field testing. This prior knowledge

saved valuable time on mission days by minimizing the need to search for elevated hydrocarbon concentrations prior to REMUS deployment.

2.5 UAS

2.5.1 UAS Payload and Missions

During the field testing, Dr. Garcia of Water Mapping conducted UAS surveys using multi-rotor quadcopters rigged with optical and thermal sensors capable of broadcasting high-resolution video in real-time to the pilot's control. For the testing at the Santa Barbara seeps, a UAS equipped with optical and thermal sensors performed three main types of missions to support operations: (1) tactical positioning, (2) monitoring and survelliance, and (3) mapping. These different mission types are described in the following sections. Results of these missions are provided in Section 3, Results and Discussion.

Tactical Positioning

The purpose of a tactical positioning-type mission is to collect aerial data that can be used to guide on-water operations. The mission provides real-time data to crew on the vessel, which can be used to select the most appropriate locations for sampling or other operations. This type of mission is useful when little information exists on the location of the oil and, thus, the UAS may spend much of the flight searching for oil, and little time actually above the oil.

Monitoring and Surveillance

A monitoring and surveillance mission is similar to a tactical positioning mission, in that it provides real-time data that can be used to guide on-water operations. However, during monitoring and surveillance missions, video data are streamed live to the internet, allowing onshore operations, vessel crews, and other responders to view the UAS aerial images in real-time. Delivery of live streaming video to the internet is accomplished by a special receiver that links the UAS ground controller (which is receiving real-time feed of the flight) to a laptop connected to the internet. As the video begins, a link is generated that can immediately be sent to onshore operations or other responders to view the video in real-time. While the exact track of the video cannot be displayed, the link to the video can be tagged at the start position of the video (or the position of the boat), to allow responders to access the video, and see the general location of the video, via the COP in real-time.

Mapping

The purpose of a mapping mission is to provide high-resolution images of the surface oil that can be included as a layer in ERMA or other platforms. As part of other projects, Water Mapping developed a computer program to link the UAS flight log information (i.e., latitude, longitude, altitude, and heading) with the aerial images collected during a flight. The program computes the geo-rectification of each individual UAS image, which allows the overlapping fields of view to be stitched together and projected onto a map. For this project, during and after the field effort, Water Mapping developed and tested a procedure for processing these high-resolution maps in near real-time. From these tests, Water Mapping was able to demonstrate the production and delivery of a map within 20 to 30 minutes of completing the UAS flight (depending on the length of the flight and the area mapped). While aboard the George Cobb, the produced map was delivered as a geotiff to NOAA and to the AUV operations team using a flash drive; however,

the geotiff could also be delivered via a secure web portal, email, or other data transfer alternative. Once delivered, the map was incorporated into ERMA and other operational platforms, allowing the data to be used within approximately an hour of data collection.

2.5.2 Oil Thickness Classification

After the field testing ended, Dr. Garcia of Water Mapping applied a previously developed semi-supervised algorithm to his maps of surface oil to produce an oil classification layer. This classification process uses concurrently collected high-resolution visual and thermal imagery to produce a dual classification of thick versus thin oil (i.e., rainbow sheen or thinner). While not collected during this field sampling effort, on-the-ground slick thickness measurements collected contemporaneously with the aerial imagery can be used to convert the qualitative classifications into quantitative slick thickness bins. In general this process is more time-intensive, and is typically completed one to two weeks following a field mission; however, with additional help in the field or onshore, this process could be done more quickly to provide data in a shorter timeframe.

3. Results and Discussion

3.1 Detection and Quantification of Oil in the Water Column by REMUS

3.1.1 REMUS-600 Missions

During the field testing expedition, the REMUS-600 undertook 19 missions over 5 days. Over these 5 days, the REMUS-600 surveyed for a total of 23 hours and 55 minutes, covering a distance of 126 km. A description of each of these missions, including date, duration, location, general search pattern, and targeted depths, is provided in Table 1.

The REMUS-600 mission tracks and optical data were retrieved, processed, and uploaded to ERMA while aboard the George Cobb in near real-time (e.g., Figure 4). Appendix C provides a detailed description of each mission; maps of the mission track lines color coded by FDOM concentrations and OBS measurements; and a scatter plot that relates the FDOM, OBS, CHL, and depth data for each mission. During these 19 missions, we tested several different search patterns and approaches for mapping the water column (see Table 1), as well as two different protocols for triggering water sampling. See Section 2.1.2 for a description of the water sampling protocols.

3.1.2 REMUS-100 Missions

In addition, the REMUS-100 conducted six missions across five days in the field. Table 2 provides a description of each mission, including date, duration, location, general search pattern, and targeted depths of the mission. In general, the REMUS-100 was used to assist the team in locating sites with oil primarily through use of EK80 echosounder data. For example, Figure 5 shows EK80 echosounder data from August 27, 2019 that was used to determine our search area for mission MSN007. In Figure 5, data features show the presence of scatterers rising in the water column. This signal, originating in deeper waters through to shallow waters, suggests the presence of rising oil droplets and/or bubbles in the area. The higher signal in the surface waters results from biological activity and interference of surface features.

Table 1. REMUS-600 mission overview

Date	Mission	Duration (hh:mm:ss)	Distance (km)	Total duration (hh:mm:ss)	Total distance (km)	Gulps	Horizontal search pattern	Vertical search pattern	Mission depth (m)	Adaptive?
8/26/2019	MSN001	01:23:31	7.111	03:34:45	15.563	0	Rectangular	Yo-yo	2–30	Yes
	MSN002	00:27:03	2.357			0	Rectangular	Yo-yo	2–30	Yes
	MSN003	00:56:52	3.599			0	Rectangular	Yo-yo	2–30	Yes
	MSN004	00:47:19	2.496			0	Circular	Set depth	13	Yes
8/27/2019	MSN005	00:22:40	2.005	05:32:59	26.366	0	Rectangular	Yo-yo	2–35	Yes
	MSN005B	00:26:17	1.895			1	Rectangular	Yo-yo	2–35	Yes
	MSN006	01:24:03	6.683			2	Rectangular	Yo-yo	2–35	Yes
	MSN007	02:00:49	8.987			6	Rectangular	Yo-yo	2–35	Yes
	MSN008	00:27:45	1.88			1	Mow-the-lawn	Yo-yo	2–35	Yes
	MSN009	00:51:25	4.916			0	Traverse	Yo-yo	2–35	Yes
8/28/2019	MSN010	01:57:19	11.722	06:02:22	33.801	0	Mow-the-lawn/ traverse	Yo-yo	2–35	No
	MSN011	01:48:12	10.509			0	Traverse/ mow-the-lawn	Set depth/ yo-yo	10, 2–35	No
	MSN012	00:23:56	1.75			0	Circular	Set depth	7	Yes
	MSN013	00:25:57	2.383			0	Rectangular	Set depth	16	Yes
	MSN014	01:26:58	7.437			0	Traverse	Yo-yo	3–25	Yes
8/29/2019	MSN015	02:44:12	16.285	5:52:41	33.407	0	Mow-the-lawn/ traverse	Yo-yo	3–20, 3–12.5, 6–12.5	Yes
	MSN016	00:53:35	5.085			1	Mow-the-lawn/ circular	Yo-yo/ set depth	3–20, 9	Yes
	MSN017	00:46:09	3.962			3	Rectangular	Yo-yo	3–20	Yes
	MSN018	01:28:45	8.075			2	Mow-the-lawn	Yo-yo/ set depth	3–20, 9	Yes
8/30/2019	MSN019	02:52:30	16.888	02:52:30	16.888	0	Mow-the-lawn/ traverse	Yo-yo	3–20	Yes

Figure 4. REMUS-600 mission tracks off the coast of Santa Barbara, California, in ERMA. The center image shows an overview of all missions, with insets at a higher zoom level showing tracks of each specific mission (labeled by mission number).
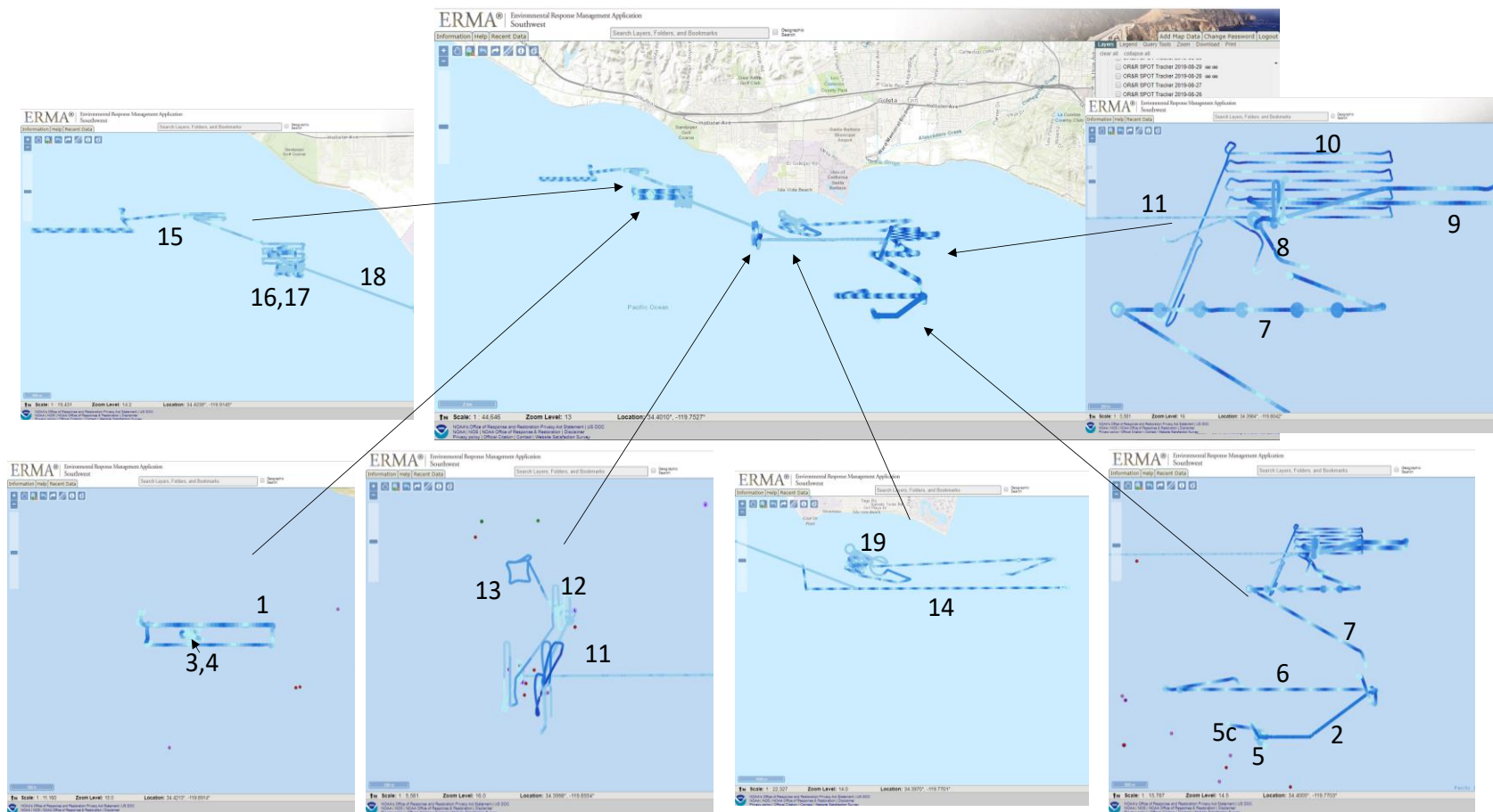
Table 2. REMUS-100 mission overview

Date	Mission	Duration (hh:mm:ss)	Distance (km)	Total duration (hh:mm:ss)	Total distance (km)	Horizontal search pattern	Vertical search pattern	Mission depth (m)
8/26/2019	MSN001	03:20:30	19.3	03:20:30	19.3	Rectangular	Set depth	30
8/27/2019	MSN002	00:59:19	2.4	04:23:26	22.8	Rectangular/ traverse	Set depth	30
	MSN003	03:24:07	20.5			Rectangular/ mow-the-lawn	Set depth/ yo-yo	30, 2–30
8/28/2019	MSN004	04:36:16	23.3	04:36:16	23.3	Mow-the-lawn/ traverse	Set depth	30, 20
8/29/2019	MSN005	01:05:47	6.8	02:50:04	16.4	Mow-the-lawn	Set depth	1.5
	MSN006	01:44:17	9.7			Mow-the-lawn	Set depth	2, 10

Figure 5. EK80 echosounder data that correspond to mission MSN007. The heat map indicates particles were detected at this location from 0 to 30 m.
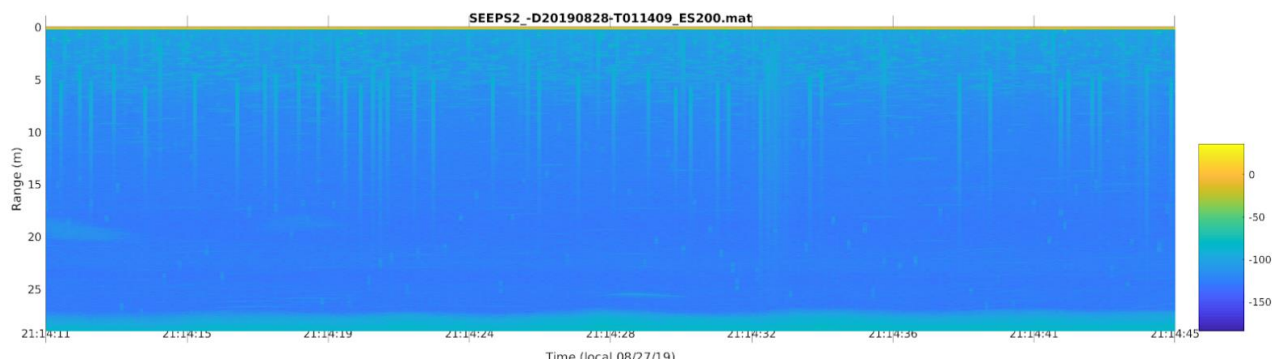
3.1.3   Support from LRAUV

Finally, an LRAUV was in operation during our field testing, conducting continuous surveys of our study area before and during the field testing. Data collected by the SeaOWL UV-A fluorometer onboard the LRAUV was used to inform and direct mission planning and sampling by the REMUS-600. As an example, Figure 6 shows data collected the evening of Sunday, August 25, 2019, before our first day in the field. These data show two main hot spots identified by the LRAUV, which the field team used as sampling locations for the initial missions.

Figure 6. LRAUV SeaOWL detections that informed REMUS missions to save time.
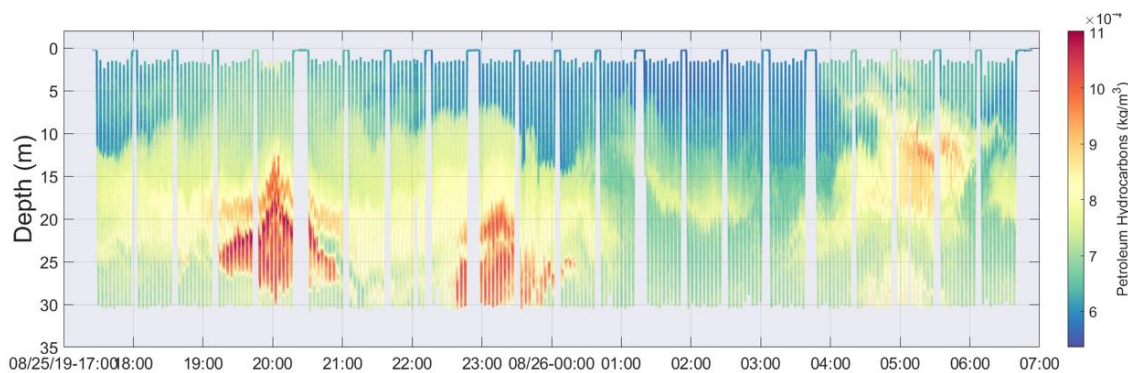
3.1.4   Converging Lines of Evidence: CTD and SeaOWL Data

When interpreting fluorometry data from the field, often a first course of action is to establish expected background FDOM concentrations for the area. In some environments, this is well-known and predictable. For example, in deep ocean waters, FDOM is typically low at around 1 ppb QSE (quinine sulfate equivalents) with very little fluctuation. This characteristically low, stable FDOM is the result of minimal biological activity and no freshwater influence in deep ocean waters. For other areas, such as shallow, coastal waters, background FDOM can be significantly higher and more variable due to increased freshwater inputs that are high in naturally occurring FDOM and increased biological activity in surface waters. For these areas, FDOM typically trends with salinity and/or with depth, and therefore salinity and depth measurements from the CTD can be used to help characterize FDOM in the area and establish a background FDOM. As a result, in areas where there is fluctuation due to various inputs of naturally occurring FDOM, oil can be detected by changes or anomalies in these predictable trends.

In Santa Barbara coastal waters, there is limited freshwater input, and subsequently limited terrestrially-derived FDOM input to the ocean. Thus, salinity is constant and high; and background FDOM is predictably stable at around 2 ppb QSE in deeper waters, slightly increasing in shallower water. Therefore, salinity is not a variable that needs to be considered within our study area. There is, however, a trend in FDOM concentrations with depth, with higher background FDOM concentrations occurring around 10–15 m below surface, and the lowest FDOM concentrations occurring at deeper depths. Figure 7 shows a typical FDOM concentration versus depth trend seen in coastal waters near Santa Barbara, California.

Another line of evidence used to distinguish oil from natural FDOM is CHL measurements. *In situ* production of FDOM in the ocean arises from phytoplankton productivity and therefore FDOM and CHL tend to trend together. On the other hand, crude oil and other petroleum products do not contain CHL. Consequently, an increase in FDOM concentrations without a corresponding increase in CHL concentrations is a good indicator that dispersed oil or dissolved hydrocarbons are present.

Finally, OBS measures particulate concentrations in the water column. Often oil in the water column will exist primarily as droplets, which this measurement corroborates. However, coincident high FDOM and high OBS can also be indicative of phytoplankton, which is where CHL can be used as additional evidence to discriminate between the two. In cases where oil and gas are being released together, OBS measurements will quantify both the oil droplets and the gas bubbles in the water column. The SeaOWL UV-A fluorometer has integrated these three sensors into one device such that these measurements can be easily collected synoptically, improving our ability to discriminate crude oil from phytoplankton and other natural sources of FDOM.

Figure 7. A typical FDOM concentration versus depth trend for coastal waters near Santa Barbara, California. The trend shows a maximum peak FDOM around 12 m below surface. Data are from REMUS-600, mission MSN005b. PPB = parts per billion.
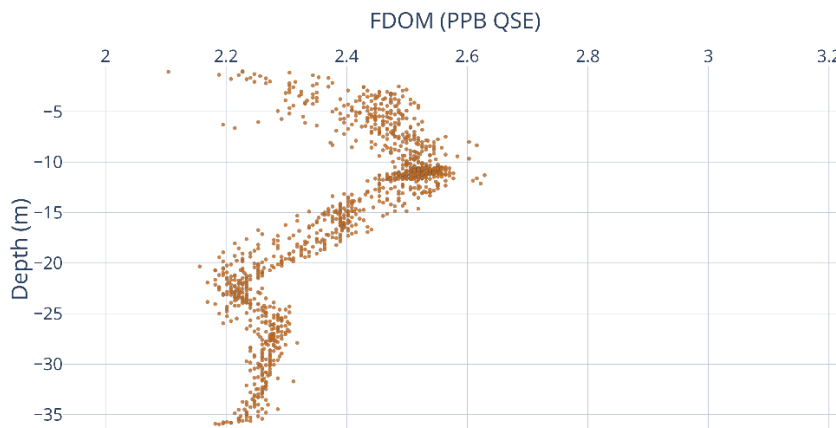
Figure 8 presents examples of these different scenarios, demonstrating how these three lines of evidence can be used in combination to distinguish a hydrocarbon signal from phytoplankton and other naturally occurring FDOM. For example, Figure 8B presents data from MSN003, where the SeaOWL observed elevated FDOM and OBS, without a corresponding increase in CHL at 30–35 m below surface. This combination of signals is an indication that the FDOM signal is likely the result of oil in the water column. This is in contrast to Figure 8A, which shows data from an area with no hydrocarbon signal. Figure 8C shows another example where FDOM and OBS are elevated without a corresponding increase in CHL at 10–15 m below surface, again indicating there are oil droplets or dissolved hydrocarbons in the water column. The case studies in Section 4 further discuss how data from the three SeaOWL UV-A sensors can be used as converging lines of evidence to detect and quantify oil in the water column.

3.1.5   Holographic Images

The holographic camera is a data-rich sensor that can take up to 10 images a second. These raw images capture the interference patterns created by particulate material within the holographic camera's beam. Using the holographic camera's digital processing program, the raw images can be reconstructed to reproduce two-dimensional (2D) and 3D renderings of the particulate material that show a silhouette of the particulate's shape. For oil spill response efforts and NRDA work, processed holographic images can provide additional evidence of oil in the water column by demonstrating (near) spherical particles (which are most likely oil droplets or gas bubbles) are present in the water column. The processed images can also be used to provide an estimate of the number and size distribution of the oil droplets or gas bubbles in the water column.

Figure 8. OBS, FDOM, and CHL versus depth for REMUS-600 missions MSN005B, MSN003, and MSN008. A) In mission MSN005B, the FDOM is consistently low and the peak maximum corresponds with the CHL maximum (grey box), indicating that the increase in FDOM between 10 and 15 m below surface (grey box) is attributable to biological sources. B) In mission MSN003, there is an increase in both OBS and FDOM between 30 and 35 m below surface (grey box) without a corresponding increase in CHL, indicating that the increase in FDOM is likely due to dispersed oil or dissolved hydrocarbons. C) In mission MSN008, the high FDOM count (above 3.0 ppb) with no corresponding increase in CHL at a depth of 12 to 15 m (grey box) provides strong evidence for oil.
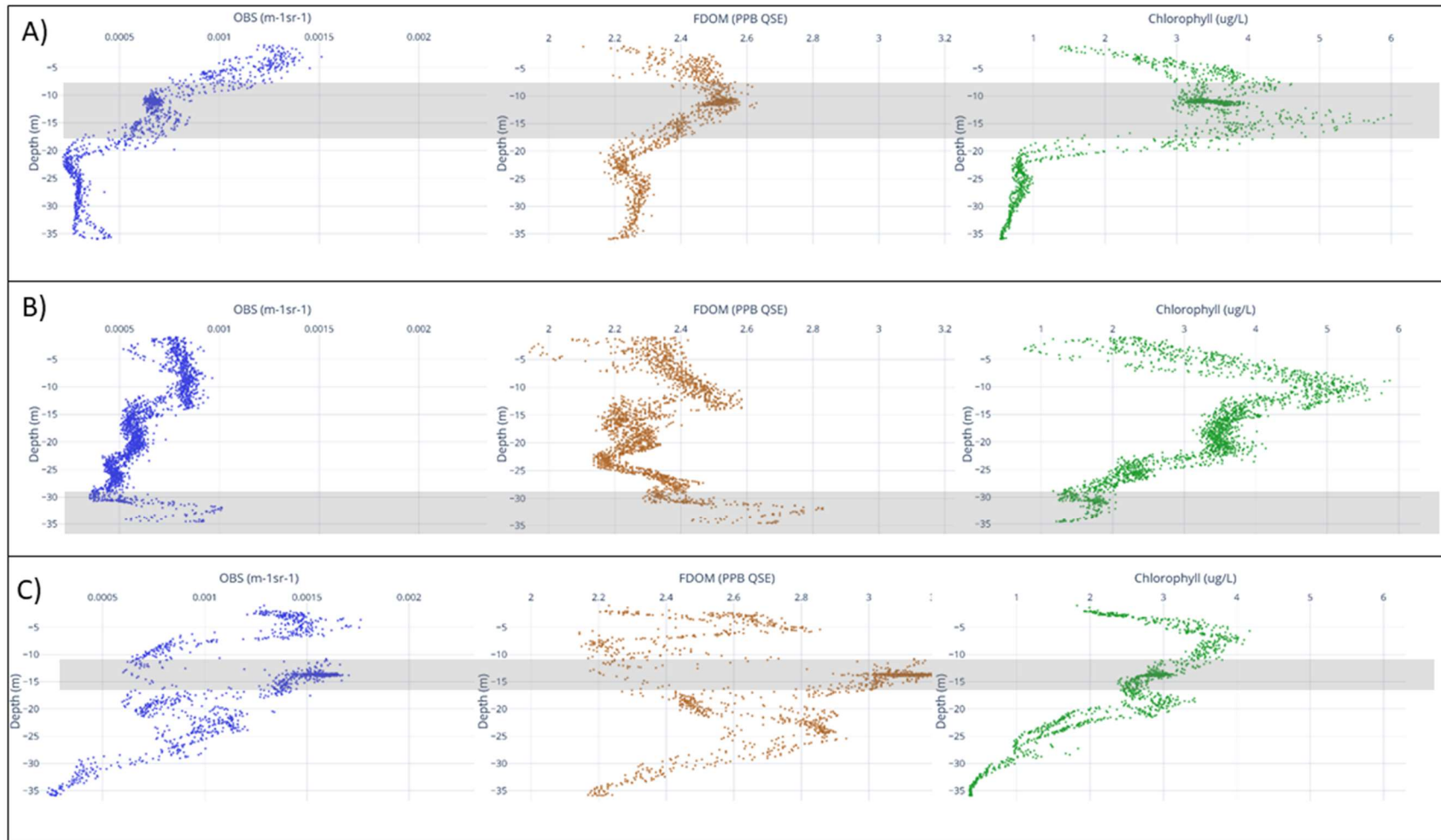
For this project, the REMUS-600 collected holographic camera data during the 19 missions. Following retrieval from the camera, the data were processed using the holographic camera software "Holo Batch" or "Holo Detail" from Seascan. These programs use the interference patterns in the holographic images stored by the holographic camera to identify and reconstruct particles in the image. It also produces a color-coded depth image that can be viewed in 3D to see the particles suspended in water. The format of the new images is a .tiff file. Figure 9 shows examples of 2D depth images and reconstructed 2D particle images from data collected at the Santa Barbara seeps. Images are processed through a routine to create a holograph where heatmap colors represent object distances from the detector, with blue being objects farthest away at 160 mm and red being objects that are closest (Figure 9, left panels). Black-and-white 2D representation of holograph images can be extracted and further refined to provide detailed shape information on the objects (Figure 9, right panels). The top panels illustrate biological activity detected by the imager, as illustrated by presence of copepods (yellow) and long-chain plankton (green). The bottom images illustrate a sample with minimal biological activity and the presence of oil spheres. Once the images have been reconstructed, particles in the image can be analyzed using standard image processing, to identify droplets of oil and determine characteristics such as size, opacity, and volume.

Dr. Fischell from WHOI wrote a script that produces oil droplet statistics using the reconstructed holographic image. For this script, Dr. Fischell assumed any particulate with a major to minor axis ratio of less than 1.1 (i.e., the mean major and minor axis dimensions were within 10% of each other) was an oil droplet or gas bubble. The oil droplet/gas bubble statistics for each image (i.e., sum volume of droplets, the number of droplets, median opacity, median droplet radius, variance of opacity, and variance of radius) are output into a .csv file, which can then be used to develop plots and other visual displays of the data (see Section 3.3).

Figure 10 shows scatter plots of droplet radius versus opacity, a relationship that was reviewed for each image processed. Using this script, Dr. Fischell processed raw holographic images from 21 interesting features that were identified in the SeaOWL and CTD data. Among these 21 features were locations of the 13 gulped water samples. Table 3 provides summary statistics for the holographic data collected during these 13 gulps. Based on these statistics, we can conclude that overall the concentrations of oil droplets/gas bubbles in the water column at the 13 gulp locations were relatively low, which is in agreement with our overall conclusion from the water chemistry (see Section 3.1.4). The highest concentrations of oil droplets/gas bubbles observed by the holographic camera were found at the following locations: the first gulp from mission MSN006, the first gulp from mission MSN007, the gulp from mission MSN008, and the gulp from mission MSN018. At the other nine gulps, very few oil droplets/gas bubbles were observed by the holographic camera. How the holographic camera data informed other data are discussed further in the case studies (Section 4).

Figure 9. (Left panels a and c) Image processing routine results for holographs collected during mission MSN007 with the holographic camera. Heat map colors in the holographs represent object distances from the detector with blue being farthest away at 160 mm. (Right panels b and d) Black and white 2D representation of extracted holograph images corresponding to left panels. Top panels (a and b) illustrate biological activity detected by the imager, as illustrated by the presence of copepods (yellow) and long-chain plankton (green). Bottom images (c and d) illustrate a sample with minimal biological activity and the presence of oil spheres.
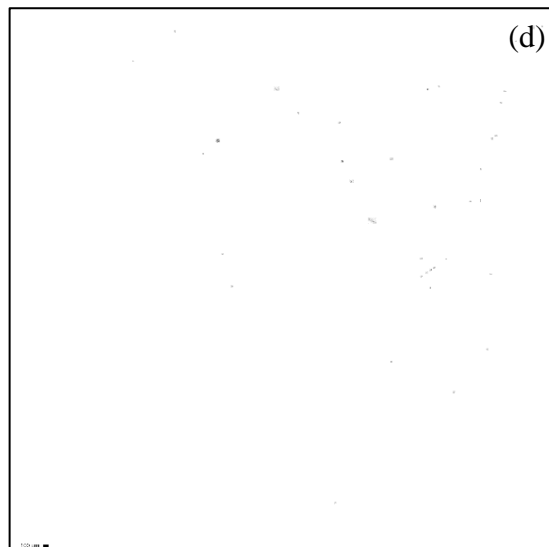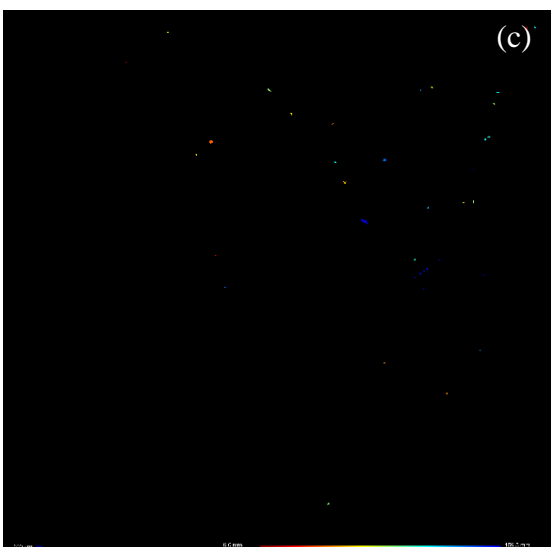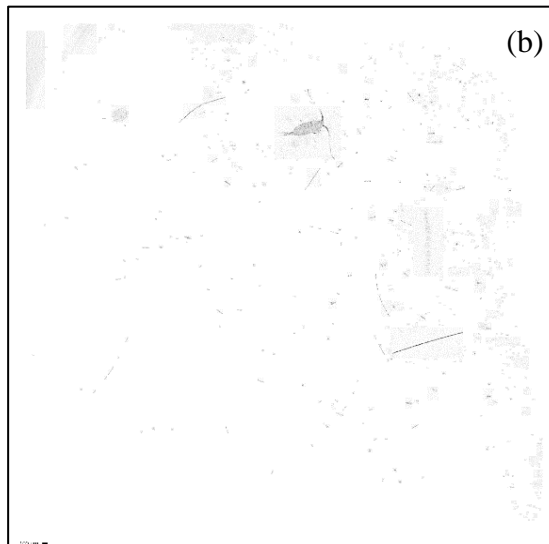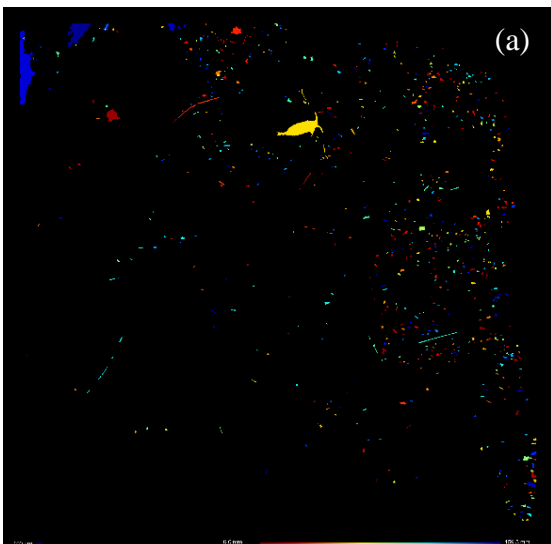
Figure 10. Examples of holographic camera statistics – opacity versus radius on detected droplets in two example images from August 26, 2019 in Santa Barbara seeps.
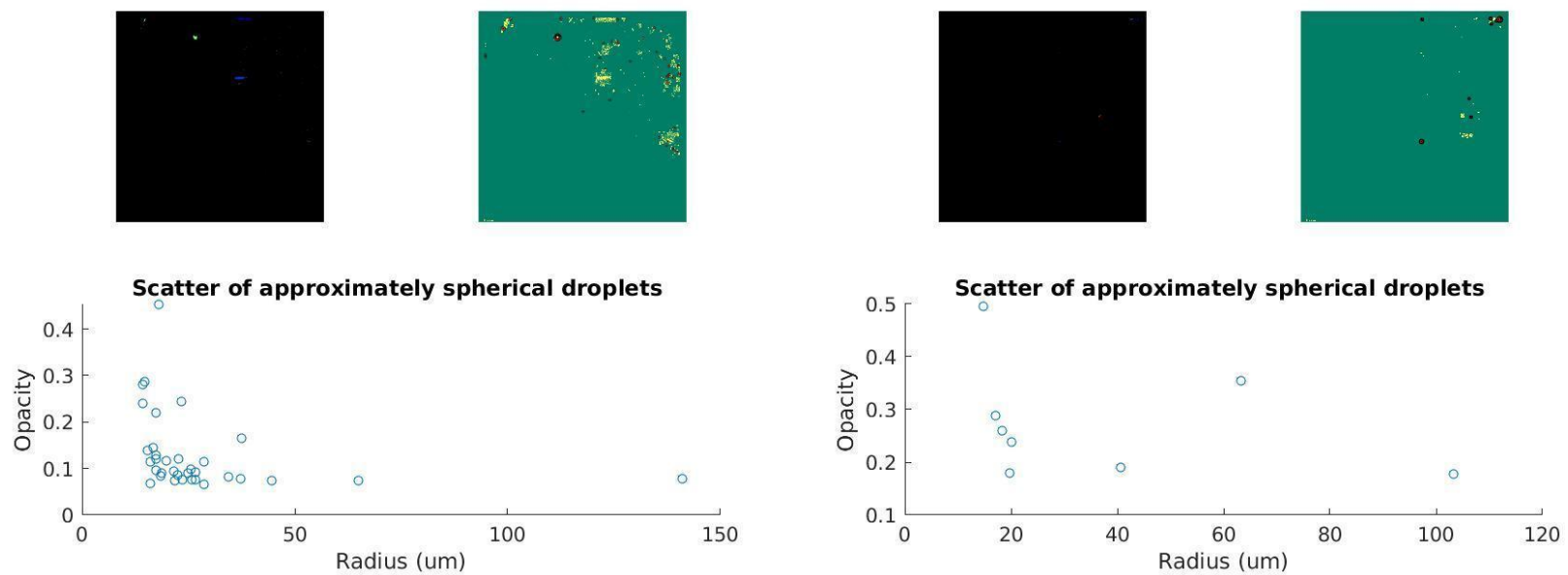
Table 3. Holographic image summary statistics for number of droplets in images collected at gulp locations.

Mission	Gulp depth (m)	Average droplets (#)	Maximum droplets (#)	Minimum droplets (#)	Median droplets (#)	Frames with ≥ 100 droplets
MSN005B	11.2	NA	NA	NA	NA	NA
MSN006	9.7	84.0	166	2	92	40
MSN006	14.1	33.9	100	3	33	1
MSN007	11.1	57.3	154	1	58	16
MSN007	11.8	46.9	107	2	50	6
MSN007	12.5	45.8	143	1	42	3
MSN007	11.4	38.2	103	2	41	1
MSN007	20.2	34.2	109	2	34	1
MSN007	20.6	28.9	80	2	28	0
MSN008	13.8	67.8	164	1	66	17
MSN016	9.0	38.5	104	2	33	2
MSN017	6.2	30.0	73	1	27	0
MSN018	11.4	59.4	152	2	57	10

NA = data not available.

3.1.6   Water Sampling

Over the 19 missions conducted by the REMUS-600 at the Santa Barbara seeps, the Water Gulper collected 16 water samples. For three of these samples, EPA determined through salinity measurements that the sampler failed to gulp. This failure may have been due to a malfunction with the pump mechanism, which is sensitive to air bubbles in the system, or may have been due to a loss of communication between the AUV and the Water Gulper during the mission. Additional testing of the Water Gulper could help elucidate reasons for these failures. Ultimately, it is good practice to check the salinity of all samples collected by the Water Gulper to verify the water used to pre-fill the sample bottle was completely replaced by sample water.

The Water Gulper collected water samples using both adaptive and non-adaptive behaviors developed during the initial phase of this project (see Section 2.1.2). The adaptive behavior was designed to identify and return to a location within a specific area or at a specific depth that has the highest measured FDOM concentrations to collect a water sample. Alternatively, the non-adaptive, point sampling mission was designed to sample pre-specified locations and depths. Figure 11 shows the track lines and FDOM raw count data from mission MSN007, an adaptive sampling mission, where the REMUS-600 surveyed the water column from a depth of ~ 5 m down to 30 m at six separate locations, collecting a water sample at the depth with the highest measured FDOM from each location.

The water chemistry from the Water Gulper samples are presented in Figure 12. Overall the hydrocarbon concentrations in the water samples were low. Furthermore, it appears there was contamination in the trip blanks and in the laboratory deionized (DI) water blank, making interpretation of the water chemistry difficult. Therefore, the water chemistry from this field effort cannot be used to verify fluorometry data. Despite the low TPH/TPAH concentrations and contamination in the blanks, we met our primary goal of demonstrating a functioning AUV water sampler with different sampling behaviors. Future missions will include additional quality assurance samples, to allow us to determine if and where contamination may be introduced into the blanks.

Figure 11. Data from the .csv files for mission MSN007 are used to plot the raw FDOM count over the course of REMUS-600's path, as it takes six separate water samples using the Water Gulper.
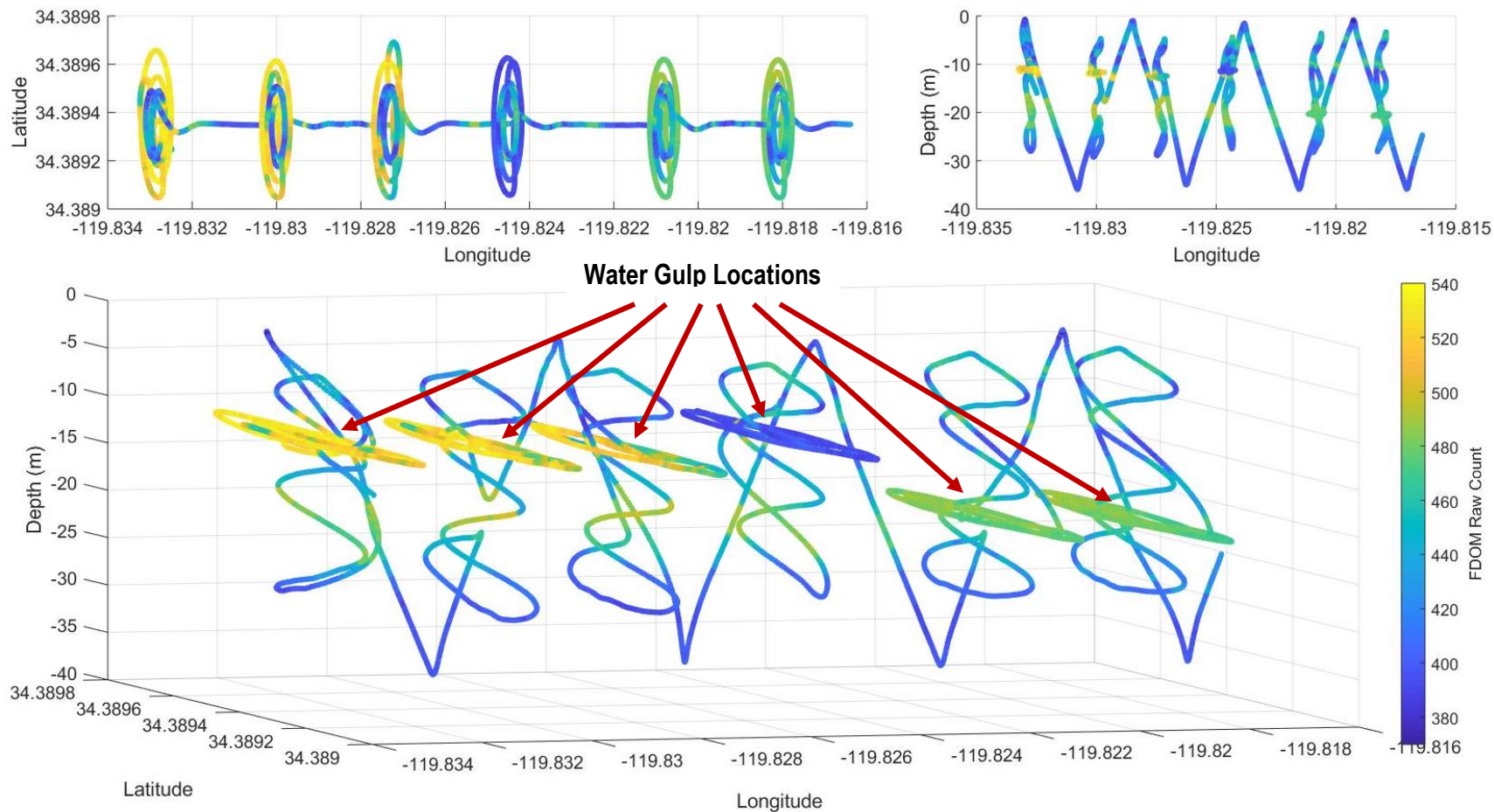
Figure 12. TPH, total PAH, total BTEX, and total alkane concentrations for quality control samples (red) and gulped samples (blue).
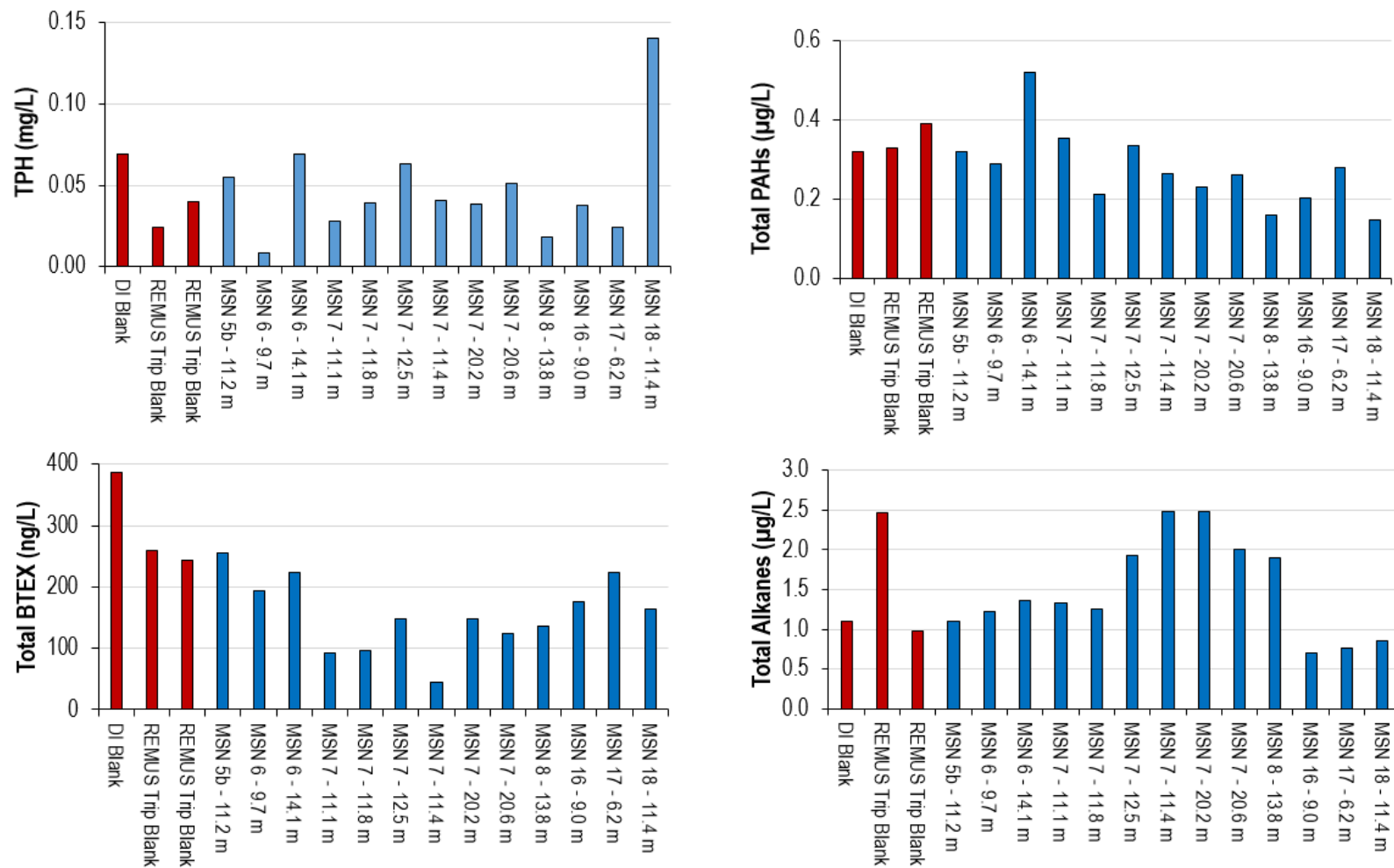
3.1.7   AUV Behaviors

During the field testing, the team explored two alternative data collection strategies for improving resolution compared to conventional mow-the-lawn search patterns for the patchy, time-varying underwater features presented by oil in the water column. For the first method, the team imaged with an acoustic sensor (EK80) on one vehicle (REMUS-100); and then directed the second vehicle, a REMUS-600, to survey specific areas identified by the EK80 to characterize water quality and contaminant concentrations. For the second technique, AUV operators used a technique referred to as "constrained adaptation," where the AUV conducts a pre-set search pattern that is interrupted when it comes across anomalies of interest. Once an anomaly is detected, the AUV is triggered to return to the location of the anomaly and conduct a more detailed survey, which could include a tighter search pattern and/or triggered water sampling. For this project, an anomaly was defined as an FDOM reading above a specific threshold. Constrained adaptation is designed to adapt the AUV search pattern based on what the AUV encounters in the environment. Figure 13 shows the FDOM data along the track lines for mission MSN017 where the REMUS-600 underwent three different adaptations (i.e., was triggered to collect a water sample) in response to FDOM maxima in the water column.

The field testing has highlighted several future AUV behavior modifications that could improve our ability to use REMUS AUVs for oil spill response efforts. First, the challenge of trying to capture complex, spatially and temporally variable oil seep information was made very clear in this experiment. A takeaway from our field testing is that the development of behaviors that include shorter, more rapid adaptation and gulping in response to detections of large anomalies may be an important additional AUV behavior to add to the toolbox. In addition, different adaptation triggers were tested throughout the week as we learned how to use them. We found that a combination of a minimum FDOM threshold for adaptation and a higher minimum FDOM threshold for gulping worked well. Second, the depth-adaptation part of the autonomy was based on altitude rather than depth, but the physical forcing for the processes is linked to depth rather than altitude. Modifying the adaptation so that it is based on depth will address issues with this incongruity and is easily changed. Finally, latitude and longitude variability were found to be much more significant than depth variability, which also suggests that with some modeling it should be possible to further constrain behaviors in depth. This was highlighted during a long transect at constant depth with the adaptation turned off, in which the highest concentrations of August 29, 2019 were not observed in the search area, but instead during the initial transect to the search area (Figure 14).

3.1.8   Data Processing and Visualization

For the REMUS-600, WHOI developed a process to stamp all sensor data retrieved as a .csv file with their corresponding latitude, longitude, and depth upon retrieval. This allowed the individual sensor data to be quickly plotted in three dimensions by any mapping or plotting software (e.g., Excel, MATLAB). In addition, to process and visualize the holographic camera data, WHOI developed a MATLAB visualization tool that displays the reconstructed images as well as the vehicle's path, the location in which the image was captured, and the plots of the droplet statistics. For example, Figure 15 shows a display of a reconstructed holographic camera image alongside droplet statistics and raw FDOM counts from mission MSN007 plotted in 3D space. Along the visualized path, this script can also display CTD, FDOM, and bathymetry or any other data proxy collected by REMUS.

Figure 13. FDOM counts during mission MSN017 (August 29, 2019), in which three adaptations (i.e., triggers to collect water samples) occurred in response to maxima in FDOM.
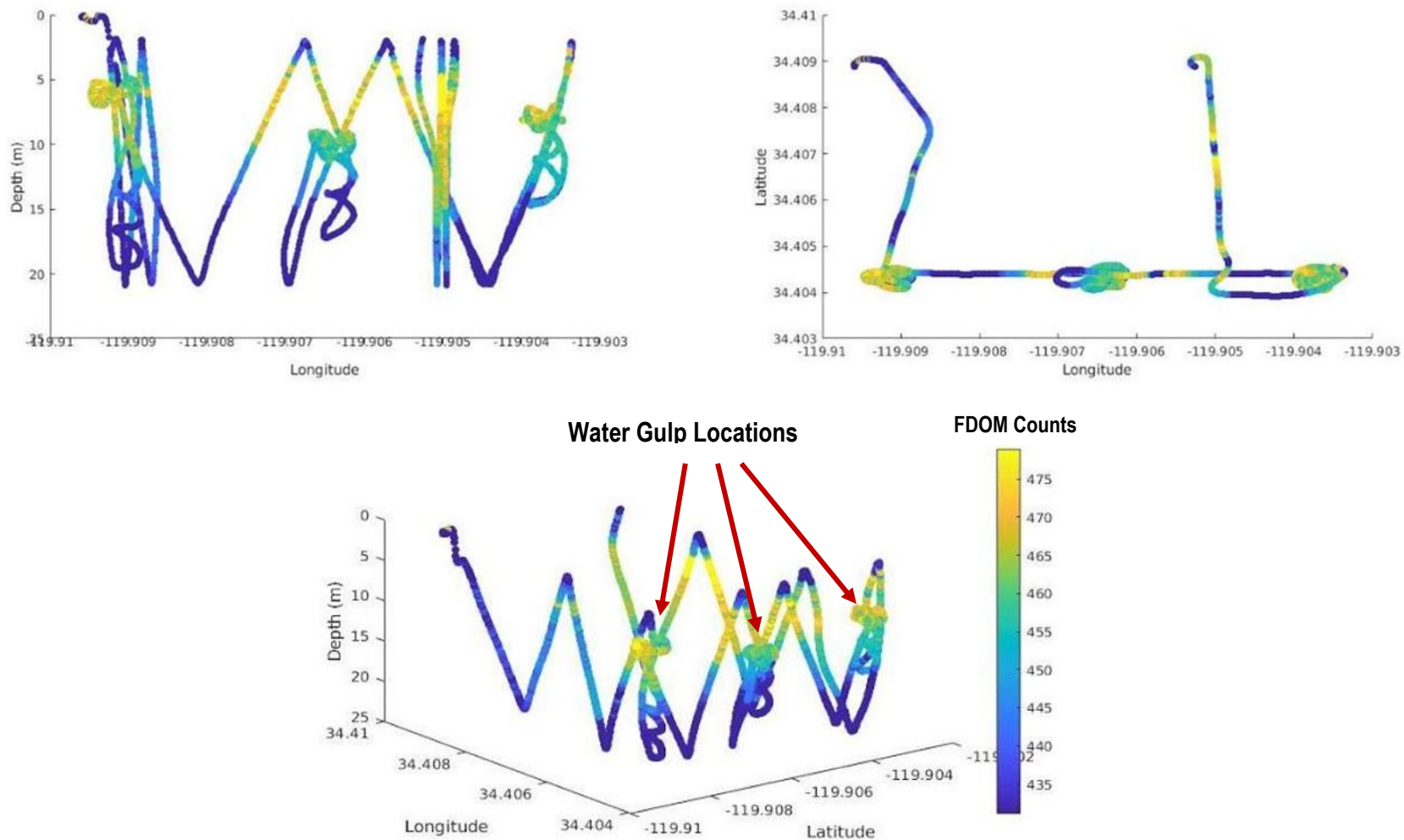
Figure 14. FDOM counts during mission MSN018 (August 29, 2019), in which the REMUS-600 traversed at a fixed depth and then began a yo-yo path.
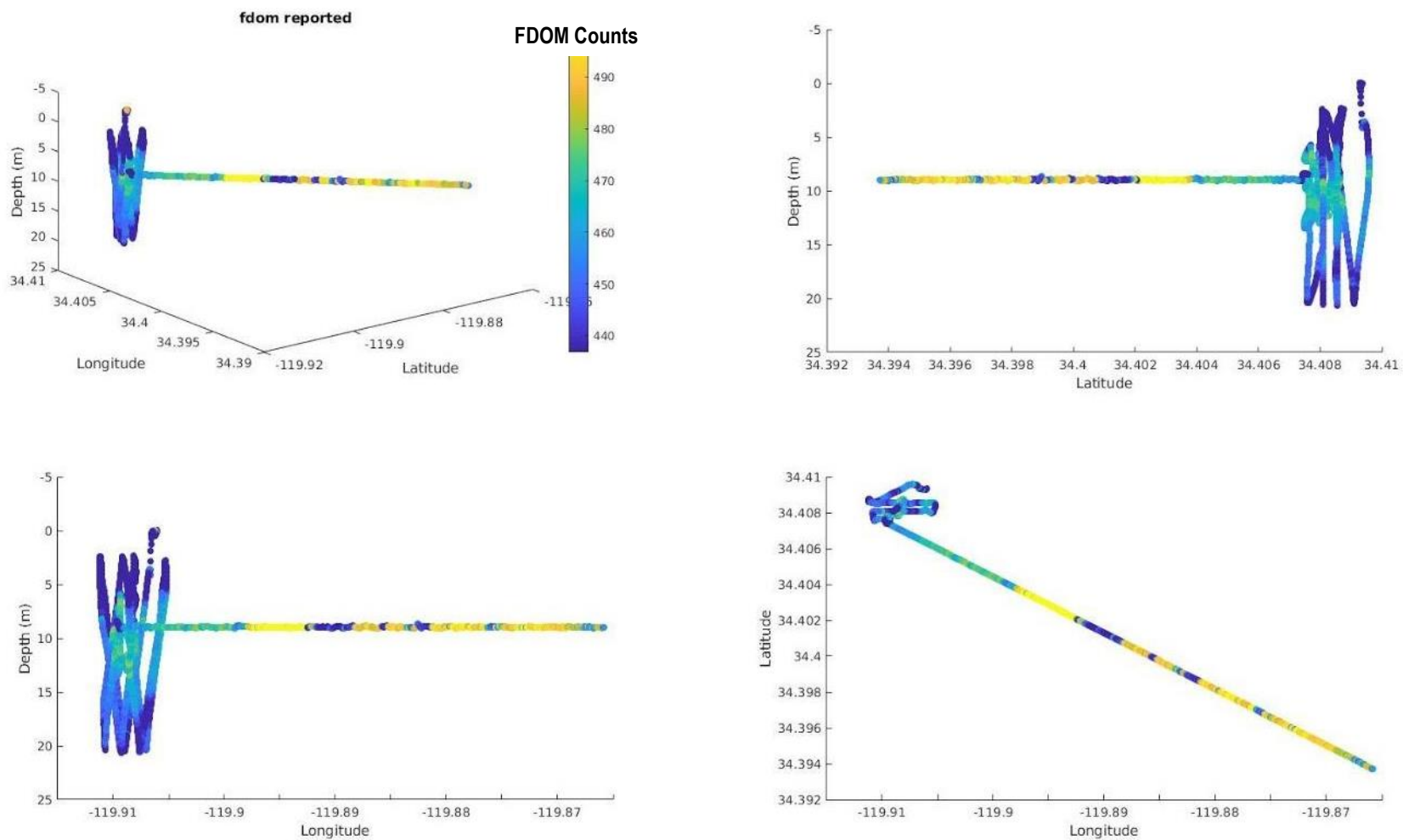
Figure 15. MATLAB visualization tool displays the reconstructed holographic image (left), alongside the vehicle path (center), and the droplet statistics (right) for an image from the second gulp of mission MSN007.
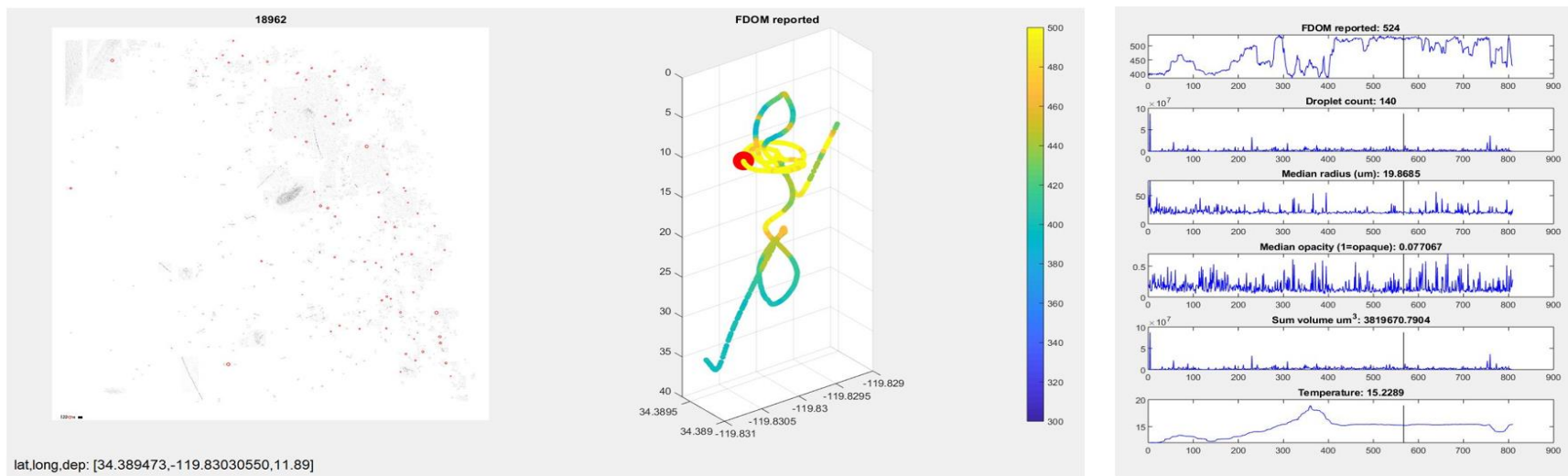
Figure 16. Plot from the VIP displays the raw FDOM count over the path of MSN007. These heat maps, which show the area the vehicle was programmed to search in meters, can be generated in near real-time.
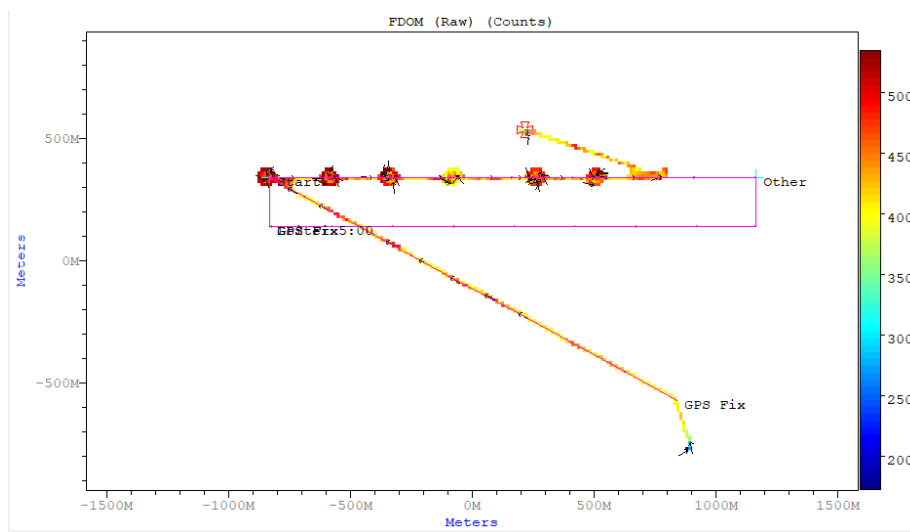
Finally, the Vehicle Interface Program (VIP) for the REMUS class of AUVs can produce near real-time heat maps using raw sensor data, which can be viewed by the onboard crew in near real-time to inform operations (Figure 16).

Following retrieval from the AUV, the SeaOWL, CTD, and DO Optode data were converted to standard units using the manufacturer's sensor calibration, and then merged. Data streams from the three sensors included conductivity, water temperature, and depth from the CTD sensor; CHL, FDOM, and OBS from the SeaOWL UV-A sensor; and DO concentration and DO saturation from the DO Optode. To merge the data from the three instruments, the data frequencies needed to be standardized. Specifically, the SeaOWL UV-A sensor collected data every 0.8 seconds, the CTD every 1.0 second, and the Optode every 1.2 seconds. To merge these datasets, the SeaOWL and Optode data were averaged by seconds and then joined to the CTD data using the collection seconds as the unique identifier. Since the sampling frequency of the Optode was less than the CTD sensor, every sixth second is missing in the Optode measurements. In the future, it is recommended that all sensors be set to the same frequency to simplify this merging process.

Once these three datasets were merged, plots and other data products were produced to aid in visualization and interpretation of the data. The resulting data products were then pushed to ERMA. Examples of the data products delivered to ERMA are provided and discussed in the case studies below (Section 4).

3.2   Slick Characterization by Remote Sensing

Water Mapping flew 14 UAS missions during the field testing (Figure 17). One mission was for tactical positioning; another five missions were for monitoring and surveillance, which also provided tactical positioning; and eight missions were for mapping missions. On the last day of UAS support (August 29, 2019), Water Mapping conducted a UAS mapping mission at the same time and covering the same footprint as REMUS-600 mission MSN016. Results from this synoptic sampling event are discussed as part of case study #3 in Section 4.

Figure 17. Overview of the footprints of all the UAS surveys.
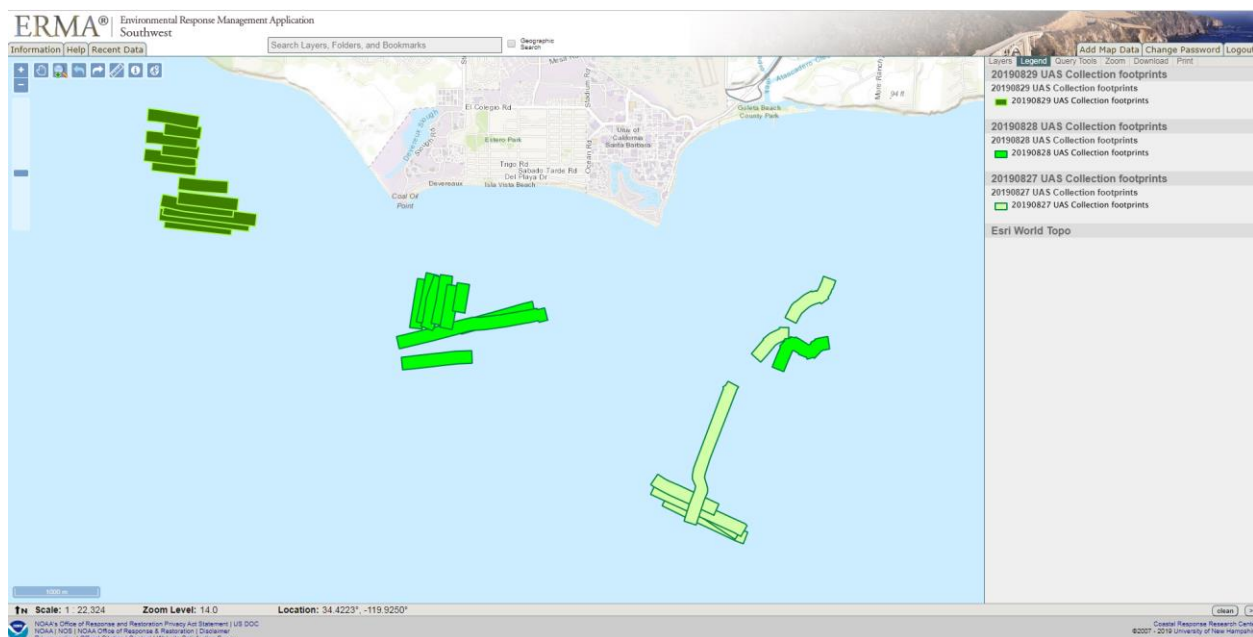
3.2.1   Real-Time Streaming of UAS Video

Over the three days Water Mapping participated in the field testing, Dr. Garcia flew five monitoring and surveillance flights, where high-resolution video from the UAS was streamed live to the internet. The real-time video displayed the high-resolution visible video on the right and the thermal video on the left, with a map showing the location and path of the UAS flight in the lower-left corner. In addition, flight statistics, date, time, and global positioning system (GPS) coordinates (decimal degrees latitude and longitude) were provided along the bottom. Figure 18 shows a screenshot of one of the videos streamed live on August 28, 2019. Table 4 contains a list of links with the real-time video transmisions.

During the field testing, UAS video was made available through ERMA in real-time. This was the first time this data delivery process was tested, demonstrating a method for quickly transferring data collected by the UAS to multiple responders and onshore operations during an oil spill response.

Table 4. Real time UAS videos

Date	Survey #	Start time (hh:mm:ss)	Duration (hh:mm:ss)	YouTube video title	YouTube link
8/28/2019	WM-RTM-01	10:56:00	00:07:45	Real-Time UAS Oil Spill Monitoring (test at Santa Barbara seeps) Test 1	https://youtu.be/UlHVgdb22kI
8/28/2019	WM-RTM-02	12:04:00	00:16:35	Real-Time UAS Oil Spill Monitoring (test at Santa Barbara seeps) Test 2	https://youtu.be/clU5burXi0l
8/28/2019	WM-RTM-03	15:28:00	00:13:01	Real-Time UAS Oil Spill Monitoring (test at Santa Barbara seeps) Test 3	https://youtu.be/qN5vA1RL7-s
8/29/2019	WM-RTM-04	11:06:00	00:11:05	Real-Time UAS Oil Spill Monitoring (test at Santa Barbara seeps) Test 4	https://youtu.be/zDXFilXfNTc
8/29/2019	WM-RTM-05	12:32:00	00:11:03	Real-Time UAS Oil Spill Monitoring (test at Santa Barbara seeps) Test 5	https://youtu.be/mprRzVORGLw

Figure 18. Live stream of high-resolution visible and thermal video collected by UAS. Bottom center shows the coordiantes and altitude of the aircraft. The left panel shows the visual camera and the right panel shows the thermal camera.
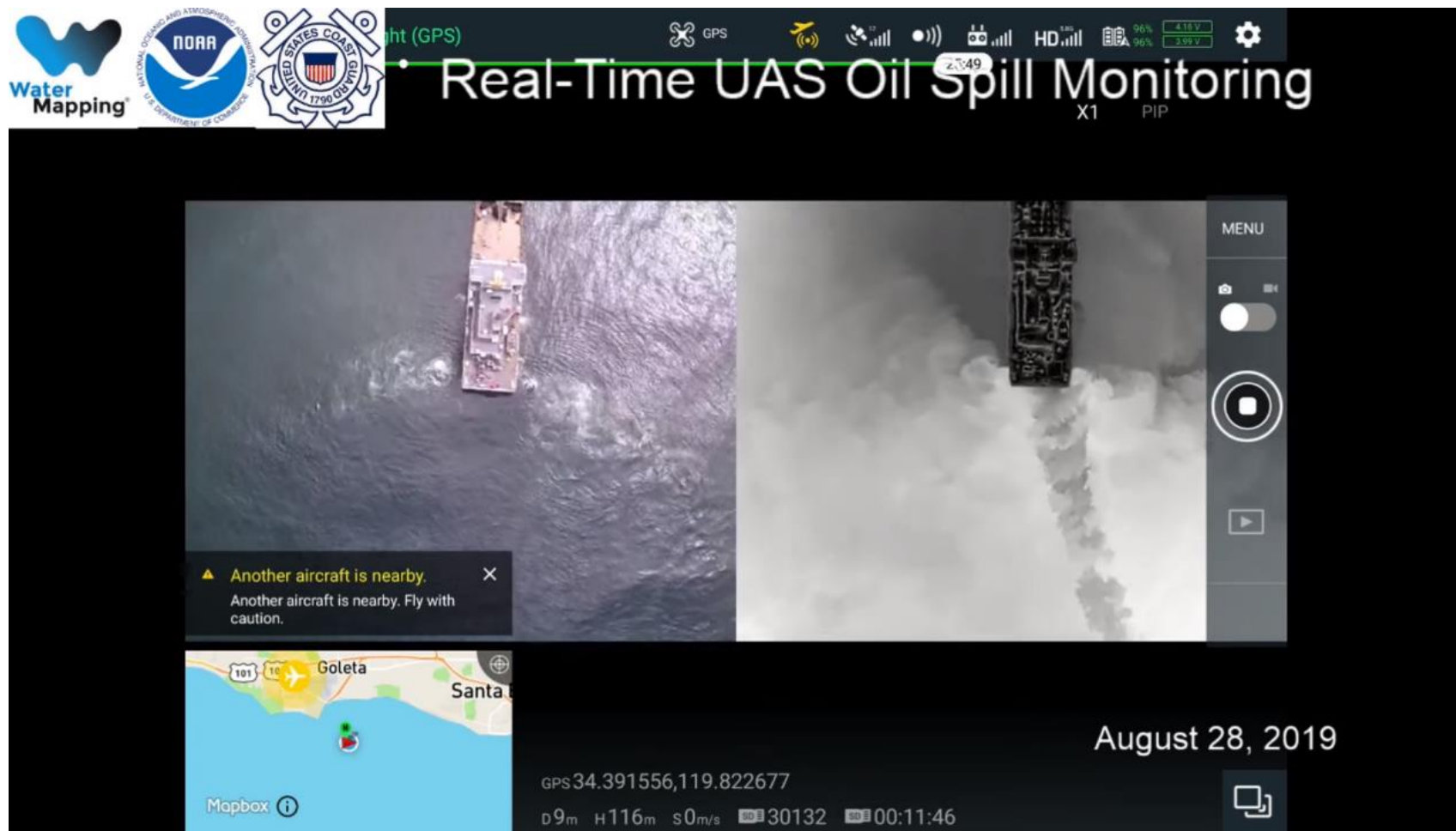
3.2.2   Mapping

Dr. Garcia also conducted eight mapping missions during the field testing at the Santa Barbara seeps. As described in Section 2.4.2, the data collected during these missions were processed using a previously developed algorithm to produce high-resolution maps. During the field testing, this process was conducted onboard the vessel, immediately after each UAS mapping mission, with a data product delivered to NOAA and the onboard AUV operations team within an hour. These maps could then be incorporated into ERMA (Figure 19) and into the AUV mission planning software (Figure 20) in near real-time.

While the overall delivery of these near real-time maps to ERMA and other platforms went smoothly during the field trials in Santa Barbara, review of the processing steps afterward presented areas where the processing could be improved. For instance, when importing the provided UAS geotiffs, the ERMA data management team struggled to remove the blank space surrounding the map. While it does not specifically impact the data presented, it was not ideal visually (see Figure 21, left). This problem can be fixed by formatting the no-data pixels so they have only one pixel value instead of two pixel values, as was done in the field. By ensuring the no-data pixels were set to one value, the data management team was able to set that particular pixel value as transparent, thus removing the blank space around the map (Figure 21, right).

3.2.3   Oil Thickness Classification

After completion of the field tests at Santa Barbara, Water Mapping generated oil classification layers for each map produced during the eight mapping missions. To generate the oil classification, Dr. Garcia applied a previously developed algorithm that generates a supervised classification of thicker, emulsified oil versus thin rainbow sheens. These oil classification maps can be used to understand locations with the thickest oil; they provide a spatial extent of the oil slick and can help with total quantity estimates of an oil spill. Figure 22 shows an example of the oil classification layer.

Figure 19. ERMA interface showing a collection of overlapping UAS flights. These maps were made available on ERMA in near real-time.
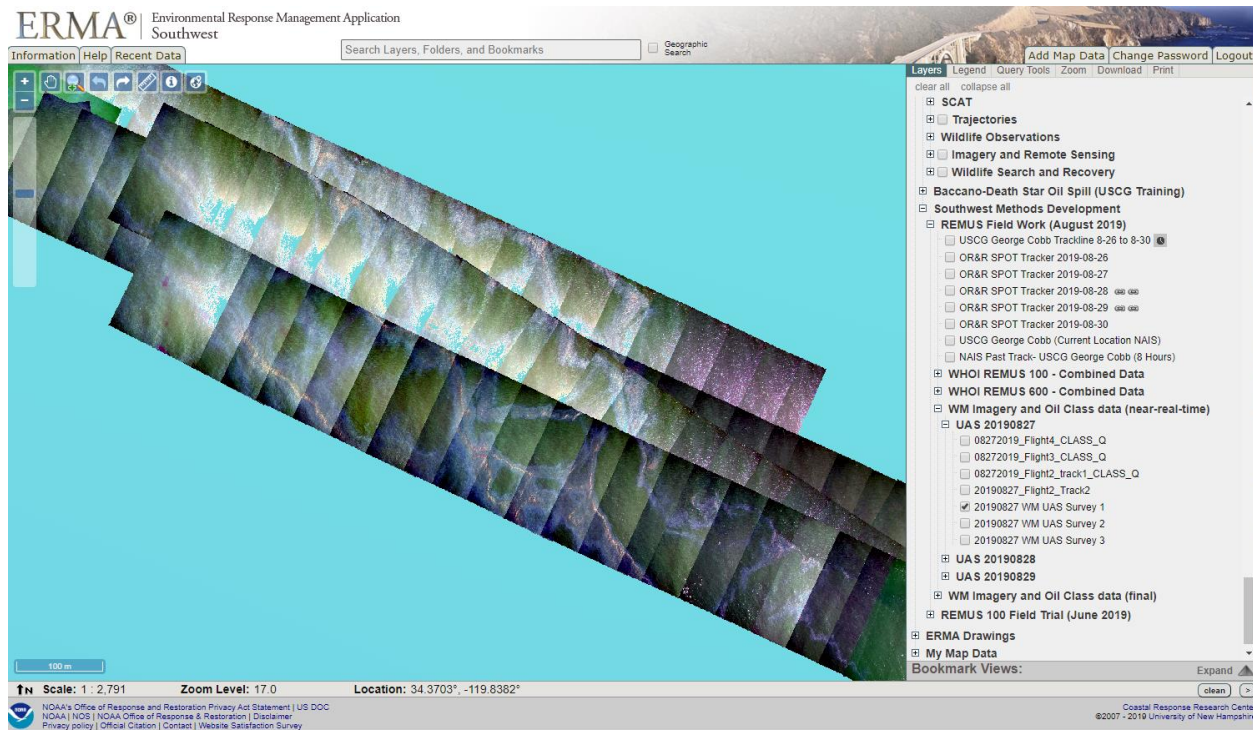
Figure 20. Example of a UAS track uploaded to the AUV mission planning software.
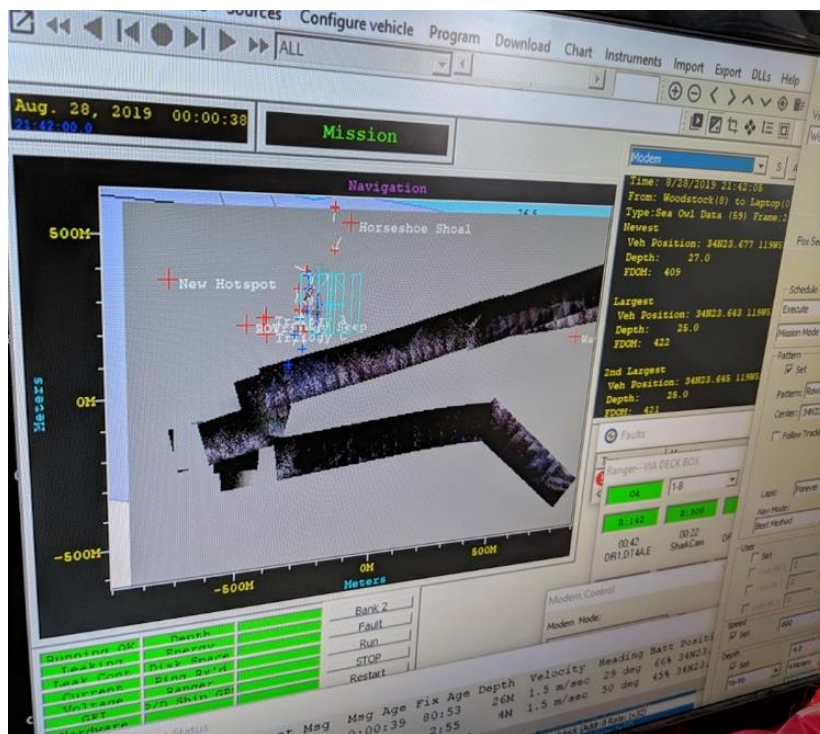
Figure 21. Original orthomosaic generated with two no-data values (left), and the newest version with only one no-data value and higher spatial resolution of approximately 7 cm (right).
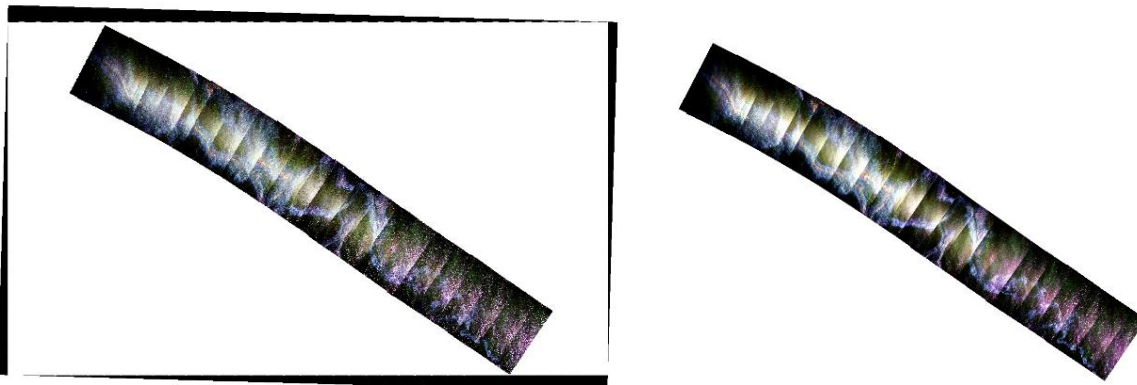
Figure 22. Example of oil classification layer.
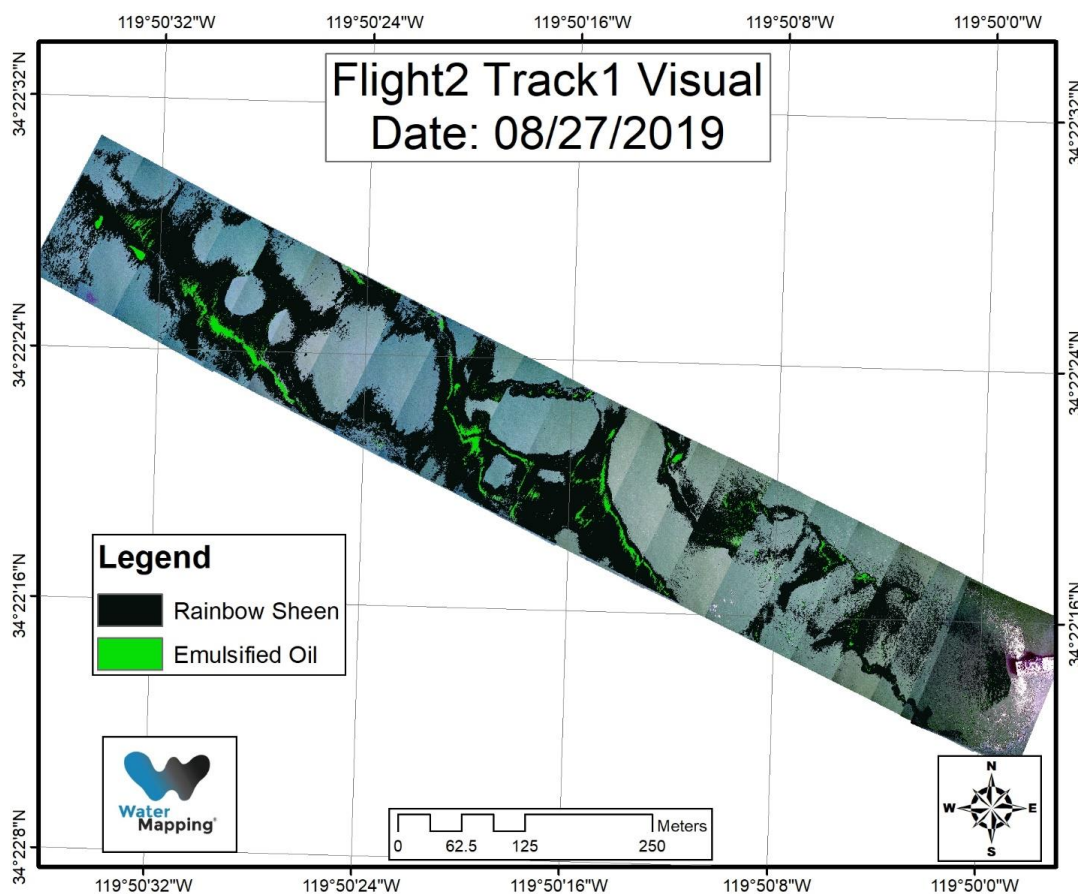
3.3   Data Delivery

An important achievement during this project was the development and demonstration of several near real-time data delivery methods for both AUV and UAS data. As shown in Table 5, typical turnaround times for delivery of most data were the same day, and often were within one–two hours of the data collection. This included delivery of SeaOWL data, which provided a 3D characterization of subsurface oil; and delivery of UAS data, which provided visual images and maps of surface oil. Other data, such as EK80 sonar data, were available the next morning and were useful in providing an overall snapshot of oil in the water column from the day before. The ability to deliver AUV and UAS data in near real-time allows responders to utilize the data to inform response decisions.

Table 5. Data delivery timeline and formats for AUV and UAS

Equipment	Instrument/ method	Data type collected	Raw data format	Delivery timeline	Processed	Processed data format
REMUS-600	SeaOWL	Fluorescence	Spreadsheet	Within 1–2 hours (caveat: REMUS must surface to download data to the web portal)	Yes	3D map of raw data (.jpeg and video), scatterplot (.jpeg)
REMUS-600	SeaOWL	Backscatter	Spreadsheet	Within 1–2 hours (caveat: REMUS must surface to download data to the web portal)	Yes	3D map of raw data (.jpeg and video), scatterplot (.jpeg)
REMUS-600	Sonde	Conductivity, water temperature, depth	Spreadsheet	Within 1–2 hours (caveat: REMUS must surface to download data to the web portal)	Yes	3D map of raw data (.jpeg and video), scatterplot (.jpeg)
REMUS-600	Camera	Video imagery	Video imagery	NA	No	NA
REMUS-600	Holographic camera	3D images	Images	1–3 weeks	Yes	Size distribution for single image, total number, and raw images
REMUS-600	Water Gulper	Sampling locations	Spreadsheet	Within 1–2 hours (caveat: REMUS must surface to download data to the web portal)	No	NA
REMUS-600	Water Gulper	Water chemistry	Spreadsheet	1–3 weeks	No	NA
REMUS-100	Echosounder	Sonar	Spreadsheet	24–48 hours	No	NA
UAS	Visible and infrared sensors	Real-time, high-definition video	Video imagery	Real-time	No	NA
UAS	Visible and infrared sensors	Visible and thermal infrared imagery with time, elevation, aspect, and off-nadir angle	Video imagery	< 24 hours	Yes	Ortho-rectified images

While the team was able to quickly process and post data to ERMA during the field testing at Santa Barbara, the data file sizes from the AUV and UAS were large and often the most time-consuming step was uploading the files from onboard computers to online platforms. From this exercise, it was apparent that one of the biggest obstacles to delivering data in near real-time during future oil spill response efforts will be the availability and speed of onboard internet connections. While NOAA's data management team, in collaboration with Abt and others, have evaluated several options for ship communications (especially with regard to remote locations in the Gulf of Mexico), continued efforts to identify and evaluate different options for onboard internet capabilities is needed to ensure field teams can support near real-time data delivery.

An additional need identified by the NOAA data management team is the development of a standardized checklist for each delivered product so the same types of information and data formats are delivered each time to more easily facilitate incorporation into the COP.

4. Case Studies

4.1 Case 1: Detection of Oil using CTD and SeaOWL Fluorometer Data

During two REMUS-600 missions, MSN003 (August 26, 2019) and MSN010 (August 28, 2019), oil and/or gas were detected near Coal Oil Point in the deepest part of the water column at 35 m below surface. For mission MSN003 southwest of Coal Oil Point, the onboard SeaOWL UV-A sensors detected elevated signatures of both FDOM and OBS, without a corresponding increase in CHL (Figures 23 and 24), a strong indication of oil in the water column. The holographic camera further supported the presence of oil droplets and/or gas bubbles in the water, detecting up to 40 spherical particles per image. The mean diameter of the particles was approximately 40 µm, with a median opacity of 13%. No water samples exist for this mission, so the data cannot be further confirmed with analytical chemistry.

For mission MSN010, southeast of Campus Point, the sensors detected an elevated OBS signal, with no corresponding increase in CHL and only a minimal increase in FDOM (Figures 25 and 26). The increase in OBS without an increase in CHL indicates the scattering is not the result of biological productivity. Furthermore, the small increase in FDOM compared to the increase in OBS suggests the increase is due to the presence of gas bubbles as opposed to oil droplets. Similar to mission MSN003, for MSN010 the holographic camera detected up to 63 spherical particles per image, further confirming the presence of gas bubbles in the water. Again, no water samples were collected during this mission, and therefore the data cannot be further confirmed with analytical chemistry.

Figure 23. Depth vertical profiles of OBS (left), FDOM (middle), and CHL (right) during mission MSN003. The CHL maximum is not coincident with elevated scattering of FDOM and OBS, suggesting anomalies at 30–35 m below surface (highlighted by grey box) are not from biological activity.
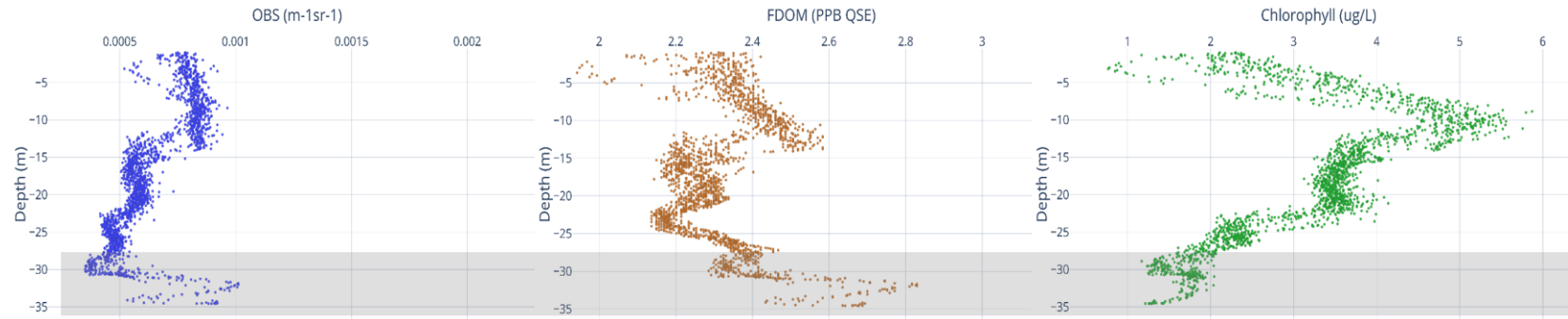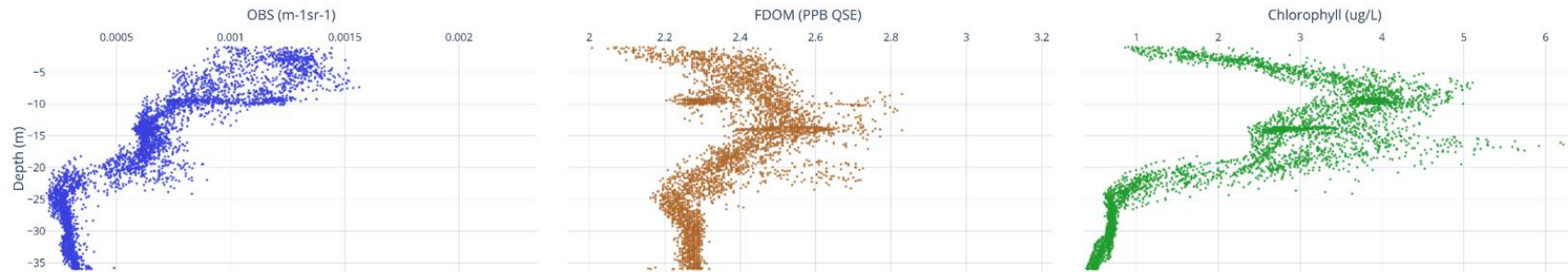
Figure 24. REMUS-600 vehicle track (top) and scatter plot of optical backscatter as a function of FDOM (bottom) for mission MSN003. For the scatter plot, CHL concentration is indicated by symbol size. Colors correspond to depth in the water column. Elevated FDOM and OBS between 30 and 35 m below surface (red circle symbols) suggest the presence of oil.
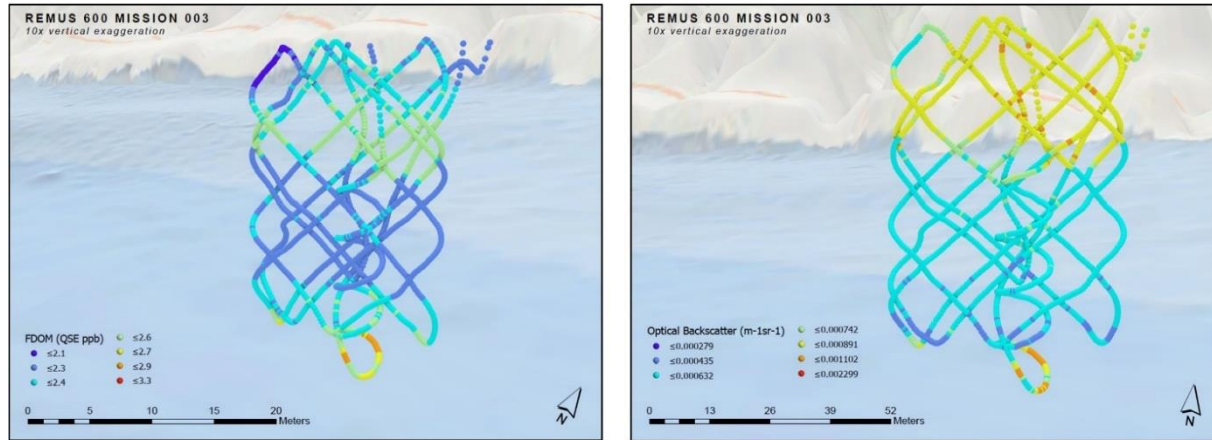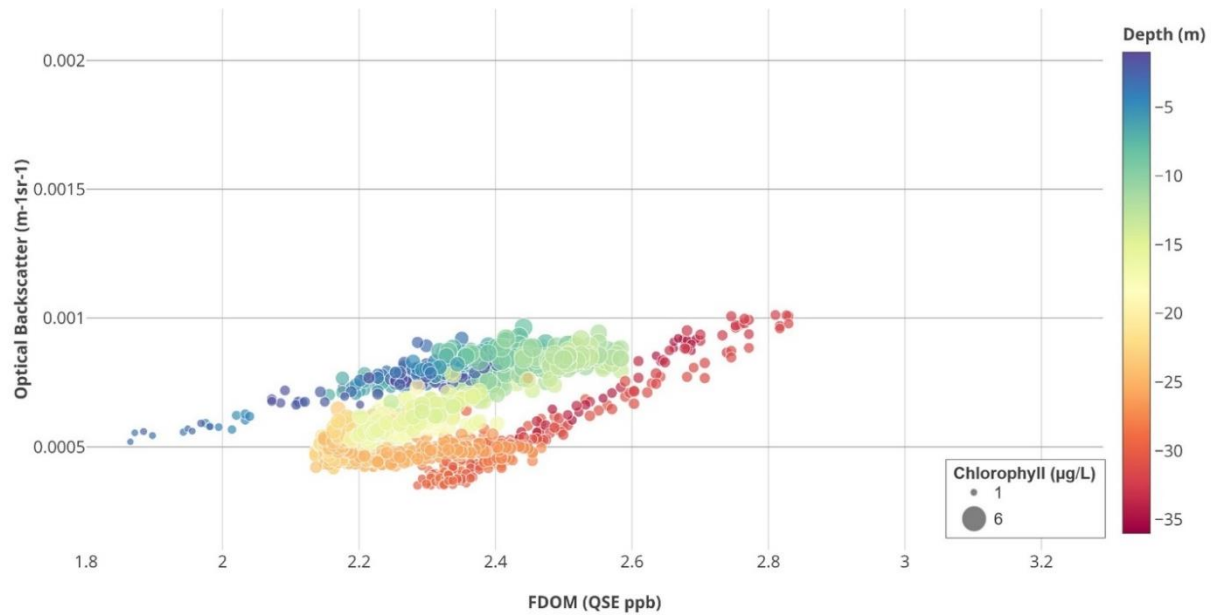
Figure 25. Depth vertical profiles of OBS (left), FDOM (middle) and CHL (right) during mission MSN010. The CHL maximum is not coincident with elevated OBS, suggesting anomalies at 35 m below surface (highlighted by grey box) are not from biological activity. Minimal increase in FDOM suggests the elevated OBS could be the result of gas bubbles as opposed to oil droplets.
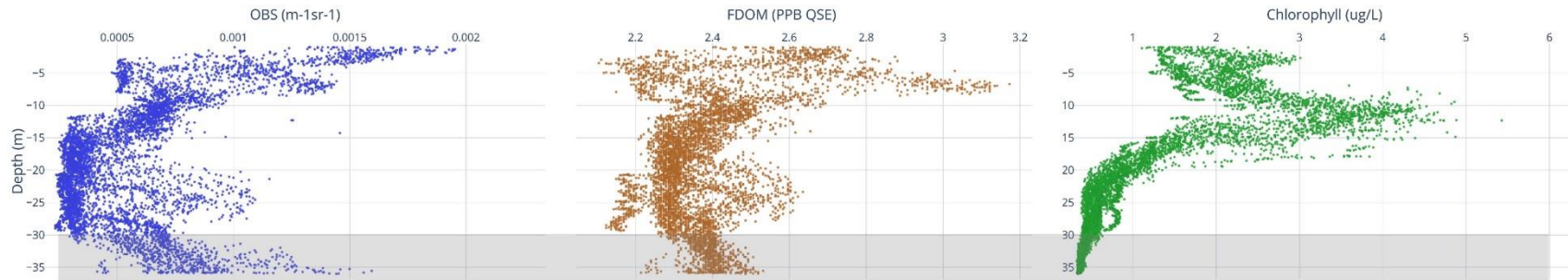
Figure 26. REMUS-600 vehicle track (top) and scatter plot of OBS as a function of FDOM (bottom) for MSN010. For the scatter plot, CHL concentration is indicated by symbol size. Colors correspond to depth in the water column. Elevated OBS between 30 and 35 m below surface (red circle symbols) with little CHL suggests the presence of gas bubbles.
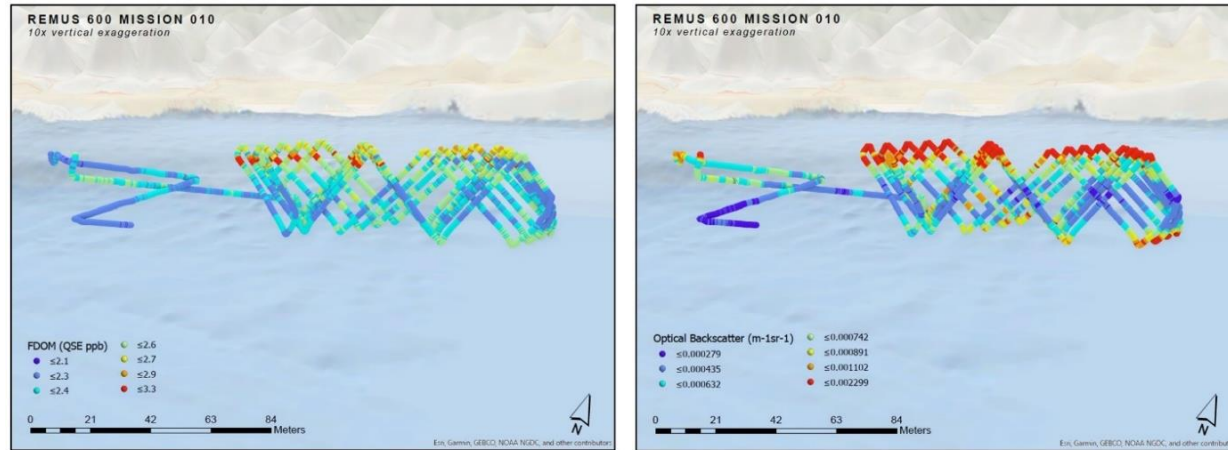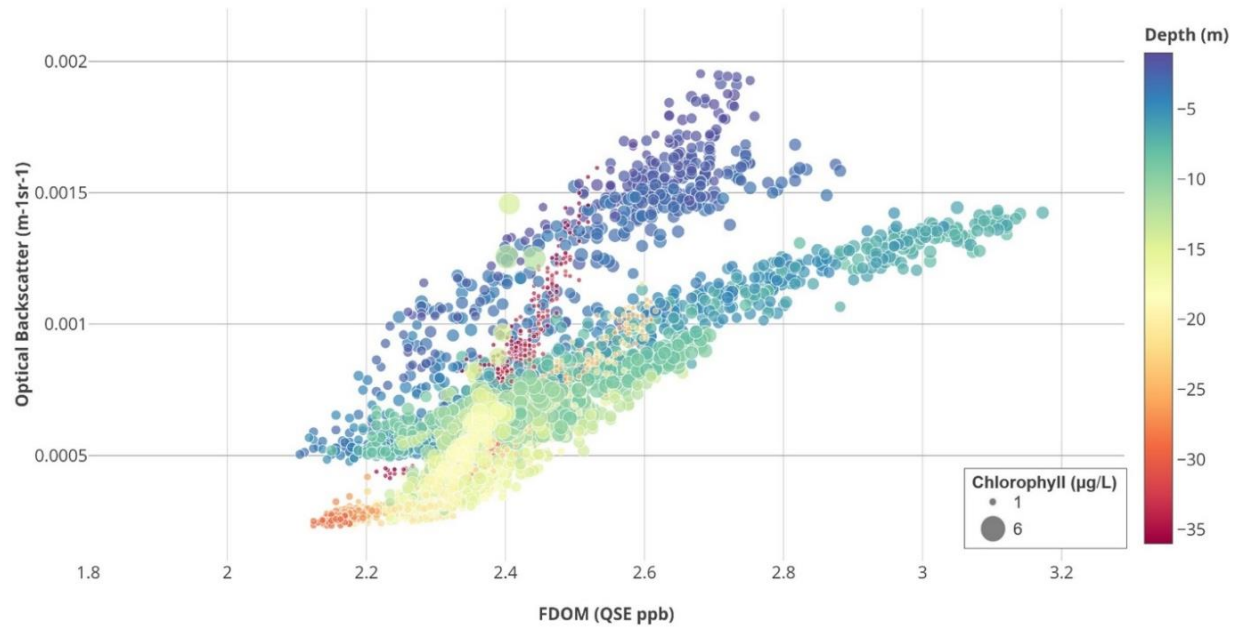
4.2 Case 2: Demonstration of AUV Adaptation and Gulped Water Samples

On our second day in the field (August 27, 2019), the team conducted two missions, MSN006 and MSN007, where samples were collected with the Water Gulper using the Circle/Spiral/Gulp Behavior, an adaptive behavior where the AUV runs a pre-set path and is programmed to return to the location of the highest FDOM reading within the path to collect a water sample.

During MSN006, the Water Gulper collected two discrete samples at depths of 9.7 m and 14.1 m. The scatter plot (Figure 27) and the vertical depth profiles (Figure 28) for MSN006 show the highest FDOM readings taken during the preprogrammed path of the AUV were taken from locations just under 10 m and just under 15 m below surface. When the preprogrammed track was completed, the AUV successfully returned to those two locations to collect samples with the Water Gulper. This demonstrates that the adaptive AUV behavior was able to successfully locate and sample locations with the highest measured FDOM during a mission.

The holographic camera data from MSN006 suggest that one of the FDOM maxima also had a high incidence of (near) spherical objects (likely oil droplet and/or gas bubbles), but the other did not. At the location of the first gulp, (near) spherical objects were present in the water column at an average frequency of 84 oil droplets/gas bubbles per image (see Table 3). This was the highest average number of droplets or bubbles detected during all of the gulped water samples. By contrast, at the second gulp location, an average of 34 droplets/bubbles were detected per image, which is one of the lower average frequencies (Table 3). This suggests that the elevated FDOM signal detected at the second gulp location was not from a high incidence of droplets/bubbles. One explanation for the differences observed between the FDOM and the holographic camera data at the second gulp location is that the oil existed mainly in a dissolved form, which would not be detected by the holographic camera, but would be detected by the SeaOWL. Additional research is needed to further evaluate and validate the oil characterization capabilities of the holographic camera.

For MSN007, the Water Gulper collected six samples, four between depths of 11 and 13 m and two at 20 m below surface. The scatter plot (Figure 29) and vertical depth profiles (Figure 30) show that the FDOM and OBS maxima occurred between 10 and 15 m for waters in this location, which was not coincident with the CHL maxima. This suggests that the elevated FDOM and OBS observed at these locations were likely not from biological activity. The holographic camera data show the presence of oil droplets/gas bubbles in the water column at each of the gulp locations for MSN007, but unlike the first gulped sample location from MSN006, none of the images from MSN007 contained anomalously high oil droplet/gas bubble values (see Table 3).

Finally, although the AUV successfully collected samples from areas of FDOM maxima, these maxima were relatively low, suggesting that oil concentrations in the water column, if present, were also low. The water chemistry confirms this FDOM observation, with TPH values under 0.1 mg/L. Unfortunately, the water used as blanks to prefill the gulper bottles and the DI water blank both had higher oil concentrations compared to many of the gulped samples, which makes the water chemistry collected during this project less reliable, but the data confirm that the petroleum concentrations were low. In future studies, the team may try to use DI water in all Water Gulper bottles, preferably Type I ultrapure DI water if available in the field, to reduce the chances of hydrocarbon detection in blanks.

Figure 27. REMUS-600 vehicle track (top) and scatter plot of optical backscatter as a function of FDOM (bottom) for mission MSN006. CHL concentration is indicated by symbol size. Colors correspond to depth in the water column. High FDOM and OBS between 10 and 15 m below surface suggest the presence of oil, confirmed by the discrete sample of petroleum oil in the water.
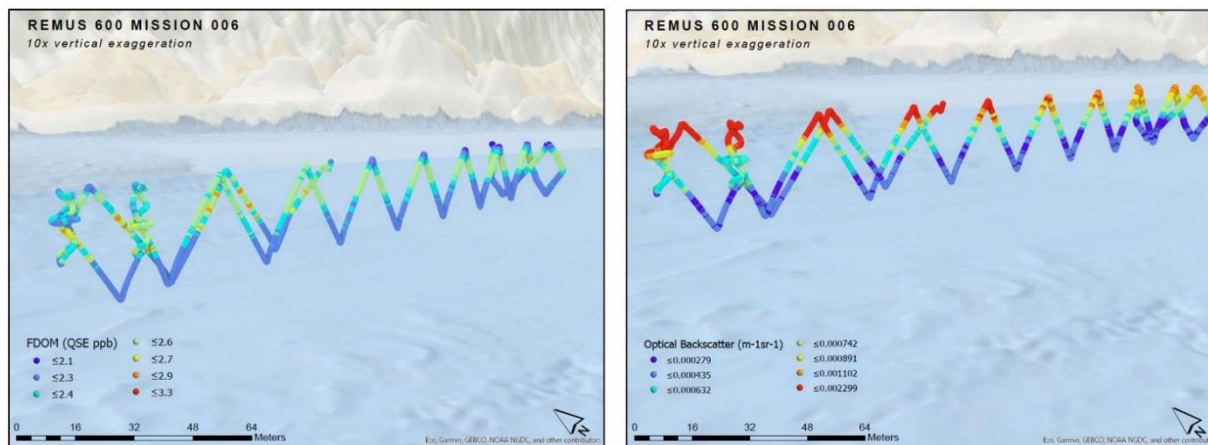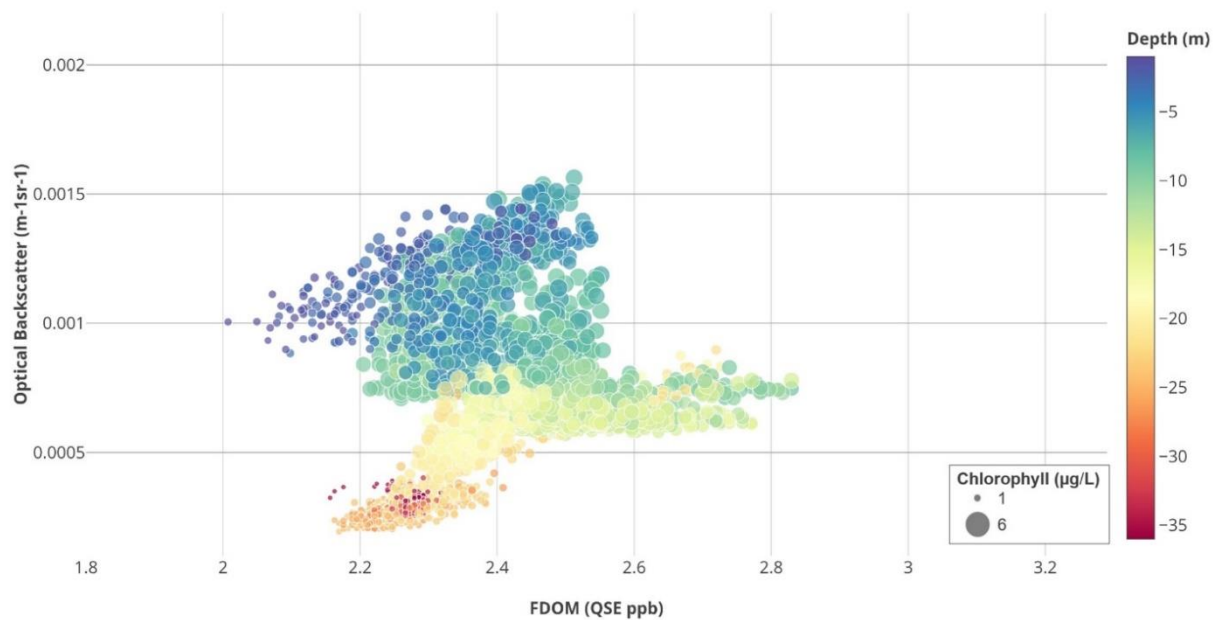
Figure 28. Depth vertical profiles of OBS (left), FDOM (middle), and CHL (right) during mission MSN007. The CHL maximum occurs between 5 and 10 m and is not coincident with elevated scattering and FDOM fluorescence, suggesting anomalies are not from biological activity below a depth of 10 m.

Figure 29. REMUS-600 vehicle track (top) and scatter plot of optical backscatter as a function of FDOM (bottom) for mission MSN007. CHL concentration is indicated by symbol size. Colors correspond to depth in the water column. High FDOM and OBS between 10 and 20 m below surface suggest the presence of oil, confirmed by discrete samples of petroleum oil in the water.
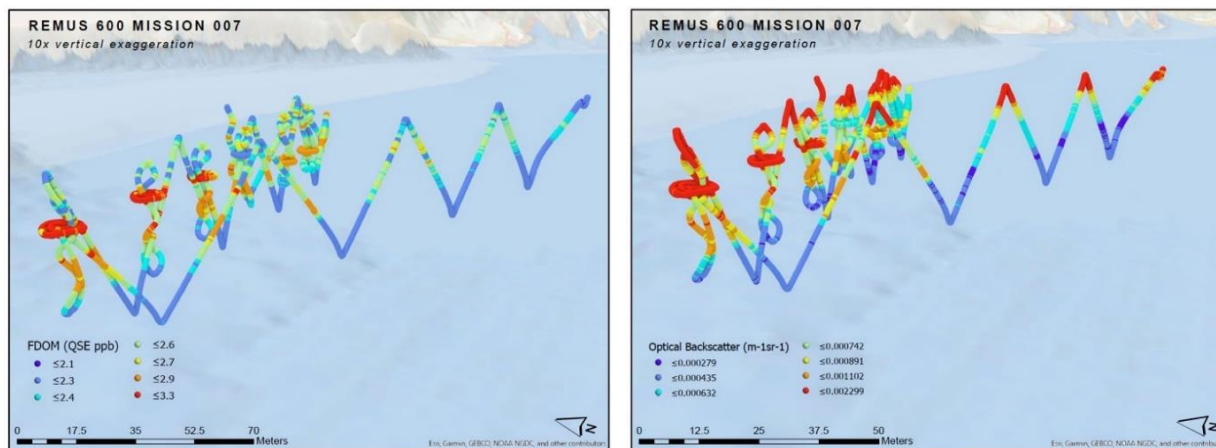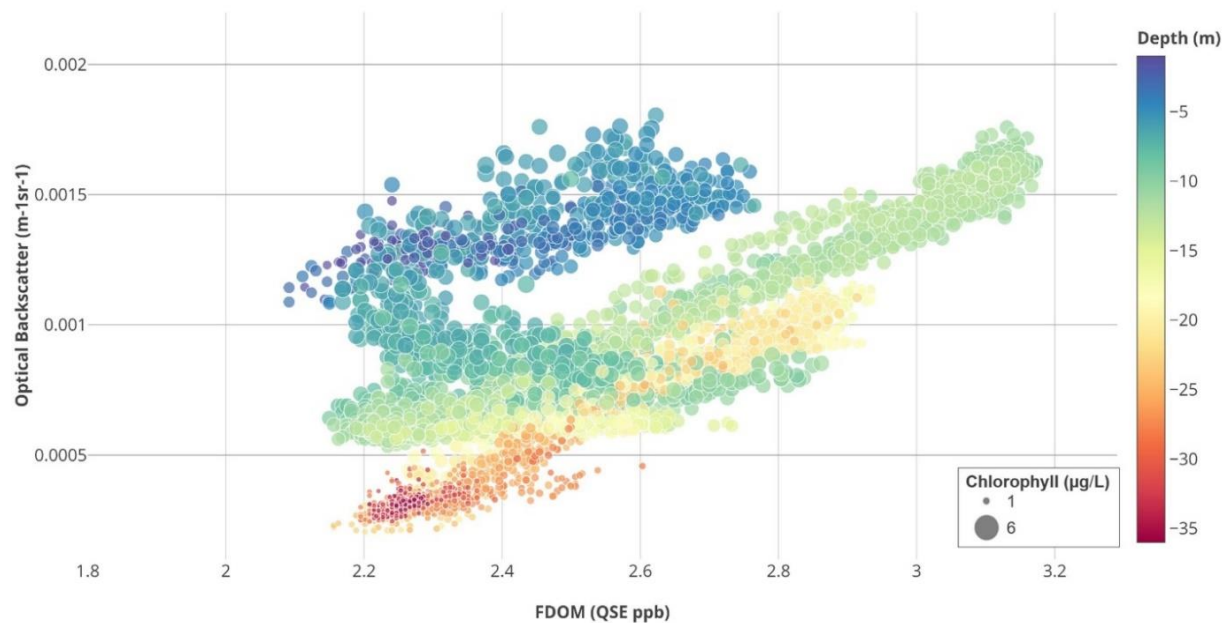
Figure 30. Depth vertical profiles of OBS (left), FDOM (middle), and CHL (right) during mission MSN007. The CHL maximum occurs between 5 and 10 m below surface and is not coincident with elevated scattering and FDOM fluorescence, suggesting anomalies are not from biological activity below depths of 10 m.
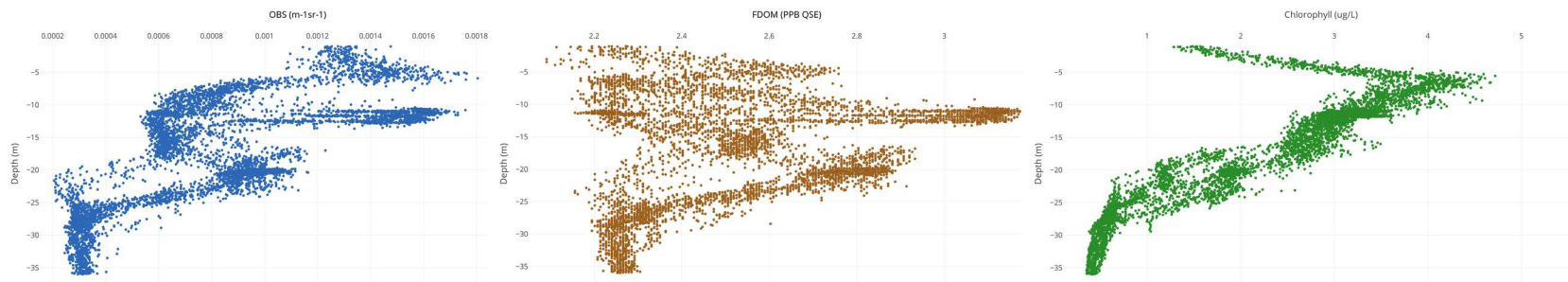
4.3   Case 3: UAS and AUV Synoptic Sampling

On the last day of UAS support (August 29, 2019), the UAS and AUV conducted synoptic surface mapping and subsurface sampling over an area southwest of Coal Oil Point during WM UAS Survey 2 and REMUS-600 mission MSN016 (Figure 31). The team conducted this synoptic sampling to practice coordination of the AUV and UAS technologies, and to demonstrate the suite of complementary data products that can be delivered both in near real-time and during post-processing by these two technologies.

During Survey 2 on August 29, 2019, the UAS captured the nature and extent of the surface oil in the area by producing ortho-rectified, high-resolution visual images of the water surface, which were delivered to ERMA within an hour of data collection (Figure 32). Following the field testing, Water Mapping used these high-resolution images to develop an oil classification layer, providing further quantification of the oil extent by classifying the oiling footprint into thicker emulsified oil or thinner sheens (Figure 33).

The REMUS-600 surveyed the area using a standard horizontal mow-the-lawn routine and vertical yo-yo pattern between 3-m and 20-m depths, followed by a mow-the-lawn routine at a set depth of 9 m. Similar to the UAS, within an hour of data retrieval from the AUV, the team was able to create and deliver FDOM, OBS, and CHL data products to ERMA (Figures 34 and 35). The FDOM 3D maps show where elevated FDOM occurs in the water column, and the corresponding plots with OBS and CHL measurements can be used to distinguish naturally occurring FDOM from hydrocarbon FDOM. Ultimately little oil was encountered in the water column during this mission (Figure 35).

Figure 31. UAS map of surface oil and the track lines for mission MSN016 from the REMUS-600, as delivered in near real-time to ERMA during the field testing.
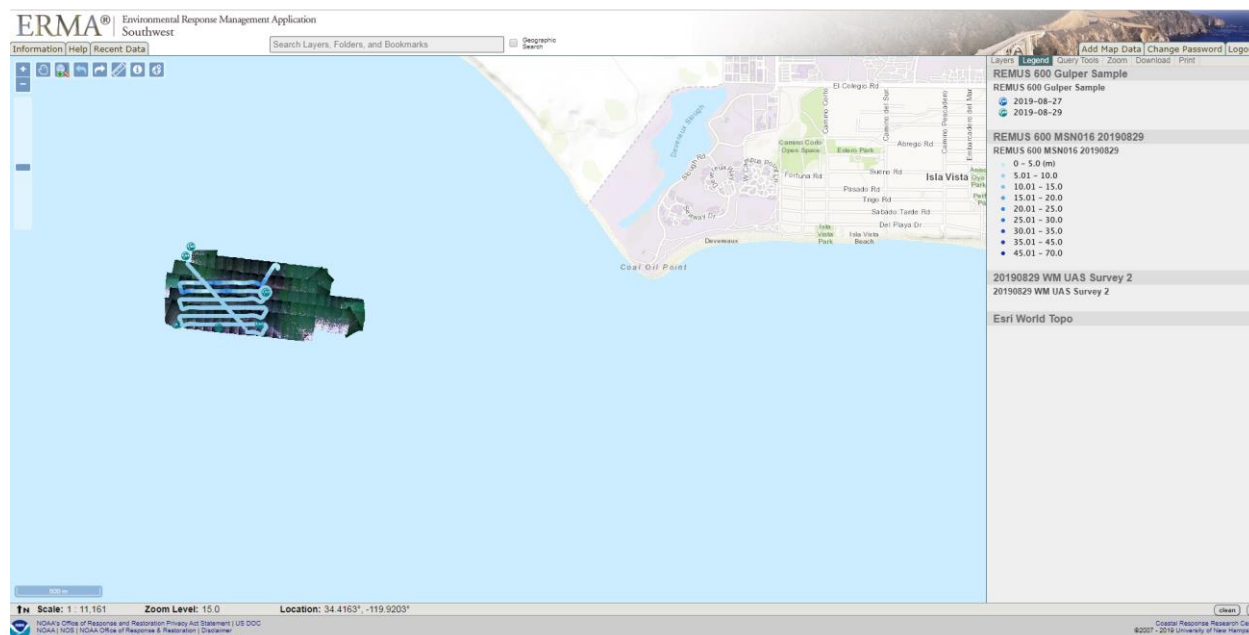
Source: ERMA.

Figure 32. High-resolution imagery from UAS Survey 2 conducted on August 29, 2019.
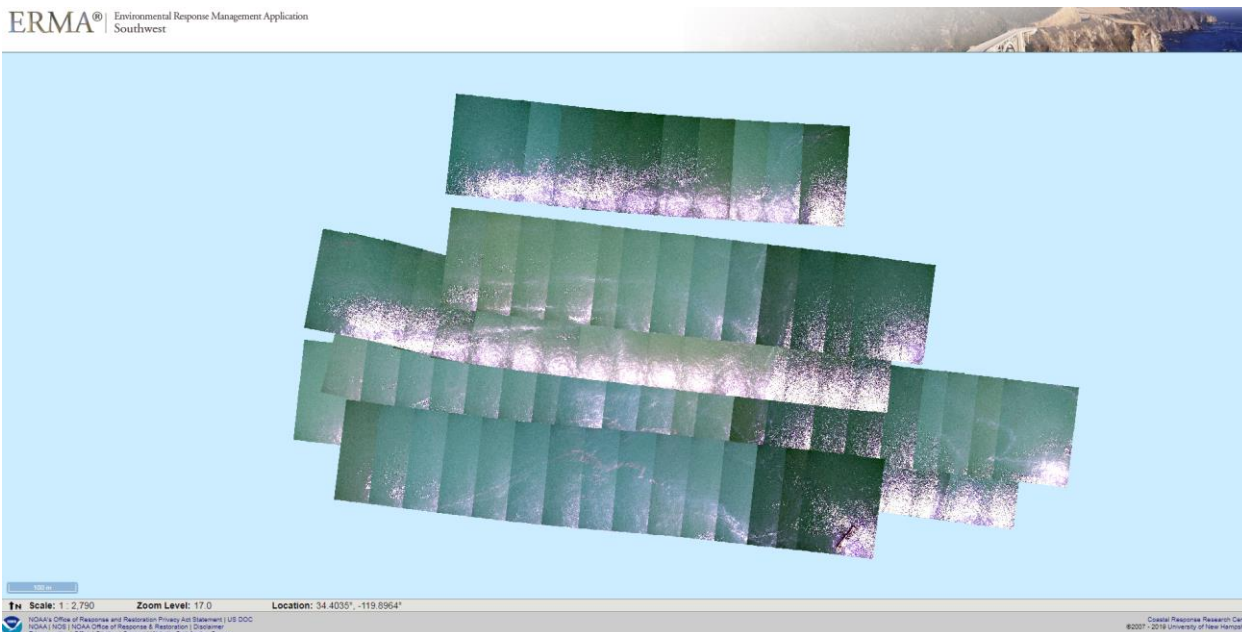
Source: ERMA.

Figure 33. Oil classification layer showing oil slick extent for UAS survey 2 conducted on August 29, 2019. Dark brown represents the thicker, emulsified oil; and light tan represents thinner sheens.
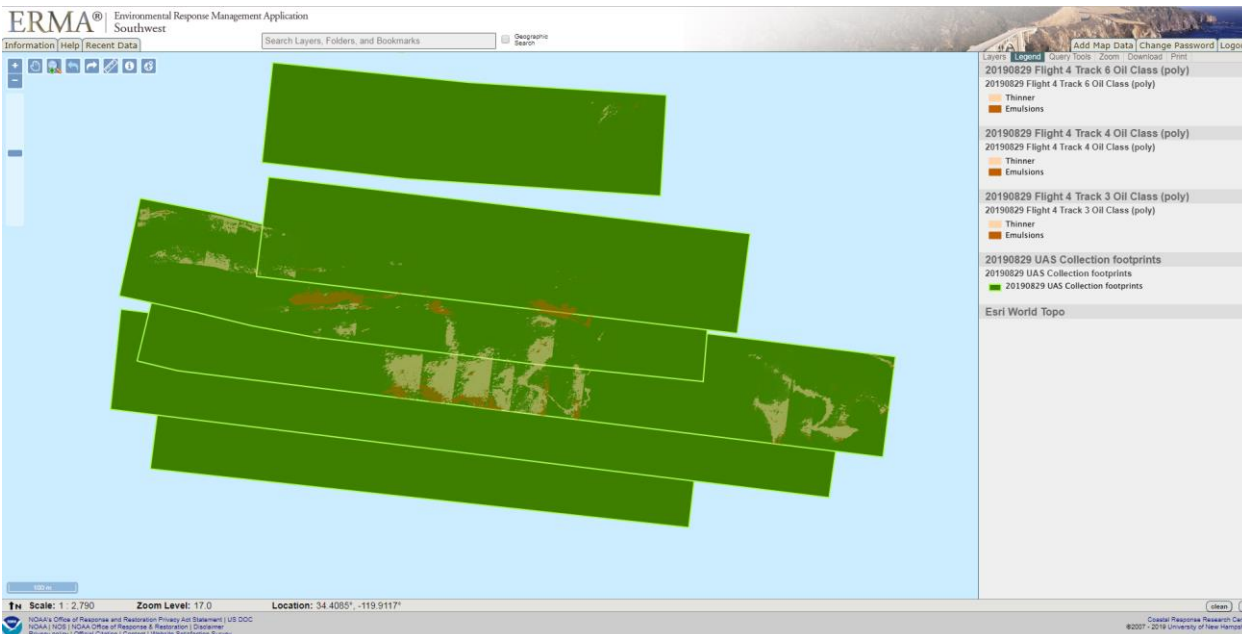
Source: ERMA.

Figure 34. FDOM and OBS measurements along the REMUS-600 vehicle track (top) for mission MSN016. Colors correspond to concentration. The scatter plot (bottom) shows OBS as a function of FDOM. CHL concentration is indicated by symbol size. Colors correspond to depth in the water column.
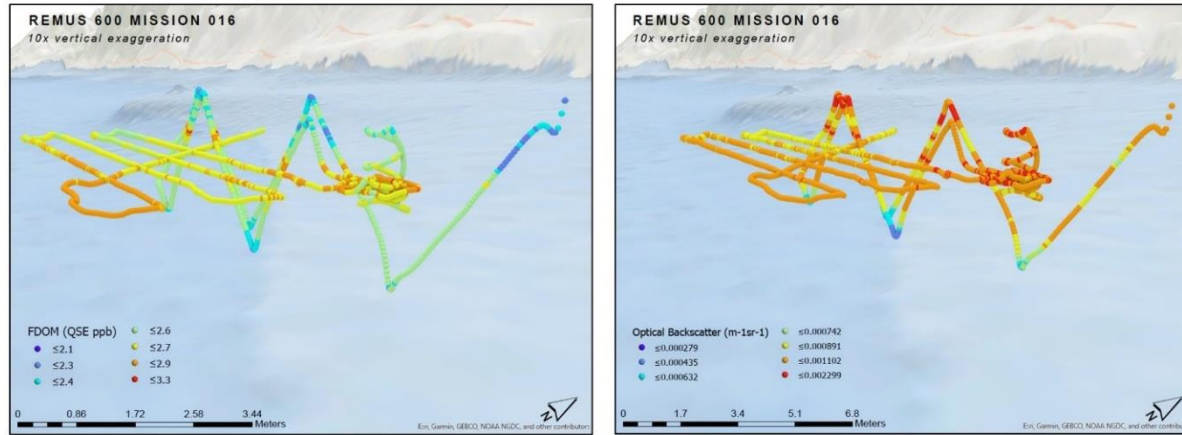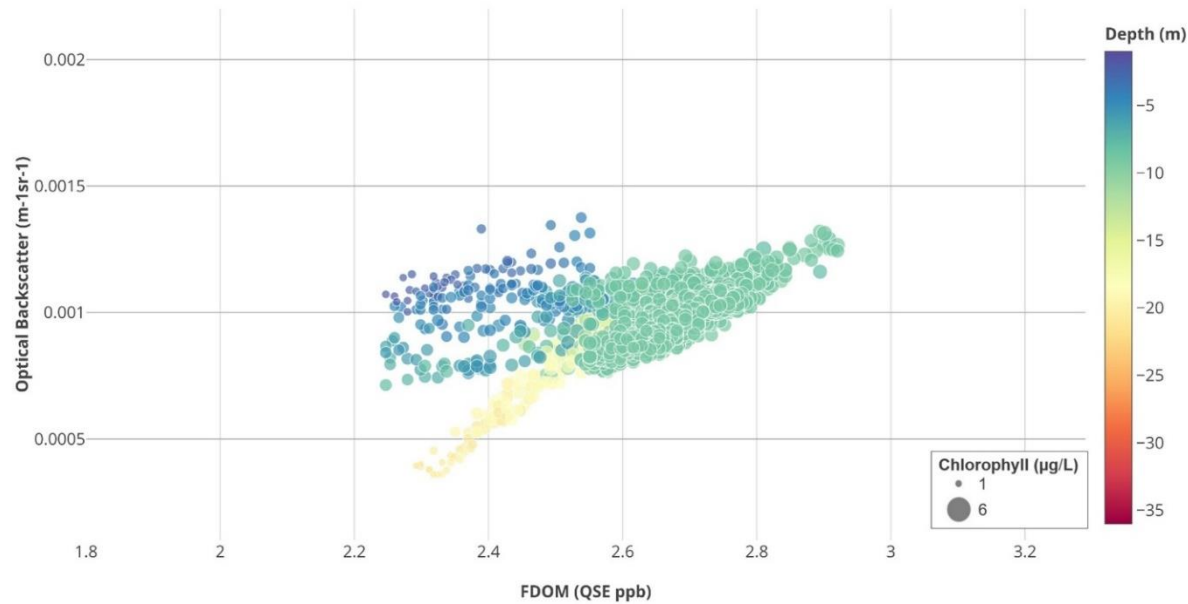
Figure 35. Depth vertical profiles of OBS (left), FDOM (middle), and CHL (right) during mission MSN016.
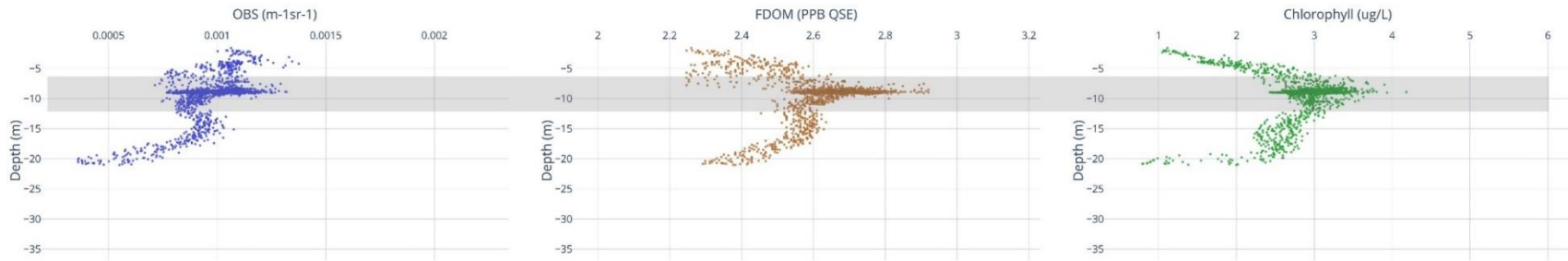
Following the field testing, WHOI processed the holographic images from select locations during each mission, which provided summary statistics on the oil droplet and/or gas bubble number, size distribution, and total volume detected in each image. In addition, EPA analyzed all water samples for BTEX, PAHs, and alkanes. These data provide additional confirmation of oil in the water column, and can also be used to develop an in situ calibration of the FDOM data.

Overall, the case study shows how the cooperation between AUV and UAS technologies can help to better inform estimates of the quantity of oil spilled by providing simultaneous information on the quantities of oil both on the water surface and beneath the surface. In addition, a combined dataset may improve our ability to estimate the nature and extent of the spilled oil throughout the ocean environment, and provide an understanding of how surface and subsurface oil relate to one another.

5. Summary and Recommendations

During and after an oil spill, responders and NRDA practitioners are seeking answers to four key questions:

- What is the nature and composition of the spilled material?
- How much material spilled?
- Where did it or could it go?
- What resources are in its path?

Answers to these questions help inform decisions regarding how and where to respond, provide an estimate of the quantity of oil spilled, and inform the nature and extent of the exposure and harm to natural resources. This study has made strides in providing responders and NRDA practitioners with additional tools and capabilities for collecting data that help address these questions. Furthermore, the study has helped improve data processing, transfer, and visualization methods to deliver the data in a format and within a timeframe that is useful to oil spill response decisions.

5.1 Project Summary

The primary purpose of this project was to develop AUV technologies and test them in an open ocean environment to improve our ability to leverage these technologies during oil spill responses. In particular, the research team at WHOI equipped a REMUS-600 with a standard set of oil characterization sensors in addition to two new oil sensing capabilities: a holographic camera and water sampling. For the new sensor, WHOI adapted a miniaturized holographic camera so that it could be mounted to a newly designed, front-end nose cap of the REMUS-600. For the water sampling, WHOI developed a new, large volume water sampler capable of collecting six 1-L samples per modular section. The samplers were designed to be modular, such that multiple samplers could be linked, allowing a user to increase or decrease the sampling capacity on the REMUS-600 as needed. To support the water sampler on the REMUS-600, WHOI also developed two new AUV behaviors that provide different approaches for collecting water samples.

In conjunction with the AUV developments, the research team also developed new data products to help visualize and interpret the data collected by the REMUS-600, as well as methods for transferring and processing the data so that these products could be made available to responders

and the COP in near real-time. The team tested these new AUV capabilities, software developments, and methods for data processing and visualization during a field effort conducted during August 26–30, 2019 at the natural seeps near Santa Barbara, California.

Finally, during the field efforts, the team tested newly developed methods for real-time delivery of UAS video and near real-time delivery of UAS visual image maps to ERMA and other operational platforms. We also practiced and demonstrated synoptic data collection by both the AUV and UAS.

5.2   Tools and Capabilities Developed

5.2.1   AUV Developments

During this project, the research team developed the following components, tools, and capabilities for use of AUV technology to detect and quantify oil in the water column:

- A new endcap that can be used on any REMUS-600 that includes wiring for all the front-end science sensors

- A nose section for the REMUS-600 that houses the holographic camera and a GoPro camera

- New AUV behaviors for detecting potential oil in the water column and collecting water samples at those locations

- Two Water Gulper payload sections with syntactic foam and frames

- Fourteen modular Water Gulper samplers complete with circuitry, pumps, cabling, and bottle plumbing

- A Water Gulper assembly and maintenance document (see Appendix B).

5.2.2   Data Processing and Visualization Developments

In addition, the team developed several new methods for data processing and visualization, including:

- A MATLAB interface for viewing data such as FDOM, CHL, and oil droplet distribution from processed holograms and .CSV files with hydrocarbon, temperature, salinity, and position/time data for quick upload to NOAA's COP, ERMA, and their data repository DIVER (Data Integration Visualization Exploration and Report)

- A holographic image classifier for post-mission analysis

- An improved process for delivering UAS high-resolution maps to ERMA in near real-time

- A new process for delivering a live video feed of high-resolution visible and thermal video to ERMA, which can be viewed by Incident Command in real-time.

5.2.3   Operational Readiness Improvements

Finally, as part of the field testing efforts, the team furthered the operational readiness of AUV and UAS technologies. Specifically, during the field efforts the team:

- Tested a full suite of sensors and capabilities for oil characterization, demonstrating how the AUV and sensors work in an open ocean environment

- Practiced planning and implementing REMUS AUV missions for oil characterization, including deployment of the AUV, AUV trouble-shooting, and coordination with a UAS for data collection.

5.3   Recommendations for Future Work

This study demonstrated how a holographic camera can provide important information in the detection and characterization of oil in the water column. However, due to the large amount of data collected and the process by which operators retrieve that data, the holographic camera did not provide (near) real-time information. Future work should include the exploration of real-time techniques for the evaluation of holographic camera images so that data may be conveyed in real-time over acoustic communications (i.e., ACOMMS) in order to inform the operator in real-time about what the camera is seeing. This would require adding an ethernet connection from the camera to the AUV such that images can be transmitted and processed in the computer backseat. Additional code is also needed to provide targeted reconstruction, and the workflow needs to be improved so that less sifting of images is required, saving time.

In addition, development of new, more nimble AUV behaviors for triggering the water sampler could provide researchers with more options and help them use the sampler more effectively. Specifically, we recommend that a new AUV behavior be developed that incorporates a shorter, more rapid adaptation to gulp based on detection of large anomalies. Such a new behavior may better handle the high spatial and temporal variability that is typical of oil in the water column.

For data delivery, it was clear during the field testing that we were pushing the limits of our current abilities to collect, process, and deliver data in the field. Continued efforts to streamline the processes developed during this study can improve the time it takes to deliver data to the COP.

Additional work is also needed to better understand how data from the different sensors can inform oil spill response and assessments. For example, we have not yet developed standard protocols for the interpretation and use of data from the holographic camera. Future missions could include development of better protocols and data products that integrate data across all sensors, including the holographic camera.

Finally, this project included a single field trial in relatively shallow waters off the coast of Santa Barbara, California. We selected this area because of the natural oil seeps, which provided us some ability to test our suite of oil characterization sensors. However, these tests were not able to demonstrate the ability of the AUV and sensors to operate in deep ocean waters such as those in the Gulf of Mexico where oil drilling operations are prevalent.

All of the data collection devices attached to the REMUS-600 (which is rated to operate at a maximum depth of 600 m) were designed to tolerate greater depths. In its current state, the holographic camera is rated to operate at depths up to 1,000 m. With a new housing, the holographic camera's depth rating could be increased. The Water Gulper was matched with the REMUS-600 for depth rating, but with the addition of pressure-tolerant electronics, it could be

tested at depths of 6,000 m or deeper. Although the parts used in this mission are expected to withstand higher pressure, pressure tolerance of such a complicated assembly is not guaranteed.

Furthermore, both the Water Gulper and holographic camera can, and have been, integrated into remotely operated vehicles (ROVs). For example, in June 2019 the WHOI team tested the miniaturized holographic camera in the field using a blue robotics ROV. This integration requires the proper mounting hardware and potentially additional software development to interface these data collection devices to the vehicle. For the Water Gulper, the AUV behaviors developed for the REMUS-600 to trigger sampling would not transfer to an ROV. However, for an ROV it is assumed that the operator would make the decision as to when to sample, and thus these autonomous behaviors would not be needed.

For future deepwater testing, we suggest the following two options:

1. Attach the existing equipment (with higher-rated housing as necessary) to an ROV that is rated to operate at depths up to 6,000 m and conduct a research mission with the primary aim of determining whether the equipment will withstand the pressures at those greater depths. If any equipment fails, we will deconstruct the failed equipment, determine the cause of failure, and redesign as necessary.

2. Conduct laboratory pressure chamber testing of specific sensors at WHOI. These pressure chambers can simulate pressure at depths of 6,000 m. While no laboratory simulation can entirely replicate conditions in the field, at a minimum we would be able to verify that sensors and sampling equipment can withstand those pressures and still operate before attempting to use the equipment in the field.

Ultimately, additional testing at other locations may be warranted to further develop the water gulper and holographic camera capabilities and address these data gaps.

References

Abt Associates. 2018. *Deepwater Horizon* Lessons Learned – Methodology and Operational Tools to Assess Future Oil Spills. Available: https://www.bsee.gov/sites/bsee.gov/files/research-reports//1079aa1.pdf. Accessed 12/18/2019.

Conmy, R.N., P.G. Coble, J. Farr, A.M. Wood, K. Lee, S. Pegau, I. Walsh, C. Koch, M.I. Abercrombie, M.S. Miles, M. Lewis, S. Ryan, B. Robinson, T. King, C. Kelble, and J. Lacoste. 2014. Performance of submersible fluorometers exposed to chemically-dispersed crude oil: Wave tank simulations for improved oil spill monitoring and evaluation of *Deepwater Horizon* spill measurements. *Environmental Science and Technology* 48(3):1803–1810.

Farrell, J.A., S. Pang, W. Li, and R. Arrieta. 2003. Chemical plume tracing experimental results with a REMUS AUV. September. In *Oceans 2003. Celebrating the Past ... Teaming Toward the Future (IEEE Cat. No. 03CH37492)* (Vol. 2, pp. 962-968). IEEE.

White, H.K, R.N. Conmy, I.R. MacDonald, and C.M. Reddy. 2016. Methods of oil detection in response to the *Deepwater Horizon* oil spill. *Oceanography* 29(3):54–65.

A. AUV Software Development

This appendix provides details on the software developments of two new AUV behaviors designed to trigger gulping (i.e., water sampling) by the Water Gulper on the REMUS-600.

A.1 Circle/Spiral/Gulp Behavior

A.1.1 Overview

The Circle / Spiral / Gulp behavior runs on the backseat 'autonomy' computer during a normal mission and will interrupt the vehicle when it finds something of interest. The interest is expressed as an elevated FDOM reading in regards to a baseline of the environment. Circle / Spiral / Gulp is suited more for exploratory missions when it is unsure as to what will be encountered.

The approach for this behavior is to define the vehicle mission plan in the REMUS VIP to explore an area with the requisite pattern, depth control, and speed, then have the backseat decide where it is worthwhile to take water samples.

A.1.2 Vehicle Setup

The crucial piece in setting up the vehicle is the control of RECON per objective. The mission plan shall have a transit to the survey which does not allow RECON, followed by a survey objective that shall allow RECON. This allocates time during the initial run-up to create a baseline of the environment. This baseline informs the backseat's search for elevated FDOM readings within the survey.

Here is an example navigate rows survey that is doing Yo-Yo depth control. As can be seen the Navigate objective between Start and WP1 has the setting "Allow RECON control" equal to "No" while the Navigate Rows objective has the setting "Allow RECON control" equal to "Yes." This pattern can be repeated numerous times within the same mission plan.

Figure A.1. A standard navigate rows mission is offset from a start point and then moves through a lawnmower pattern.

A.1.3 Backseat Computer Setup

While the backseat configuration files provides a lot of flexibility in how the vehicle will respond, once configured the settings will remain fairly consistent throughout a deployment. The exceptions to this would be if the vehicle operator wishes to select a different behavior or toggle on/off gulper sampling.

The editable seek_oil.ini file found on the backseat computer primarily deals with the Circle / Spiral / Gulp behavior as this is the more complex task. The following will detail each relevant section for this behavior.

A.1.4 Trigger

The Trigger section defines the conditions in which the backseat will interject with front seat operations. The thresh_inflate value determines how much greater a FDOM reading must be in order to trigger the behavior. This FDOM reading must also be within the thresh_min and thrsh_max value to satisfy the triggering requirements. Once an elevated location is found and the behavior is tripped, the operator can determine secondary limits to determine whether or not to take a water sample. Using gulp_sample_thresh sets another level of requirements that must be met in order to sample. Lastly, gulping can be entirely shut off by using the gulp_sample_on variable.

A.1.5 Circle Action

The Circle Action, Spiral Action, and Gulp Action sections all detail out the same variables as they are defining the parameters of a RECON Circle action. They are just being utilized in different ways. The circle action is meant to detail out a cylinder searching pattern sampling at multiple depths to find the depth in which contains the highest FDOM read outs. This part of the behavior will update the depth that the spiral and gulp will take place at.

```
[CIRCLE ACTION]
circle_radius = 20.0
radius_rate = 0.0
direction = CCW
revolutions = 1
# 'same' to use current speed or enter number
velocity = 2
# units = [knots, m_per_s]
velocity_units = knots
# depth_mode = [constant_depth, constant_altitude, triangle_depth]
# 'constant_depth' = [depth(meters), min_altitude(meters)]
# 'constant_altitude' = [altitude(meters), max_depth(meters)]
# 'triangle_depth' = [min_depth(meters), min_altitude(meters), rate(m/min), max_depth(meters)]
depth_mode = constant_depth
depth_params = [15.0, 5.0]
```

A.1.6 Spiral Action

The Circle Action, Spiral Action, and Gulp Action sections all detail out the same variables as they are defining the parameters of a RECON Circle action. They are just being utilized in different ways. The spiral action is the second part of the behavior and operates at a depth informed by the circle action. This action spirals out at the constant depth finding the latlon with the highest FDOM to take a gulp at depth_mode and depth_params are technically not used as these values are overridden by the Feedback from the Circle action.

```
[SPIRAL ACTION]
circle_radius = 15.0
radius_rate = 5.0
direction = CCW
revolutions = 1
# 'same' to use current speed or enter number
velocity = 2
# units = [knots, m_per_s]
velocity_units = knots
# depth_mode = [constant_depth, constant_altitude, triangle_depth]
# 'constant_depth' = [depth(meters), min_altitude(meters)]
# 'constant_altitude' = [altitude(meters), max_depth(meters)]
# 'triangle_depth' = [min_depth(meters), min_altitude(meters), rate(m/min), max_depth(meters)]
depth_mode = constant_depth
depth_params = [10.0, 5.0]
```

A.1.7   Gulp Action

The Circle Action, Spiral Action, and Gulp Action sections all detail out the same variables as they are defining the parameters of a RECON Circle action. They are just being utilized in different ways. The gulp action is the final aspect of the behavior, actually taking the water sample. The location and depth are defined by the previous two sections, and therefore depth_mode and depth_params are technically not used as these values are overridden by the Feedback from the Circle and Spiral Action.

```
[GULP ACTION]
circle_radius = 15.0
radius_rate = 5.0
direction = CCW
revolutions = 1
# 'same' to use current speed or enter number
velocity = 2
# units = [knots, m_per_s]
velocity_units = knots
# depth_mode = [constant_depth, constant_altitude, triangle_depth]
# 'constant_depth' = [depth(meters), min_altitude(meters)]
# 'constant_altitude' = [altitude(meters), max_depth(meters)]
# 'triangle_depth' = [min_depth(meters), min_altitude(meters), rate(m/min), max_depth(meters)]
depth_mode = constant_depth
depth_params = [5.0, 5.0]
```

A.2   Point and Gulp Behavior

The Point and Gulp behavior runs on the backseat during a normal mission and provides additive instead of augmenting actions. This mode does not interrupt control of the vehicle and therefore puts all of the onus onto the front seat within the mission plan. Use this behavior when a specific point in latlon and depth desired to sample at. The backseat will trigger a sample when the RECON allowed flag transitions from No to Yes. Only one sample is taken per transition, however many transitions can be generated within the mission plan.

A.2.1   Vehicle Setup

The crucial piece in setting up the vehicle is the control of RECON per objective. The mission plan shall have a transit to the point location which does not allow RECON, followed by a circle objective that shall allow RECON. This transition is utilized to active the gulpers to take a sample. This pattern can be repeated numerous times within the same mission plan. There are two ways to approach the mission planning for this.

A. Navigate to the latlon point at the depth desired for gulping with RECON OFF. At the desired point, perform 2 revolutions of a 20 m radius circle running at a speed of 2 knots with RECON ON.

B. Navigate to the latlon point at any transit depth with RECON OFF. At the desired point, perform 2-3 revolutions of a 20 m radius circle running at a speed of 2 knots set at your desired depth with RECON OFF. At the desired point, perform 2 revolutions of a 20 m radius circle running at a speed of 2 knots with RECON ON.

It is important to operate the circle at 2 knots with a radius of 20 keep the vehicle closer to the collection point. While the gulping should be finished within the first revolution of the circle, two revolutions was prescribed as insurance due to the current lack of feedback for the action.

Here is an example mission plan with two collection points utilizing the aforementioned A approach. As a note, the desired gulping depth in this mission is 5 meters. As can be seen the Navigate objective between Start and WP1 is running at a constant depth of 5 meters and has the setting "Allow RECON control" equal to "No." The Navigate objective is followed by a Circle objective running at constant depth of 5 meters, 2 knots, radius of 20 meters, 2 revolutions, and has the setting "Allow RECON control" equal to "Yes." This pattern can be repeated numerous times within the same mission plan.

Figure A.2. Example Point and Gulp behavior. The vehicle is set to navigate from start with RECON off and then complete two circles with RECON on.
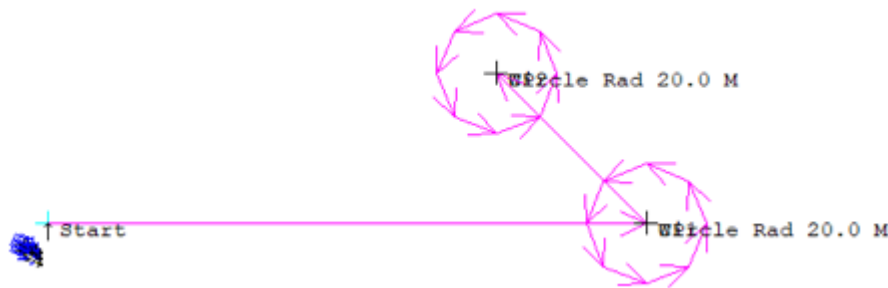
A.2.2 Backseat Computer Setup

➔ Currently there are only two options to choose from, Circle and Point. For this behavior, select Point.

```
[BEHAVIOR MODE]
# mode = ['Circle', 'Box', 'Point']
mode = Point
```

➔ This mode does not utilize any of the other sections. Once RECON control is allowed, the vehicle collects the one sample per state transition.

A.3   AUV Software Decision Tree

Two sampling strategies are presented below by software decision tree diagrams:

Figure A.3. Adaptive sampling decision diagram.
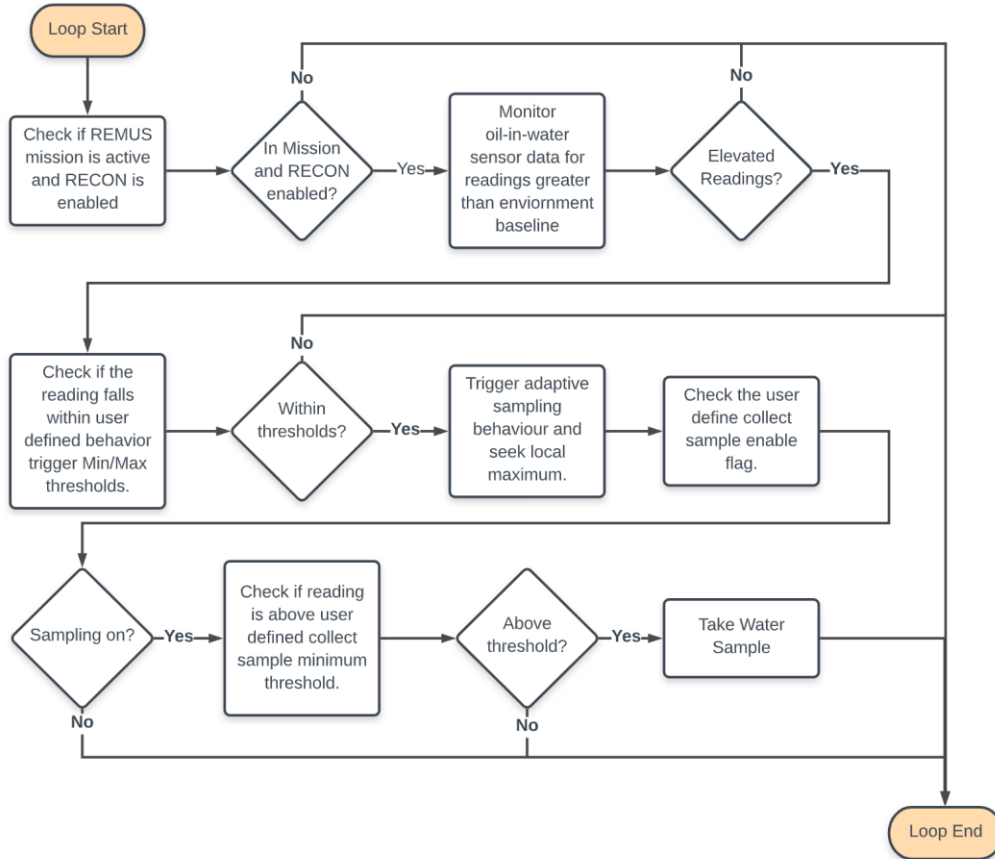
Figure A.4. Non-adaptive, point sampling decision diagram.
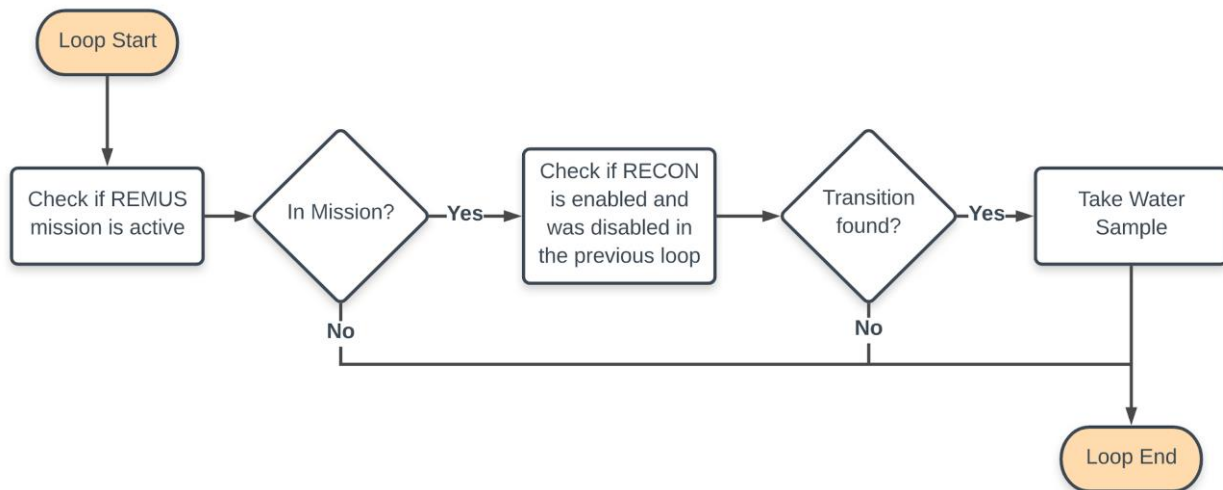
B.   Gulper Bottle Handling Procedures

AUV (REMUS-600) - Gulper HydroPump Sampler

Liam Cross, Daniel Gomez-Ibanez, Manyu Belani, Amy Kukulya
Woods Hole Oceanographic Institution
August 2019

Bottle Handling Procedures:

Abstract: This document identifies the steps that must be met in order to prepare the Gulper hydro-pump sampling assembly for mission deployment. In order to deliver uncontaminated samples, the following sections must be met in order, such that all procedures meet speculation. Please see as follows:

- **Section A: Mass Pre-filling of Bottles**
- **Section B: Priming Station Setup**
- **Section C: Pre-Sample Procedure**
- **Section D: Post-Sample Procedure**

Section A: Amber-Glass Bottles, Pre-Filling

Step 01a: All bottles will be prefilled with clean, fresh water prior to mission deployment. *(This will reduce the amount of time it takes to prime each hydro-pump, therefore reducing the overall assembly preparation time) … Remove cap, fill bottle, re-apply cap*

Step 02a: Record the general date / time and water source that bottles were filled from. (This information will be needed for post-sampling)

        Note: After all of the bottles have been pre-filled, proceed to the next section "Priming Station Setup")

Section B: Priming Station Setup

Step 01b: Retrieve a *Gulper Maintenance Fixture* and position in a workable Location

Step 02b: Fill a large reservoir with fresh / clean water, place this reservoir next To the *Gulper Maintenance Fixture*

Step 03b: Retrieve the peristaltic pump-head, motor-drive and motor-controller. Place the pump-head to the left of the *Gulper Maintenance Fixture.* Connect the motor-controller to a 110-volt power source

Step 04b: Utilizing the semi-translucent peristaltic .500" OD tubing, outfit the Peristaltic pump's motor head to be equipped with about 2-3ft of tubing. The Intake-end of the peristaltic tubing should be attached to a male-male ⅜" brass hose barb

Step 05b: Making using of the clear / firm ⅜" tubing, cut a length at about 3ft. Attach one end of this tubing to the free-end of the ⅜" brass hose Barb mentioned in the previous step. Outfit the other end with a Secondary plastic male-male ⅜" plastic hose barb

        Note: The secondary barb is used as a quick disconnect down-stream of the Exhaust lines on hydro-pumps 01-06 on each of the gulper tray assemblies)

Step 06b: Utilizing the .500" OD clear / firm tubing, cut about a 4ft length. This Tubing will be connected between the fresh-water reservoir and each

Of the intake valves leading to bottles 01 - 06

End of Priming Station Setup, please follow to next section "Pre-Sample Procedure"

Section C: Pre-Sample Procedure

Step 01c: Retrieve qty 1 "*Gulper tray assembly*". Place onto the "*Gulper Maintenance Fixture*" facing upside-down, such that each of the six O-rings can be inspected

Step 02c: Inspect each of the 6 O-rings. If any one O-ring shows sign of wear or tare, replace it with a new O-ring and lubricate with <mark>Krytox</mark>

Step 03c: While the *Gulper tray assembly* is situated upside-down, it is a good Time to install the qty 6 stainless steel inlet straws

Note: Make sure that the tray assembly is secured to the fixture by Use of the holding clamps

Step 04c: Press each of the stainless steel inlet straws into place until they are Secured firmly by a collision interference

Step 05c: Now that inlet straws are installed, undo the holding clamps and reposition the *Gulper tray assembly* in the maintenance fixture such That it is oriented right-side up. Re-secure the holding clamps and Prepare to install the qty 6 amber-glass bottles

… … …
The following steps will verify an Incremental procedure for installing each of the 6 amber-glass bottle, contaminant-free
… … …

Step 06c: Retrieve qty 6 pre-filled amber-glass bottles

Step 07c: Targeting only 1 of the 6 amber-glass bottles at a time, remove the cap from the bottle. Store this cap in a safe / clean Location

Note: After a sample is taken, the bottle will be immediately re-capped

Step 08c: With the cap removed, fasten the amber-glass bottle to the gulper
Tray assembly. Verify that the bottle is properly seated into the
Seal-threaded interface

Step 09c: Repeat steps 07c & 08c until all of the 6 amber-glass bottles have been
Installed to the gulper tray assembly

Step 10c: Retrieve a hosing kit, outfit the gulper tray assembly with the hoses
01 - 06 according to the photos below. Each of the hoses are
Labelled accordingly w 01 - 06:
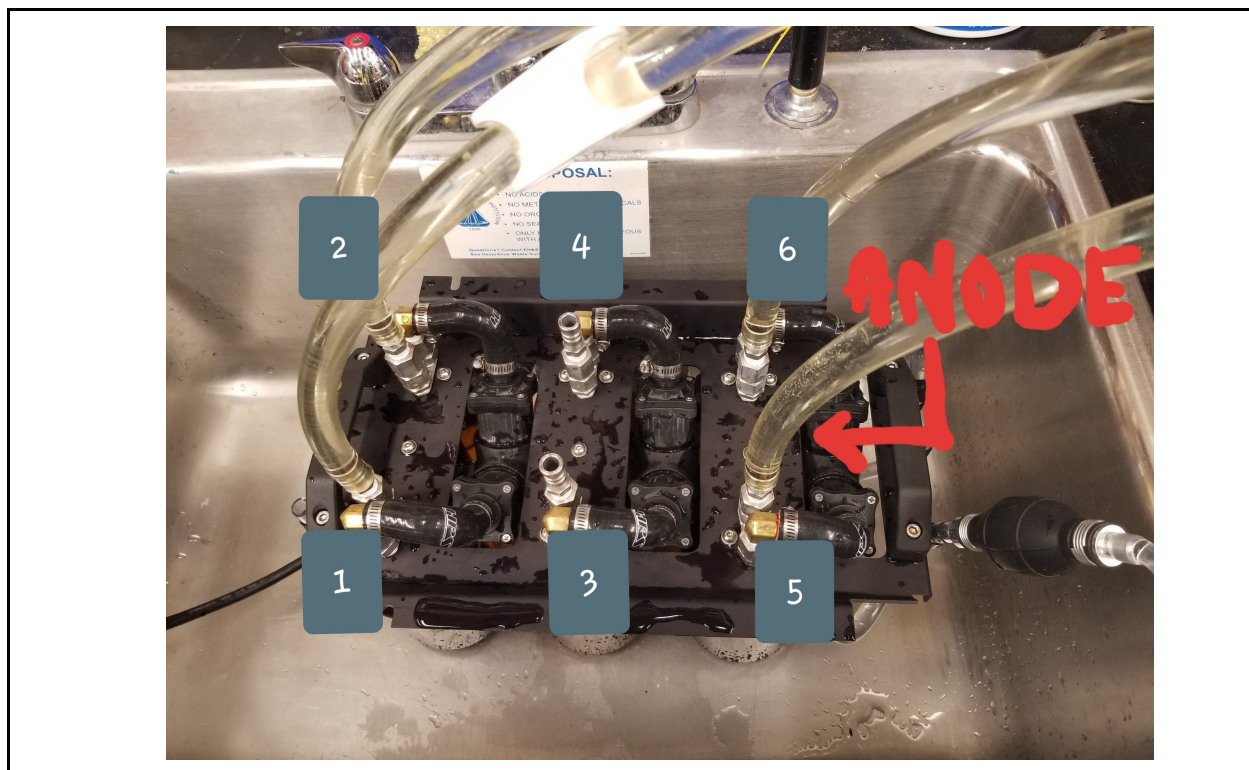
Figure: Bottle / Tube 01 - 06 Reference to Anode Location on Tray
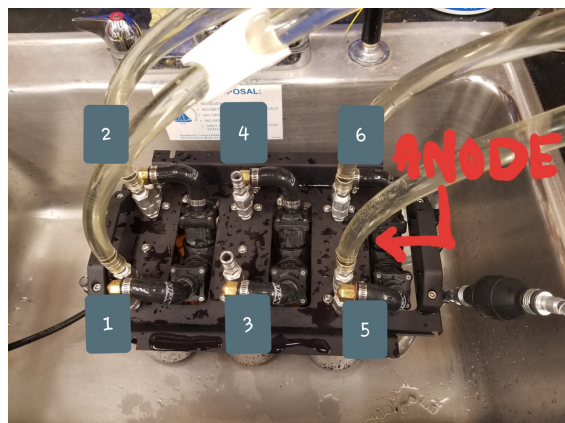
Figure: Bottle / Tube 01, 02, 04 Routing Solution (Non-Anode End)
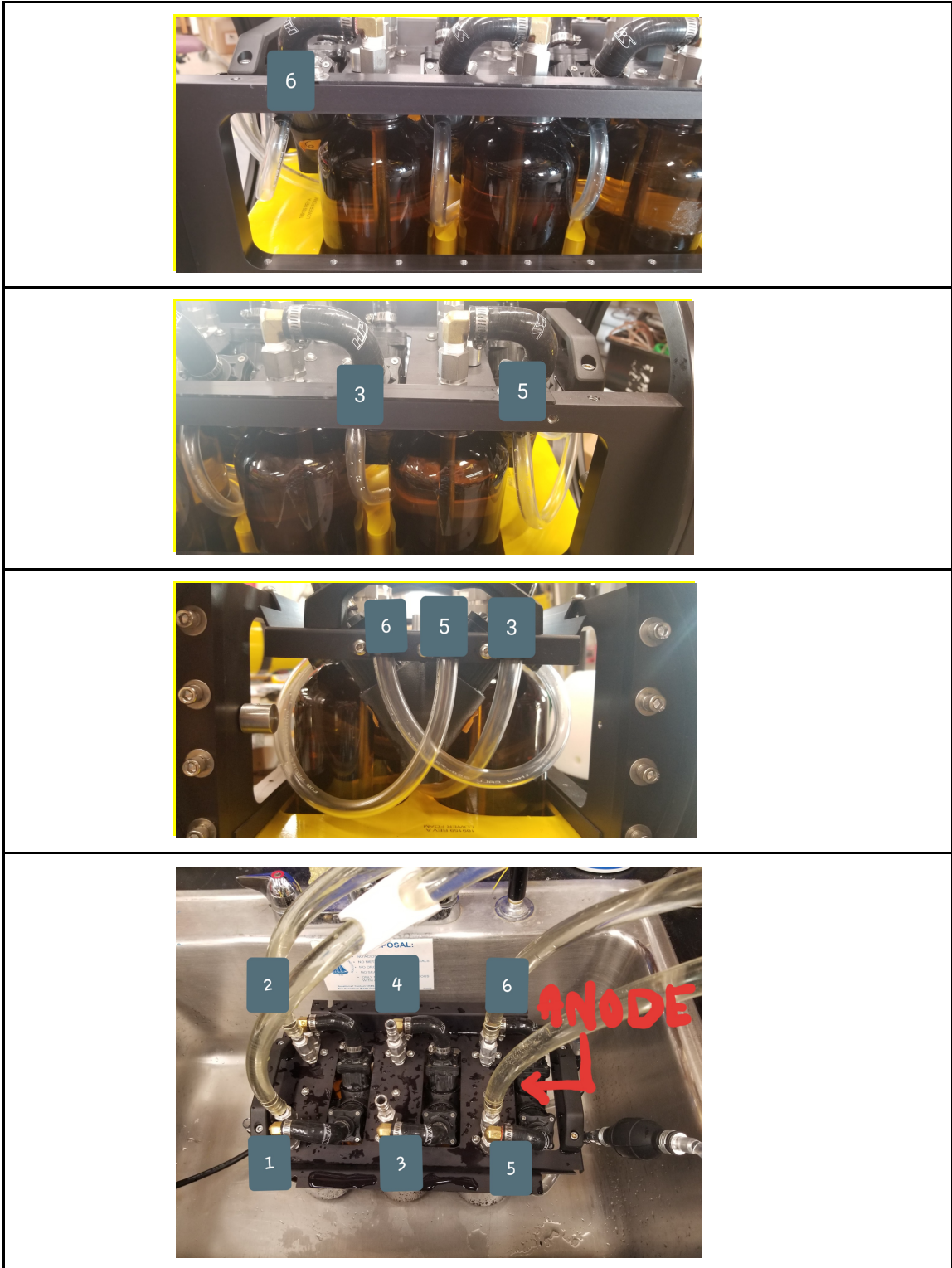
Figure: Bottle / Tube 03, 05, 06 Routing Solution (Anode End)

Amber-Glass bottles and exhaust hoses have now been installed to the tray assembly, hydropumps / lines are now ready to be burped free of air bubbles

Step 11c: Utilizing the .500" OD clear / firm tubing that was cut during priming station setup, insert one end of the tubing into the fresh-water reservoir. Affix this tubing stationary. Attach the other end of the tubing to the intake valve upstream a bottle you wish to prime now

Note: Reference back to the ⅜" OD clear / firm tubing from the Priming Station setup, note that one end of the ⅜" OD tubing is connected with the peristaltic tubing via the brass male-male hose barb. However, the free end is attached to a plastic male-male ⅜" hose barb. Use this plastic barb to interface between the peristaltic pump and exhaust lines 01 through 06 on the tray assembly

Step 12c: Connect the plastic hose barb to the end of an exhaust line down-stream from the associated pump

Note: A closed-system has now been completed, vacuum is pulled by the peristaltic pump, which will burp the line free of ai**r**

Step 13c: With the peristaltic tubing feeding through the peristaltic pump-head, close the pump-head.

Note: The running end of the peristaltic tubing should dump back into the fresh-water reservoir (closed-loop), or to some drain location

IMPORTANT: When actuating the peristaltic pump, make sure to Pull a vacuum in the direction that the check-valves flow. Therefore, the pump should pull vacuum through the intake Check-valve, down the stainless steel straw, out through the exhaust Check-valve, through the hydropump, and out the exhaust tubing. Actuating the pump in the opposite direction could can damage the check-valves

Step 14c: Turn on the pump head, pulse from setting 2 - 7 for approximately 25 seconds in order to burp all air out of the line

Note: If no vacuum is pulled by the peristaltic pump during actuation, Check the associated o-ring to verify that it is intact

Step 15c: Turn off the peristaltic pump, and disconnect the plastic male-male
Hose barb from down-stream the respective exhaust tubing

Step 16c: *This hydro pump / tubing section has now been primed*

Step 17c: Repeat <mark>steps 11c - steps 17c</mark> for the remaining bottles

… … ...

Step 18c: Now that all hydropumps / bottles / exhaust tubes have been burped,
It is time to install the gulper assembly to the Remus 600

Step 19c: Install each gulper assembly onto the Remus 600. Record the serial
Number of each tray, and whether it is connected to the forward or
Aft gulper section

Step 20c: Fasten all hardware in place and re-install the vehicle's syntactic
Foam

Step 21c: Apply qty 6 clean / teflon straws to each of the gulper assemblies
onboard Remus 600. (Forward / Aft)

Step 22c: The Gulper Assemblies onboard the Remus 600 are now ready for
Mission deployment

Section D: Post Sample

Step 01d: **POWER OFF THE REMUS 600**

Step 02d: Remove the teflon snorkels from the Remus 600 Gulper sections

Step 03d: Remove the syntactic foam / fastening hardware from the Remus
600 Gulper sections

Step 04d: Disconnect each Gulper JBox Cable from its cable connection (Forward /
Aft)

Step 05d: Remove each gulper assembly from the Remus-600, placing each on a Gulper Maintenance Stand

Step 06d: Targeting only one bottle, carefully unscrew the amber-glass bottle from The Gulper tray assembly

Note: Immediately re-cap this bottle to preserve the contained sample

Step 07d: A printed sticker with the following contents will be adhered to the body of each amber-glass bottle:

Priming Water 01, Date / Time (UTC): *mm/dd/yy, hh:mm*
Water Source, 01: *Bulk-fill of bottles*
Priming Water 02, Date / Time (UTC): *mm/dd/yy, hh:mm*
Water Source, 02: *Burping each bottle from reservoir*
Sampler SN: ###
Bottle ##: ##

Step 08d: Fill in all of the sticker contents, pertaining to the bottle at hand

Note: Priming Water 01 pertains to the event / water source when Initially filling all of the amber glass bottles

Note: Priming Water 02 pertains to the event / water source when Burping the air bubbles from the hydro-pump / bottle / exhaust Tubing

Step 09d: Store this bottle in a safe / shaded location. (Deliver to EPA)

Step 10d: Repeat steps 06d - 09d for the remaining bottles in the assembly

Step 11d: Remove the 6x SS inlet straws & exhaust tubing from the assembly. Store These items in a contained bag

Step 12d: Place gulper tray back into its storage container, taking into account that That it has already been used during mission deployment

Step 13d: Post Sampling for the Gulper bottles is now complete

C.   REMUS AUV Missions

C.1   Day 6 for WHOI Team (first day of missions): Monday, August 26, 2019

The research team left the dock for the USCG buoy tender, the George Cobb at 7:00 (local) aboard the "Lil Toot." Once aboard the vessel, the gulpers were primed and both vehicles checked out without an issue. The Arctic buoy for the LRAUV was launched, and then the Cobb proceeded to the Holly hot spot where the REMUS-600 was launched, and the REMUS-100 shortly after. The launch area for the vehicles was decided based on the data gathered by the LRAUV the night before. The LRAUV had been sent on a path off the coast of Coal Point, and the uploaded data showed a spike in the concentration of petroleum hydrocarbons near the oil rig Holly.

Figure C.1. LRAUV tracklines showing mission tracks that informed REMUS vehicle deployments and mission planning.
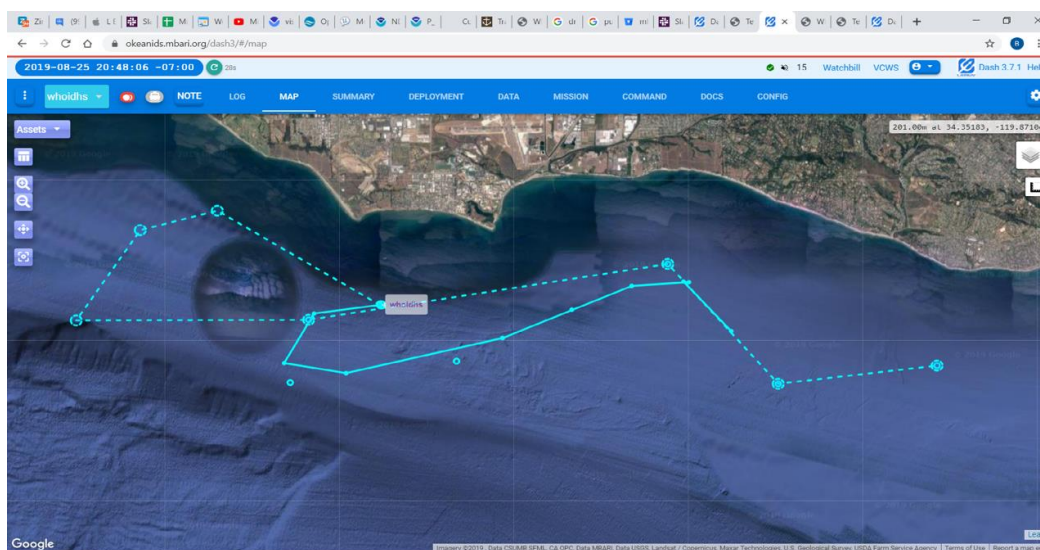
Figure C.2. LRAUV SeaOWL detections that informed REMUS missions in order to save time.
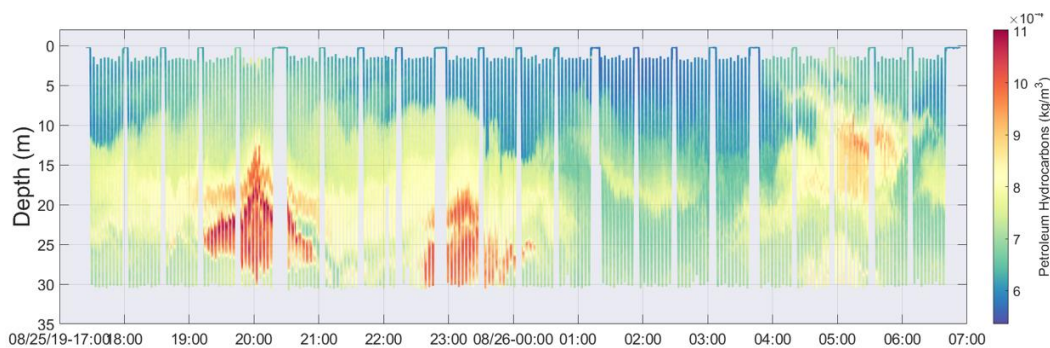
C.1.1 REMUS-600 MSN001

The first mission was programed for the REMUS-600 to do a yo-yo path in a rectangle around the Holly hot spot located at 34N24.462 119W55.176, which the LRAUV had identified the night before. The start point was offset from the hot spot by 100-m North and 500-m West, and the proceeding rectangle was 1,500 m by 200 m. The REMUS-600 was intended to run 2 laps around the rectangle (4 rows in the mission) while waiting for the SeaOWL to hit a point of interest (above the FDOM threshold of 500 raw FDOM counts), and trigger the vehicle into an adaptive mission. The REMUS-600 was launched and the mission started at 11:29 PST (local).

The REMUS-600 never triggered into its adaptive mission during MSN001 and it completed its fourth row and surfaced for a GPS fix, where it was put into manual mode and the mission was ended. It was suspected that the adaptive program never triggered because the rectangular path kept the vehicle too far from the hot spot (at its nearest point it was 100 m away). The next REMUS-600 mission was changed to go closer to the hot spot.

Figure C.3. REMUS-600 preprogrammed mission around Platform Holly.
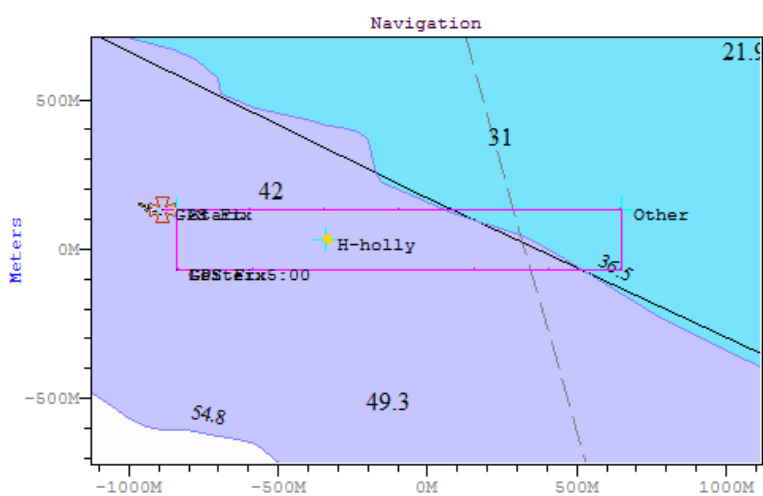
Figure C.4. FDOM and optical backscatter measurements along the REMUS-600 vehicle track (top) for Mission 1. Colors correspond to concentration. Scatter plot of optical backscatter as a function of FDOM (bottom). Chlorophyll concentration is indicated by symbol size. Colors correspond to depth in the water column.
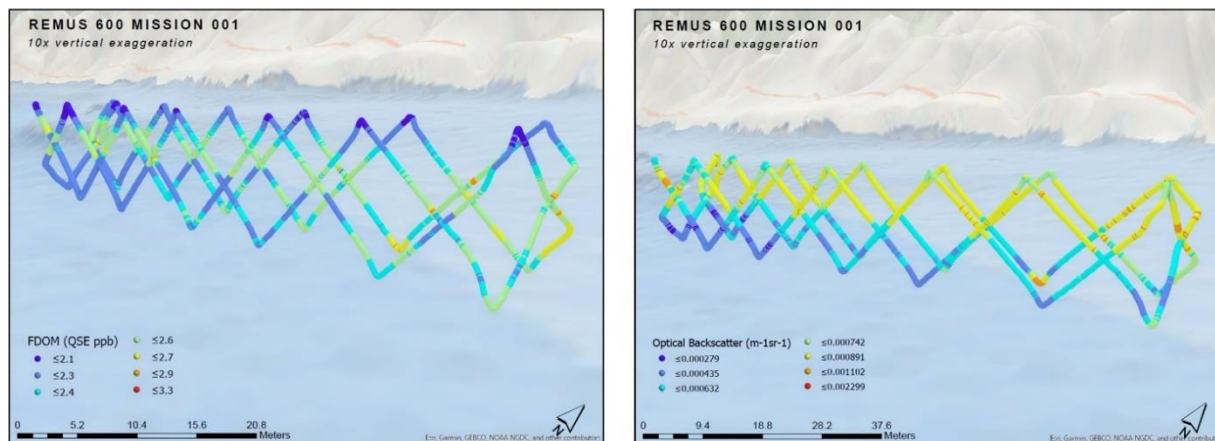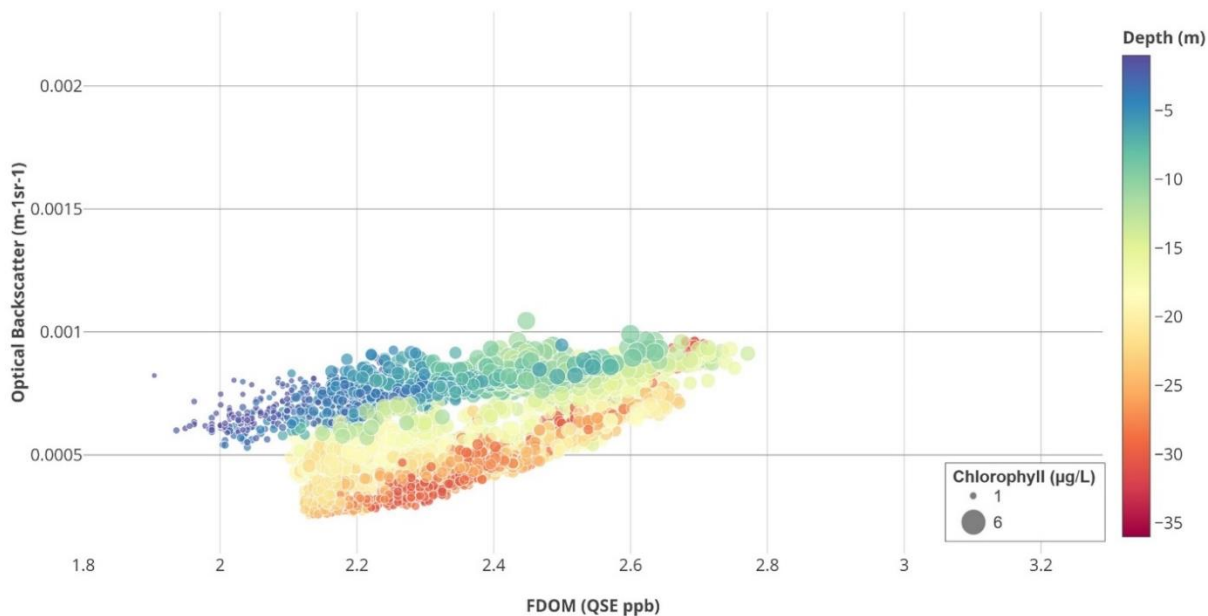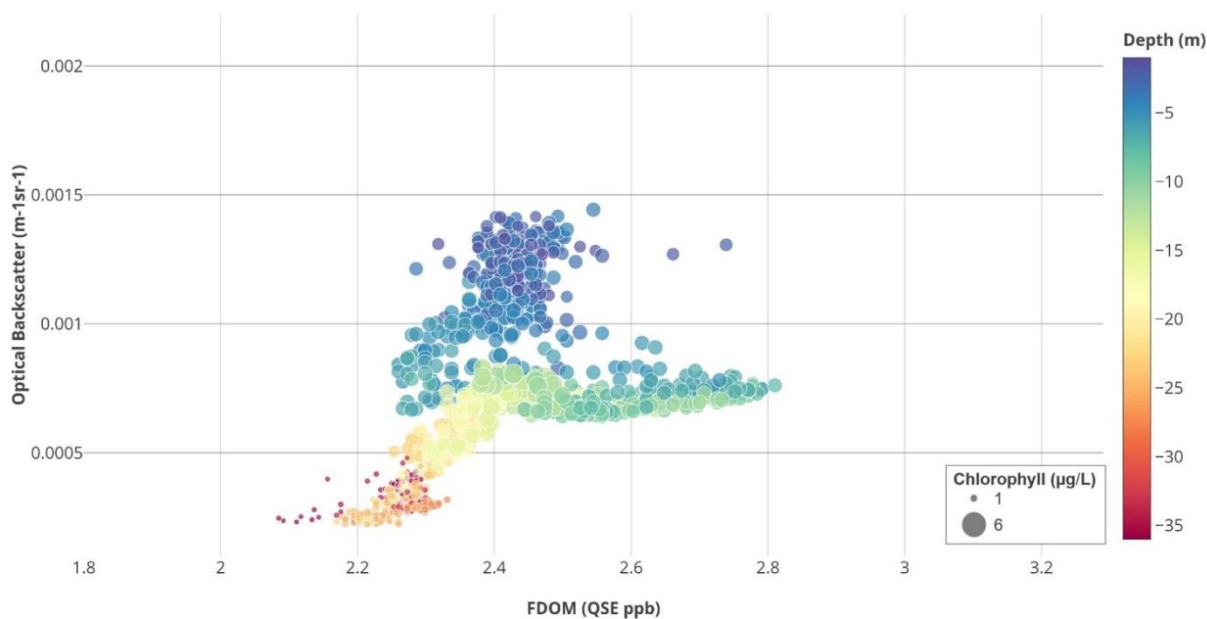
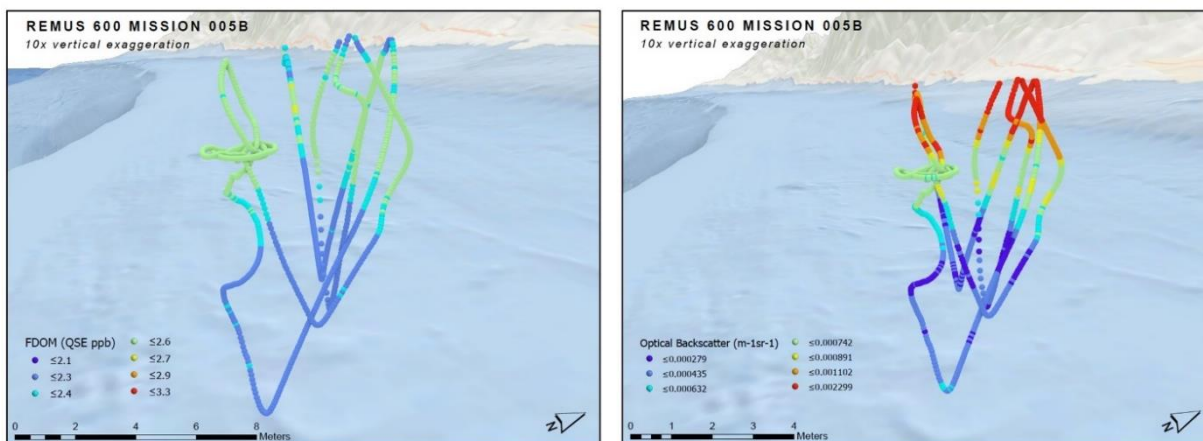**Figure C.5. Depth vertical profiles of OBS (left), FDOM (middle), and CHL (right) during REMUS-600 MSN001.**
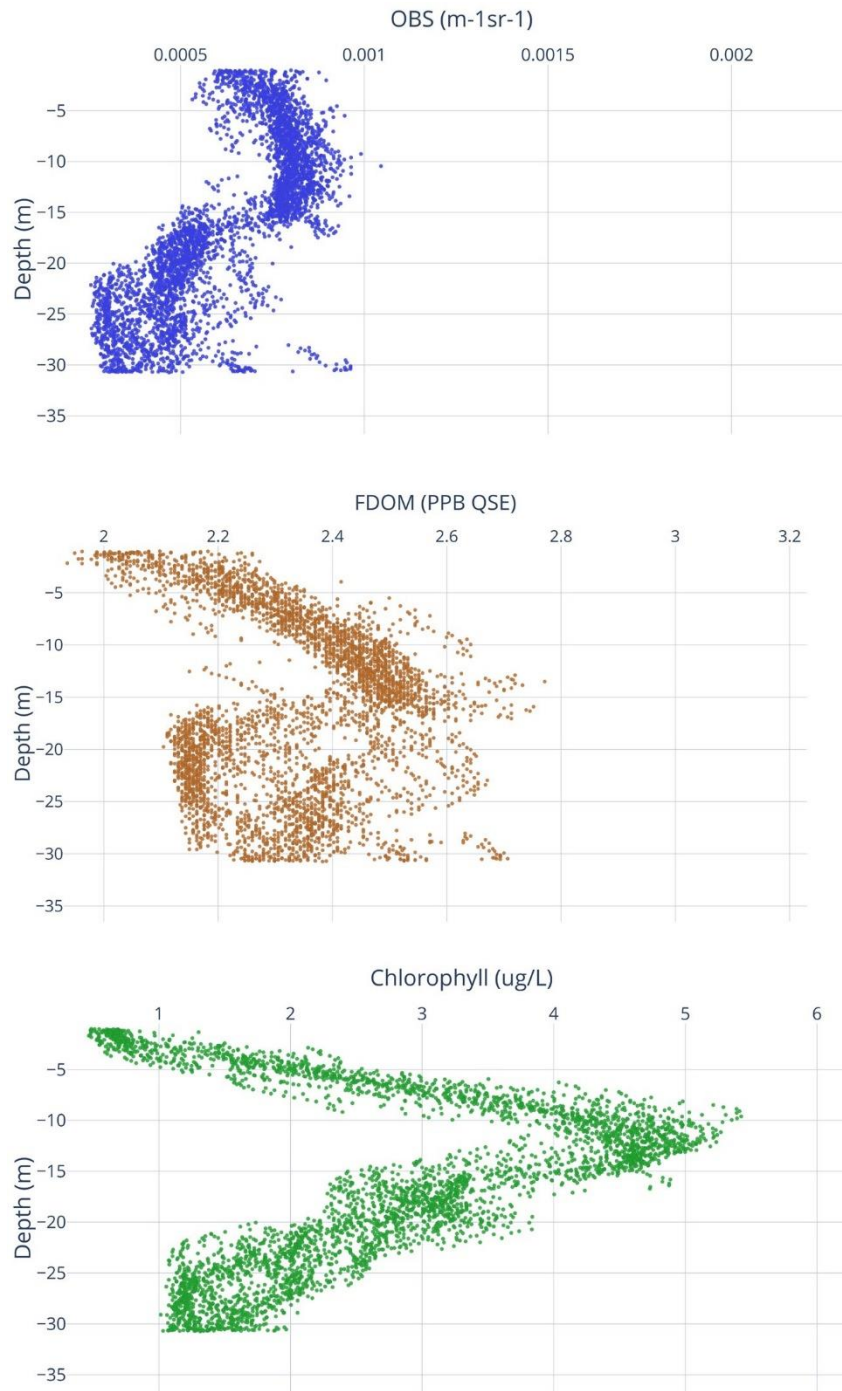
C.1.2   REMUS-100 MSN001

The REMUS-100 was checked out on deck and launched at about noon PST local time with the same rectangular path as the original REMUS-600 mission, but at a constant depth of 30 m in order to gather sidescan data and EK80 splitbeam sonar data over the same area, and to have comparisons for the sensors aboard the REMUS-600. This mission began at 12:14 (local) and ran until 12:37 (local) when it was redirected to make a diamond in the center of the original rectangle, around the hot spot. It continued in this mission for the duration of its deployment, until it was aborted at 15:34 (local).

Figure C.6. The REMUS-100 ran one mission on August 26, first making a large rectangle around the Holly hot spot, and then shorter passes through it.

Figure C.7. FDOM and optical backscatter measurements along the REMUS-100 vehicle track (top) for Mission 1. Colors correspond to concentration. Scatter plot of optical backscatter as a function of FDOM (bottom). Chlorophyll concentration is indicated by symbol size. Colors correspond to depth in the water column.
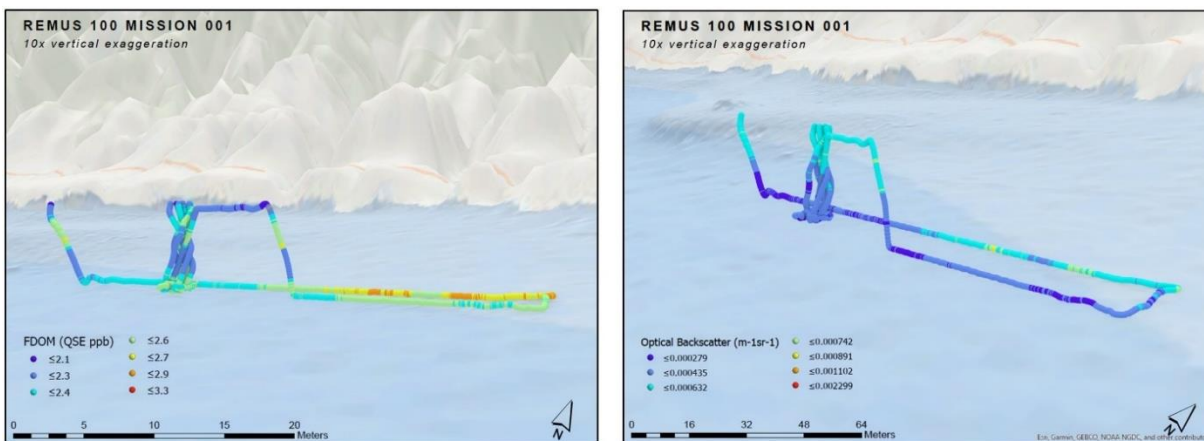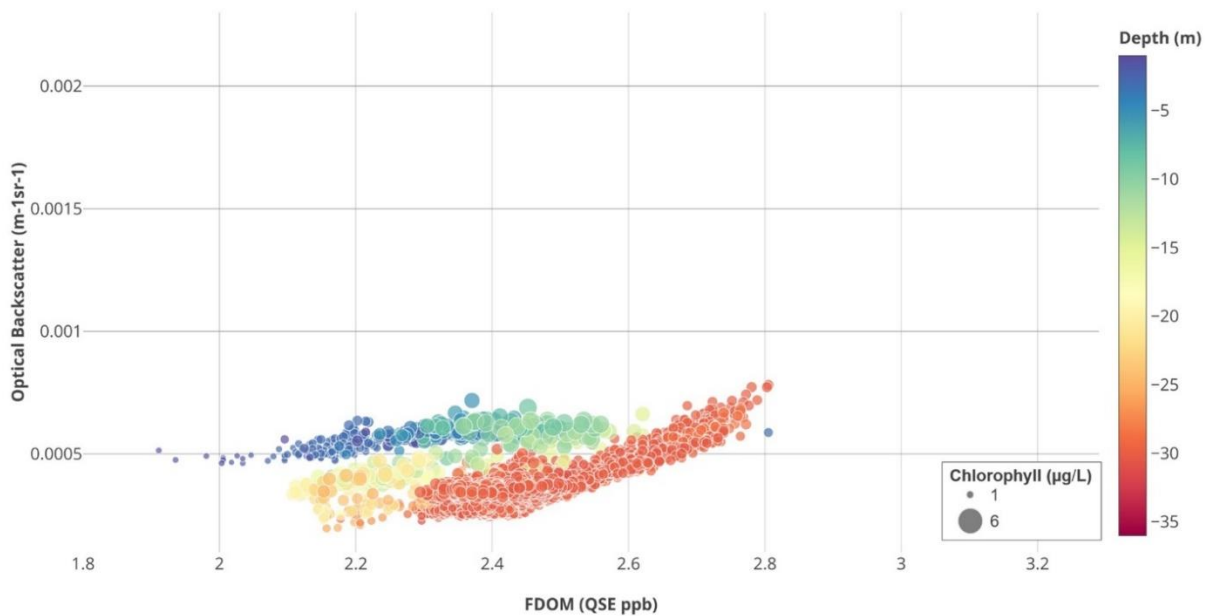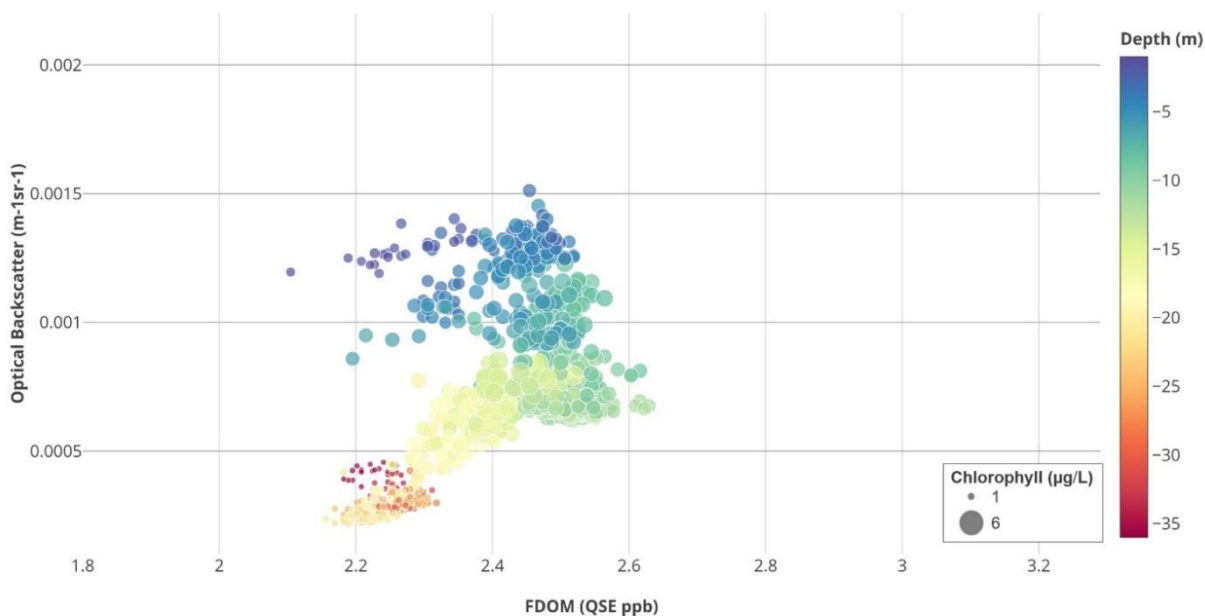
C.1.3   REMUS-600 MSN002

The second REMUS-600 mission was started at 13:27 (local) in a yo-yo path along a rectangular path, and this time moved closer to the hot spot. The *Start* point was offset from the Holly hot spot with one of the long legs of the rectangle passing through the center of the Holly hot spot. However, the vehicle still did not trigger and at 14:02:26 (local) it was sent to get a GPS fix (command 11). The SeaOWL raw FDOM counts spiked in shallow water, due to old oil rising and forming a thin slick, and when the vehicle surfaced it triggered the adaptive mission. It began its circular path but was then put into manual mode and the mission was ended. It is important to note that variables such as detection threshold and depth to trigger autonomy behavior to gulp are all user changeable and can be adapted via WiFi on the fly (and eventually via acoustic modem).

Figure C.8. The second REMUS-600 mission was a yo-yo path in a rectangle passing through the Holly hot spot.

Figure C.9. FDOM and optical backscatter measurements along the REMUS-600 vehicle track (top) for Mission 2. Colors correspond to concentration. Scatter plot of optical backscatter as a function of FDOM (bottom). Chlorophyll concentration is indicated by symbol size. Colors correspond to depth in the water column.
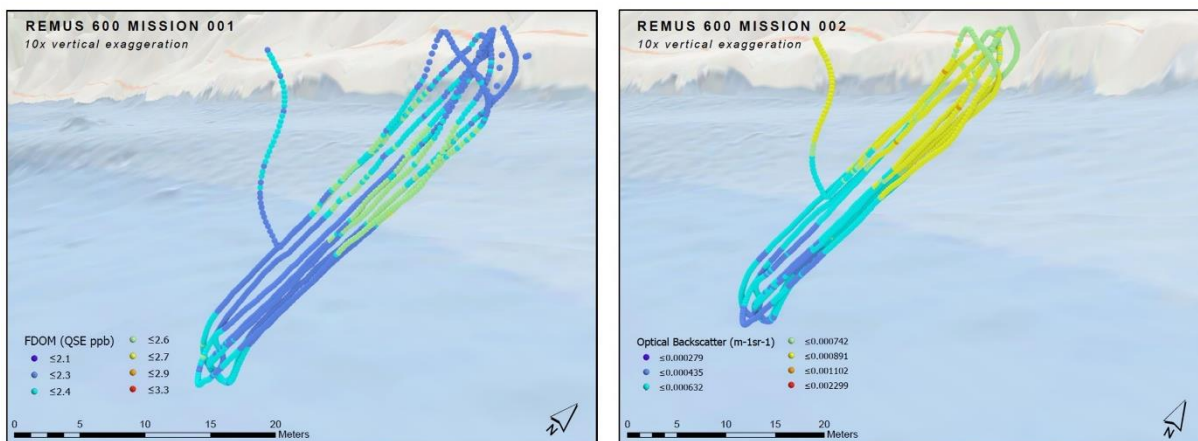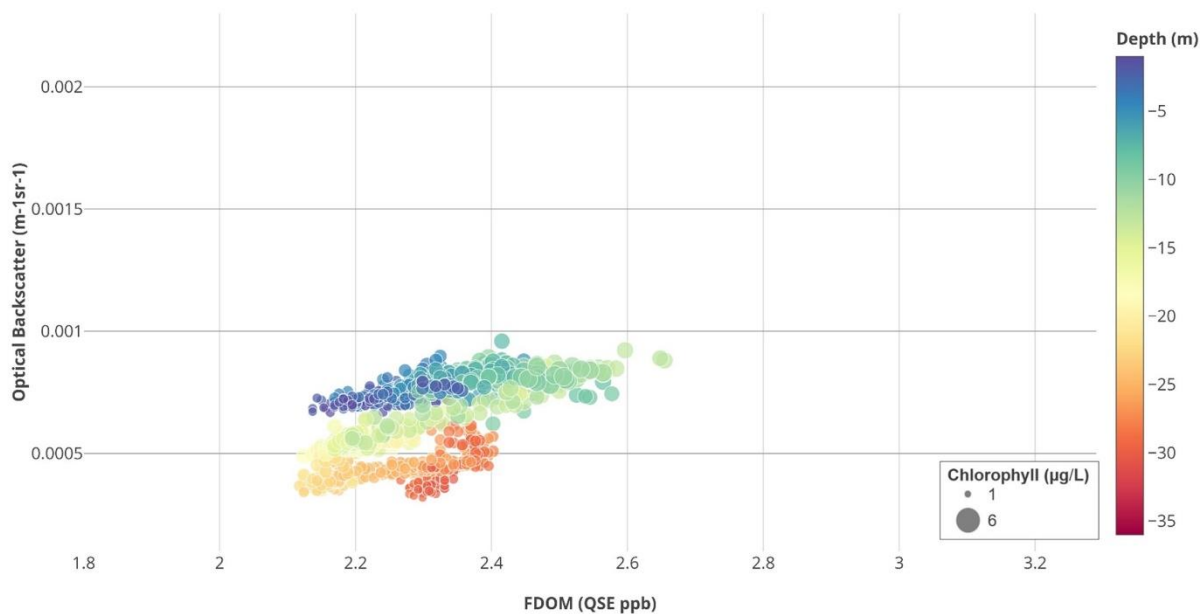
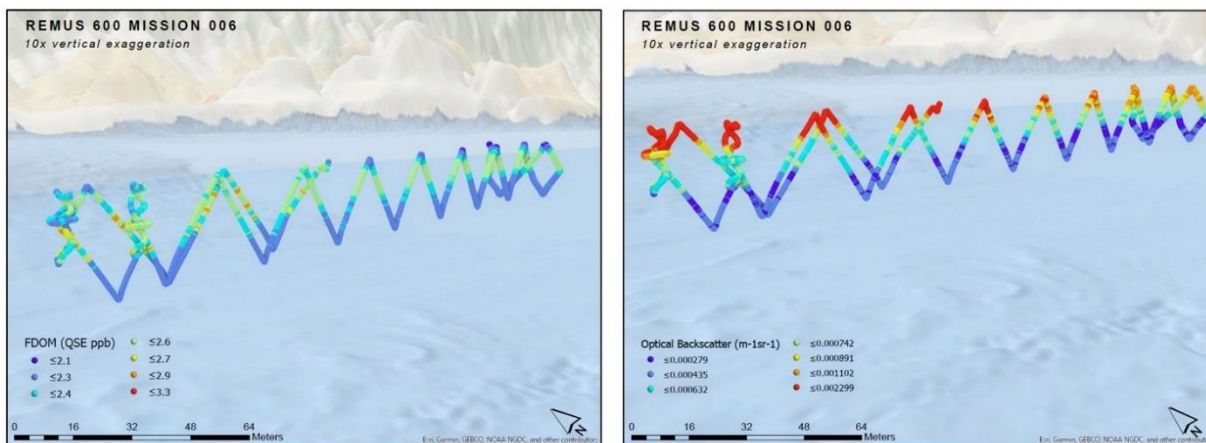**Figure C.10. Depth vertical profiles of OBS (left), FDOM (middle), and CHL (right) during REMUS-600 MSN002.**
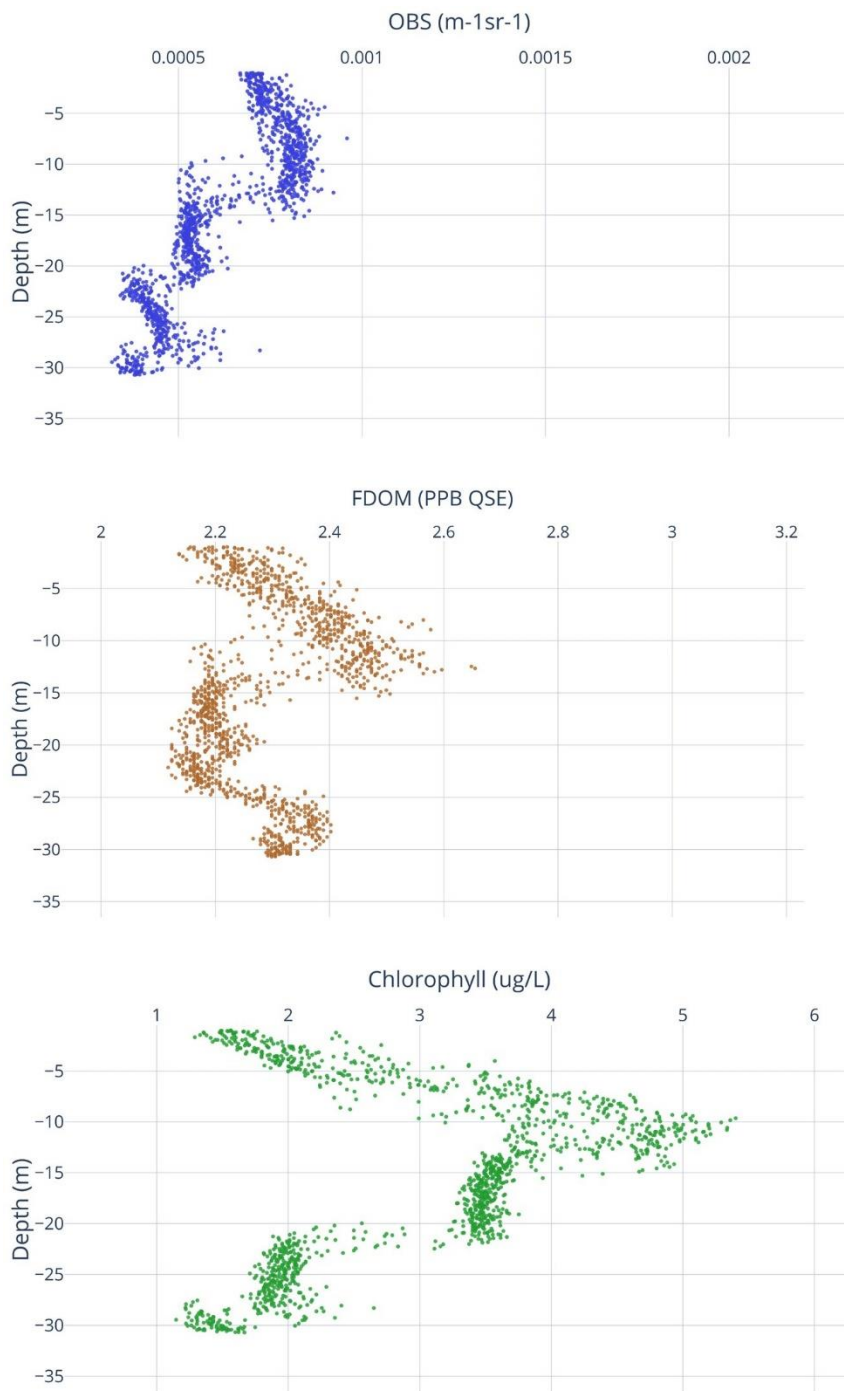
C.1.4   REMUS-600 MSN003

During REMUS-600 MSN002, it was observed that the SeaOWL on the REMUS-100 was recording much higher FDOM raw counts than the SeaOWL on the REMUS-600. This is because the company that manufactures the SeaOWL calibrates each one differently. However, the trigger point had been determined by the SeaOWL readings from the REMUS-100, so the REMUS-600 never triggered into an adaptive mission. The trigger threshold was lowered for the REMUS-600 and another rectangular "navigate rows" mission was started. The third mission began at 14:15 (local). At 14:41:46 (local), the vehicle was sent for another GPS fix, displaying the same behavior as before where the high SeaOWL FDOM reading triggered an adaptive mission. It was then taken over in manual mode and the mission ended at 15:12 (local).

Figure C.11. The REMUS-600 MSN003 was set to be the same path as MSN002 moving through the Holly hot spot. When it surfaced the adaptive mission was falsely triggered resulting in the circular path in the center.

Figure C.12. FDOM and optical backscatter measurements along the REMUS-600 vehicle track (top) for Mission 3. Colors correspond to concentration. Scatter plot of optical backscatter as a function of FDOM (bottom). Chlorophyll concentration is indicated by symbol size. Colors correspond to depth in the water column.
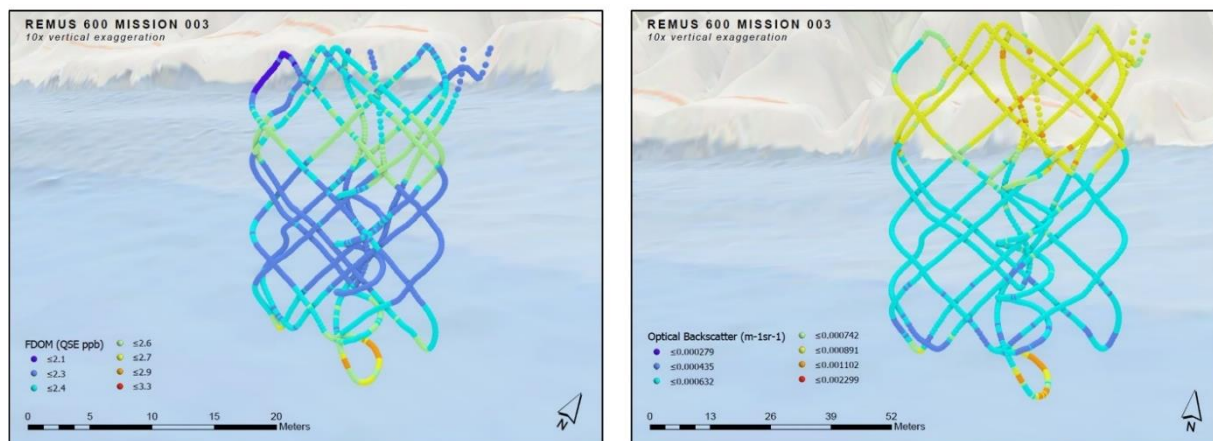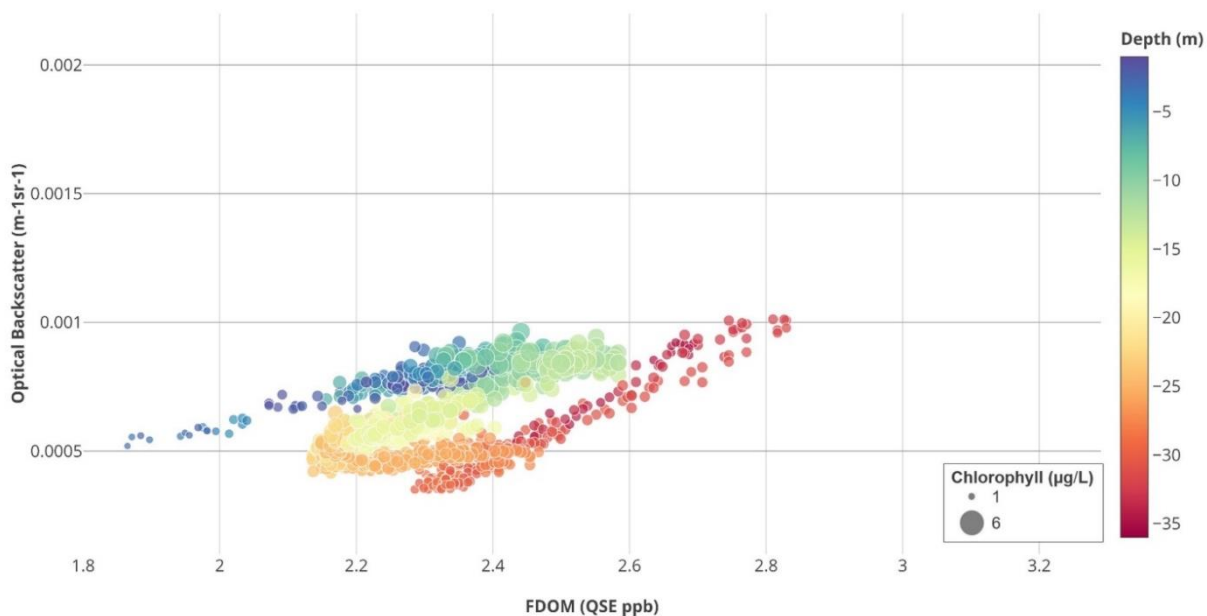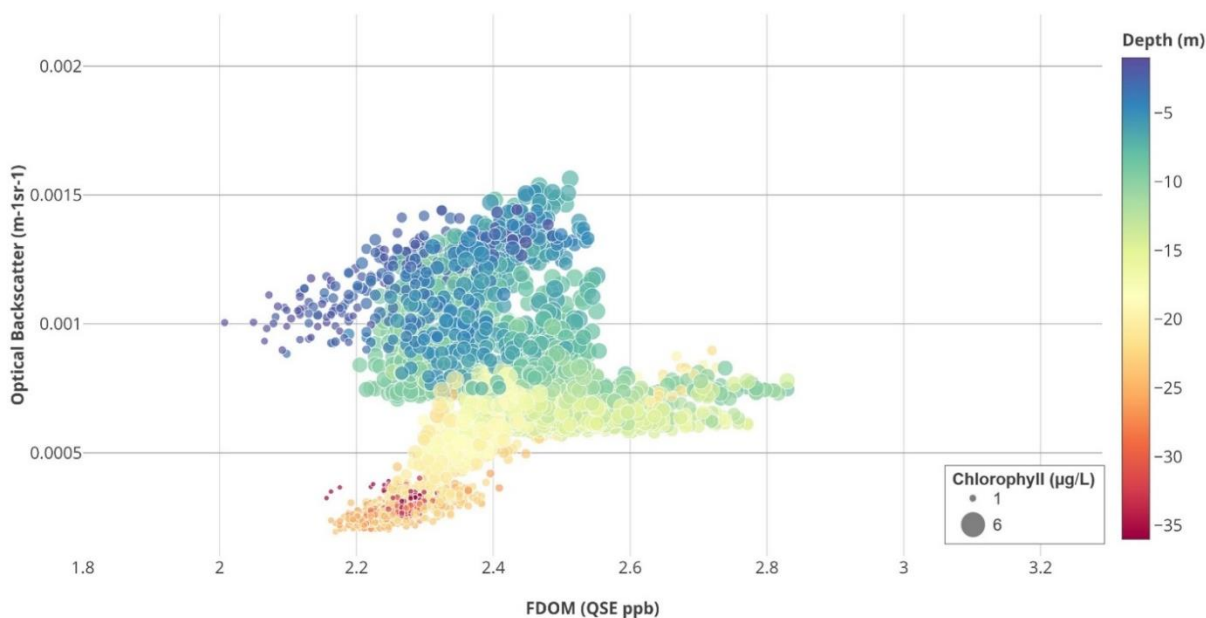
**Figure C.13. Depth vertical profiles of OBS (left), FDOM (middle), and CHL (right) during REMUS-600 MSN003.**
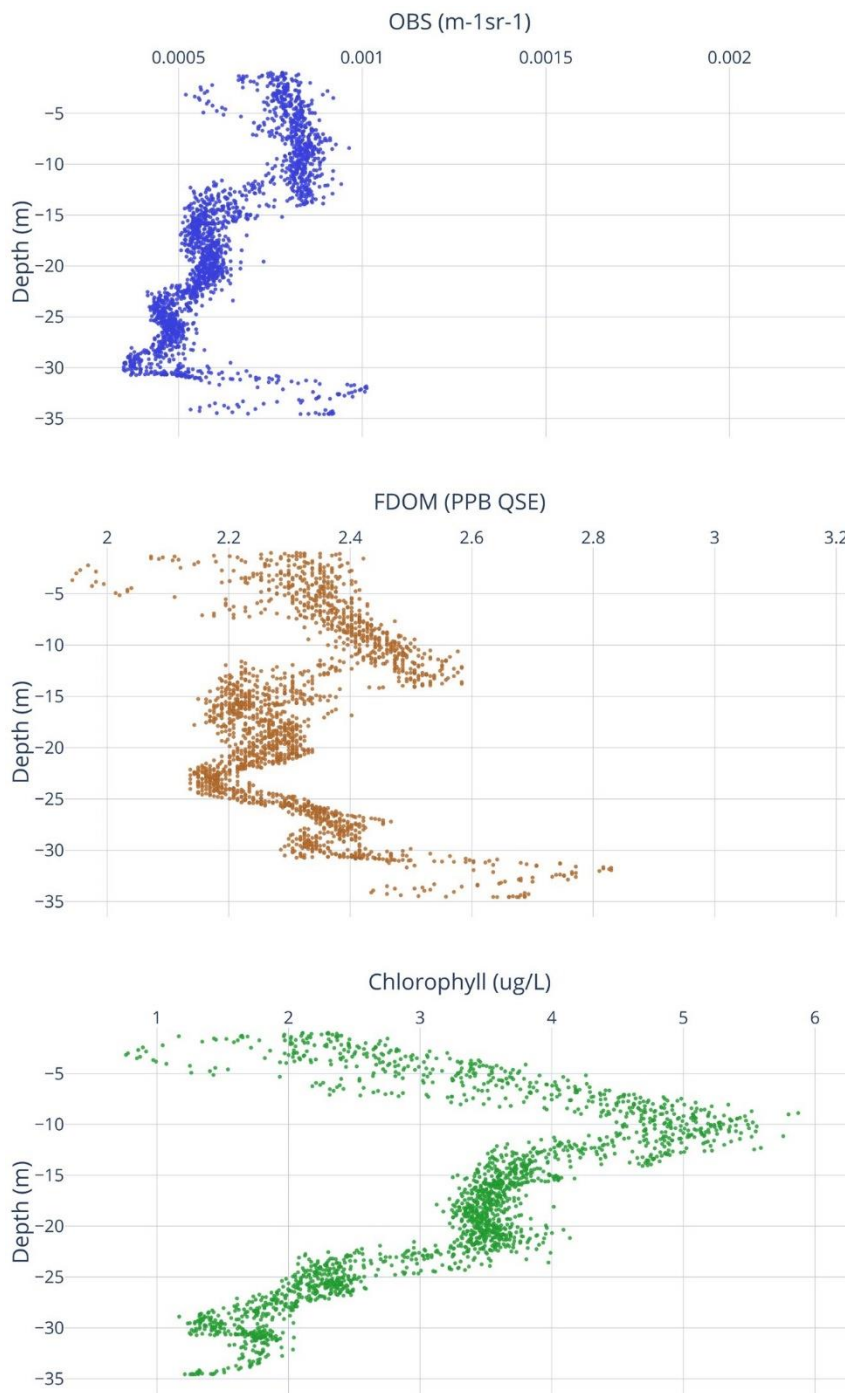
C.1.5   REMUS-600 MSN004

The goal of the final mission was simply to test the vehicle's ability to gulp without using the autonomy mission. MSN004 was a backseat mission that sent the REMUS-600 to a specific point where it would then go into spirals through a minimum and maximum preprogrammed depth of the adaptive mission and take a gulp. The REMUS-600 went through the circle and spiral behavior but never gulped, and was then put into manual mode and the mission ended at 16:04 (local).

Figure C.14. The final mission of August 26 was a circular point and gulp mission at the Holly hot spot; however, while the vehicle went into its adaptive behavior, it did not gulp.

Figure C.15. FDOM and optical backscatter measurements along the REMUS-600 vehicle track (top) for Mission 4. Colors correspond to concentration. Scatter plot of optical backscatter as a function of FDOM (bottom). Chlorophyll concentration is indicated by symbol size. Colors correspond to depth in the water column.
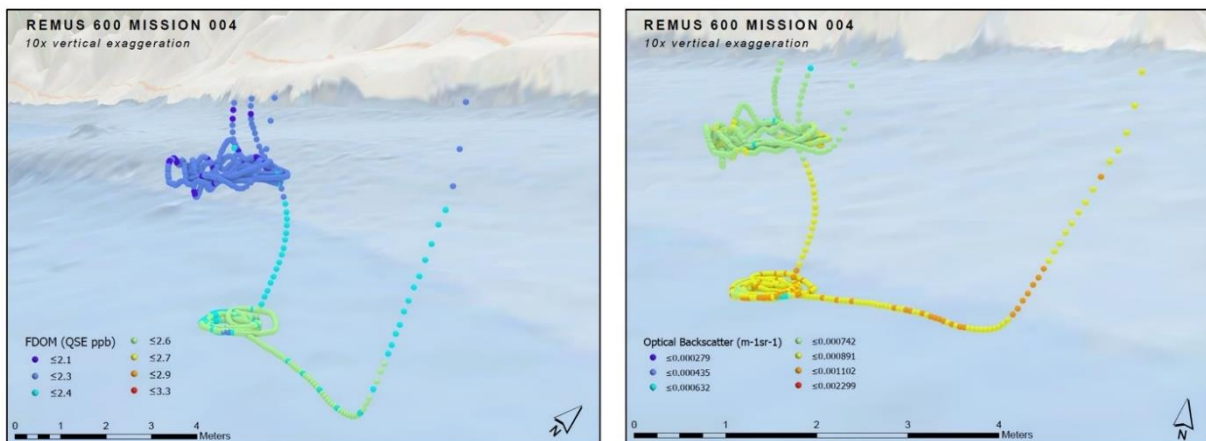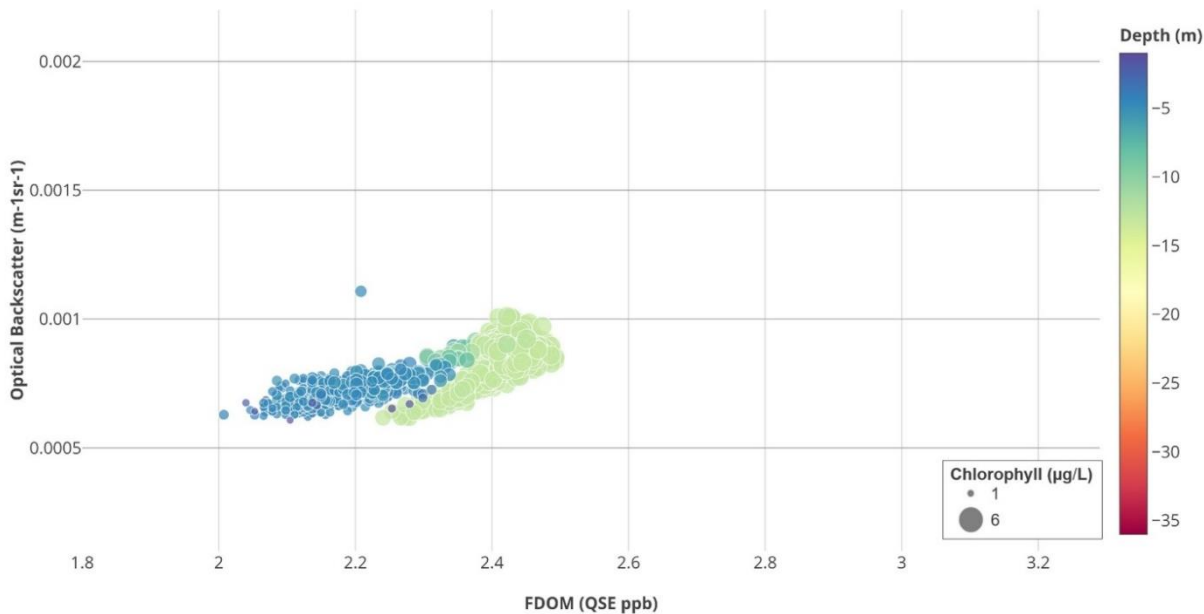
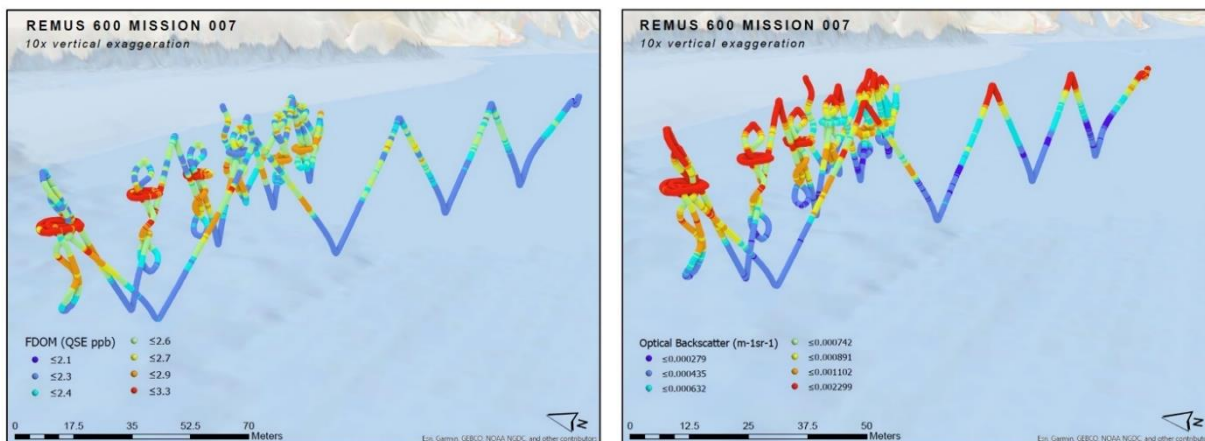**Figure C.16. Depth vertical profiles of OBS (left), FDOM (middle), and CHL (right) during REMUS-600 MSN004.**
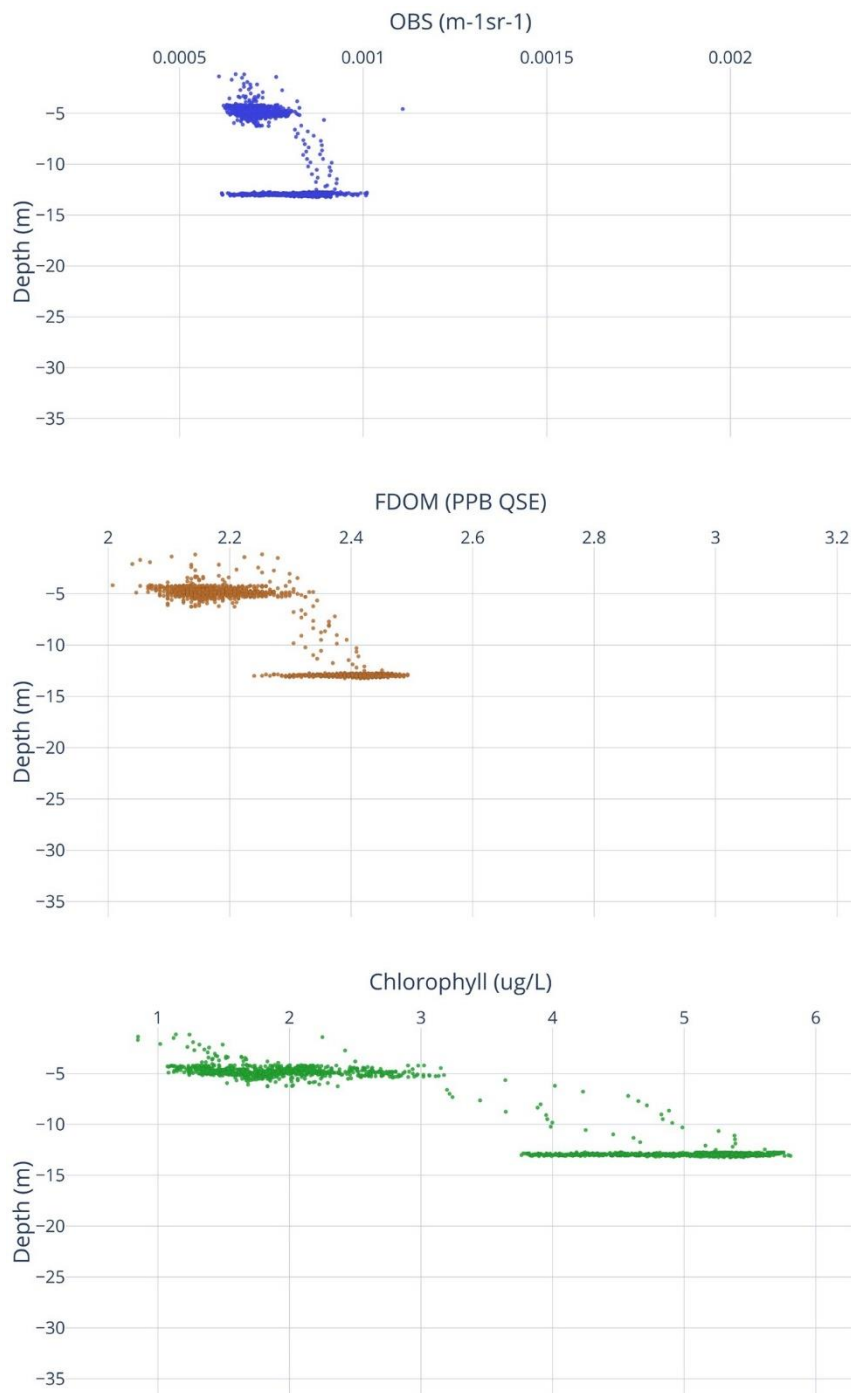
C.1.6   Post-Mission

The post-mission analysis revealed that the gulpers never took a sample because they were not properly initialized, most likely due to a bug caused by the updated gulper code that was loaded on the vehicle after the vehicle checkouts in Woods Hole. The older versions of the code were recovered in order to roll back the vehicle to the version it was at when tested at Woods Hole. The gulper bottles were not removed as they were never used.

C.2   Day 7: Tuesday, August 27, 2019

The REMUS-600 was rolled back to a previous version of the code that had been more thoroughly tested, and a test gulp was successfully performed on deck. The length between GPS fixes was extended from 5,000 to 10,000 m so that it would not interrupt missions. The REMUS-600 was set to send acoustic data every 20 seconds. The operator can then prioritize what messages to receive. Due to the adaptive testing that was underway, we made the SeaOWL data message the top priority followed by vehicle state updates. The goal for the day was to confirm the gulpers were working with the REMUS-600 and identify and take oil samples. The REMUS-100 was used to gather overlaying data with the REMUS-600, as well as occasionally to scout different areas for oil signals.

Figure C.17. Shows acoustic message from REMUS that shows the newest, largest, and second-largest raw FDOM value and matching depth. This near real-time information allows an operator in the loop to make informed decisions on where oil is or is not during the mission. Further software development can turn these data into a heatmap for quick visual interpretation across latitude, longitude, and depth.
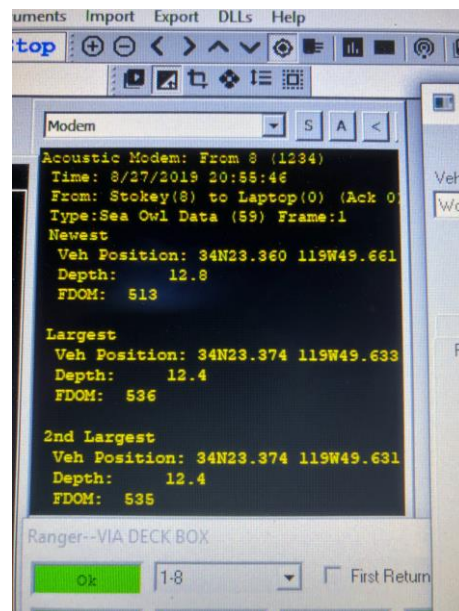
Figure C.18. The red tracks show the different REMUS-600 missions and the yellow tracks the REMUS-100 missions from August 27. Vehicles started where the LRAUV initially sensed oil and then were redirected further inland following stronger signals.
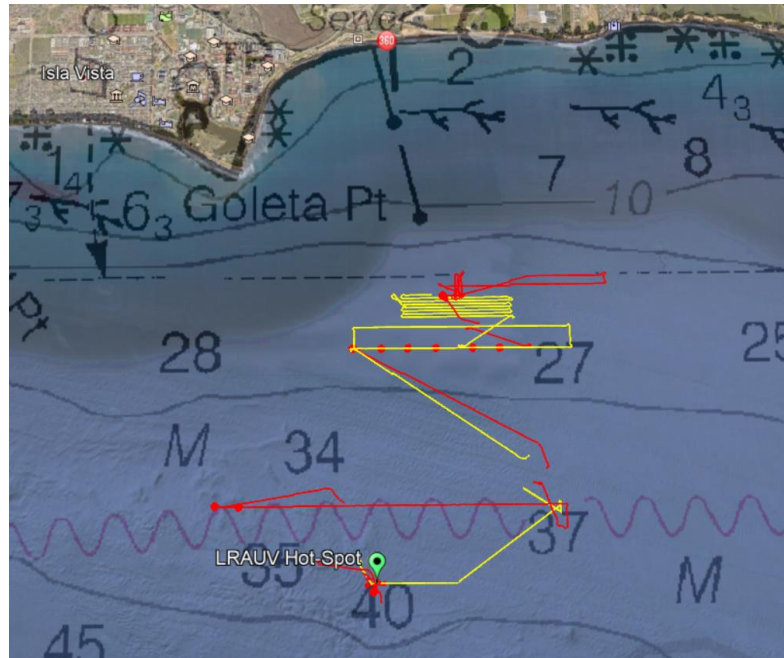
C.2.1   REMUS-600 MSN005

The REMUS-600 was launched and the mission started at 9:04 (local). It was sent to do a rectangular path and then a test gulp. The vehicle was sent some C3 commands (acoustic command language onboard the AUV and topside tracking gear) in order to test polling and successful performance while polling in 1x32 sent to 6x32. When the vehicle surfaced it started doing a PHINS inertial navigation calibration (without being directed to do so – an error we saw at Woods Hole as well), and the end of the mission file was cut. The vehicle also did not gulp because the highest SeaOWL reading occurred during the transit to the mission start point (where the vehicle was not programed to gulp), which raised the learned threshold and prevented the gulp from triggering during the rectangular path. This was changed in the backseat programming for the following mission.

Figure C.19. The first mission for the REMUS-600 on August 27 was a rectangular path during which it would test the gulper. No gulps were taken, however.

Figure C.20. FDOM and optical backscatter measurements along the REMUS-600 vehicle track (top) for Mission 5. Colors correspond to concentration. Scatter plot of optical backscatter as a function of FDOM (bottom). Chlorophyll concentration is indicated by symbol size. Colors correspond to depth in the water column.
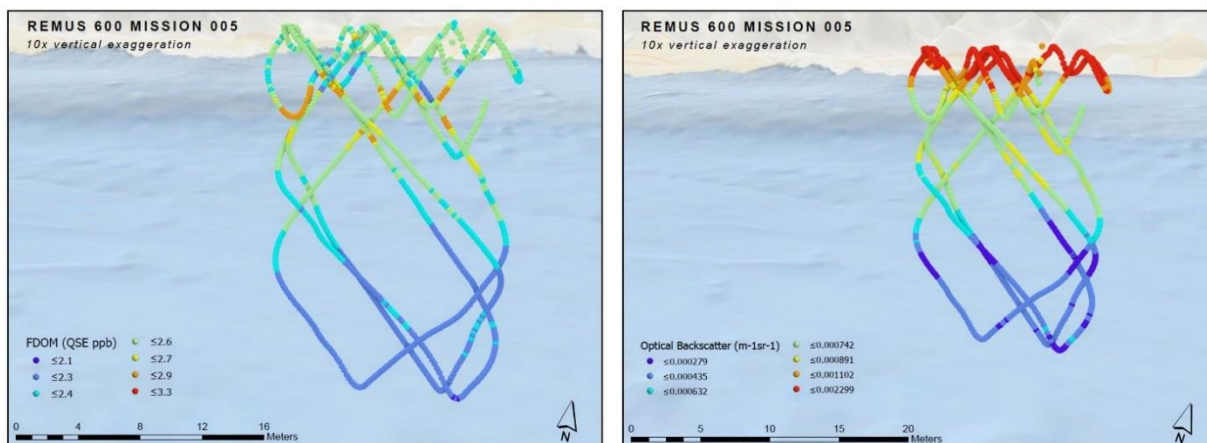
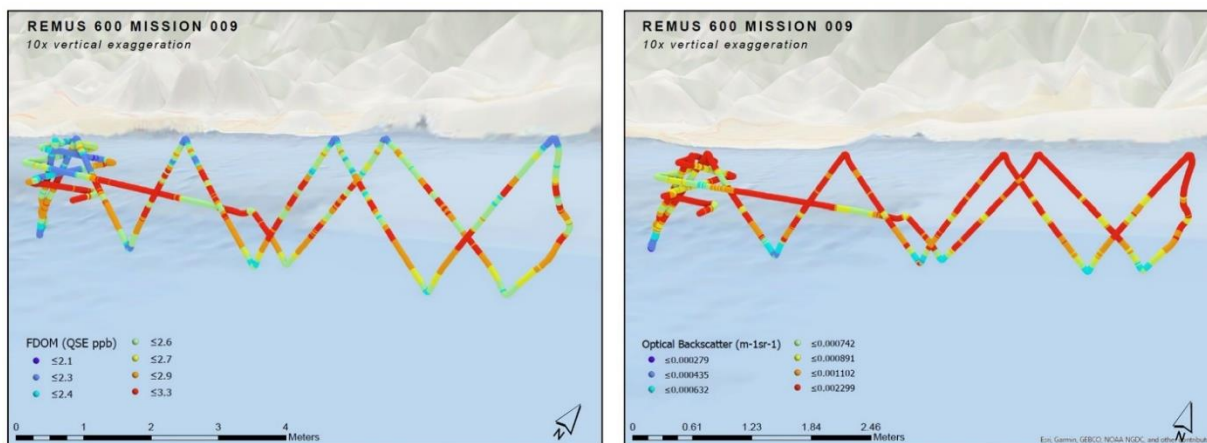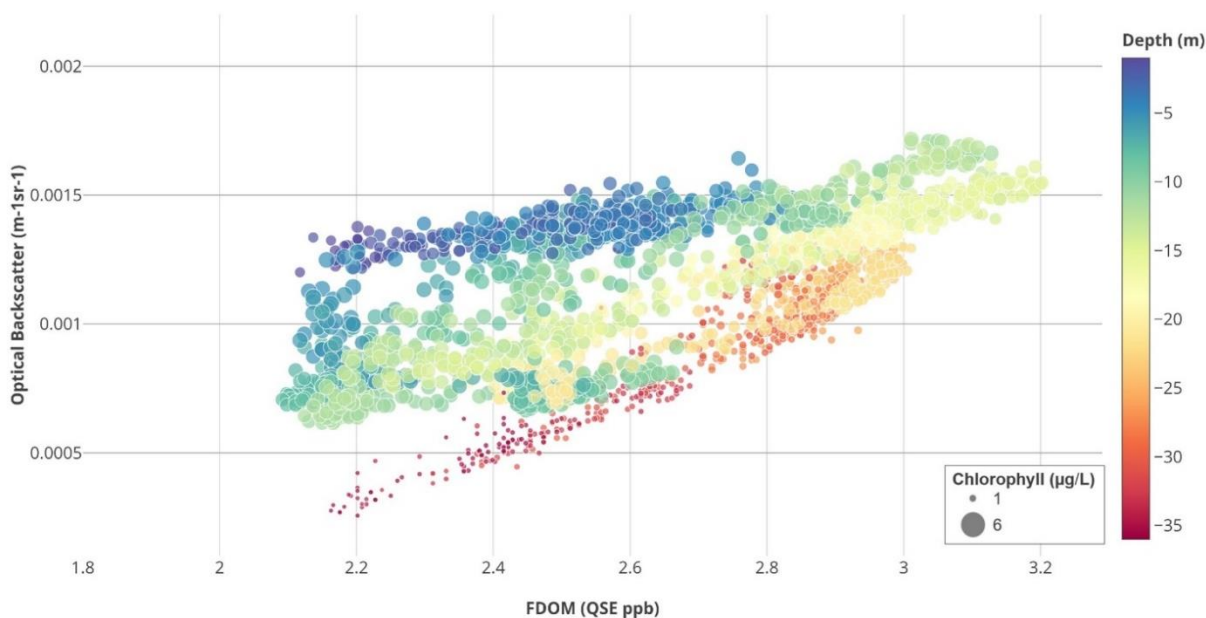**Figure C.21. Depth vertical profiles of OBS (left), FDOM (middle), and CHL (right) during REMUS-600 MSN005.**
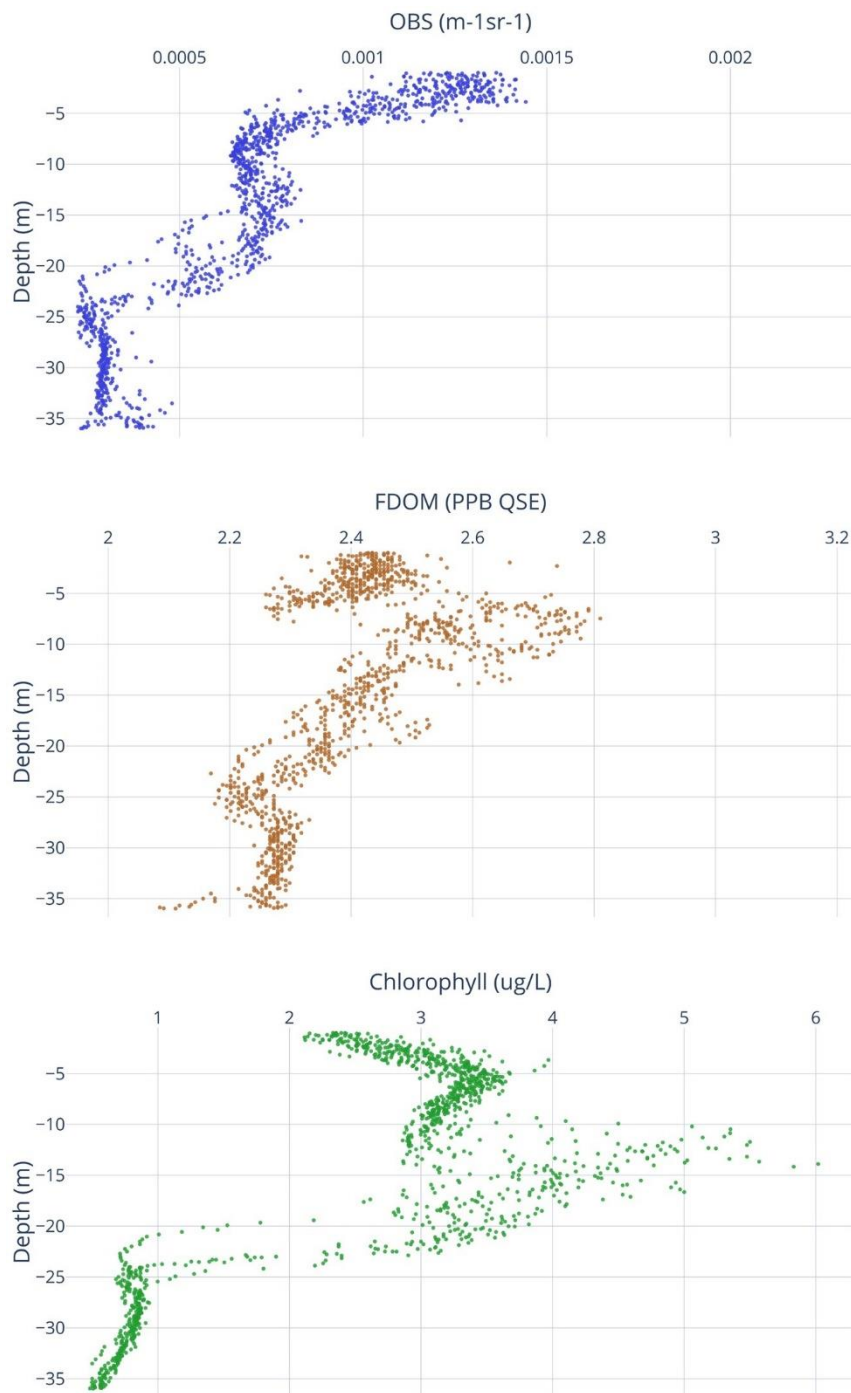
C.2.2   REMUS-600 MSN005B

The rectangular mission for a single gulp was re-run, after fixing the error in the backseat program, and this new version started at 9:57 (local). This time it successfully gulped and the mission was ended so that the vehicle could be redirected to an oil location.

Figure C.22. The path from REMUS-600 MSN005 was rerun as MSN005B, and this time the vehicle triggered its adaptive mission as seen by the spiral path.

Figure C.23. FDOM and optical backscatter measurements along the REMUS-600 vehicle track (top) for Mission 5B. Colors correspond to concentration. Scatter plot of optical backscatter as a function of FDOM (bottom). Chlorophyll concentration is indicated by symbol size. Colors correspond to depth in the water column.

Figure C.24. Depth vertical profiles of OBS (left), FDOM (middle), and CHL (right) during REMUS-600 MSN005B.
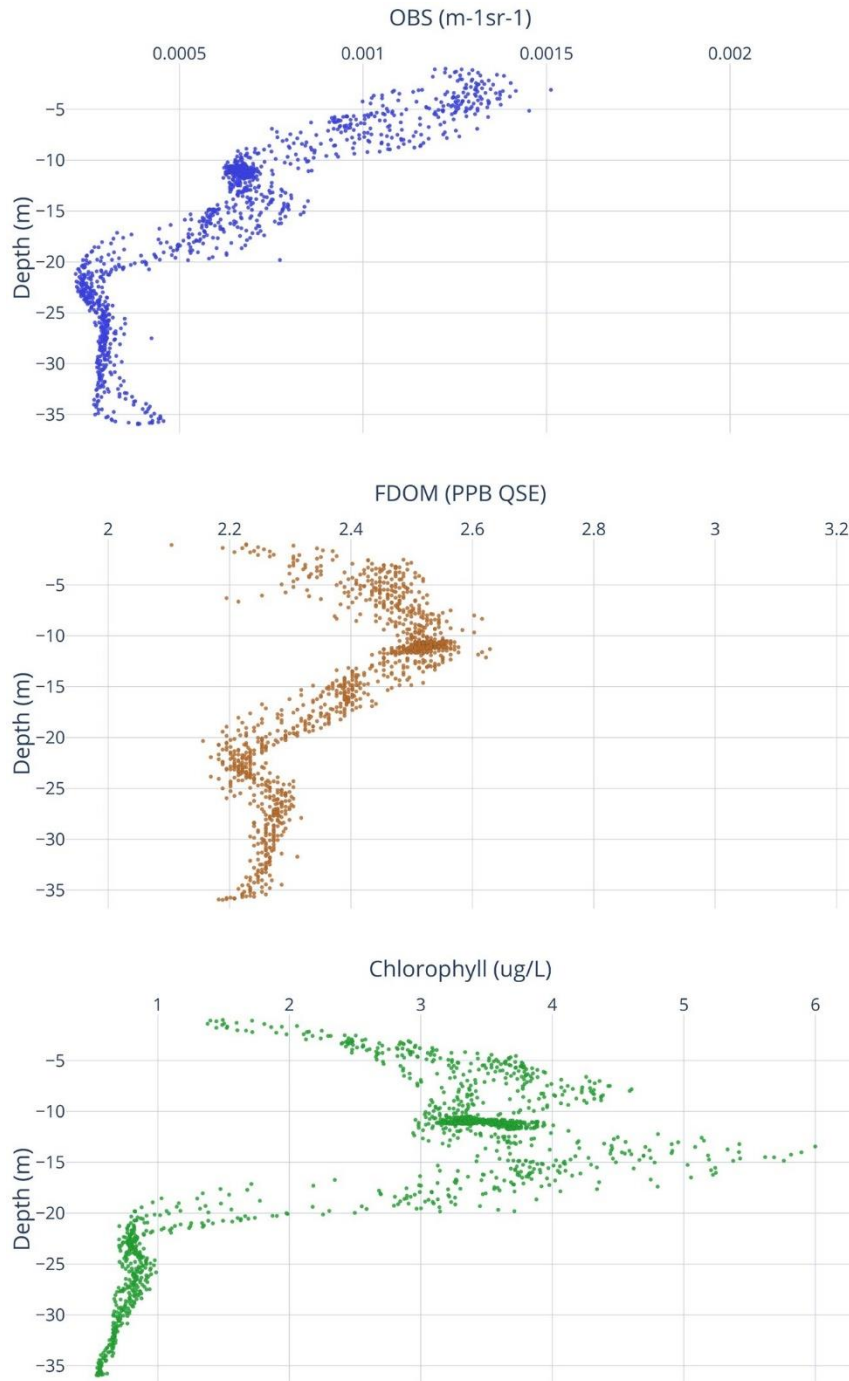
C.2.3   REMUS-100 MSN002

The REMUS-100 was launched and the mission started at 10:56. The mission was another rectangular rows mission but it only completed one leg before it was observed that the vehicle was moving unusually slow (only about 0.5 m/s) so the mission was aborted at 12:52 and the vehicle brought to the surface to visually confirm whether something was stuck in the propellers. The vehicle's speed was not caused by a prop catch but by the vehicle reaching its ballard limit, which caused it to cut out its thrusters. This also happened in June with the REMUS-100 Darter, but it is unclear why. The bollard limit was raised from 50 to 100 in order to prevent this issue from occurring.

Figure C.25. The REMUS-100's first mission on August 27 was a path through the hot spot identified by the LRAUV.
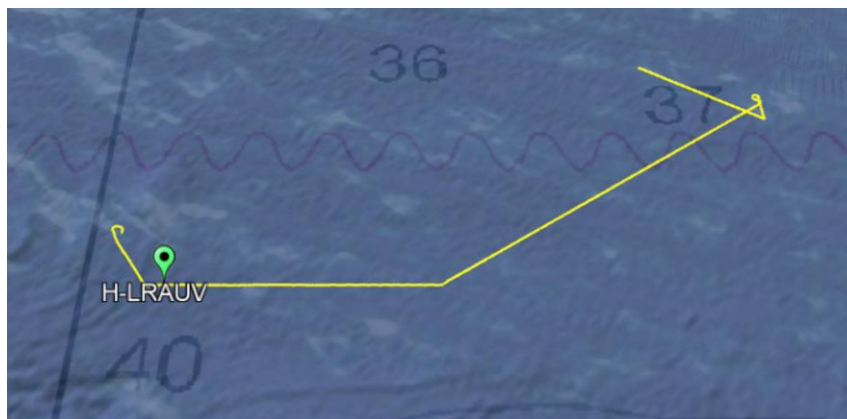
Figure C.26. FDOM and optical backscatter measurements along the REMUS-100 vehicle track (top) for Mission 2. Colors correspond to concentration. Scatter plot of optical backscatter as a function of FDOM (bottom). Chlorophyll concentration is indicated by symbol size. Colors correspond to depth in the water column.
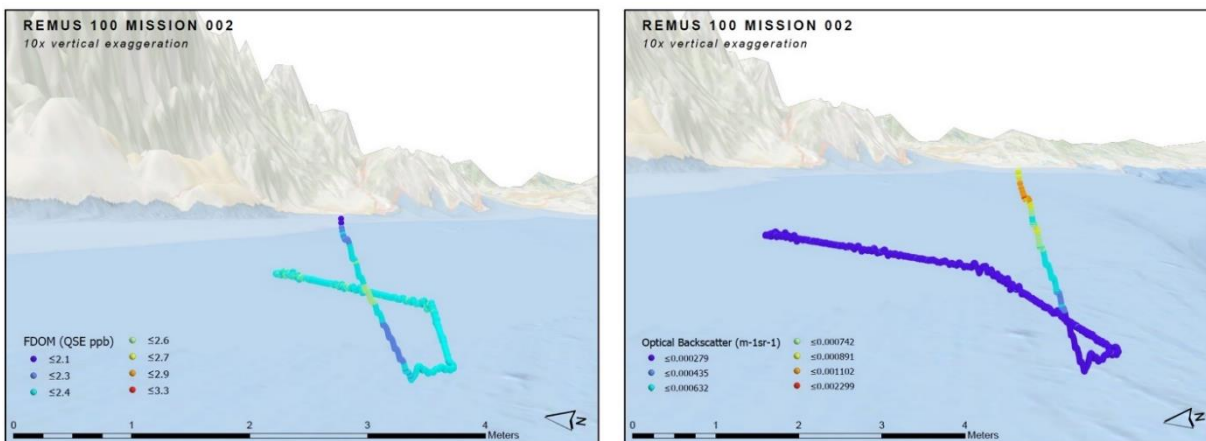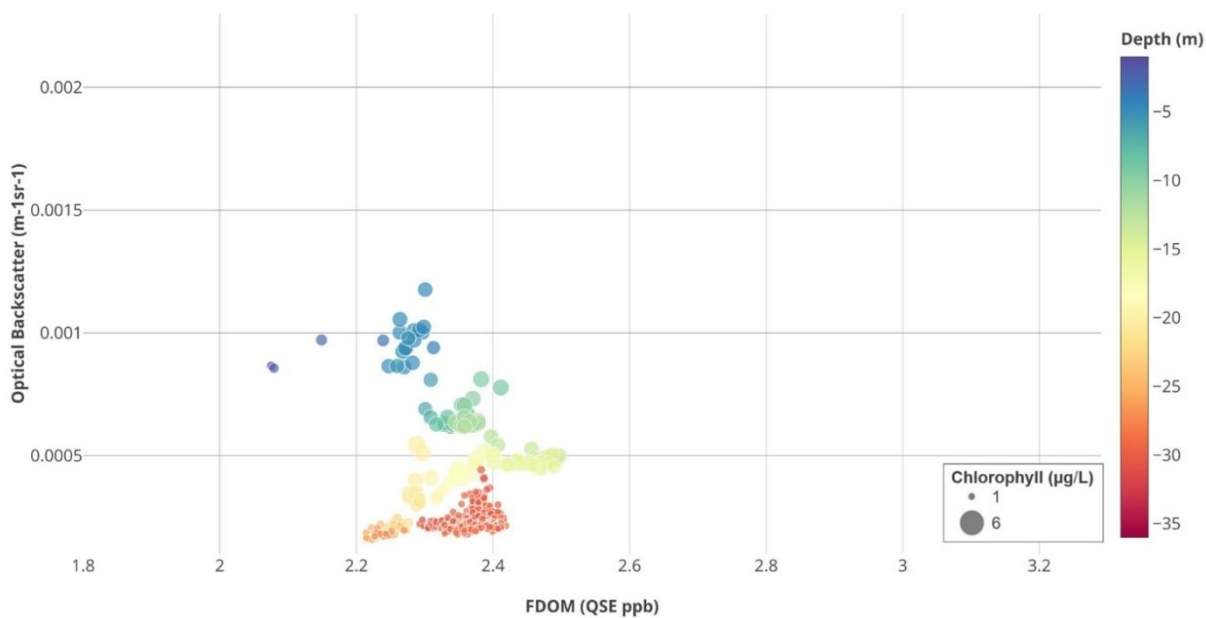
C.2.4   REMUS-600 MSN006

The vehicle was directed to a point of interest discovered by the LRAUV earlier in the day and was set to do a rectangular "rows" mission that began at 11:14 (local). It completed two gulps before the mission was aborted in order to confirm gulping (RECON messages had been turned off to limit vehicle state and SeaOWL data). The mission ended at 12:37 (local).

Figure C.27. In REMUS-600 MSN006 two gulps took place before the vehicle was redirected to another location.

Figure C.28. FDOM and optical backscatter measurements along the REMUS-600 vehicle track (top) for Mission 6. Colors correspond to concentration. Scatter plot of optical backscatter as a function of FDOM (bottom). Chlorophyll concentration is indicated by symbol size. Colors correspond to depth in the water column.
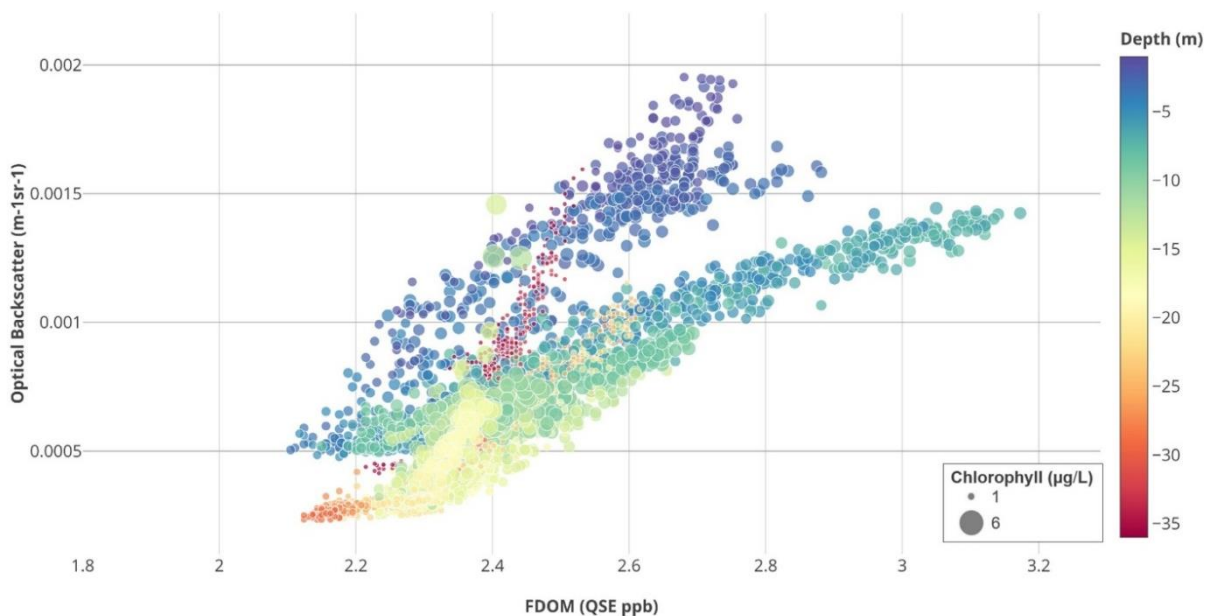
Figure C.29. Depth vertical profiles of OBS (left), FDOM (middle), and CHL (right) during REMUS-600 MSN006.
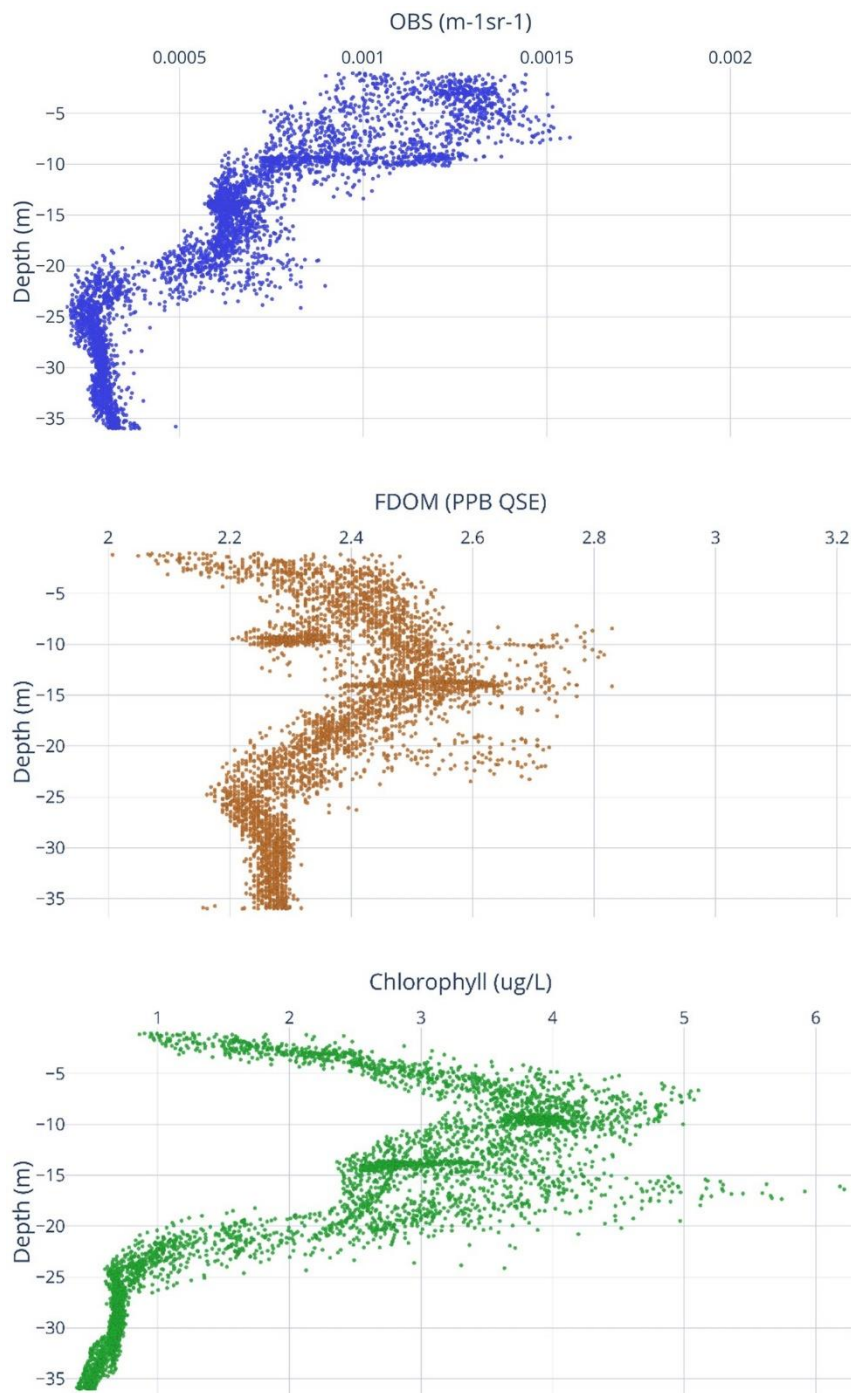
C.2.5 REMUS-100 MSN003

With the new ballard limit, the REMUS-100 started a new rectangular rows mission at 12:25 (local), which overlapped the gulps of the REMUS-600 missions. This mission continued for the rest of the day until it was aborted at 15:47 for recovery.

Figure C.30. The REMUS-100 MSN003 worked its way inland to survey the same area as the REMUS-600.

Figure C.31. FDOM and optical backscatter measurements along the REMUS-100 vehicle track (top) for Mission 3. Colors correspond to concentration. Scatter plot of optical backscatter as a function of FDOM (bottom). Chlorophyll concentration is indicated by symbol size. Colors correspond to depth in the water column.
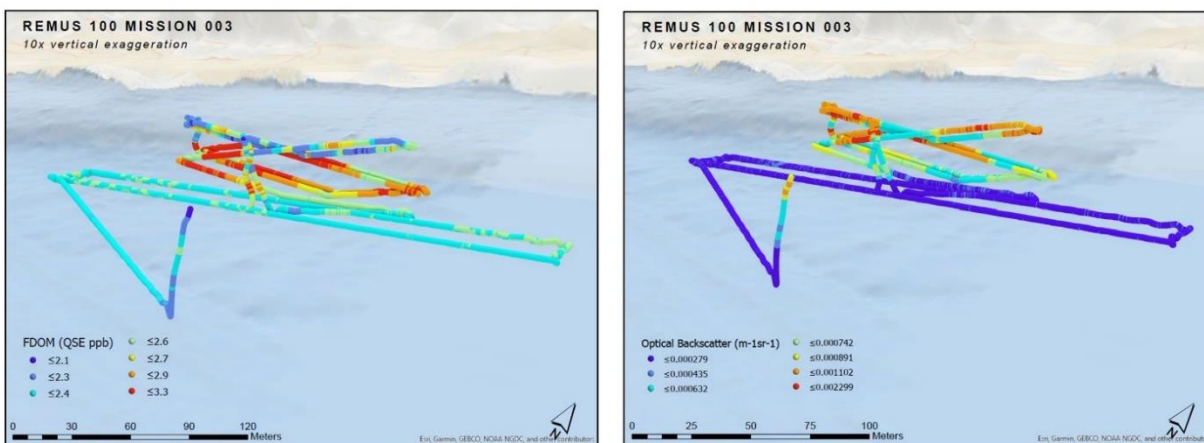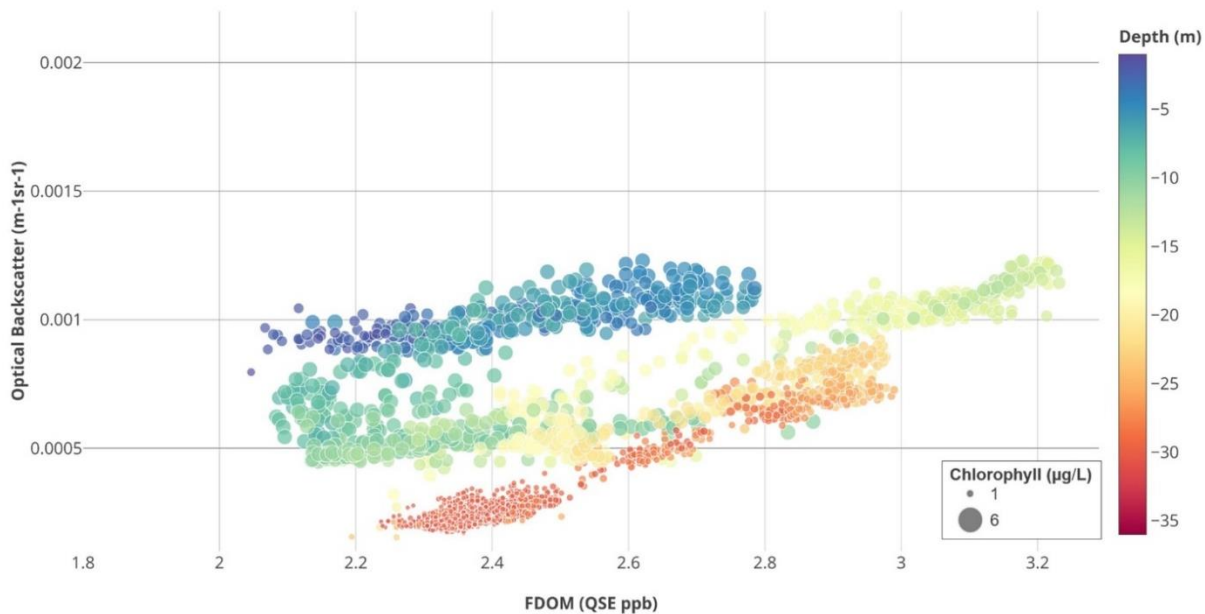
C.2.6 REMUS-600 MSN007

After gulps had been confirmed, the REMUS-600 was sent into another rectangular rows mission slightly inland of the last one. This mission started at 12:53 (local) and took 6 gulps before it was ended at 14:53 so that the REMUS could be programed for a lawnmower mission instead of repeating continuously over the same rectangle.

Figure C.32. During REMUS-600 MSN007 the vehicle completed six separate gulps during the first leg of the mission.

Figure C.33. FDOM and optical backscatter measurements along the REMUS-600 vehicle track (top) for Mission 7. Colors correspond to concentration. Scatter plot of optical backscatter as a function of FDOM (bottom). Chlorophyll concentration is indicated by symbol size. Colors correspond to depth in the water column.
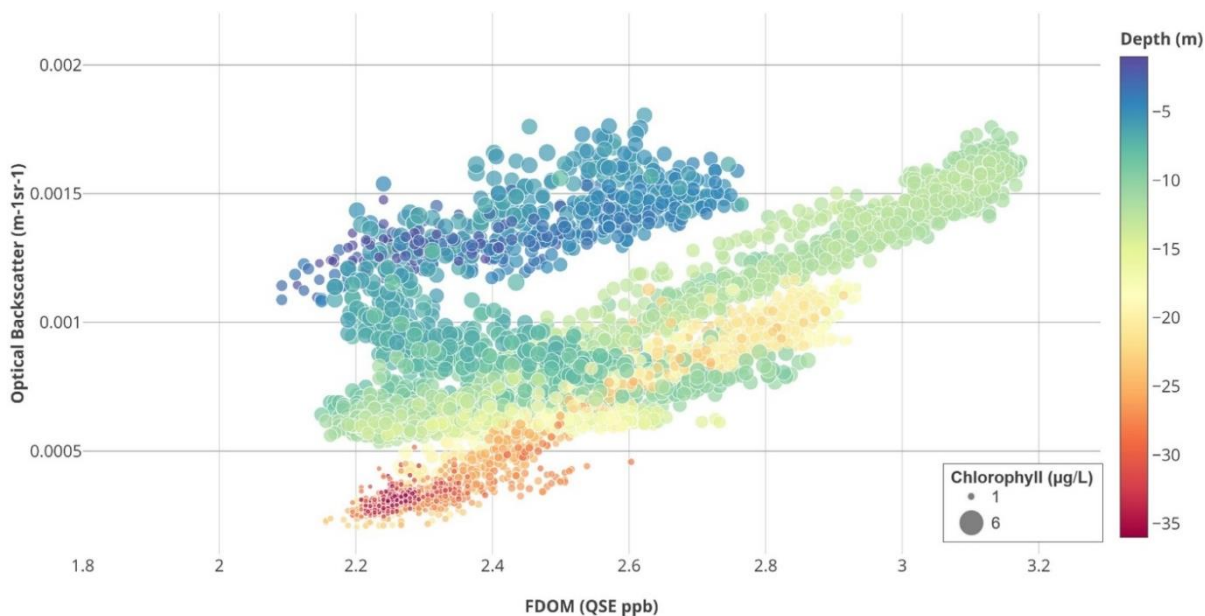
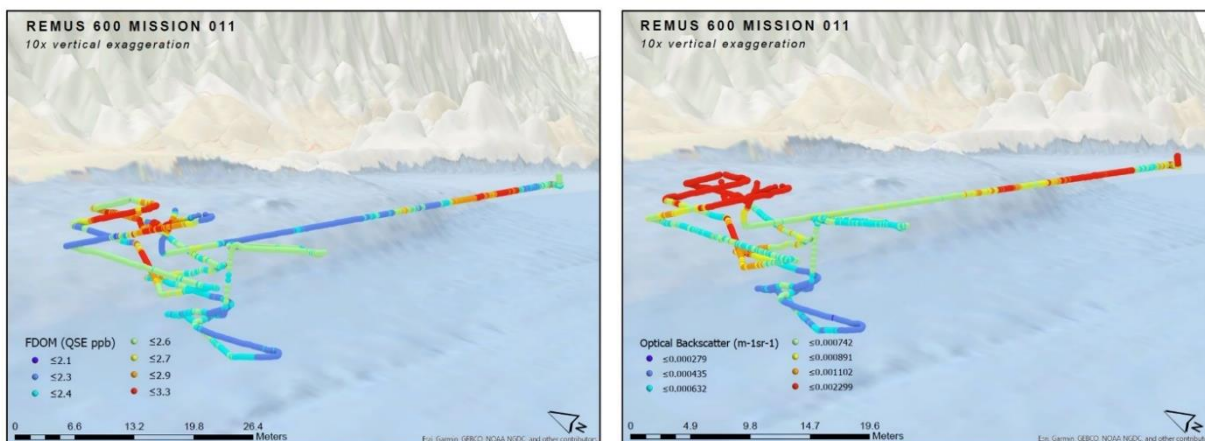**Figure C.34. Depth vertical profiles of OBS (left), FDOM (middle), and CHL (right) during REMUS-600 MSN007.**
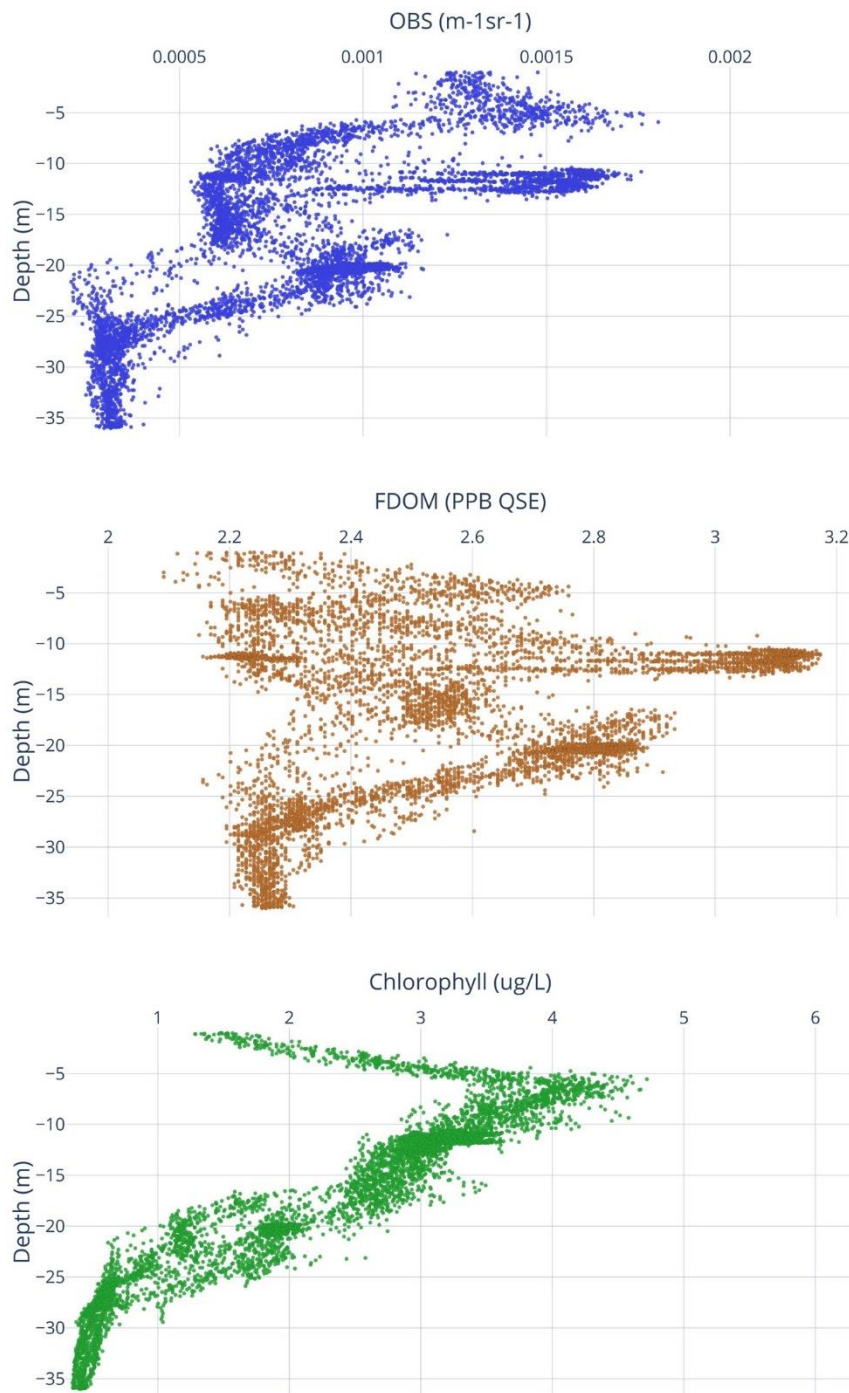
C.2.7   REMUS-600 MSN008

The seventh mission was a yo-yo pattern along a lawnmower path moving more and more inland. The mission began at 15:12 and around this time the REMUS-100 was also redirected to follow this path without beginning a new mission. One gulp was taken during this mission, but the mission was aborted soon after, at 15:39, in order to raise the threshold for SeaOWL triggering. Since the samples take five days to process and use methane and other gases in order to do so, low-level oil samples are undesirable.

Figure C.35. Two gulps were taken during REMUS-600 MSN008 before it was aborted to change gulping parameters.

Figure C.36. FDOM and optical backscatter measurements along the REMUS-600 vehicle track (top) for Mission 8. Colors correspond to concentration. Scatter plot of optical backscatter as a function of FDOM (bottom). Chlorophyll concentration is indicated by symbol size. Colors correspond to depth in the water column.
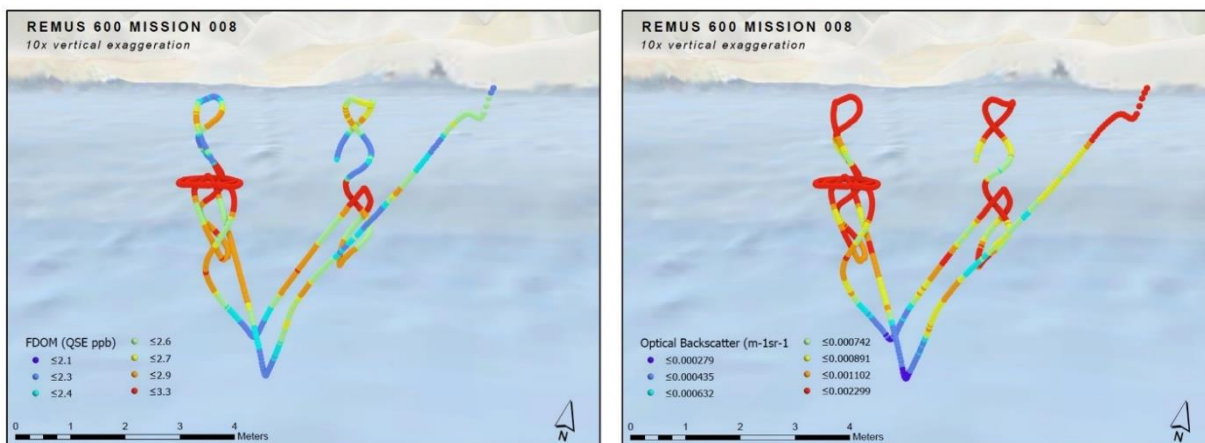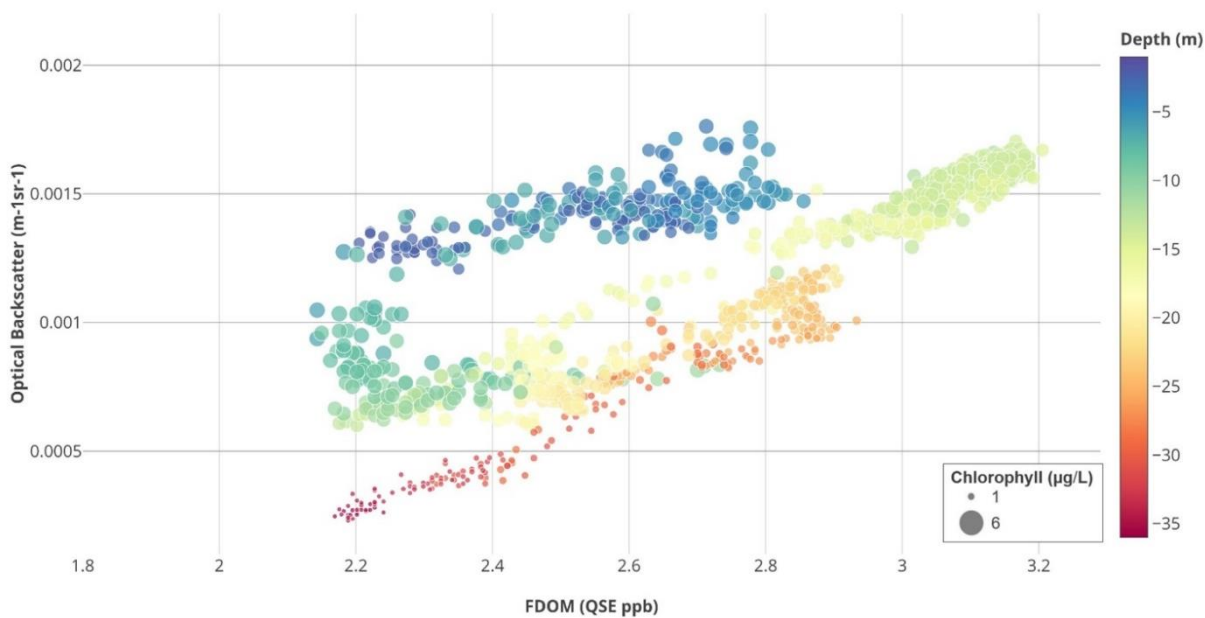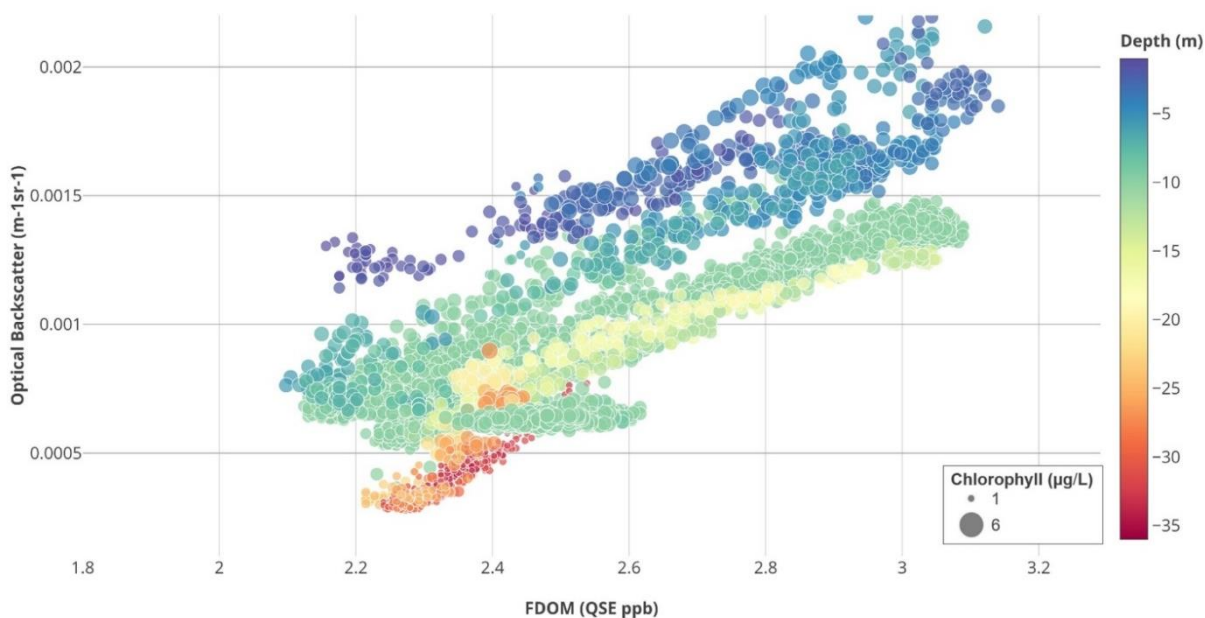
Figure C.37. Depth vertical profiles of OBS (left), FDOM (middle), and CHL (right) during REMUS-600 MSN008.
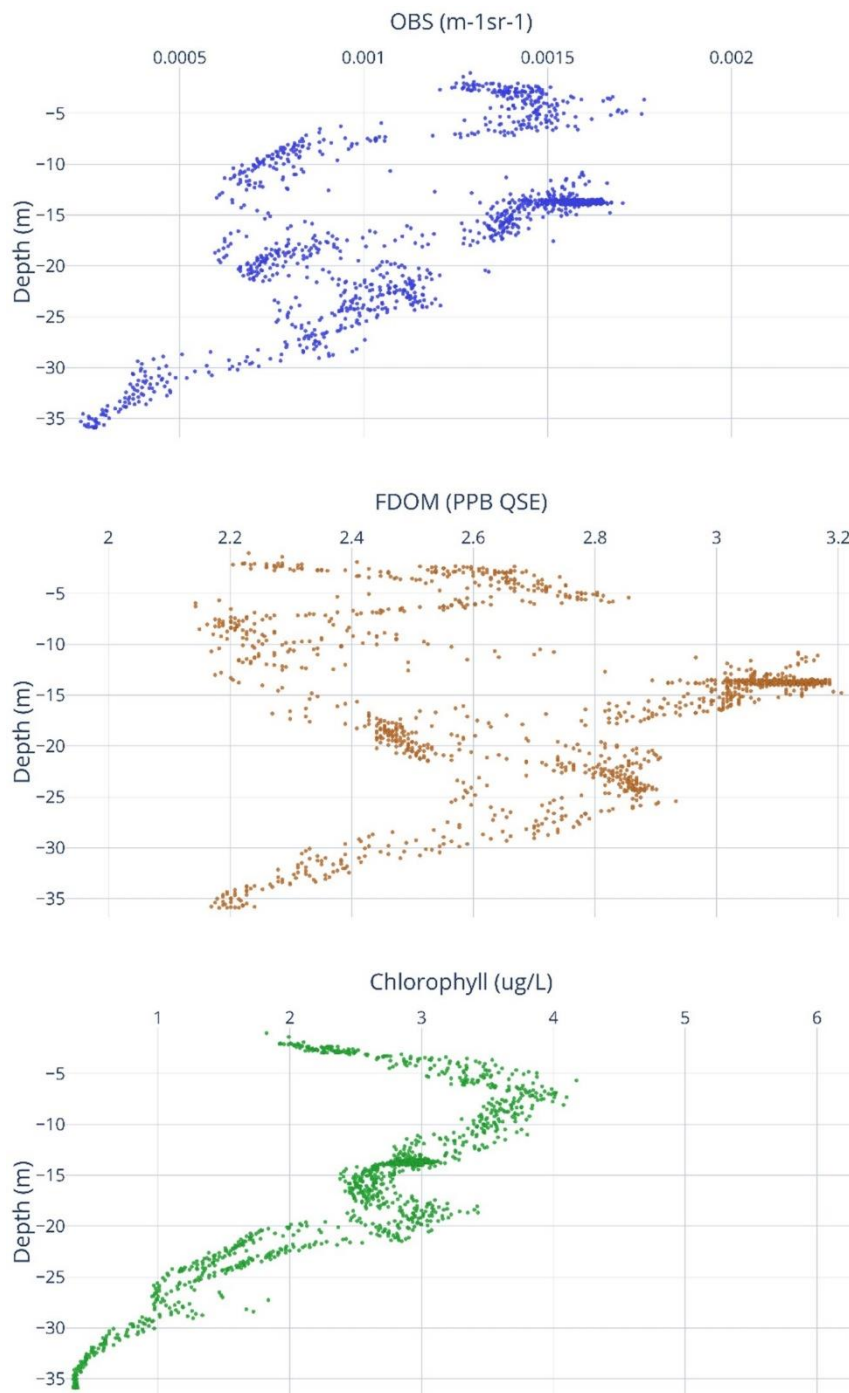
C.2.8 REMUS-600 MSN009

The final mission of the day began at 15:45; however, because of the two trip blanks, all bottles were already filled and the mission was aborted at 16:35 for recovery.

Figure C.38. During the final mission of the day, REMUS-600 MSN009, the vehicle traversed a large area, not gulping since the bottles were already filled.

Figure C.39. FDOM and optical backscatter measurements along the REMUS-600 vehicle track (top) for Mission 9. Colors correspond to concentration. Scatter plot of optical backscatter as a function of FDOM (bottom). Chlorophyll concentration is indicated by symbol size. Colors correspond to depth in the water column.

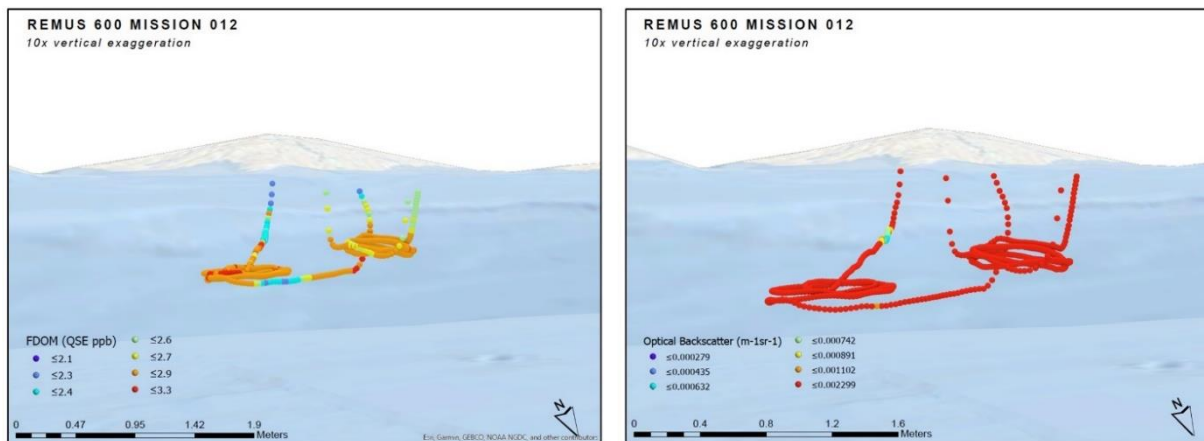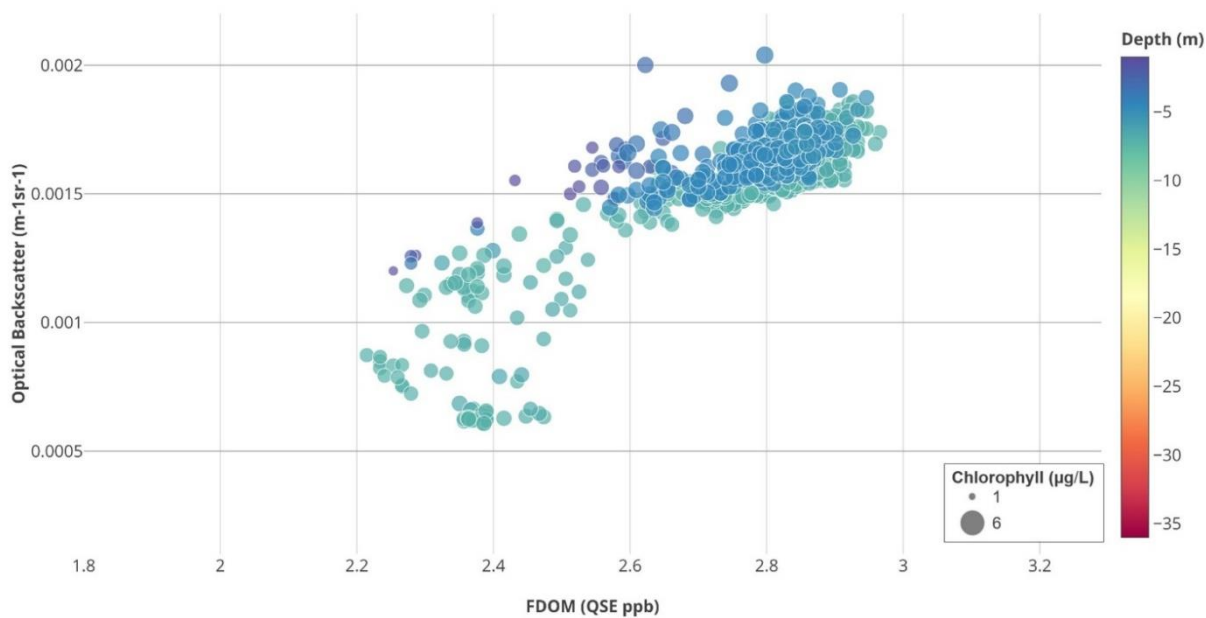**Figure C.40. Depth vertical profiles of OBS (left), FDOM (middle), and CHL (right) during REMUS-600 MSN009.**
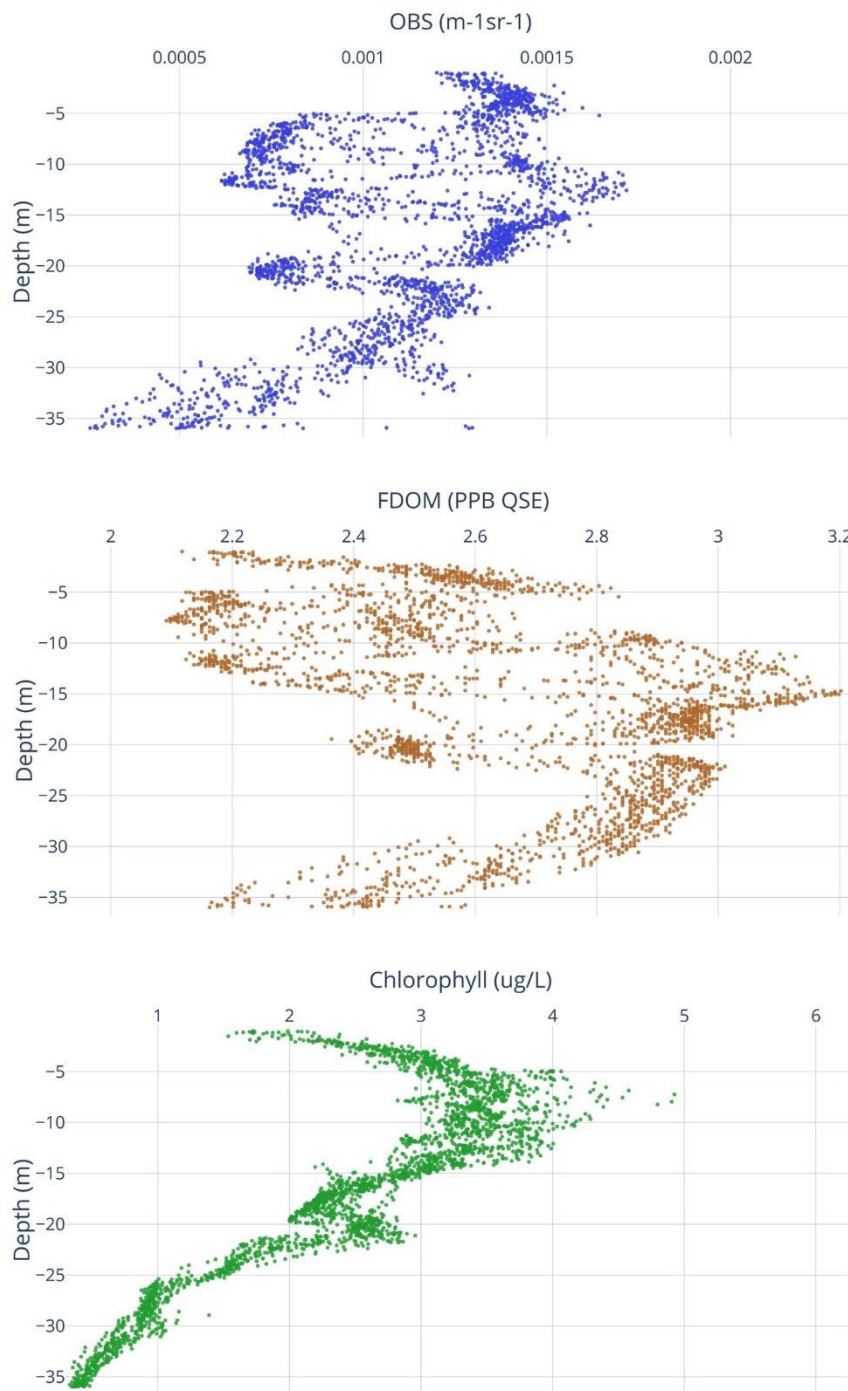
C.3   Day 8: Wednesday, August 28, 2019

The main objective of the August 28 deployment was to survey a large area, identify some hot spots, and bring the REMUS-600 back to those hot spots to take gulps. Additionally, the drone from the NOAA contractor, Water Mapper, would be flown over the same area as the vehicles. So far the oil slicks identified by the drone were not able to inform where to send the vehicle, since the surface oil did not seem to correspond with oil in the water column; however, the overlay of drone footage and vehicle data are still useful information. Unfortunately, despite seeing oil bubbling to the surface in different areas throughout the day, FDOM signals picked up by the vehicles were extremely low for the entire day, and no gulps were taken. The EPA did take manual bulk oil samples from the surface, to be used for their analysis of the water oil mixtures later. It is suspected that because of the calm weather, the oil rose through the water in contained bubbles, and was not dispersed enough for the vehicle to pick up a strong sustained signal.

The location of the first mission was chosen based on REMUS-100 EK80 data from the night before, where we observed what looked like bubbles or oil droplets rising to the surface.

Figure C.41. The red tracks are the REMUS-600 mission and the yellow tracks are the REMUS-100 missions from August 28. The vehicles began at a hot spot identified by the LRAUV and then transited to the known hot spot Trilogy.
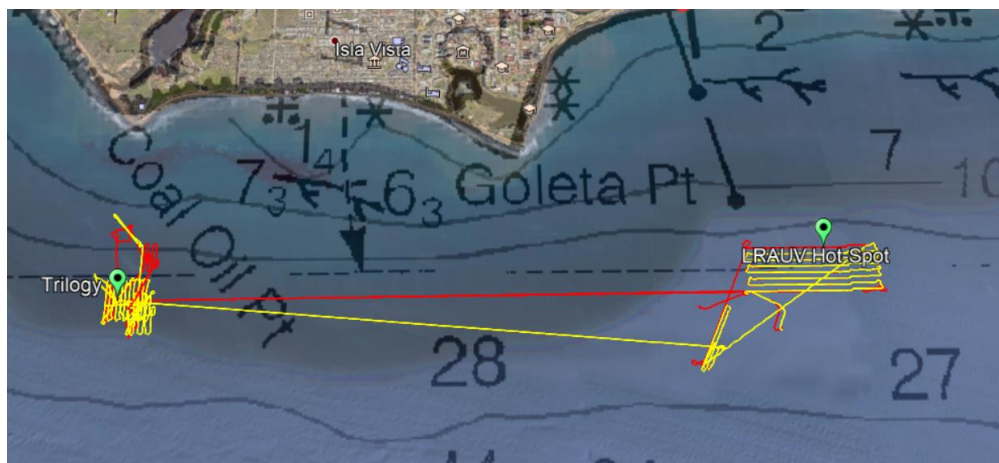
C.3.1 REMUS-600 MSN010

The REMUS-600 was launched near the EK80 signals from the day before at 34N23.508, 119W49.410 and the first mission of the day, MSN010, was started at 10:45. The mission was a lawnmower path in order to survey the area for potential oil hot spots. At 12:17, having not recorded any high FDOM counts, the vehicle was rerouted to survey a different area. The C3 was sent topside and the vehicle began a new, slightly offset lawnmower path; however, it then displayed the behavior where it reset itself in order to recalibrate PHINS, so the mission was aborted around 12:45 and the end of the mission was lost. Further analysis showed that the vehicle software has a feature that can be rectified back at Woods Hole. This "feature," now known, did not interrupt the remaining missions.

Figure C.42. The REMUS-600 MSN010 was a lawnmower path surveying the area identified as a hot spot by the LRAUV the night before.
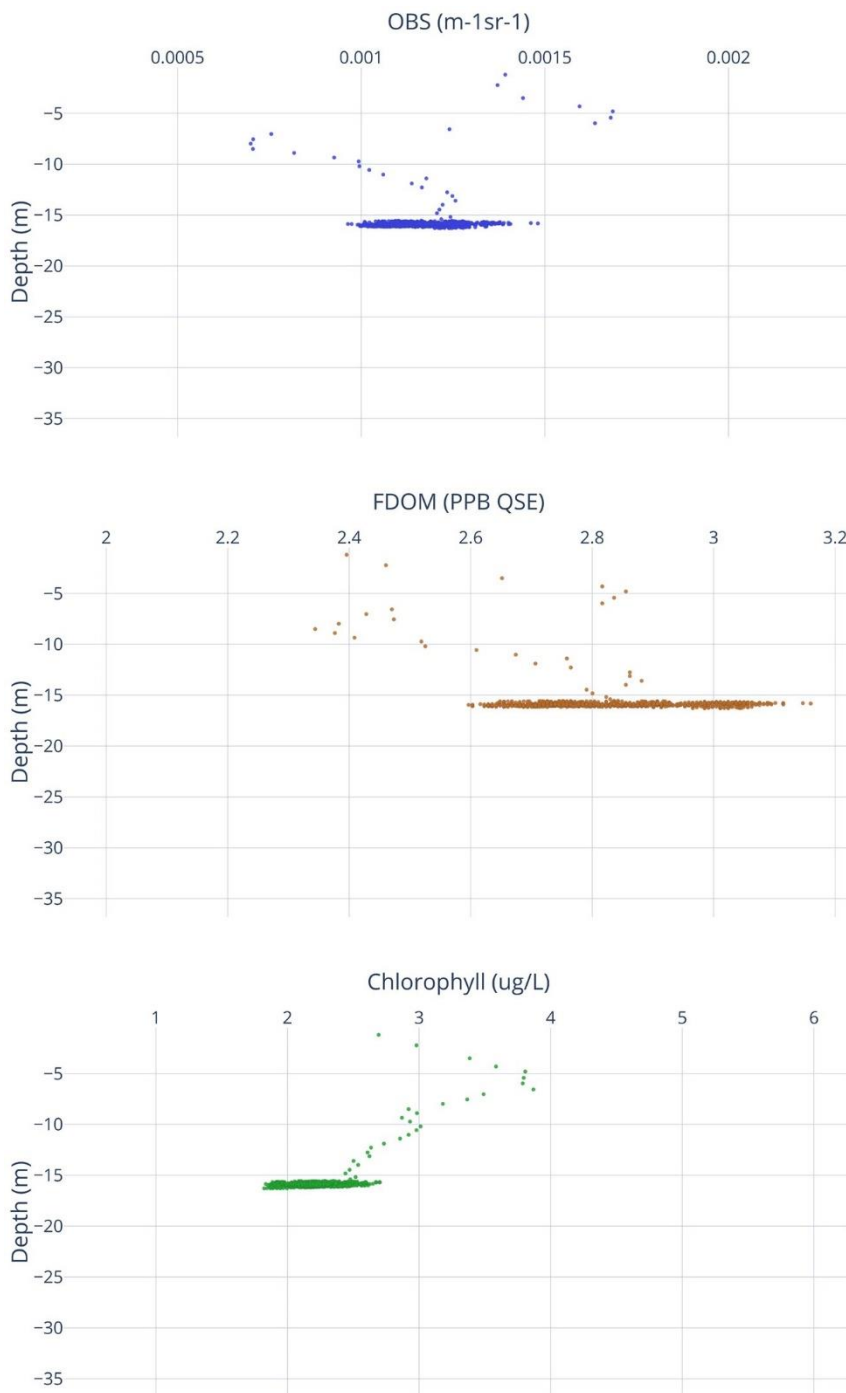
Figure C.43. FDOM and optical backscatter measurements along the REMUS-600 vehicle track (top) for Mission 10. Colors correspond to concentration. Scatter plot of optical backscatter as a function of FDOM (bottom). Chlorophyll concentration is indicated by symbol size. Colors correspond to depth in the water column.
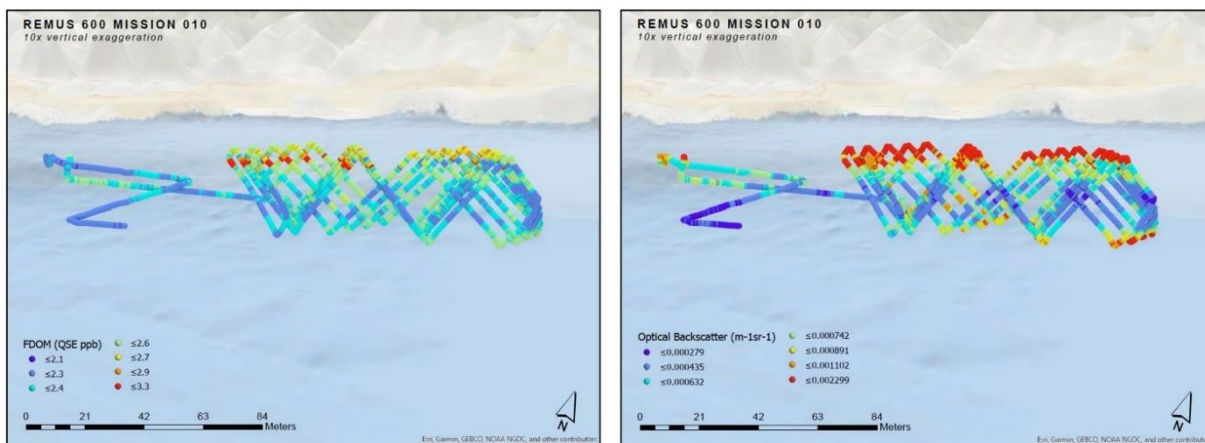
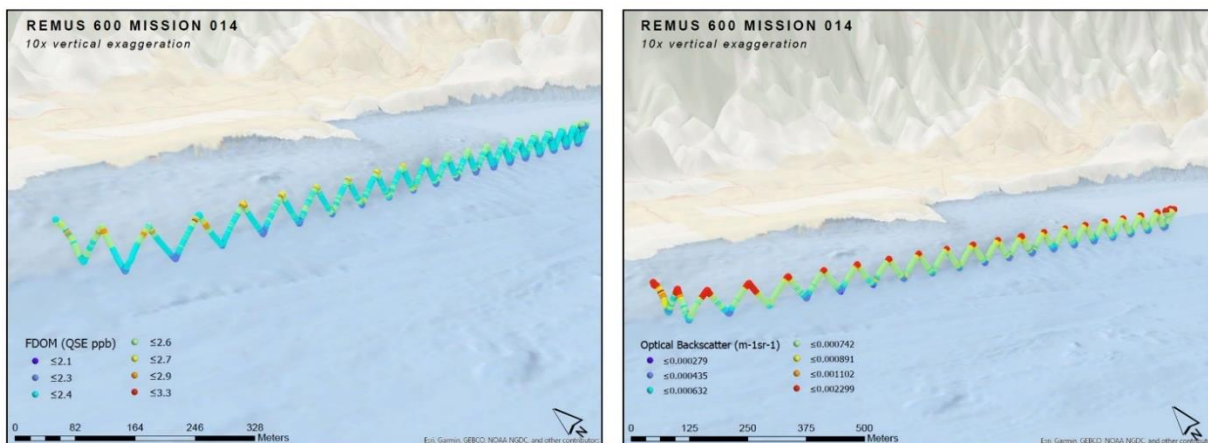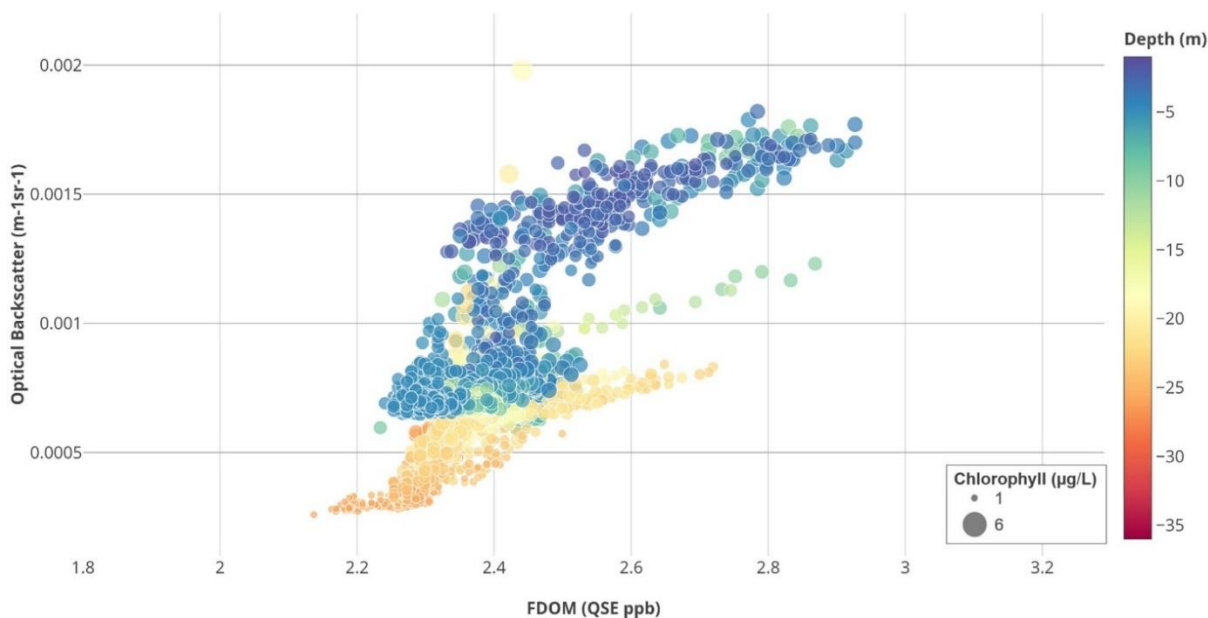**Figure C.44. Depth vertical profiles of OBS (left), FDOM (middle), and CHL (right) during REMUS-600 MSN010.**
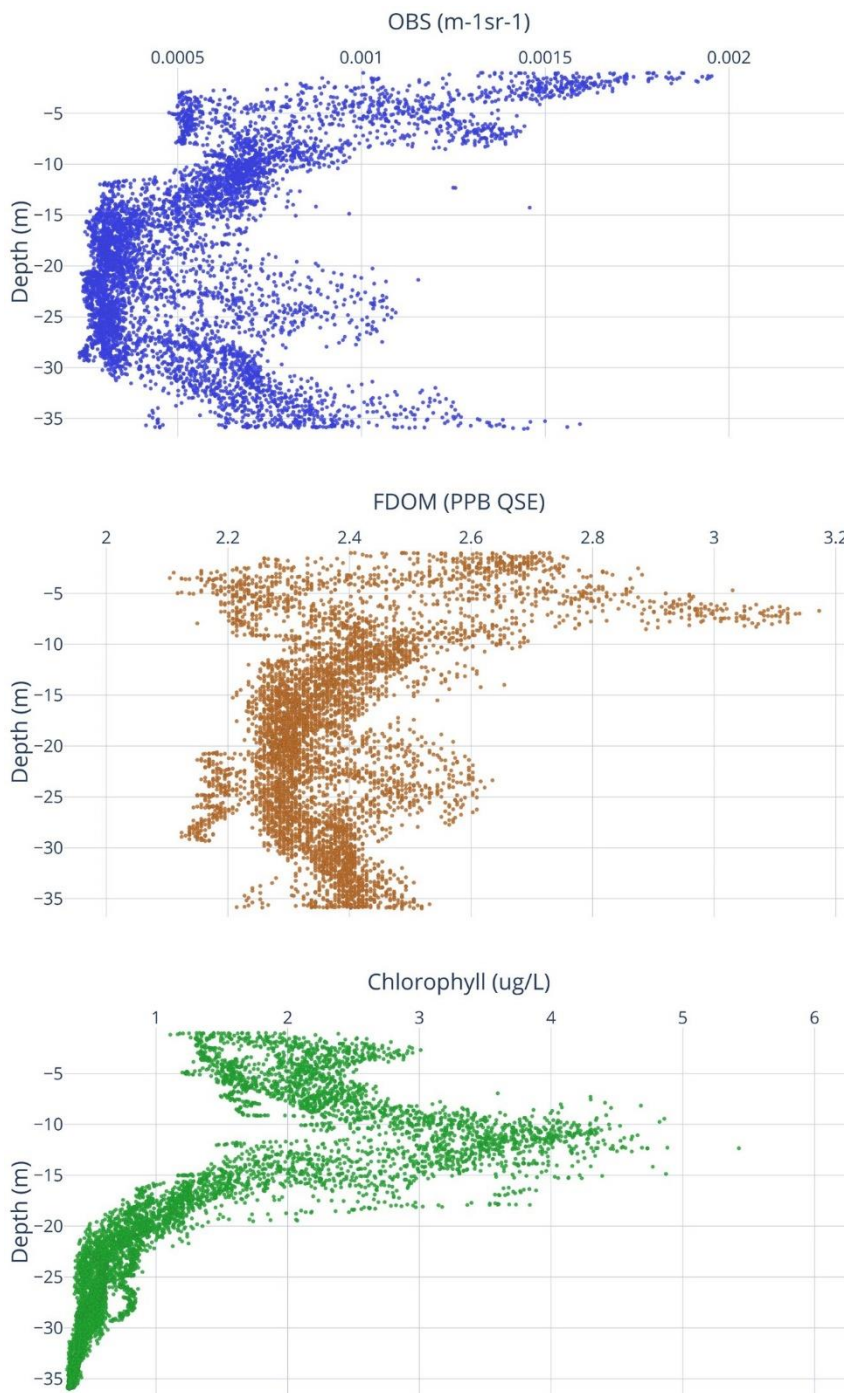
C.3.2   REMUS-100 MSN004

The REMUS-100 ran only one mission for the full day, which began at 10:59; however, it was redirected many times to survey different areas. Generally, it was used to survey slightly offset areas from the REMUS-600 in order to broaden our search area. At 15:32, the REMUS-100's battery ran out and went dead in the water. It was spotted from the George Cobb based on its last location and was recovered without issue. Both launches and recoveries went much smoother than the day before, and neither vehicle hit the side during any point.

Figure C.45. The REMUS-100 ran one mission on August 28, first surveying the area of the LRAUV-identified hot spot and then transitioning to survey the area around the known Trilogy hot spot.

Figure C.46. FDOM and optical backscatter measurements along the REMUS-100 vehicle track (top) for Mission 4. Colors correspond to concentration. Scatter plot of optical backscatter as a function of FDOM (bottom). Chlorophyll concentration is indicated by symbol size. Colors correspond to depth in the water column.
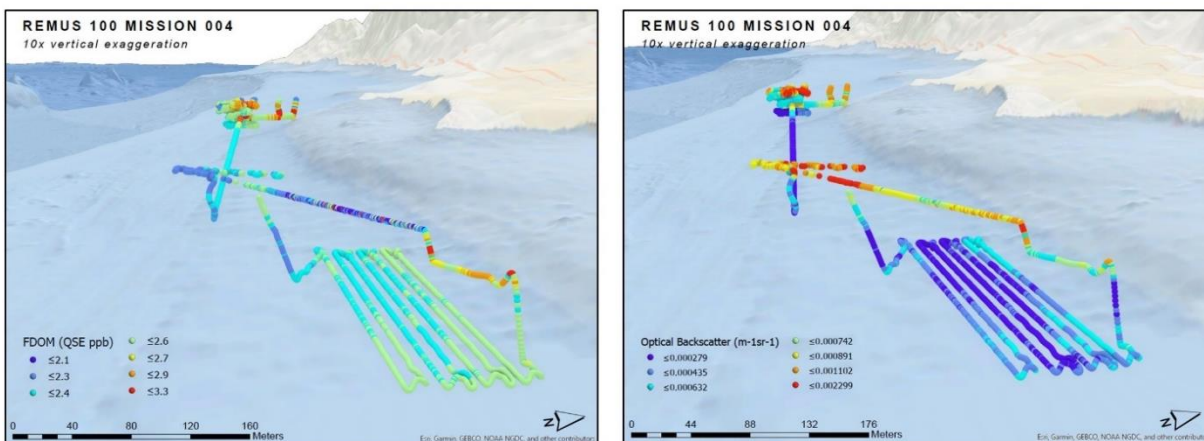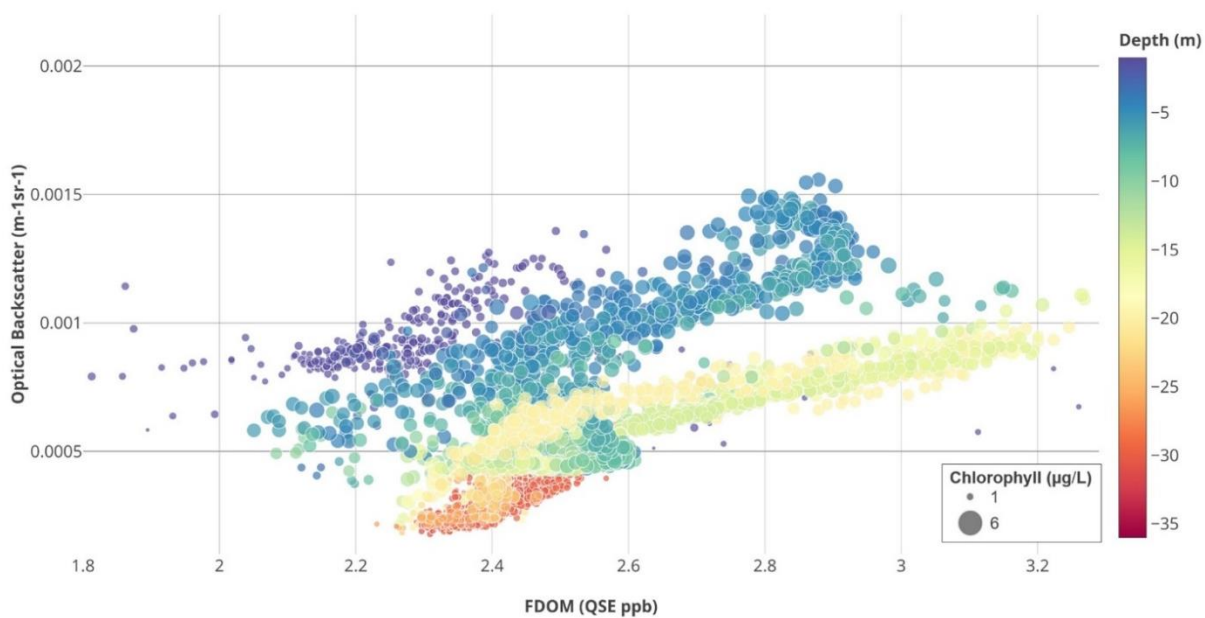
C.3.3   REMUS-600 MSN011

After the mission was aborted due to the PHINS reset, the vehicle's new mission began at 13:09 (local), where it was directed to transit to the hot spot Trilogy off the coast of Coal Point. This area displayed high oil counts in the past, and is locally known as the area of a very active seep. The vehicle reached this location and at 14:10 it was directed to begin a lawnmower path, but no high FDOM counts were recorded, and at 14:20, the vehicle was redirected again. It began another lawnmower path more inland near Horseshoe seep, another known seep in the area. It was relocated once more at 14:32 to begin a lawnmower path in a more southern area based on a high reading from the REMUS-100, which turned out to be an anomaly. At 14:58 the mission was aborted in order to reprogram the vehicle, and allow it to adaptively gulp if it found anything interesting, rather than just survey.

Figure C.47. During MSN011, the REMUS-600 transited from the LRAUV hot spot to a known seep in the area, Trilogy.
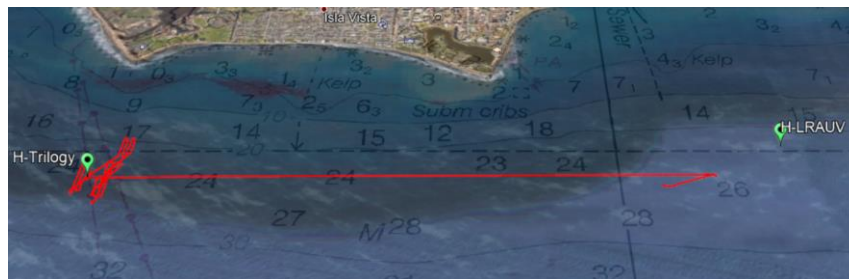
Figure C.48. FDOM and optical backscatter measurements along the REMUS-600 vehicle track (top) for Mission 11. Colors correspond to concentration. Scatter plot of optical backscatter as a function of FDOM (bottom). Chlorophyll concentration is indicated by symbol size. Colors correspond to depth in the water column.
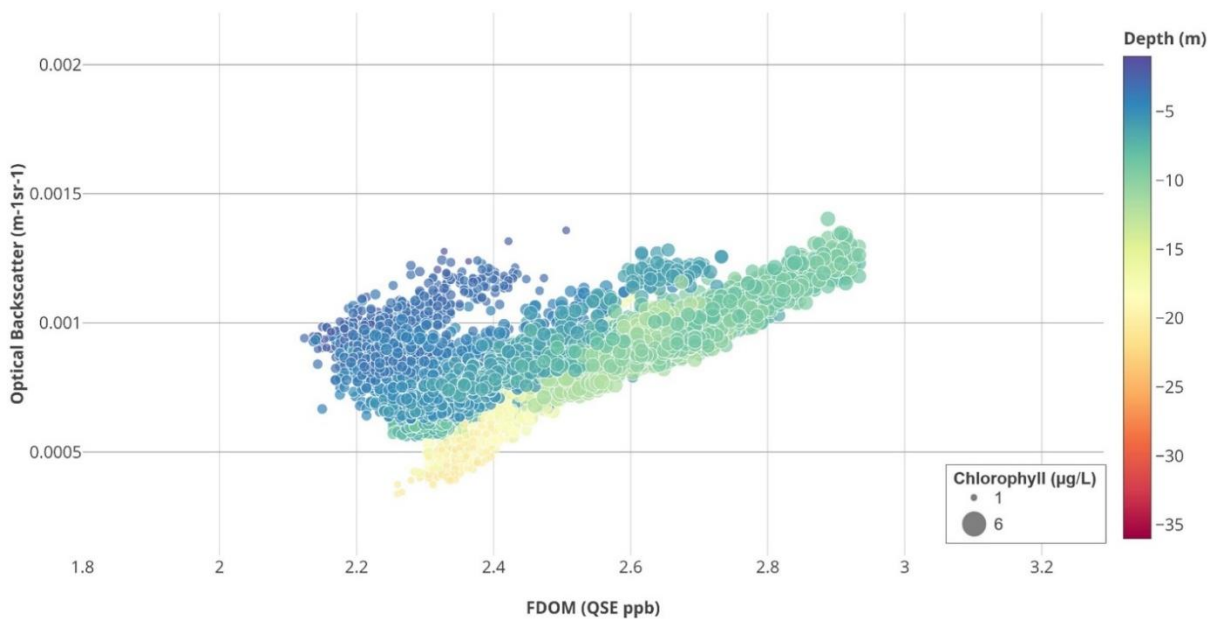
Figure C.49. Depth vertical profiles of OBS (left), FDOM (middle), and CHL (right) during REMUS-600 MSN011.
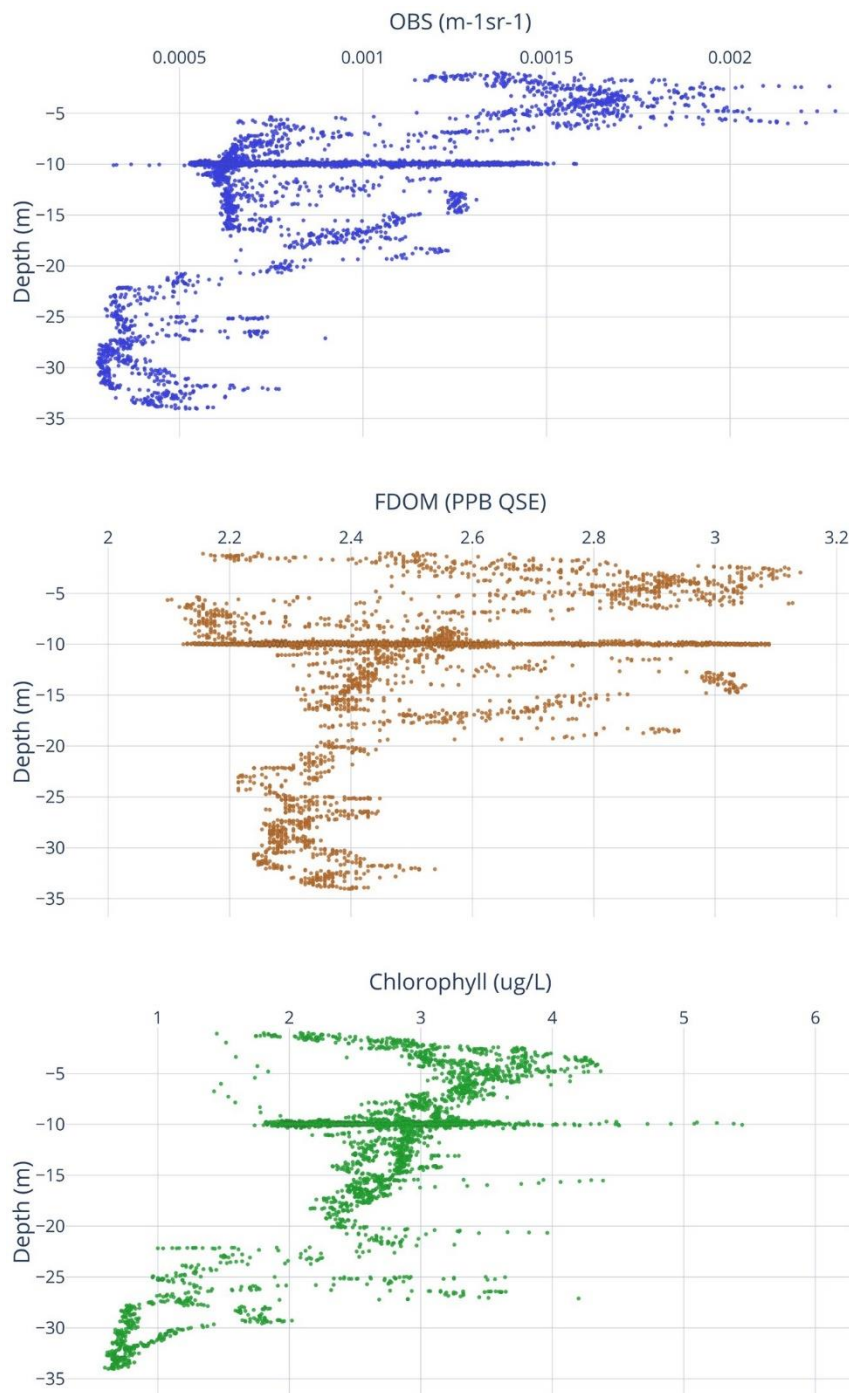
C.3.4 REMUS-600 MSN012

At 15:13, the twelfth mission began – the vehicle had been programed to drive in two circles and trigger an adaptive mission if it hit a signal of 30% above a 520 threshold. The adaptive mission never triggered due to extremely low oil signal in the area and the mission was aborted at 15:37 so the parameters could be changed and the vehicle moved to a different location.

Figure C.50. For MSN012, the REMUS-600 drove in two circles.

Figure C.51. FDOM and optical backscatter measurements along the REMUS-600 vehicle track (top) for Mission 12. Colors correspond to concentration. Scatter plot of optical backscatter as a function of FDOM (bottom). Chlorophyll concentration is indicated by symbol size. Colors correspond to depth in the water column.

**Figure C.52. Depth vertical profiles of OBS (left), FDOM (middle), and CHL (right) during REMUS-600 MSN012.**
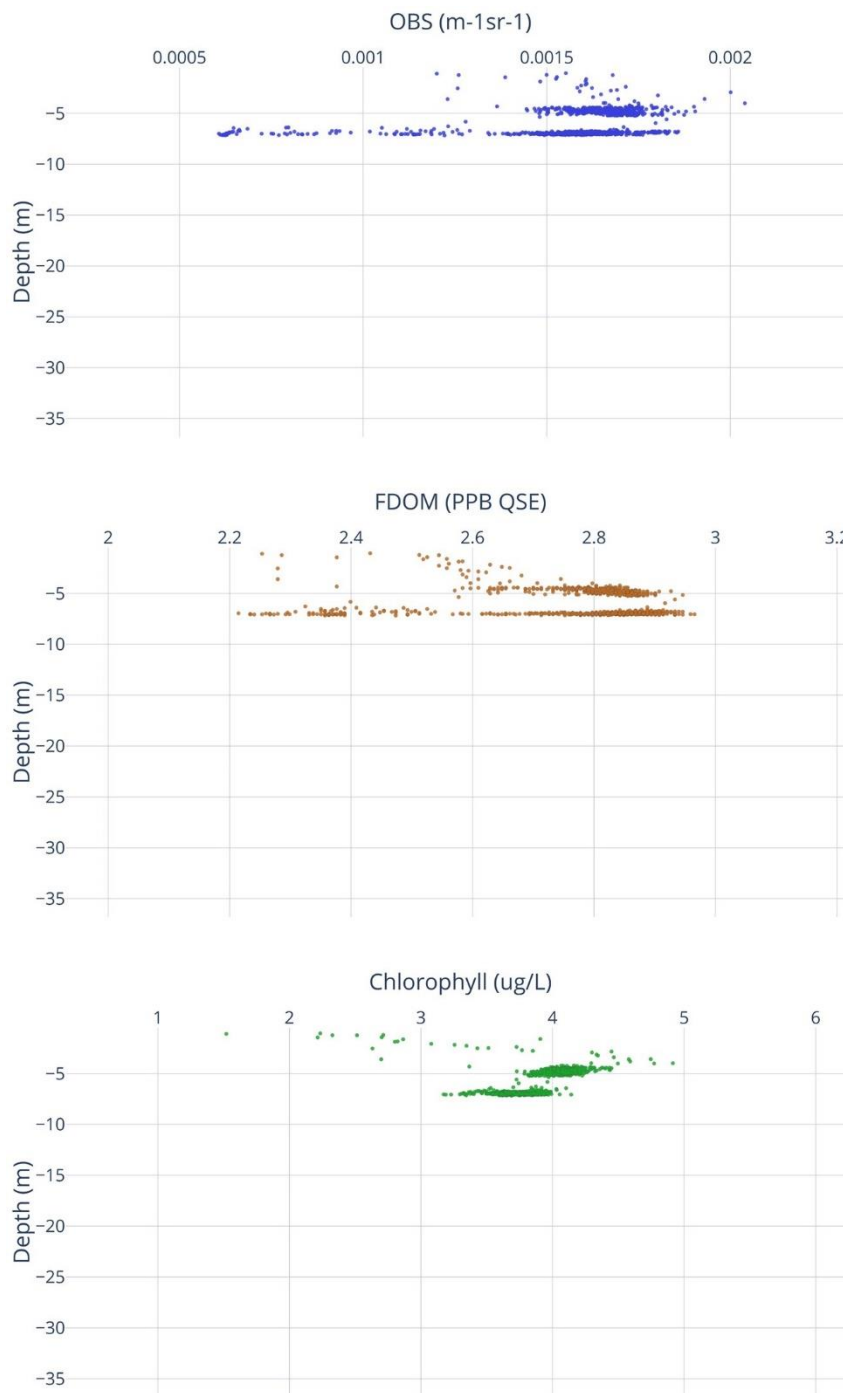
C.3.5 REMUS-600 MSN013

At 15:49 (local), a new mission began, this time in a square with the trigger for the adaptive mission set for when the vehicle detected a reading 10% above a 500 count threshold. Again, the vehicle did not encounter more than a baseline signal and never gulped. The past three missions were conducted off the coast of Coal Point, so at 16:15 the mission was aborted to give time for the vehicle to get back to the ship.

Figure C.53. The REMUS-600 drove in a square for MSN013, waiting for the adaptive mission to be triggered.

Figure C.54. FDOM and optical backscatter measurements along the REMUS-600 vehicle track (top) for Mission 13. Colors correspond to concentration. Scatter plot of optical backscatter as a function of FDOM (bottom). Chlorophyll concentration is indicated by symbol size. Colors correspond to depth in the water column.
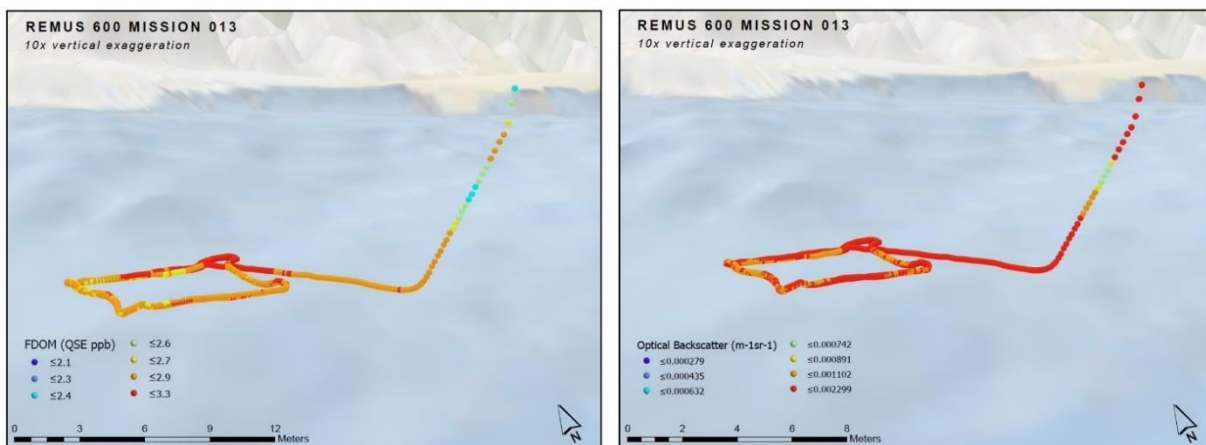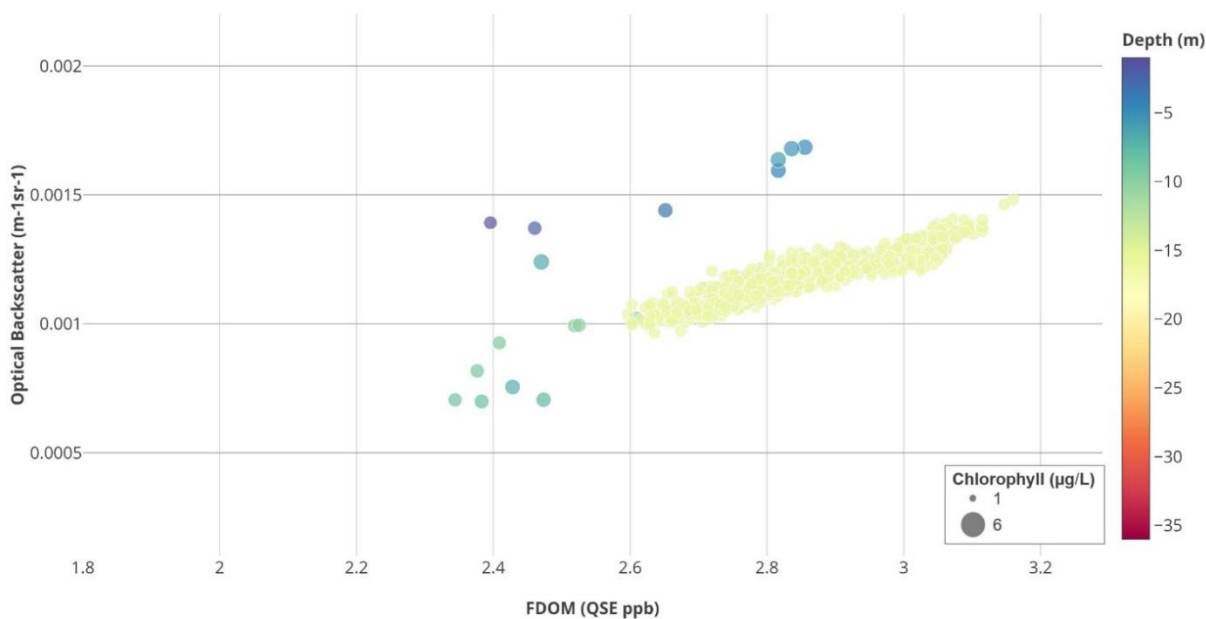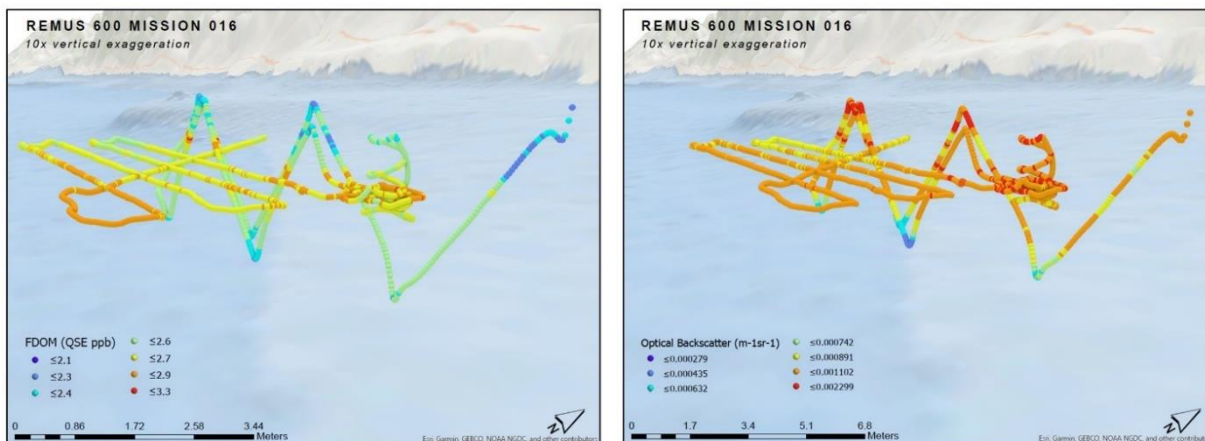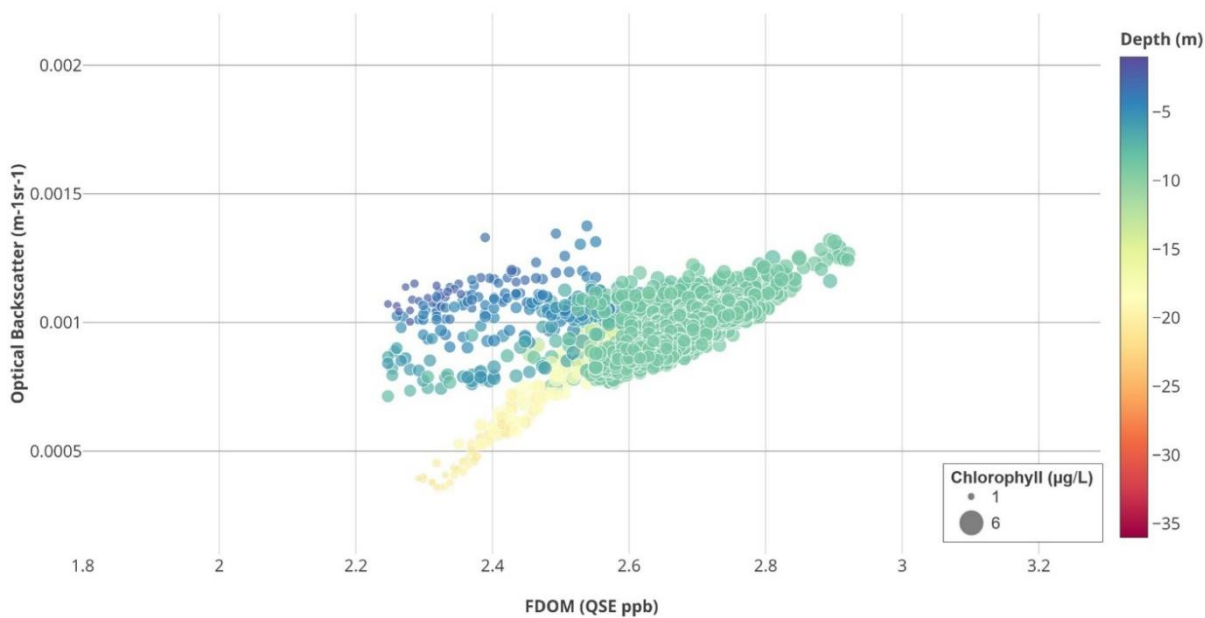
Figure C.55. Depth vertical profiles of OBS (left), FDOM (middle), and CHL (right) during REMUS-600 MSN013.

C.3.6   REMUS-600 MSN014

At 16:33 the vehicle started its final mission, which was a transit line back the way it had come before. The adaptive option was still set, but it never encountered a meaningful signal and never triggered. The mission was aborted at 17:59 and the vehicle was recovered successfully.

Figure C.56. In MSN014, the final mission of the day, the REMUS-600 transited back toward the LRAUV hot spot.
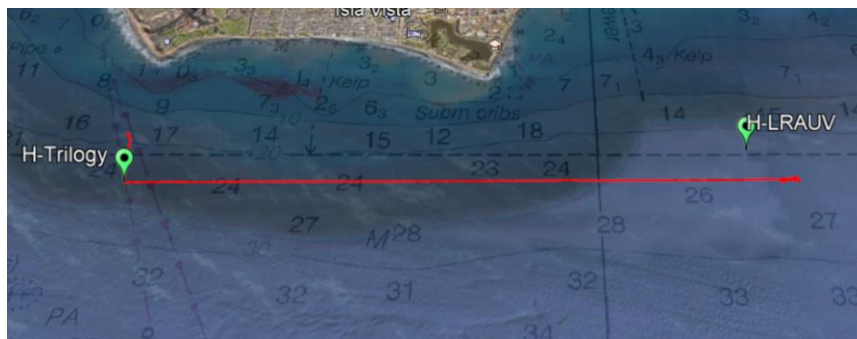
Figure C.57. FDOM and optical backscatter measurements along the REMUS-600 vehicle track (top) for Mission 14. Colors correspond to concentration. Scatter plot of optical backscatter as a function of FDOM (bottom). Chlorophyll concentration is indicated by symbol size. Colors correspond to depth in the water column.

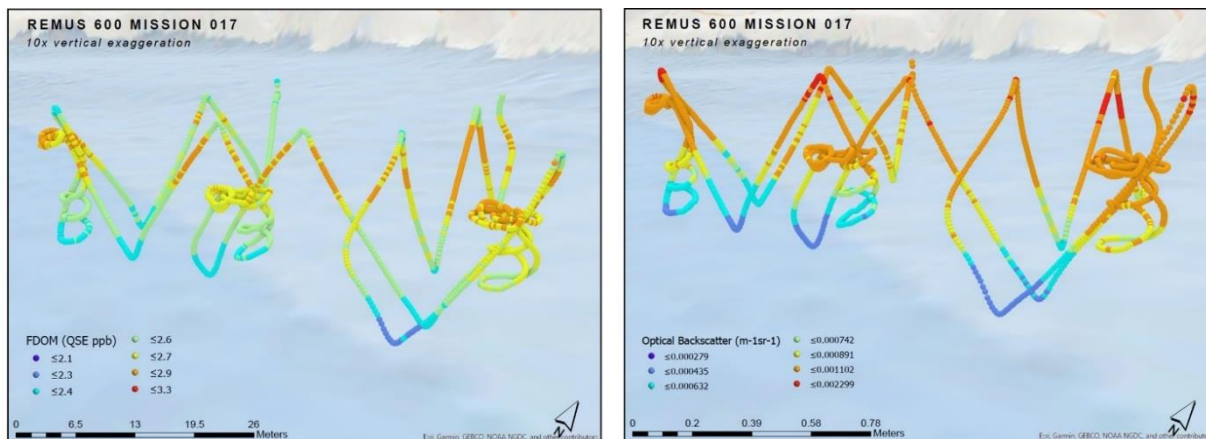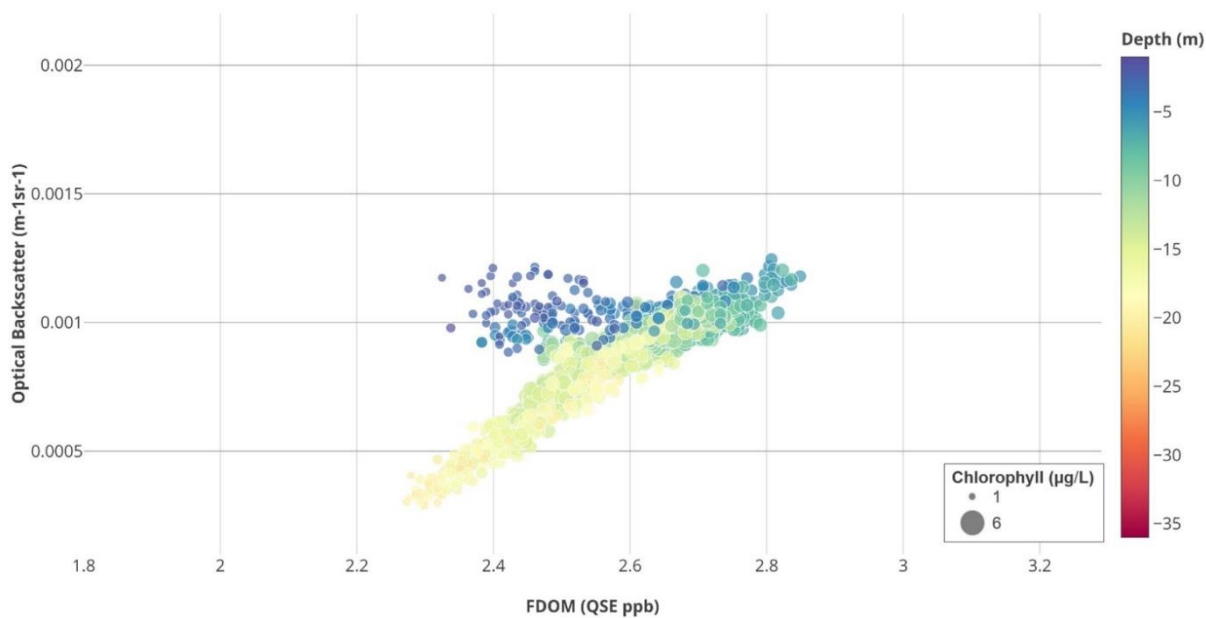**Figure C.58. Depth vertical profiles of OBS (left), FDOM (middle), and CHL (right) during REMUS-600 MSN014.**
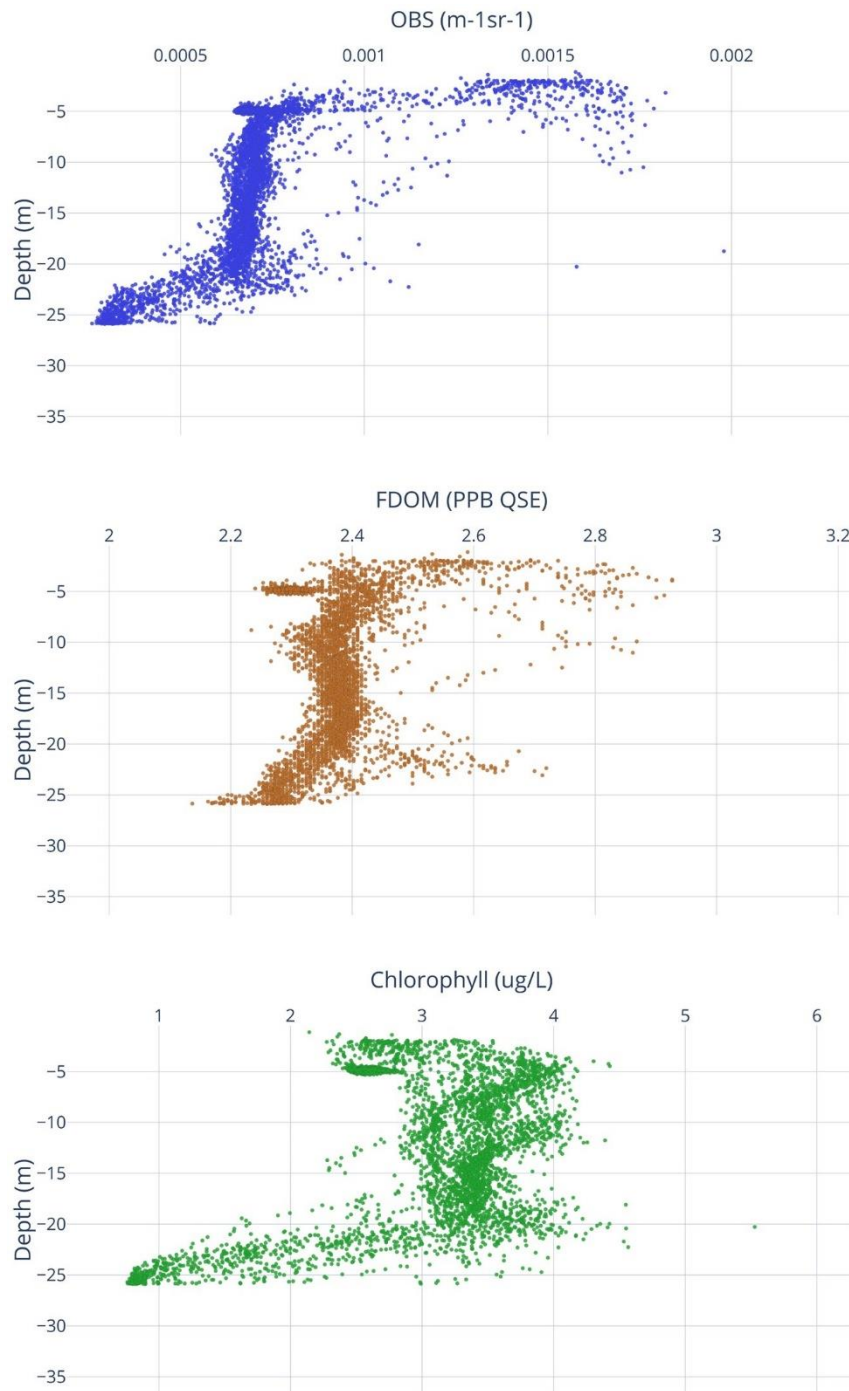
C.4 Day 9: Thursday, August 29, 2019

The objective of the day was to find high oil signals and sample, however, the lack of mixing of the oil seeps prevented the vehicles from finding very high FDOM counts at depths the REMUS-600 could gulp. LRAUV swam through the entire seep area the previous day, evening, and morning and also found lower signals in the water. Some light oil was encountered at the surface where the oil spreads out after the surface tension of the rising oil bubbles is disturbed, but the peristaltic pumps do not work if air from the surface is taken in; therefore, we do not pump while at the surface, just below at ~ 0.5 m. Instead of gulping at the surface with the REMUS-600, the REMUS-100 was run at a 1.5-m depth and samples were taken by hand using a boat pole, so the EPA could still have bottle samples that confirmed the SeaOWL readings from the AUV. The REMUS-600 continued to search for oil at depth, and tested a new double-gulp behavior.

Figure C.59. The missions on August 29 began at another hot spot identified by the LRAUV and then moved back east, searching for high oil signals.

C.4.1   REMUS-600 MSN015

The vehicle was initially deployed west of the Holly hot spot and sent in a lawnmower mission in order to search for elevated oil signals. Since only low FDOM counts were detected, the REMUS-100 deployment was initially held off. It was redirected twice (at 10:26 and 11:37) to lawnmower paths farther east, but oil was still not detected, and the mission was aborted at 12:24 (local).

Figure C.60. REMUS-600 MSN015 began near an LRAUV hot spot and then moved east toward the Holly hot spot as it searched for oil.

Figure C.61. FDOM and optical backscatter measurements along the REMUS-600 vehicle track (top) for Mission 15. Colors correspond to concentration. Scatter plot of optical backscatter as a function of FDOM (bottom). Chlorophyll concentration is indicated by symbol size. Colors correspond to depth in the water column.
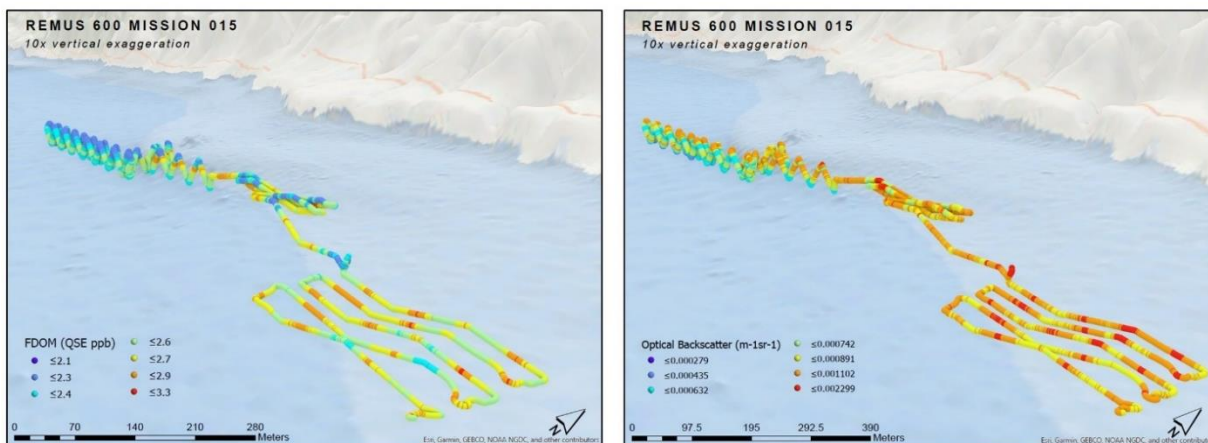
**Figure C.62. Depth vertical profiles of OBS (left), FDOM (middle), and CHL (right) during REMUS-600 MSN015.**
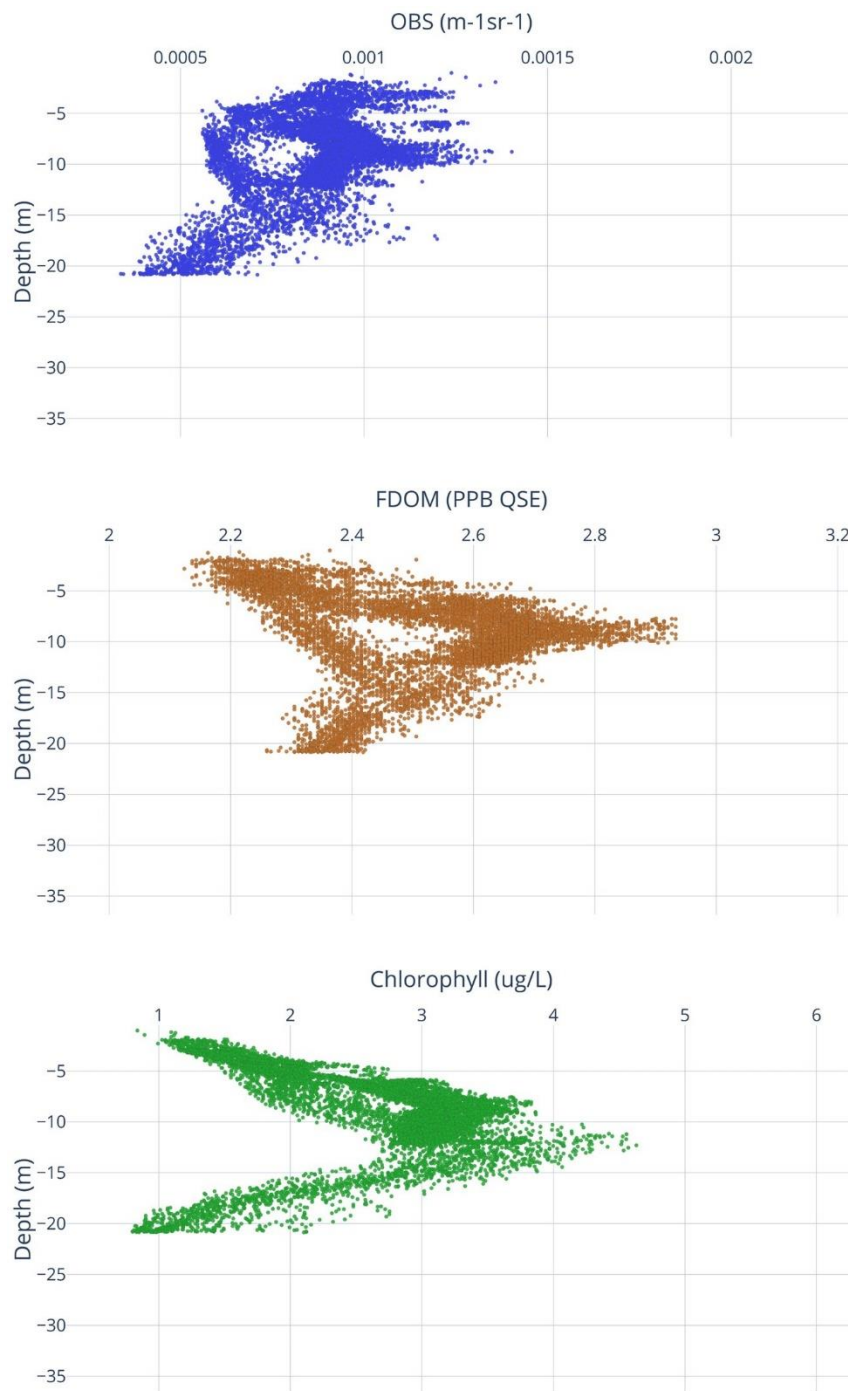
C.4.2 REMUS-100 MSN005

The REMUS-100 was launched and began its first mission at 12:10 (local), where it ran a lawnmower path set to a 1.5-m depth (in reality the vehicle fluctuated between surfacing and a 2-m depth). The mission was aborted at 13:16 so that the Cobb could approach, and the EPA gathered bottle samples next to the vehicle.

Figure C.63. During MSN005, the REMUS-100 made a lawnmower path east of the Holly hot spot.

Figure C.64. FDOM and optical backscatter measurements along the REMUS-100 vehicle track (top) for Mission 5. Colors correspond to concentration. Scatter plot of optical backscatter as a function of FDOM (bottom). Chlorophyll concentration is indicated by symbol size. Colors correspond to depth in the water column.
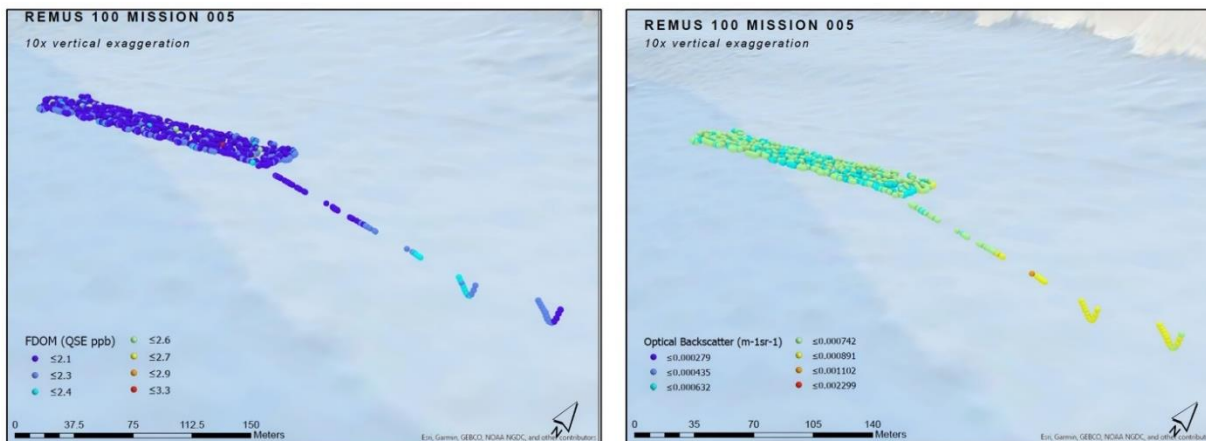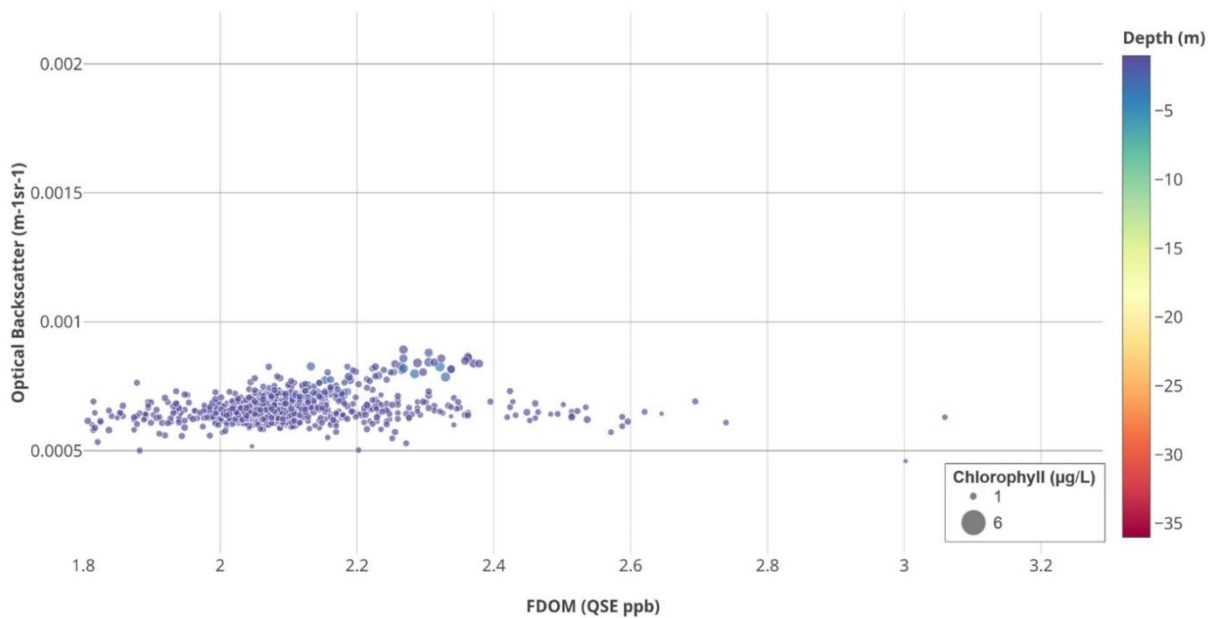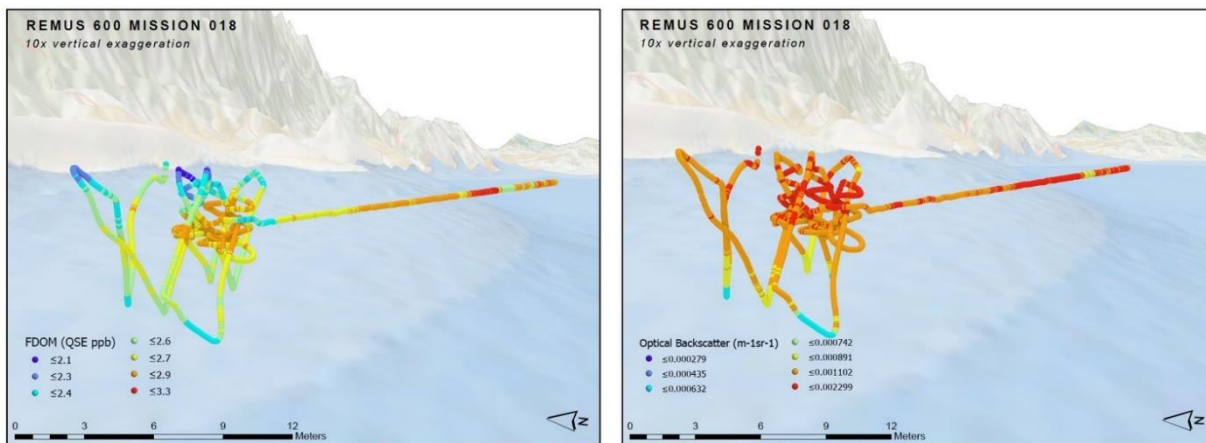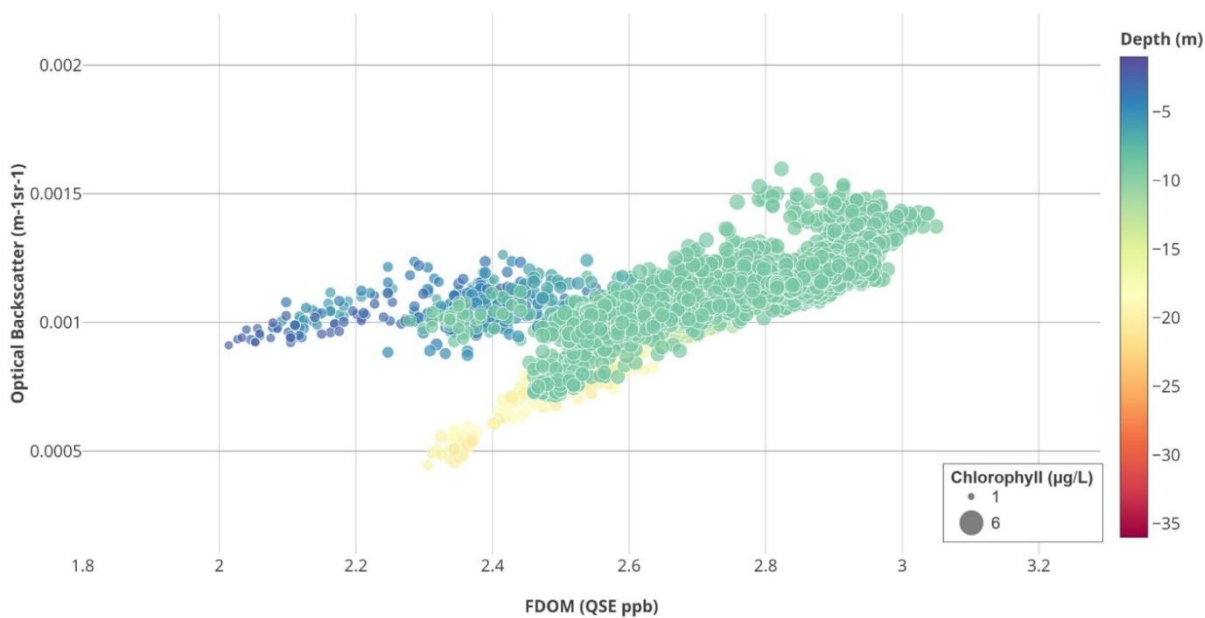
C.4.3   REMUS-600 MSN016

At 12:40 the REMUS-600 was sent on a double-gulp mission, where it went through a lawnmower path with two circles during which the gulpers took a "double gulp" filling two bottles sequentially. The double gulp was a behavior requested by the EPA in order to increase the volume of the samples gathered from an area. The WHOI team was able to adapt the vehicle code on scene and enable this new behavior. The mission was aborted to confirm the gulp at 1:33 (local).

Figure C.65. In MSN016 the REMUS 600 made a lawnmower path east of the Holly hot spot. The adaptive behavior was triggered and it took a double gulp filling two bottles.

Figure C.66. FDOM and optical backscatter measurements along the REMUS-600 vehicle track (top) for Mission 16. Colors correspond to concentration. Scatter plot of optical backscatter as a function of FDOM (bottom). Chlorophyll concentration is indicated by symbol size. Colors correspond to depth in the water column.

Figure C.67. Depth vertical profiles of OBS (left), FDOM (middle), and CHL (right) during REMUS-600 MSN016.
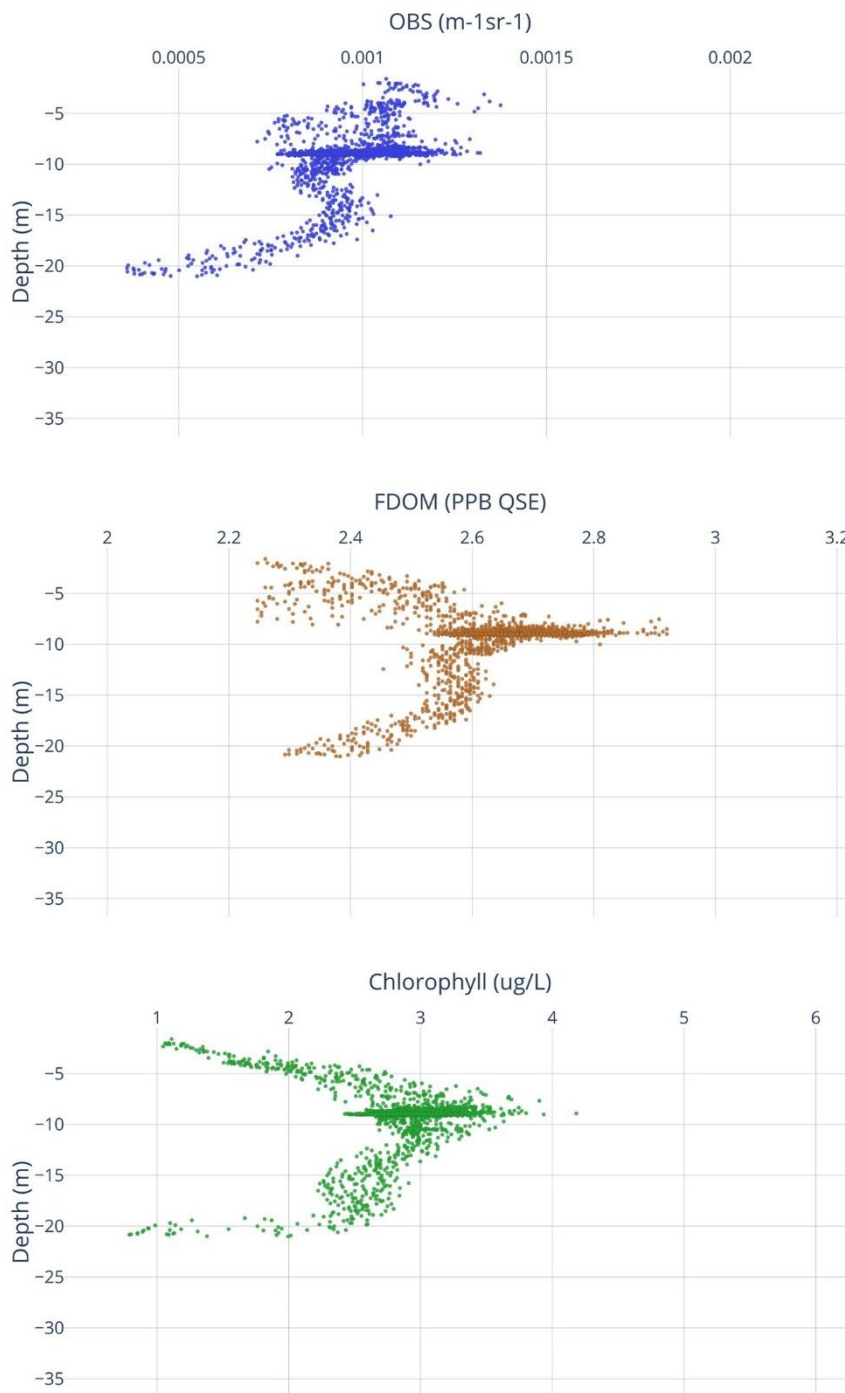
C.4.4   REMUS-600 MSN017

At 13:44 (local), the REMUS-600 ran another double-gulp mission, taking three double gulps before being aborted at 14:30 (local). After this mission, eight bottles had been filled and the vehicle was recovered onto the Cobb to replace the full gulper. This served a few purposes: practicing the switch of a gulper, ensuring the RECON mission could be reset to use the new gulper, as well as giving the EPA a chance to begin preparing the samples for the journey back.

Figure C.68. REMUS-600 MSN017 was a large square path, during which the adaptive behavior triggered three times, filling six bottles through double gulps.

Figure C.69. FDOM and optical backscatter measurements along the REMUS-600 vehicle track (top) for Mission 17. Colors correspond to concentration. Scatter plot of optical backscatter as a function of FDOM (bottom). Chlorophyll concentration is indicated by symbol size. Colors correspond to depth in the water column.

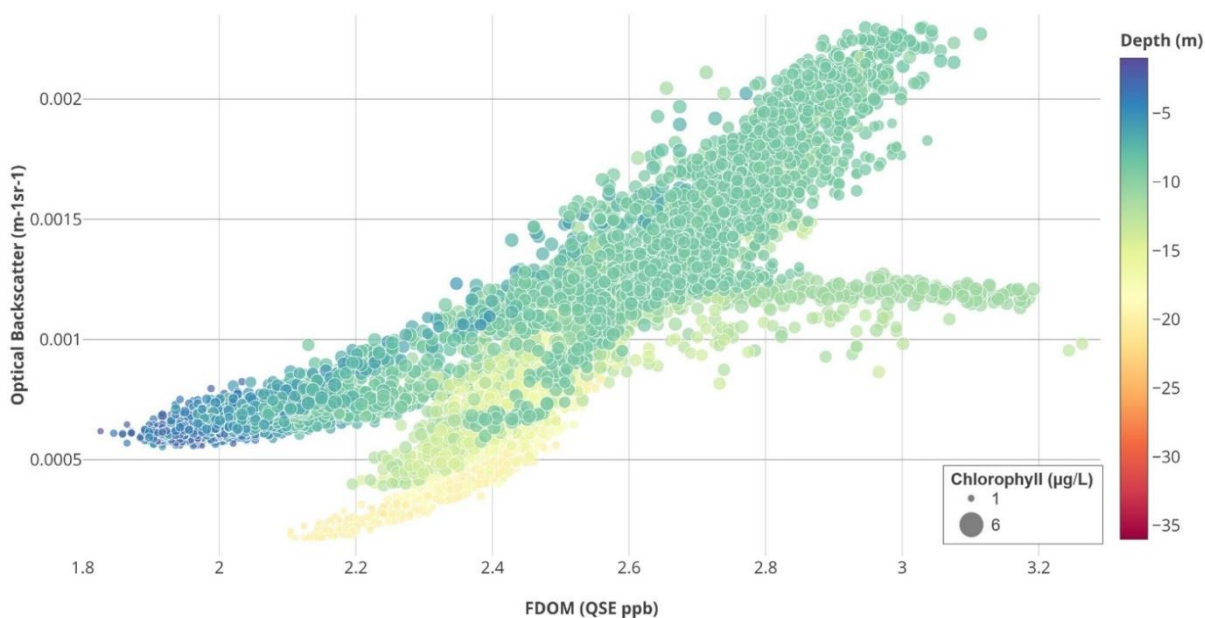**Figure C.70. Depth vertical profiles of OBS (left), FDOM (middle), and CHL (right) during REMUS-600 MSN017.**
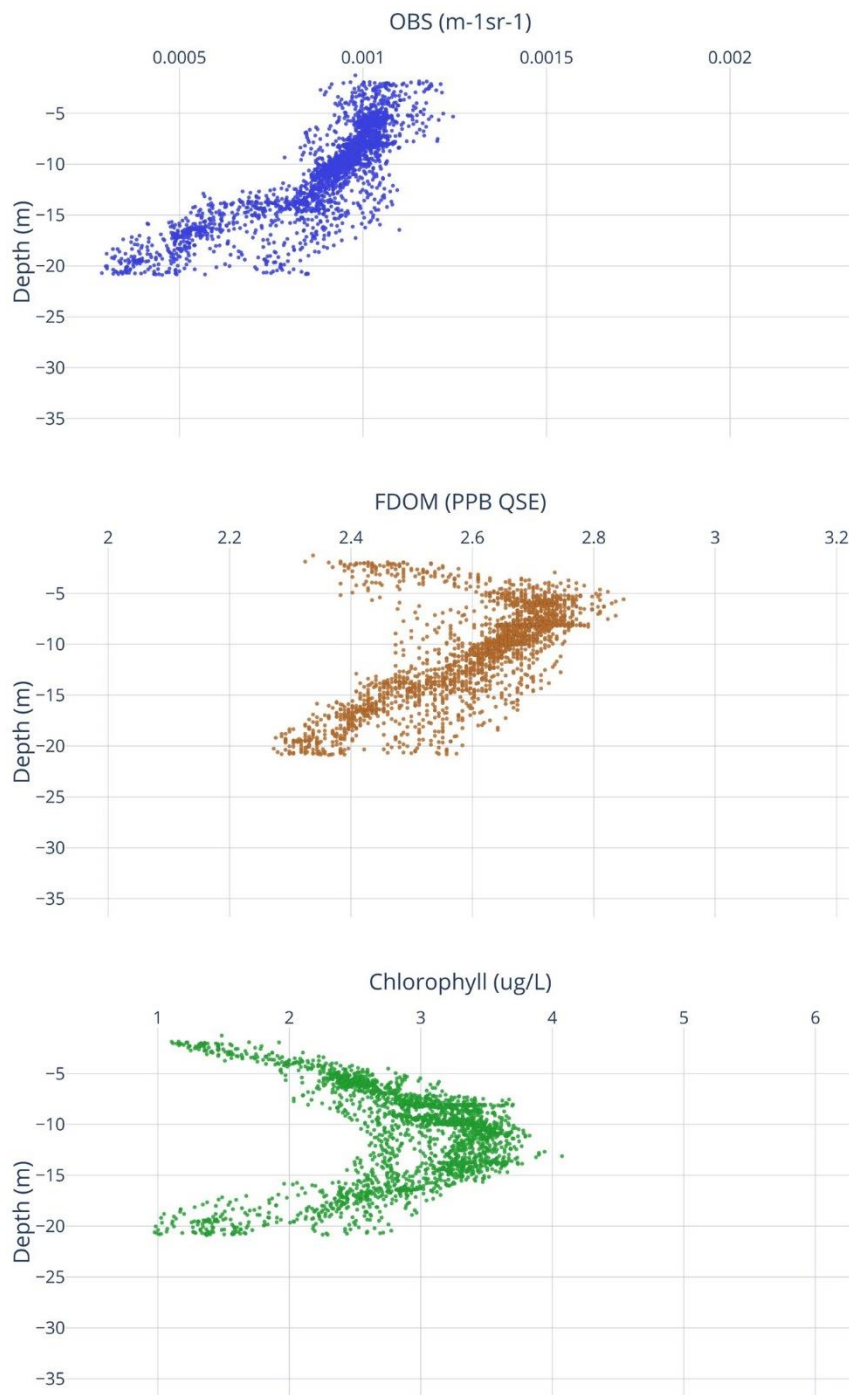
C.4.5   REMUS-100 MSN006

At 13:50 the REMUS-100 was started in another shallow lawnmower mission. This lawnmower path was allowed to run to completion, and the vehicle was finally aborted at 15:35 and was recovered for the day.

Figure C.71. The REMUS-100 ran a second lawnmower path for MSN006, only slightly offset from its path in MSN005.

Figure C.72. FDOM and optical backscatter measurements along the REMUS-100 vehicle track (top) for Mission 6. Colors correspond to concentration. Scatter plot of optical backscatter as a function of FDOM (bottom). Chlorophyll concentration is indicated by symbol size. Colors correspond to depth in the water column.
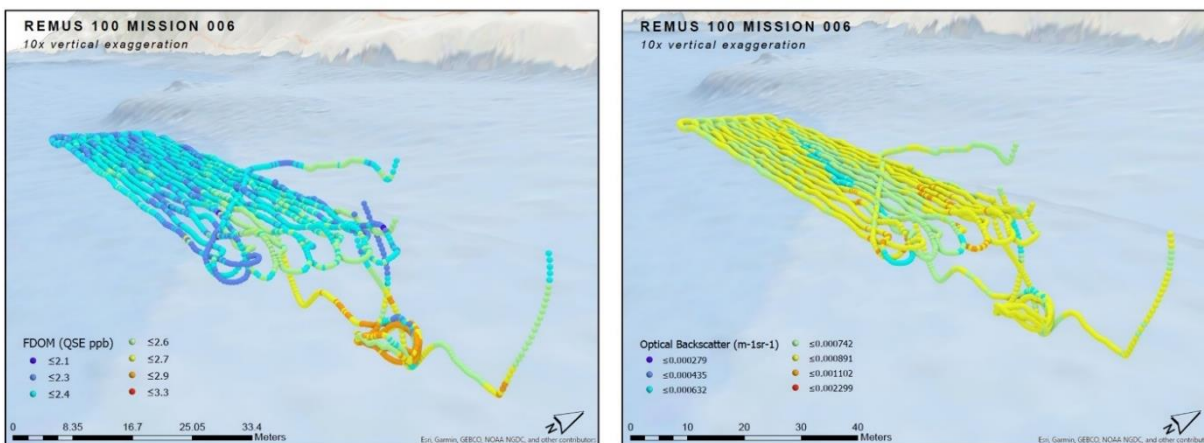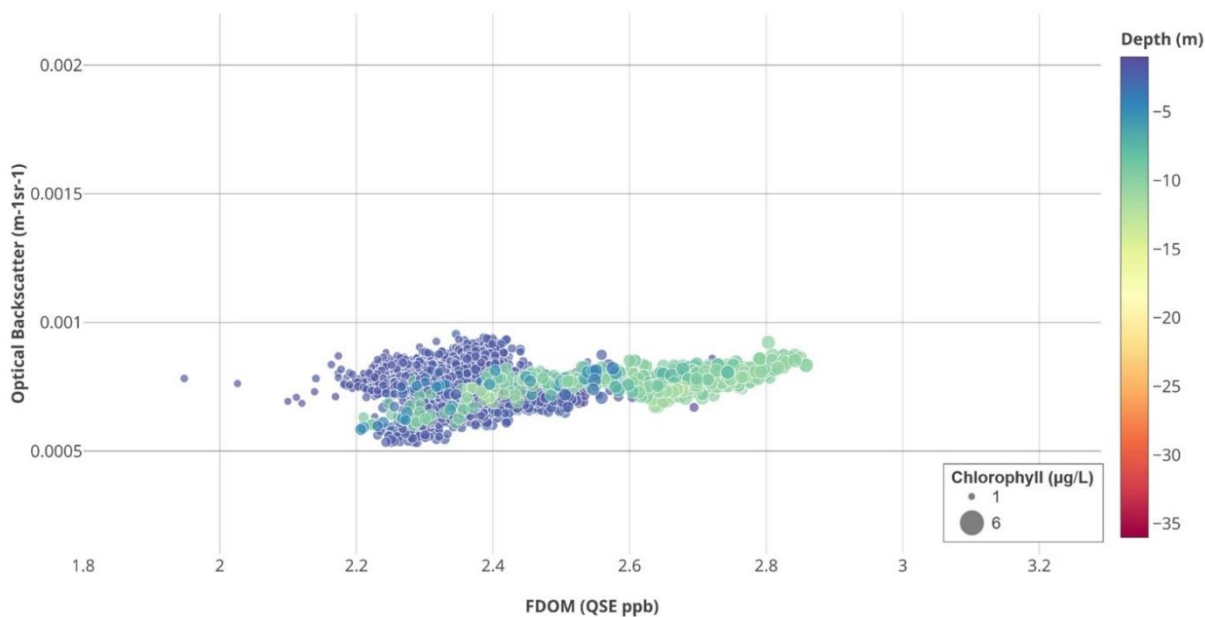
C.4.6   REMUS-600 MSN018

The REMUS-600 was relaunched and at 15:15 (local) it began another lawnmower and gulp mission to use the new gulper. Two more double gulps were taken, and then the mission was aborted at 16:43 to be recovered for the day.

Figure C.73. The REMUS-600 MSN018 was the final mission of the day and the vehicle took two double gulps before transiting back past the Trilogy hot spot.
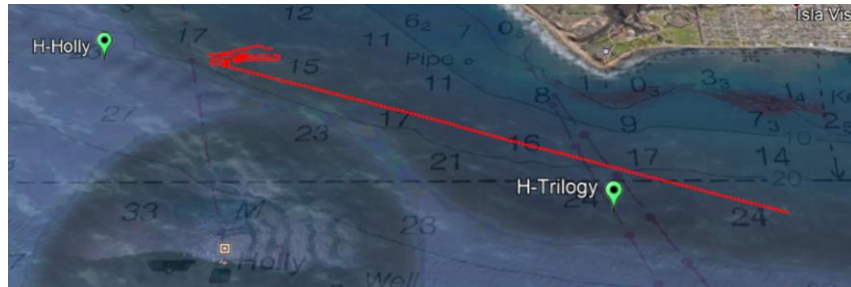
Figure C.74. FDOM and optical backscatter measurements along the REMUS-600 vehicle track (top) for Mission 18. Colors correspond to concentration. Scatter plot of optical backscatter as a function of FDOM (bottom). Chlorophyll concentration is indicated by symbol size. Colors correspond to depth in the water column.

Figure C.75. Depth vertical profiles of OBS (left), FDOM (middle), and CHL (right) during REMUS-600 MSN018.
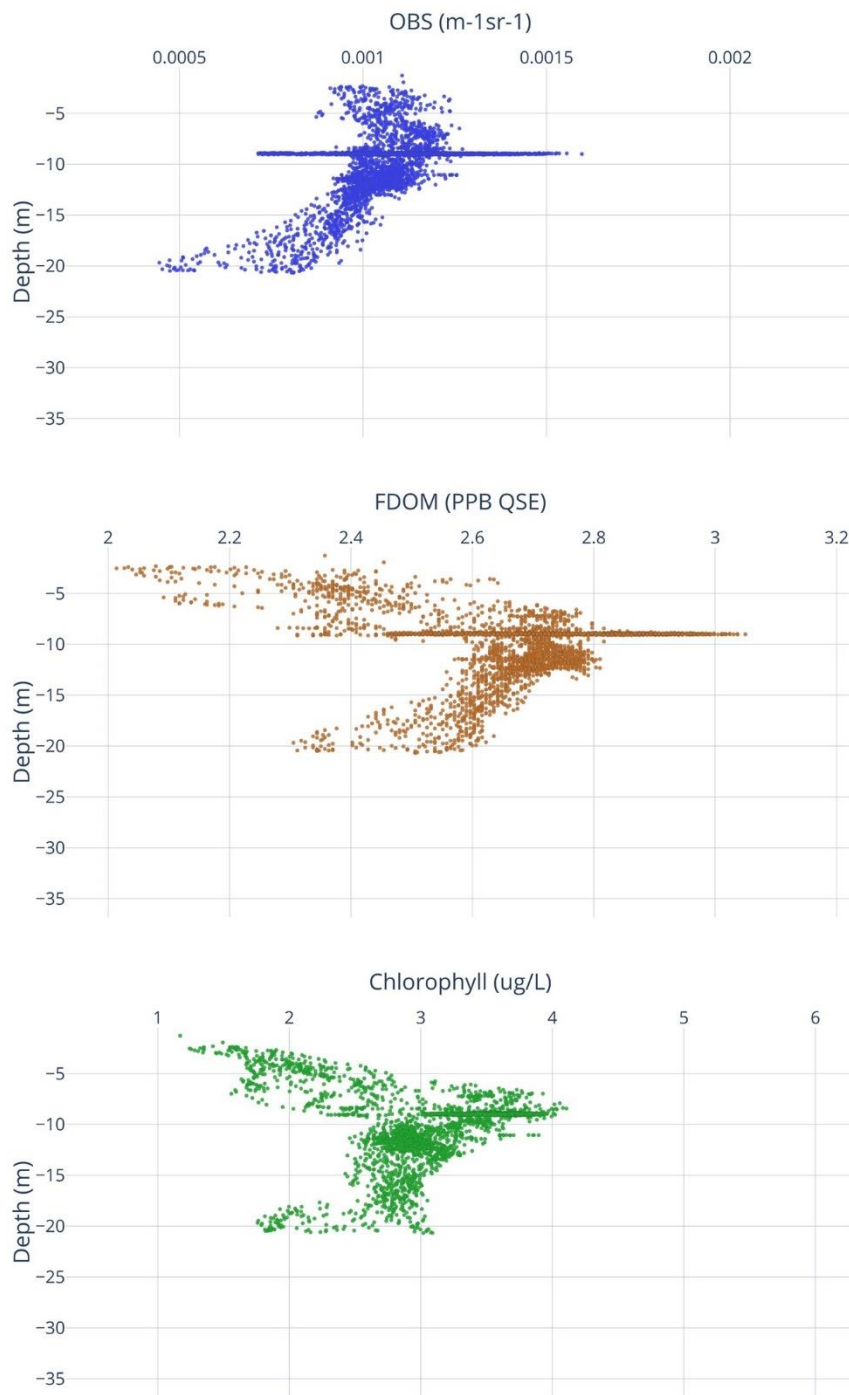
C.5   Day 10: Friday, August 30, 2019

C.5.1   REMUS-600 MSN019

The final day of deployment, the REMUS-600 was sent on a long mission between two different hot spots, and then to the location of the LRAUV buoy where it would reunite with the Cobb, which was retrieving the buoy. This path consisted of a long transit and then a lawnmower path. The vehicle had a lower threshold for triggering the autonomy behavior, to gather more data on the vehicle's autonomy performance; however, the threshold for taking a gulp was set above 600 FDOM count so that it would not gather unnecessary samples. The mission began at 8:50 (local) and was aborted for the final recovery at 16:42 (local) without any gulps taken.

Figure C.76. On the final day, August 29, only the REMUS-600 was run. It covered area from the Trilogy hot spot to an LRAUV hot spot from a previous day running both lawnmower paths and circular paths.

Figure C.77. FDOM and optical backscatter measurements along the REMUS-600 vehicle track (top) for Mission 19. Colors correspond to concentration. Scatter plot of optical backscatter as a function of FDOM (bottom). Chlorophyll concentration is indicated by symbol size. Colors correspond to depth in the water column.
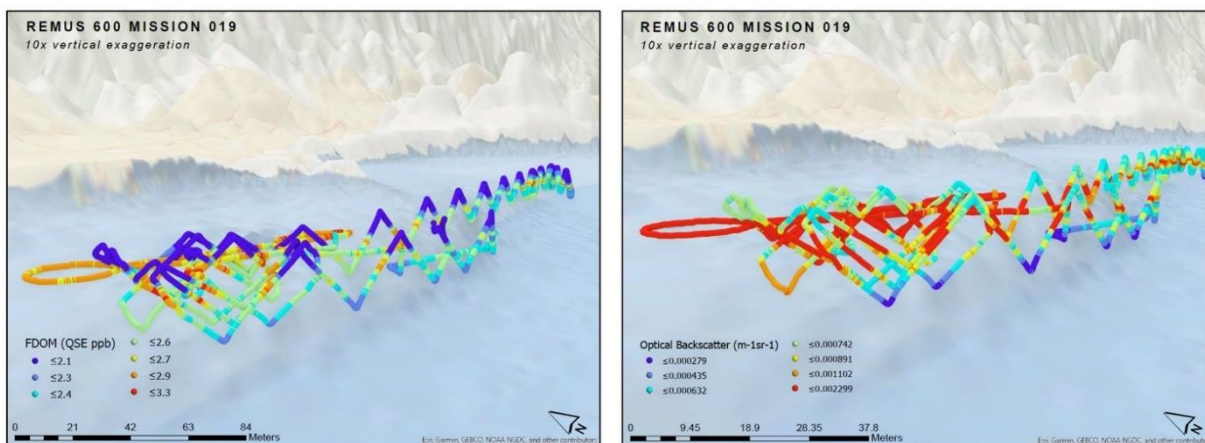
Figure C.78. Depth vertical profiles of OBS (left), FDOM (middle) and CHL (right) during REMUS-600 MSN019.
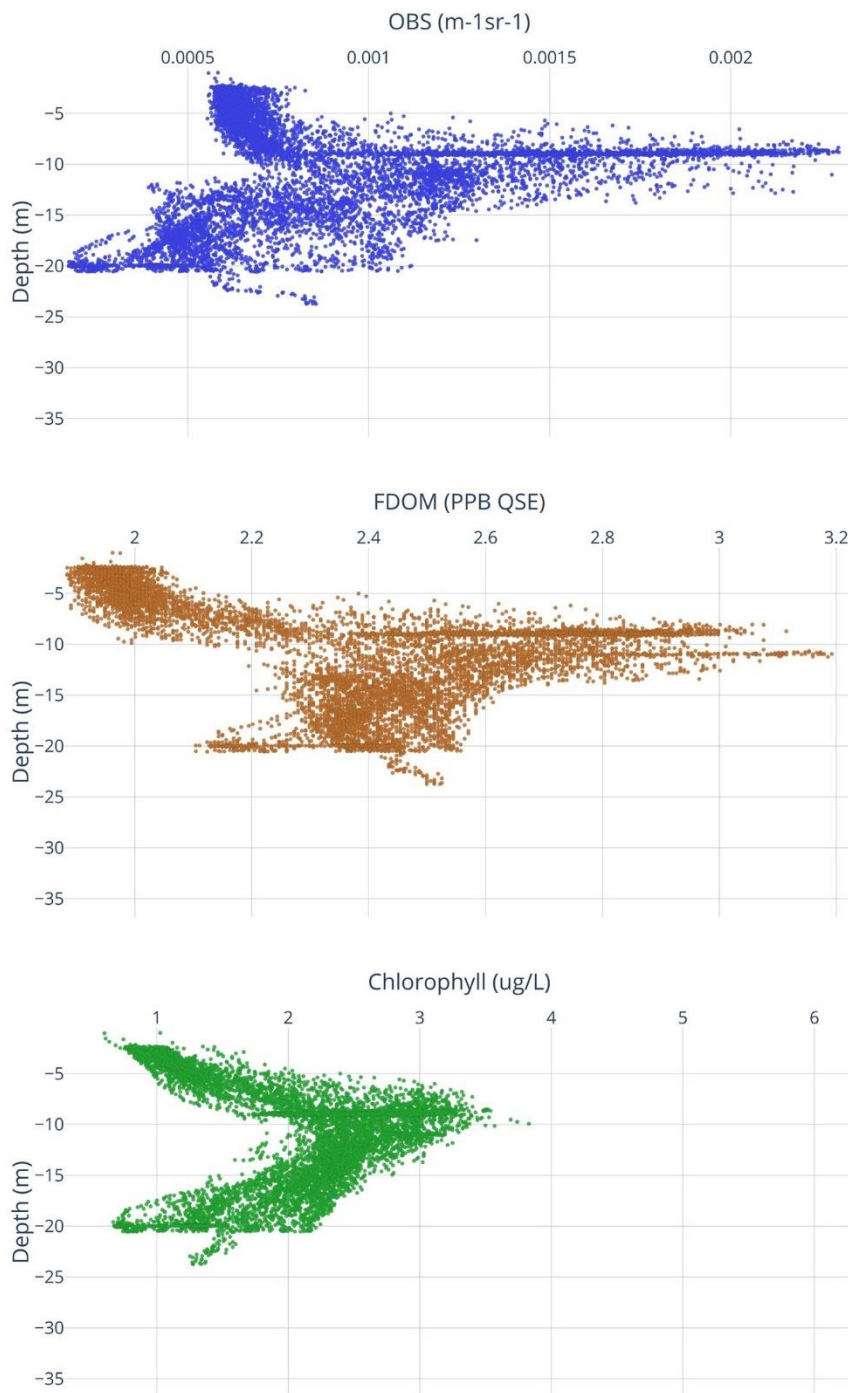
# D.   Appendix D: Maps of UAS Survey Tracks

Figure D.1. Oil classifcation of the map generated during Flight 2 Track 1 on 8/27/2019.
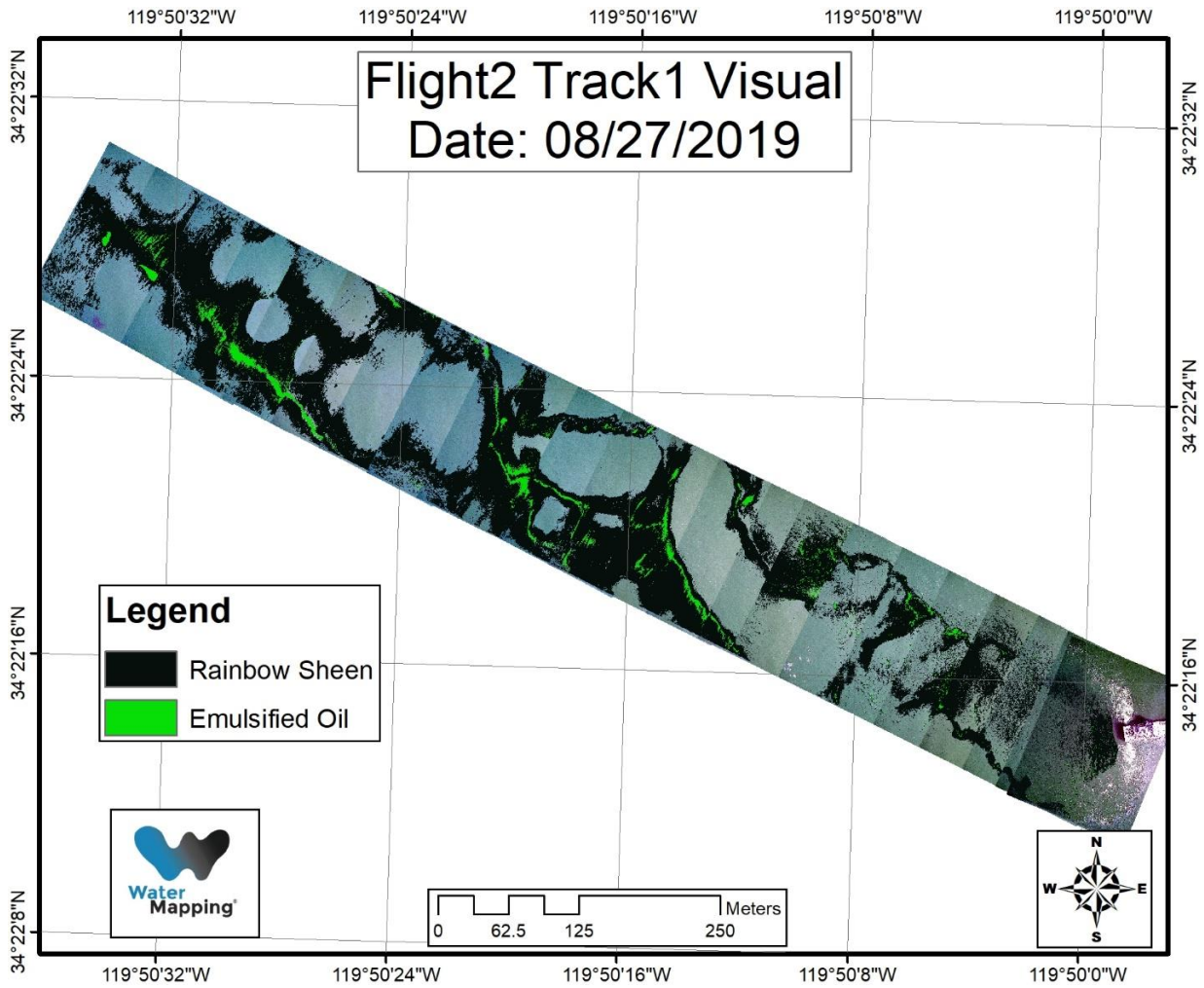
Figure D.2. Oil classifcation of the map generated during Flight 2 Track 2 on 8/27/2019.
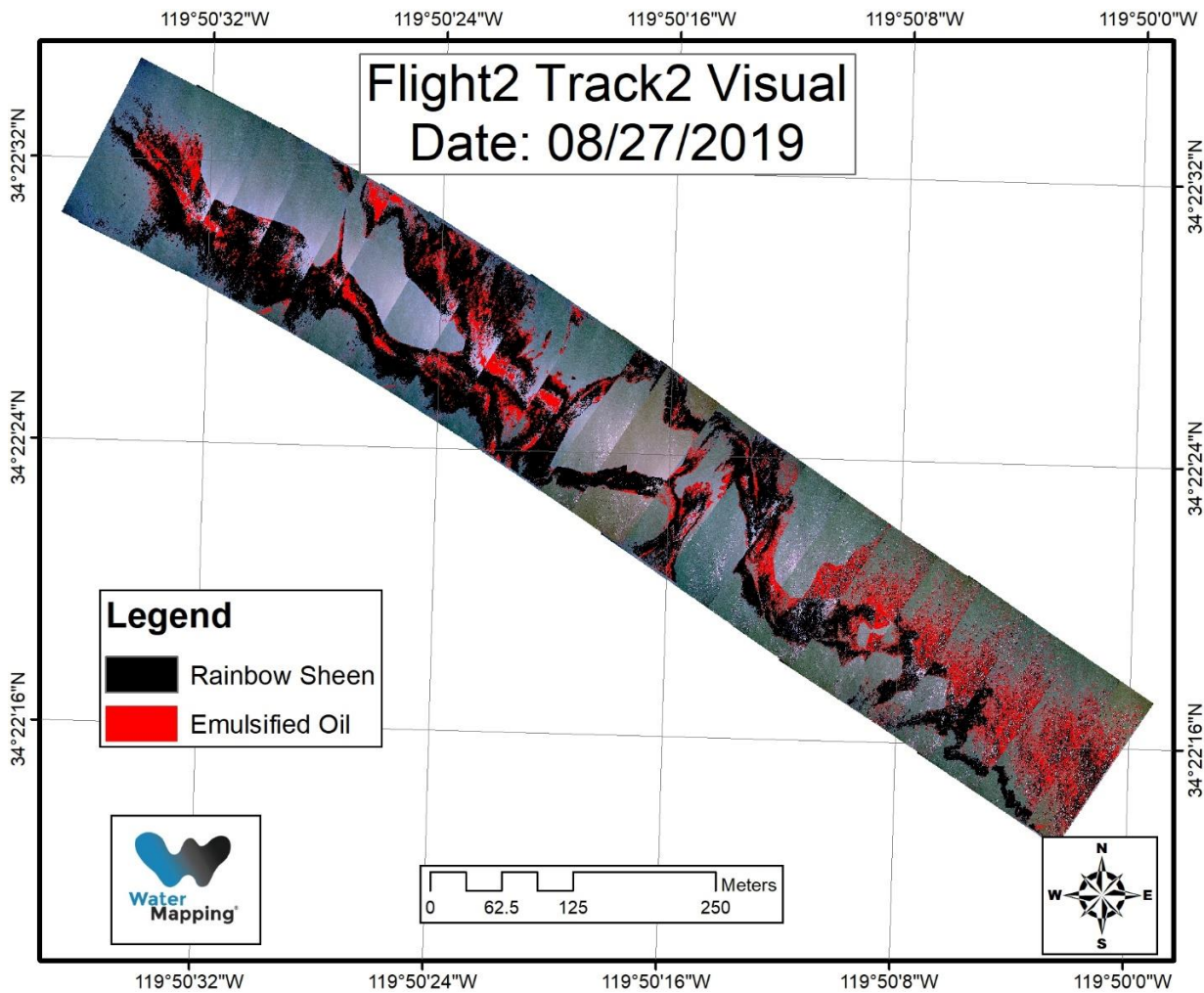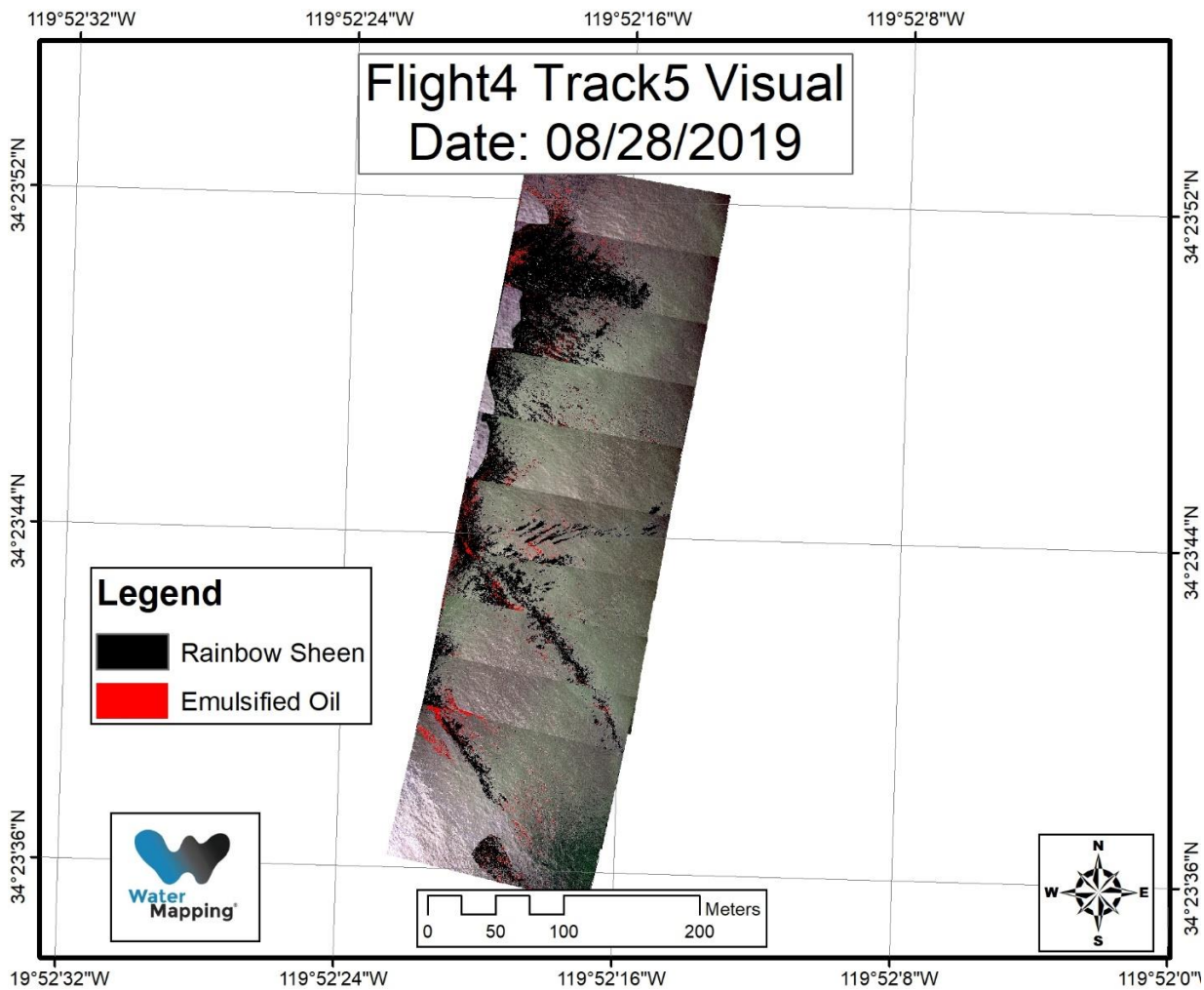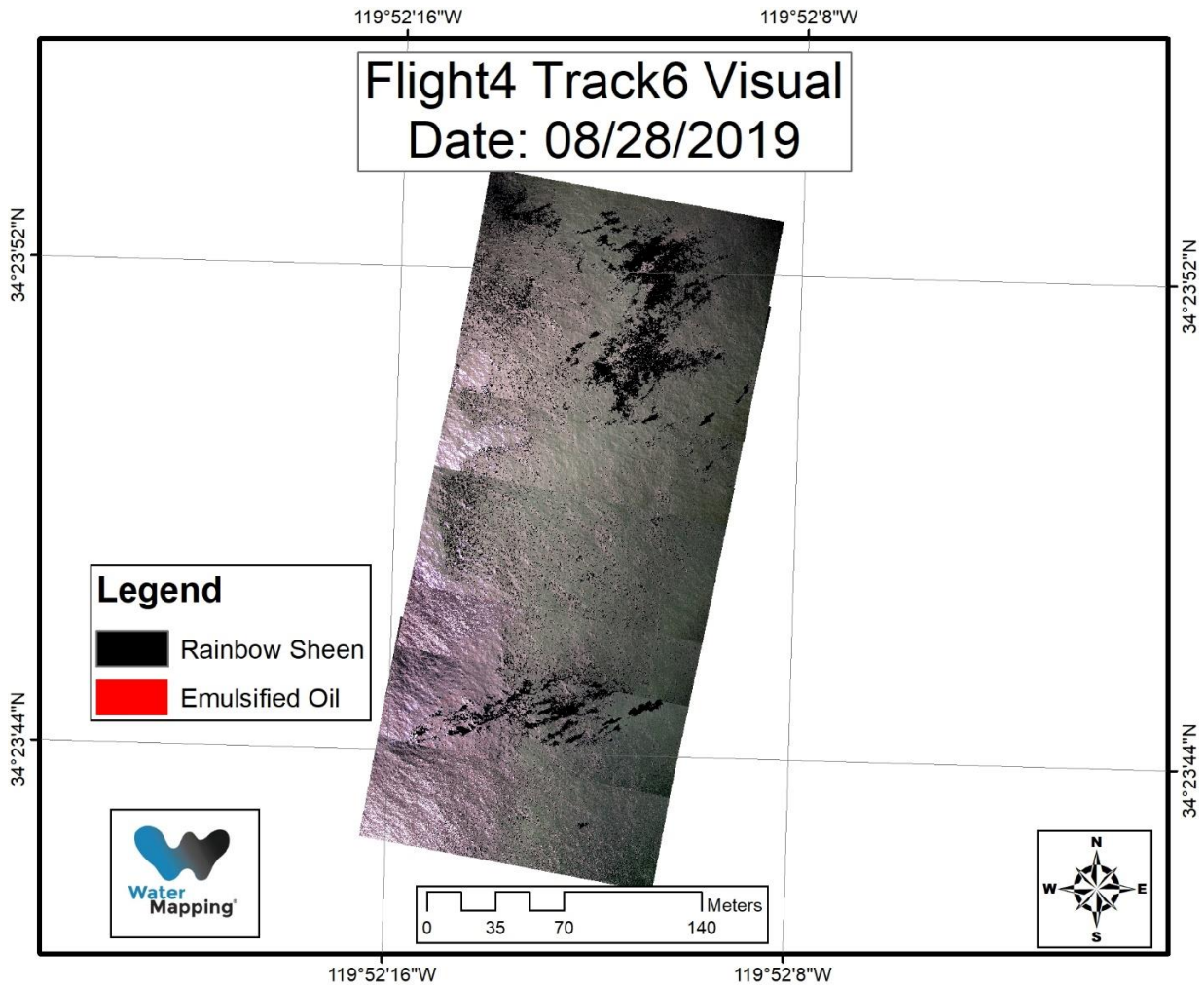
Figure D.3. Oil classifcation of the map generated during Flight 2 Track 3 on 8/27/2019.
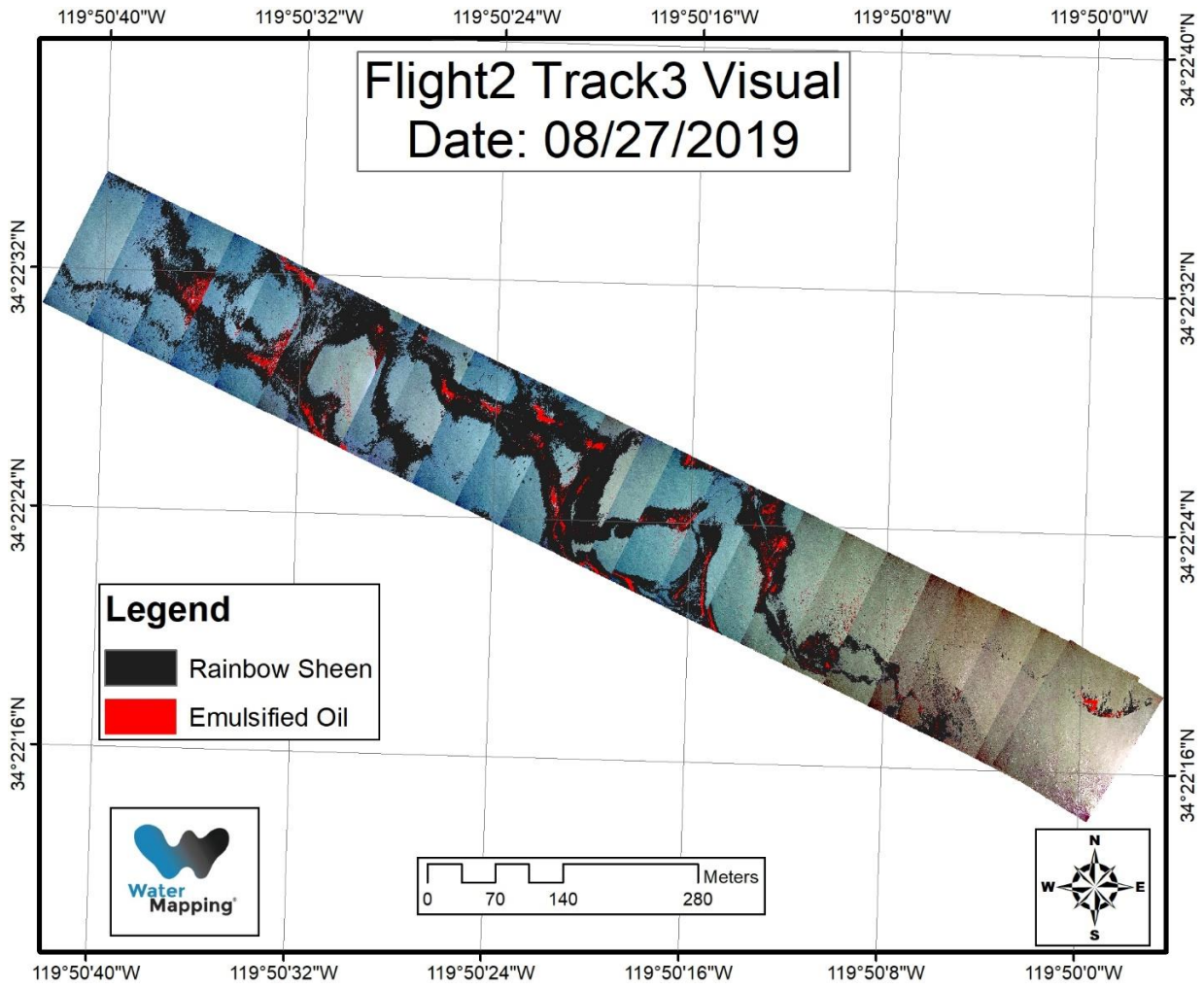
Figure D.4. Oil classifcation of the map generated during Flight 2 Track 4 on 8/27/2019.
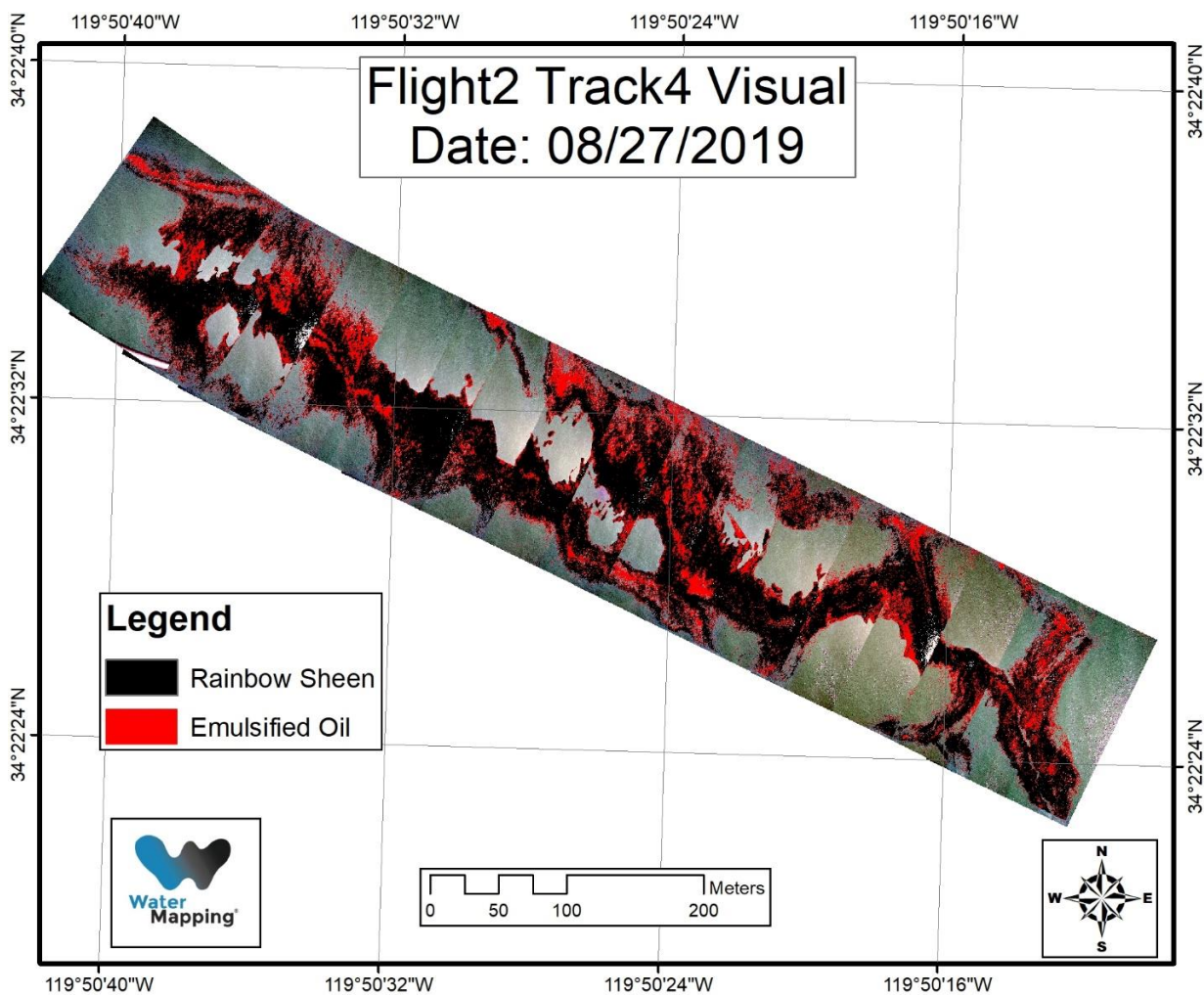
Figure D.5. Oil classifcation of the map generated during Flight 3 on 8/27/2019.
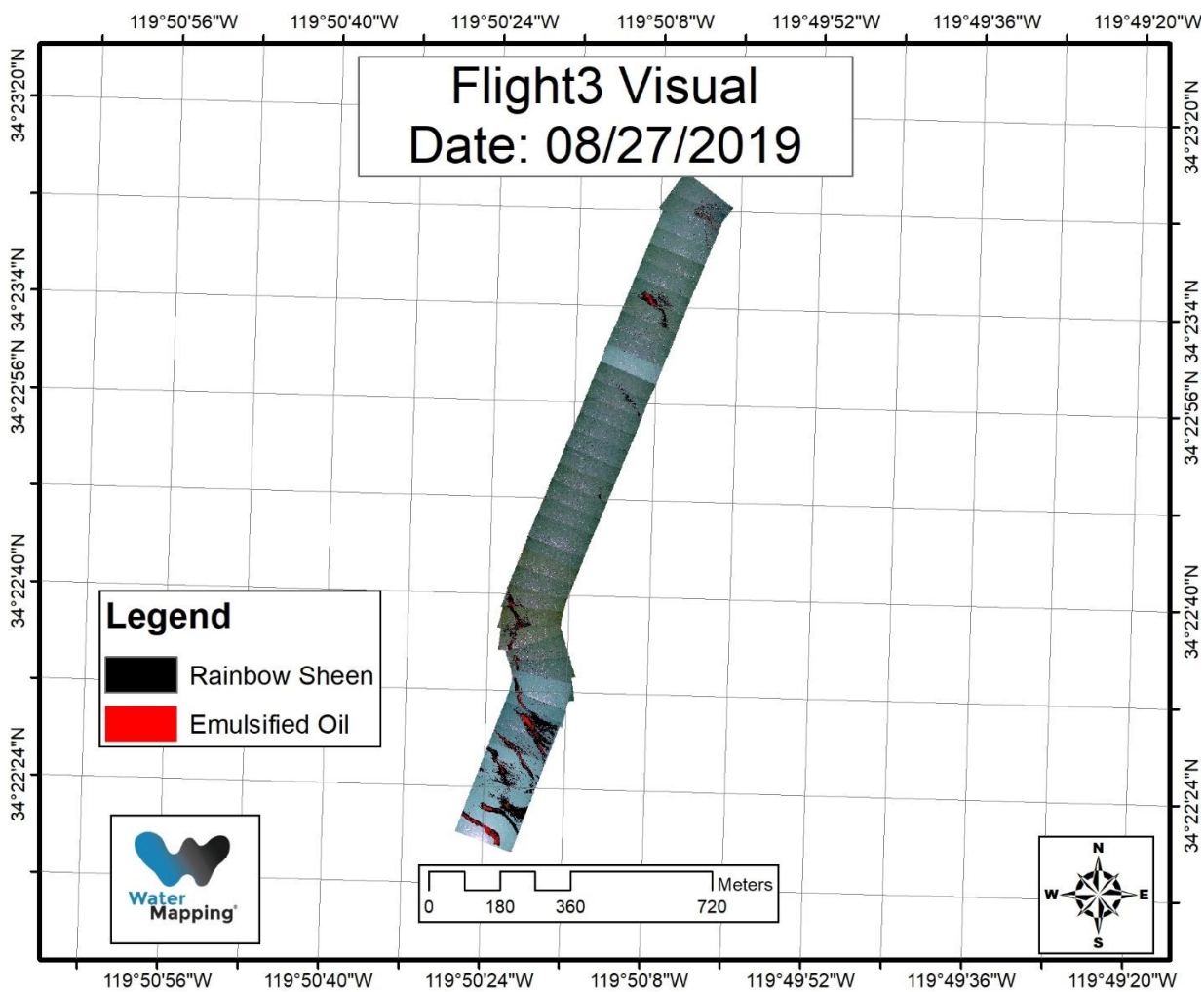
Figure D.6. Oil classifcation of the map generated during Flight 4 on 8/27/2019.
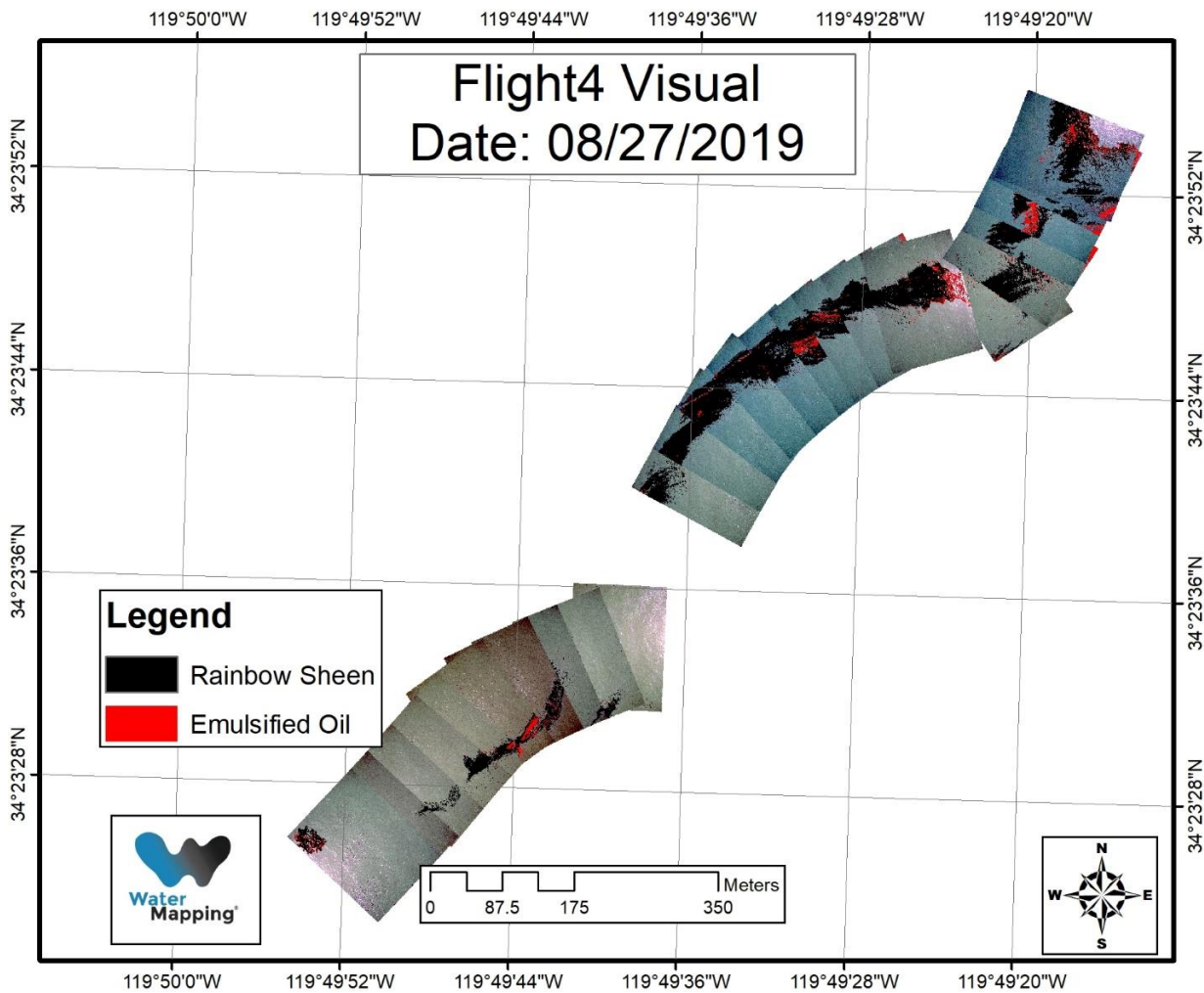
Figure D.7. Oil classifcation of the map generated during Flight 1 on 8/28/2019.
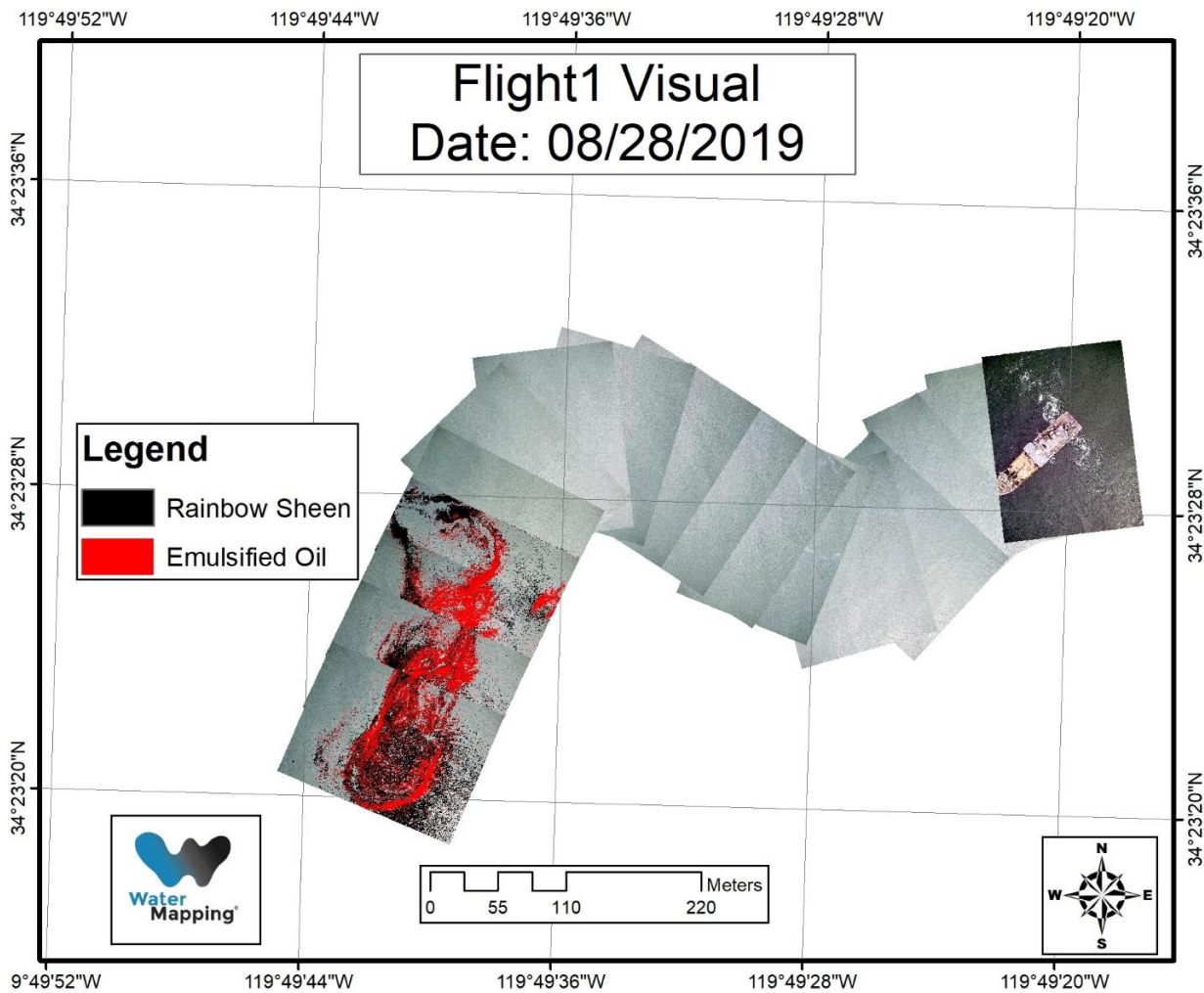
Figure D.8. Oil classifcation of the map generated during Flight 3 Track 1 on 8/28/2019.
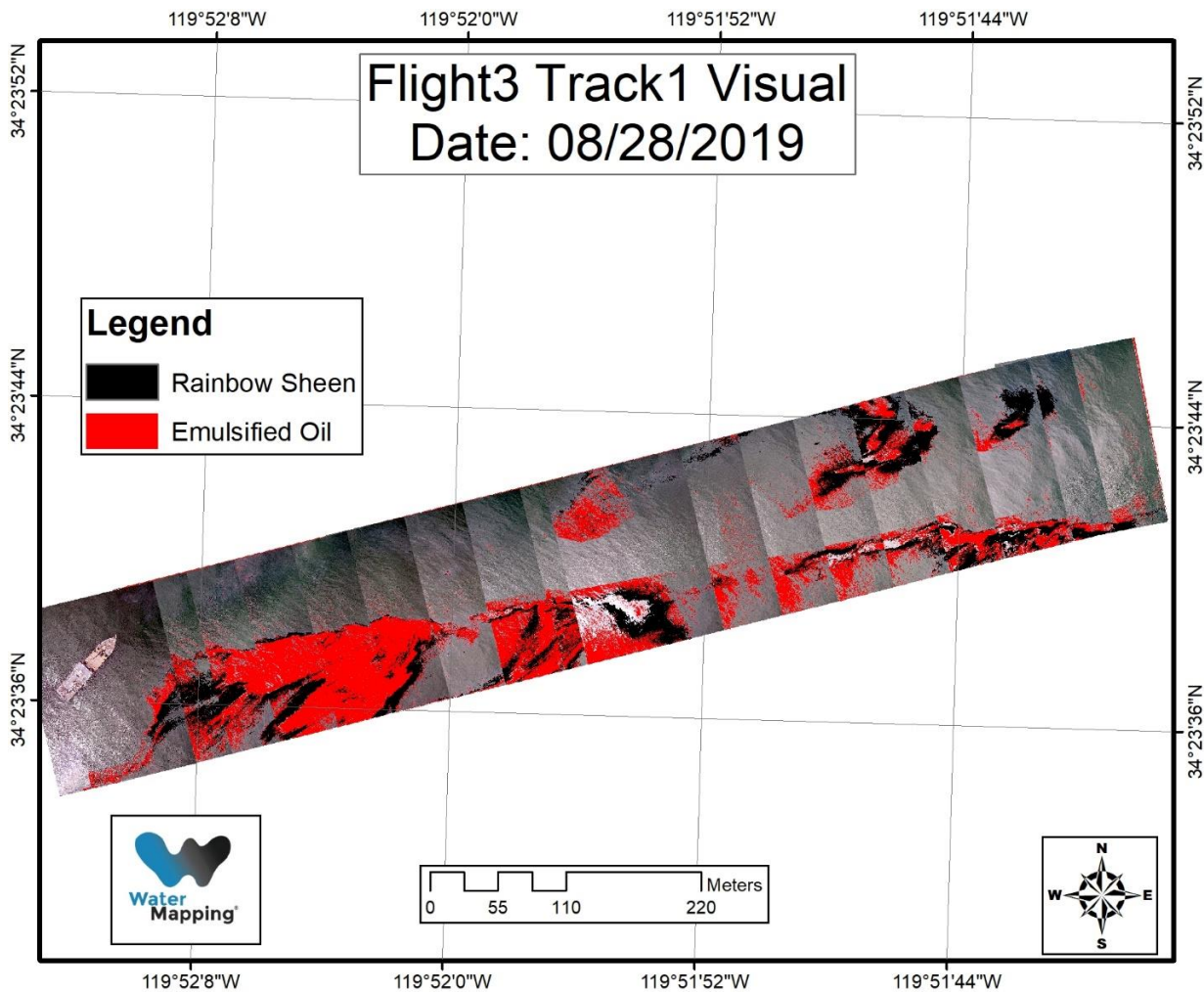
Figure D.9. Oil classifcation of the map generated during Flight 3 Track 2 on 8/28/2019.
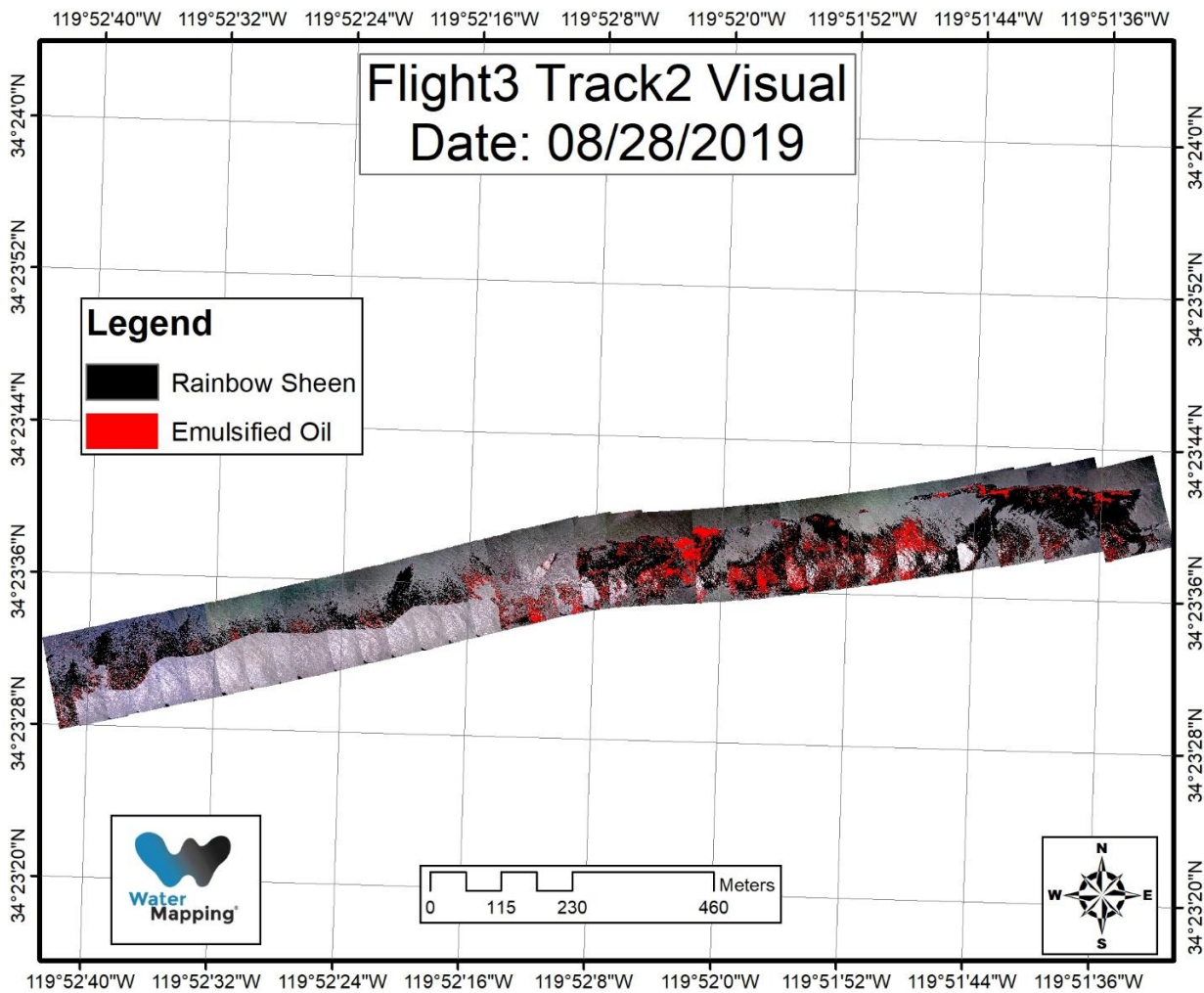
Figure D.10. Oil classifcation of the map generated during Flight 3 Track 2 on 8/28/2019.
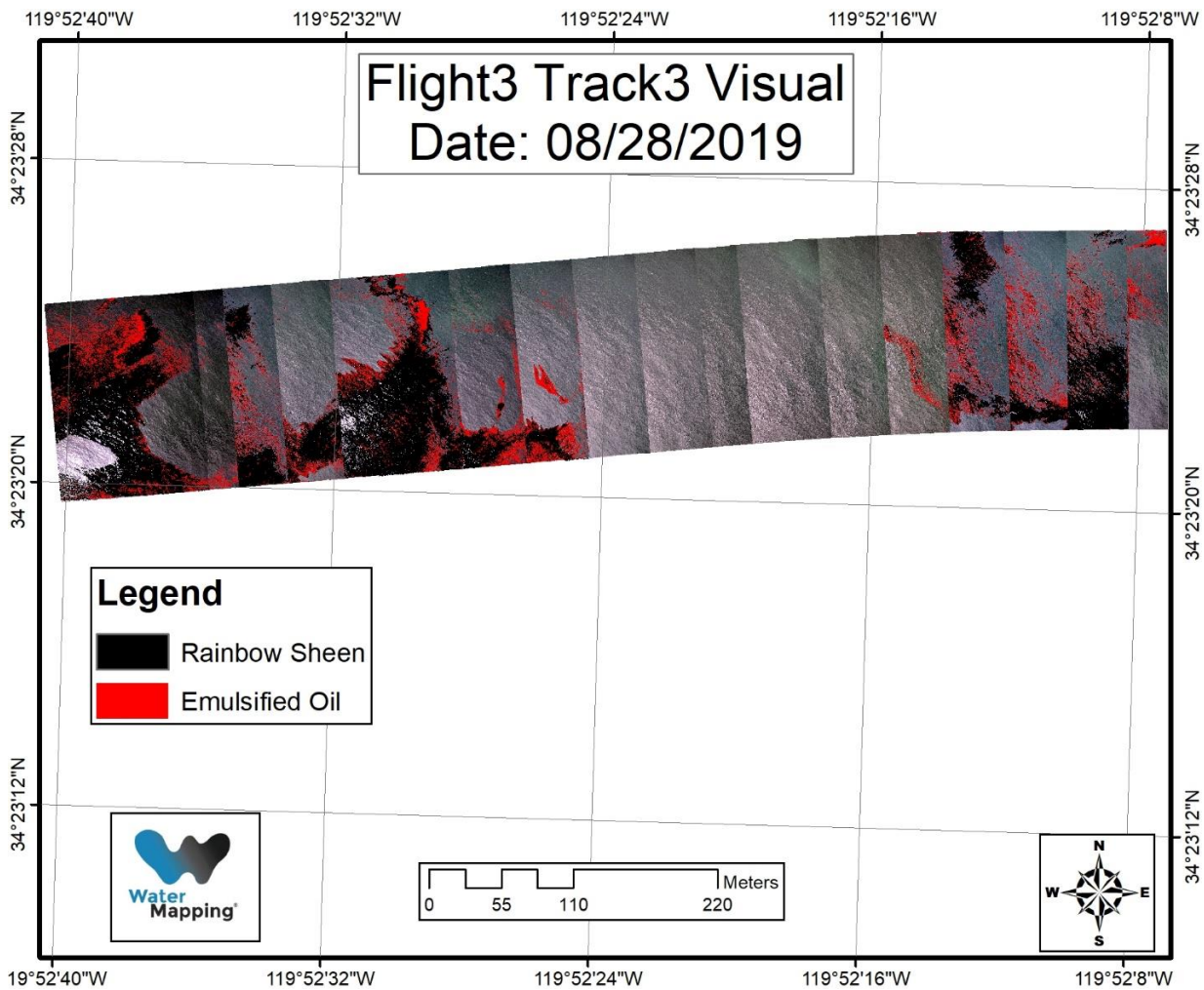
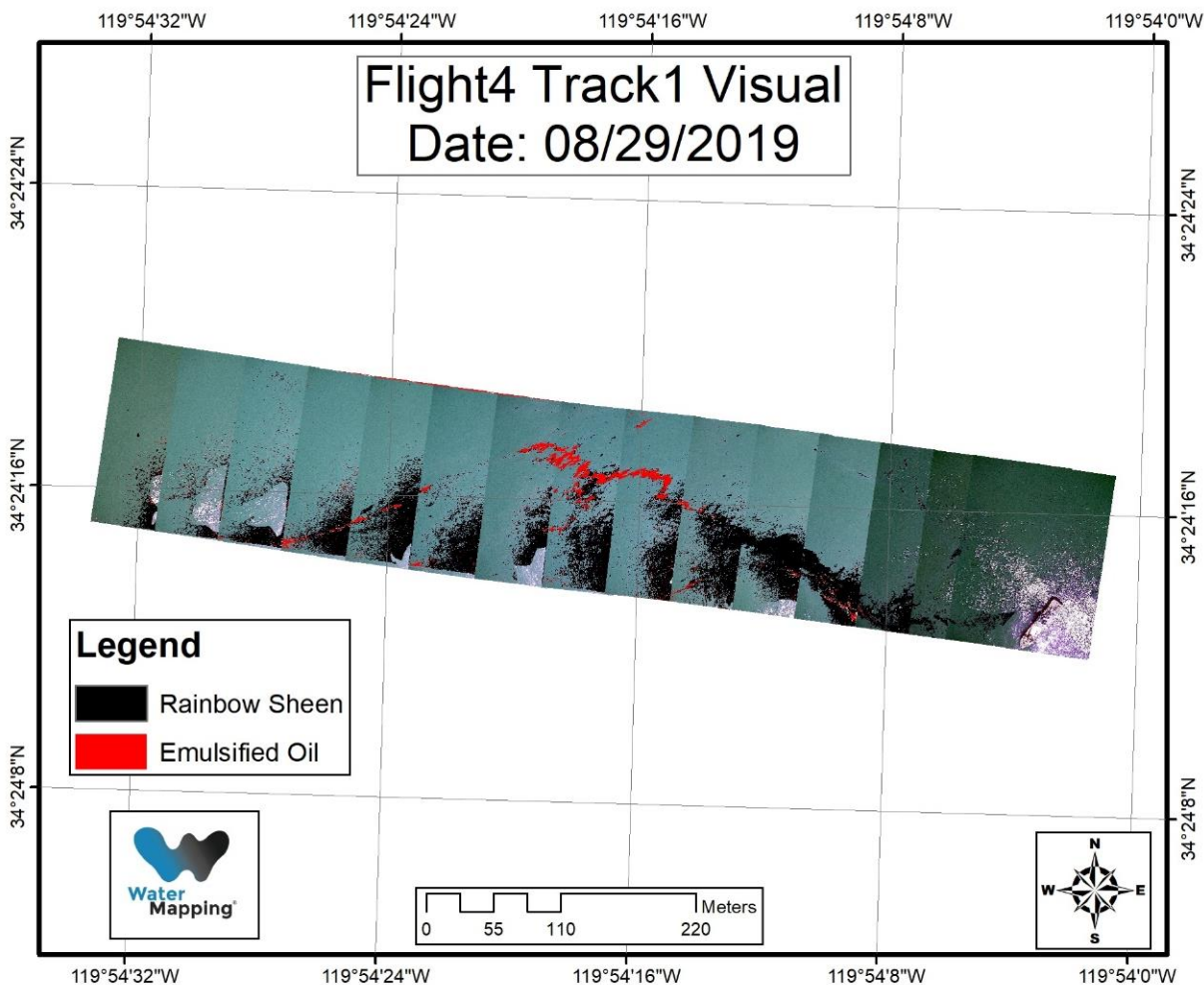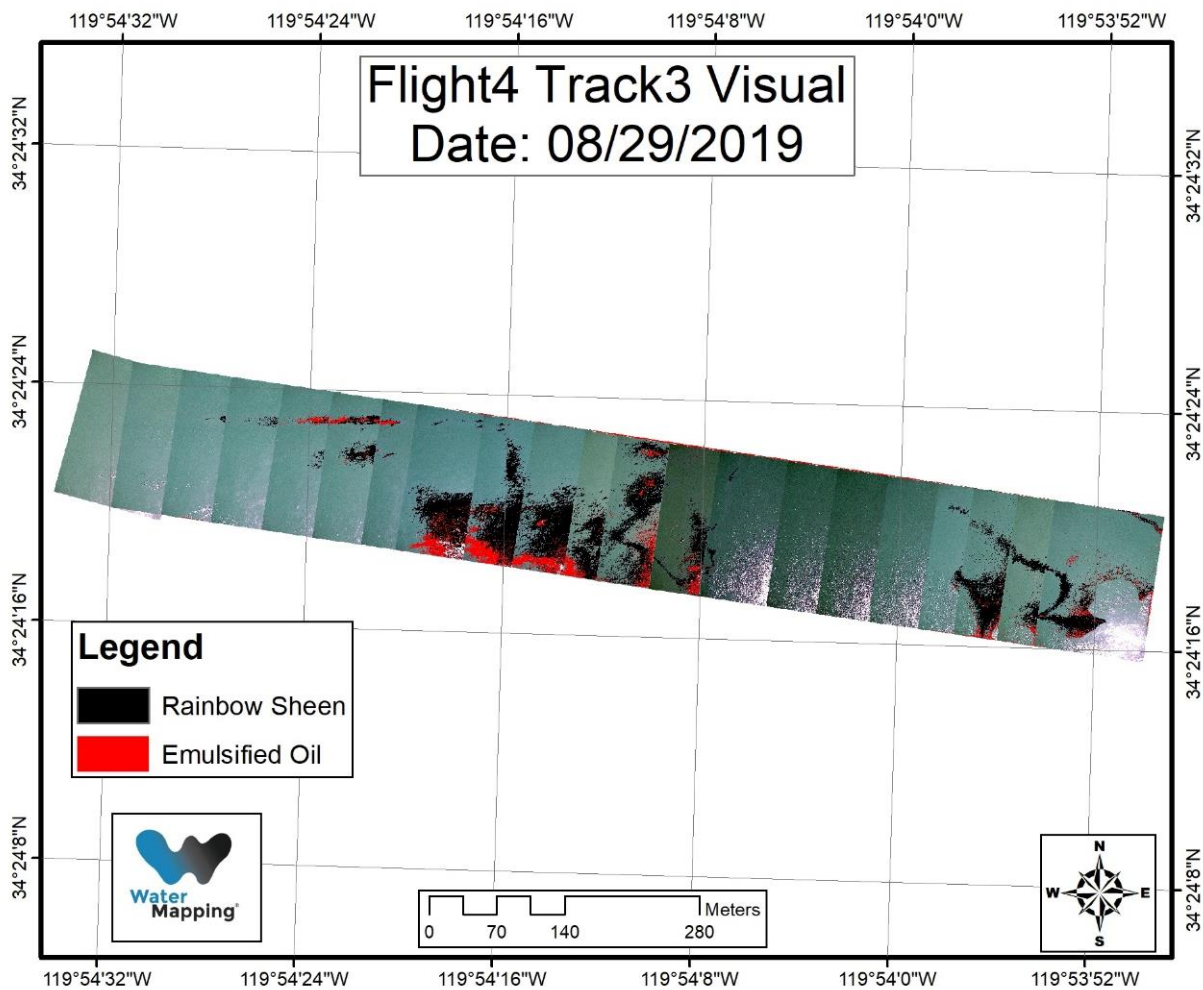**Figure D.11. Oil classifcation of the map generated during Flight 4 Track 1 on 8/28/2019.**
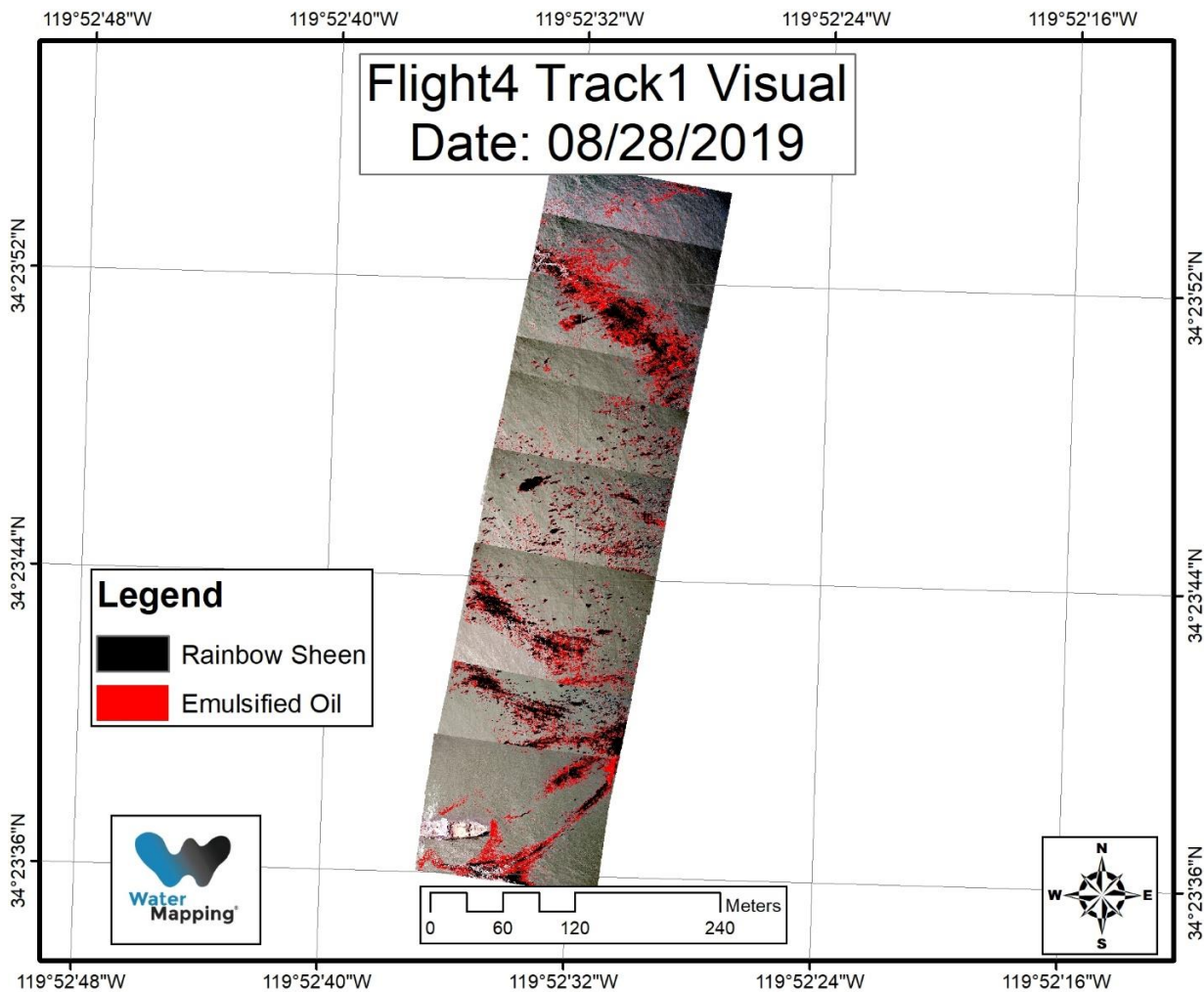
Figure D.12. Oil classifcation of the map generated during Flight 4 Track 2 on 8/28/2019.
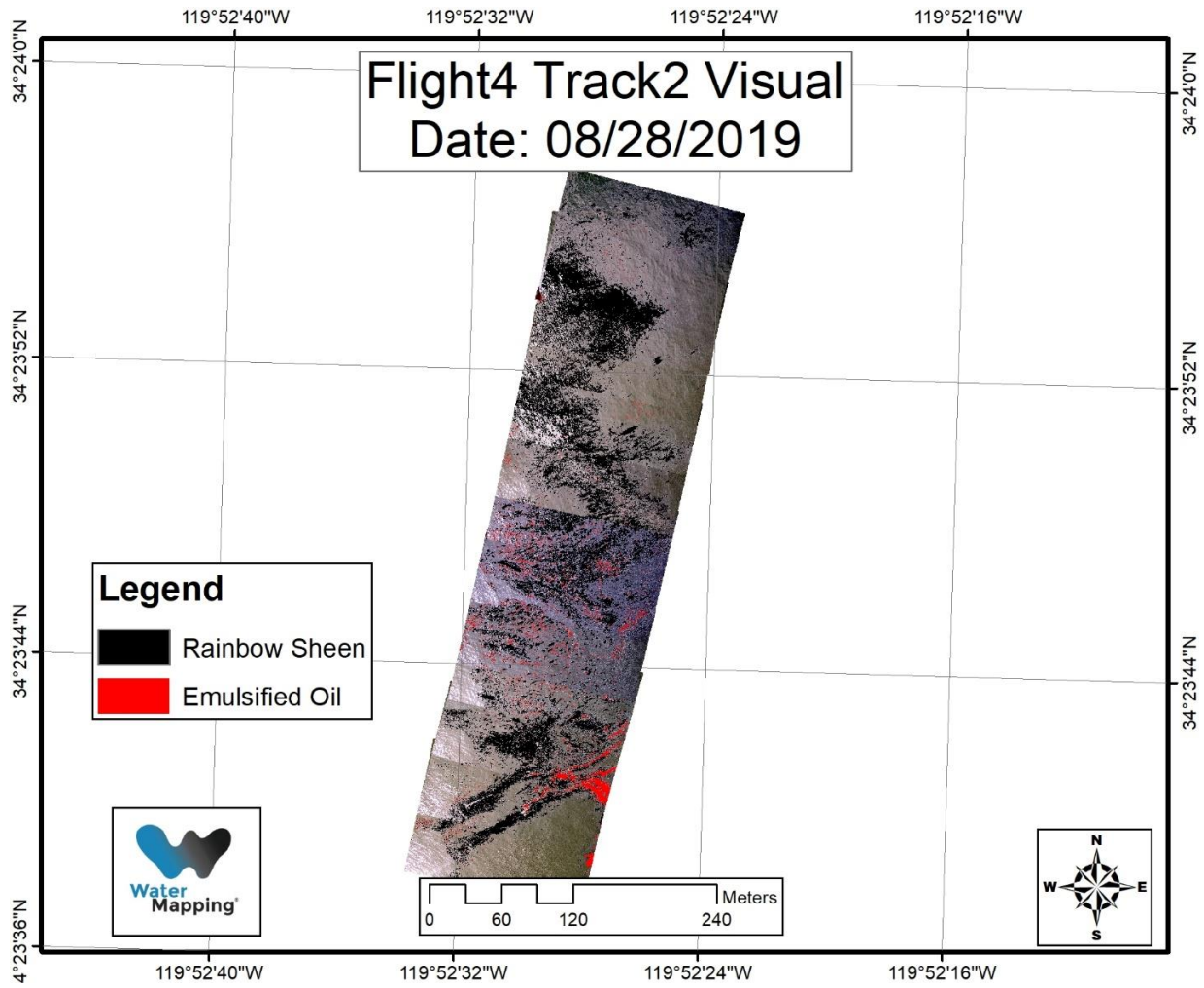
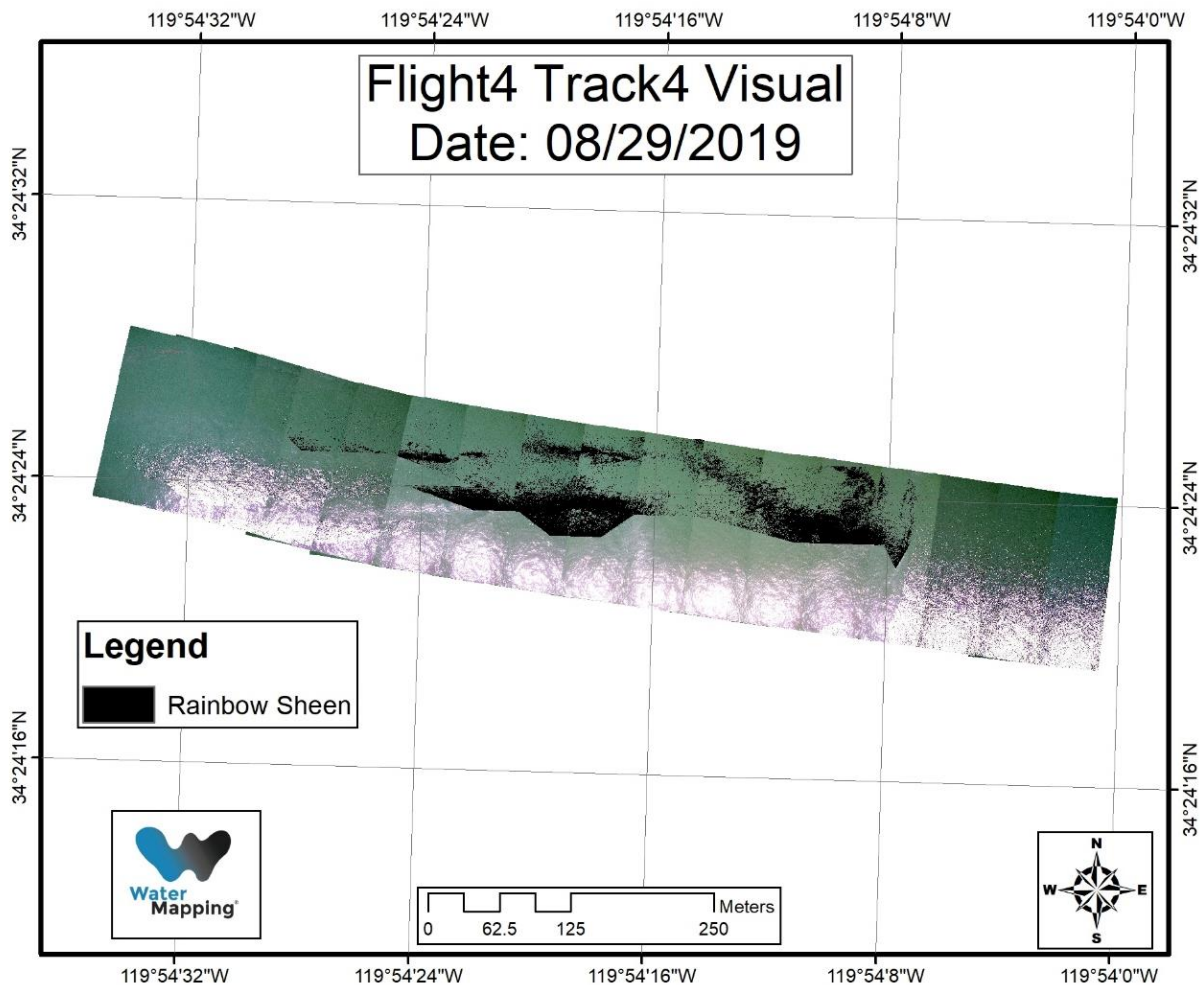**Figure D.13. Oil classifcation of the map generated during Flight 4 Track 3 on 8/28/2019.**
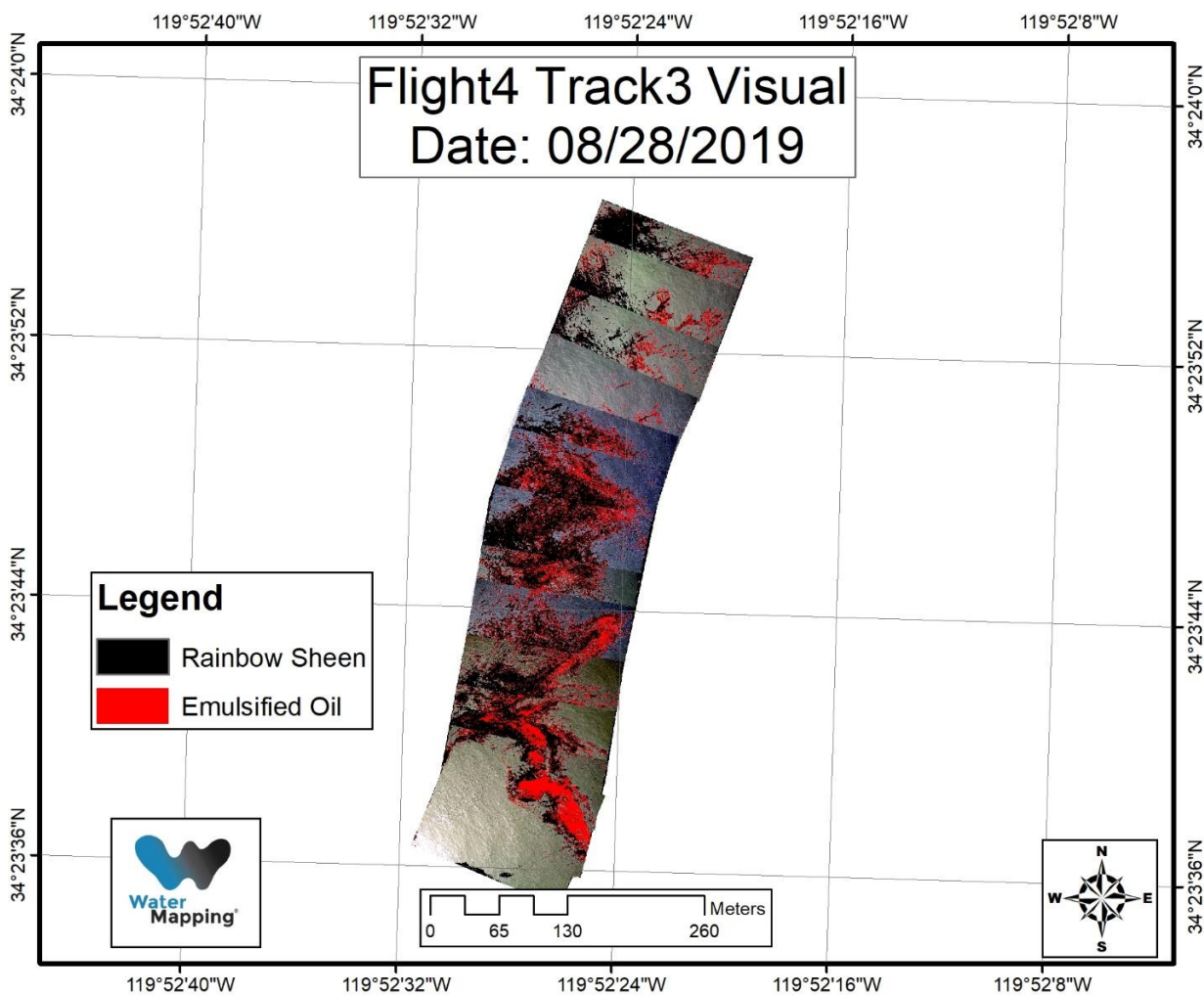
Figure D.14. Oil classifcation of the map generated during Flight 4 Track 5 on 8/28/2019.

Figure D.15. Oil classifcation of the map generated during Flight 4 Track 6 on 8/28/2019.

Figure D.16. Oil classifcation of the map generated during Flight 4 Track 1 on 8/29/2019.

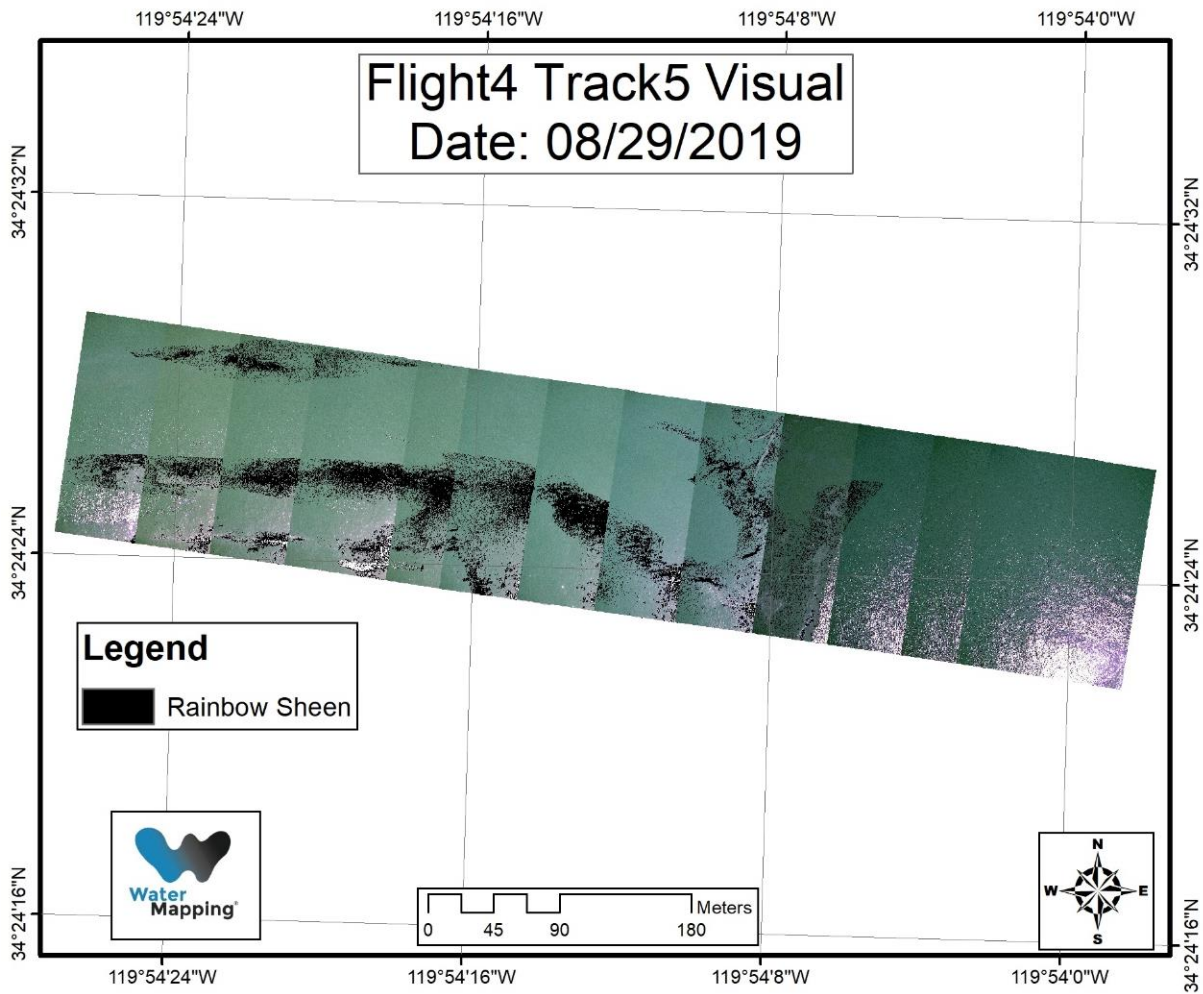**Figure D.17. Oil classifcation of the map generated during Flight 4 Track 3 on 8/29/2019.**
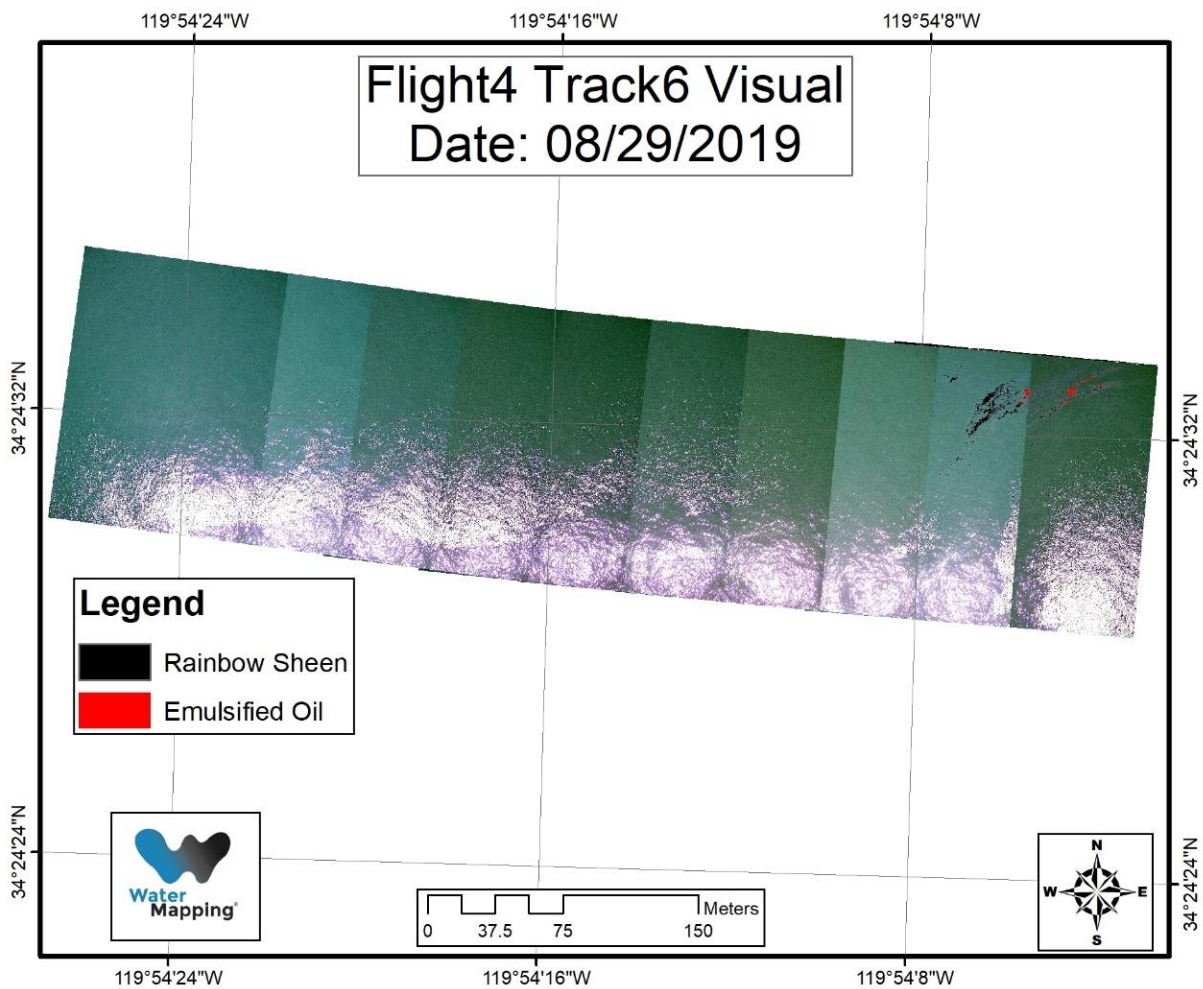
Figure D.18. Oil classifcation of the map generated during Flight 4 Track 4 on 8/29/2019.

Figure D.19. Oil classifcation of the map generated during Flight 4 Track 5 on 8/29/2019.

Figure D.20. Oil classifcation of the map generated during Flight 4 Track 6 on 8/29/2019.

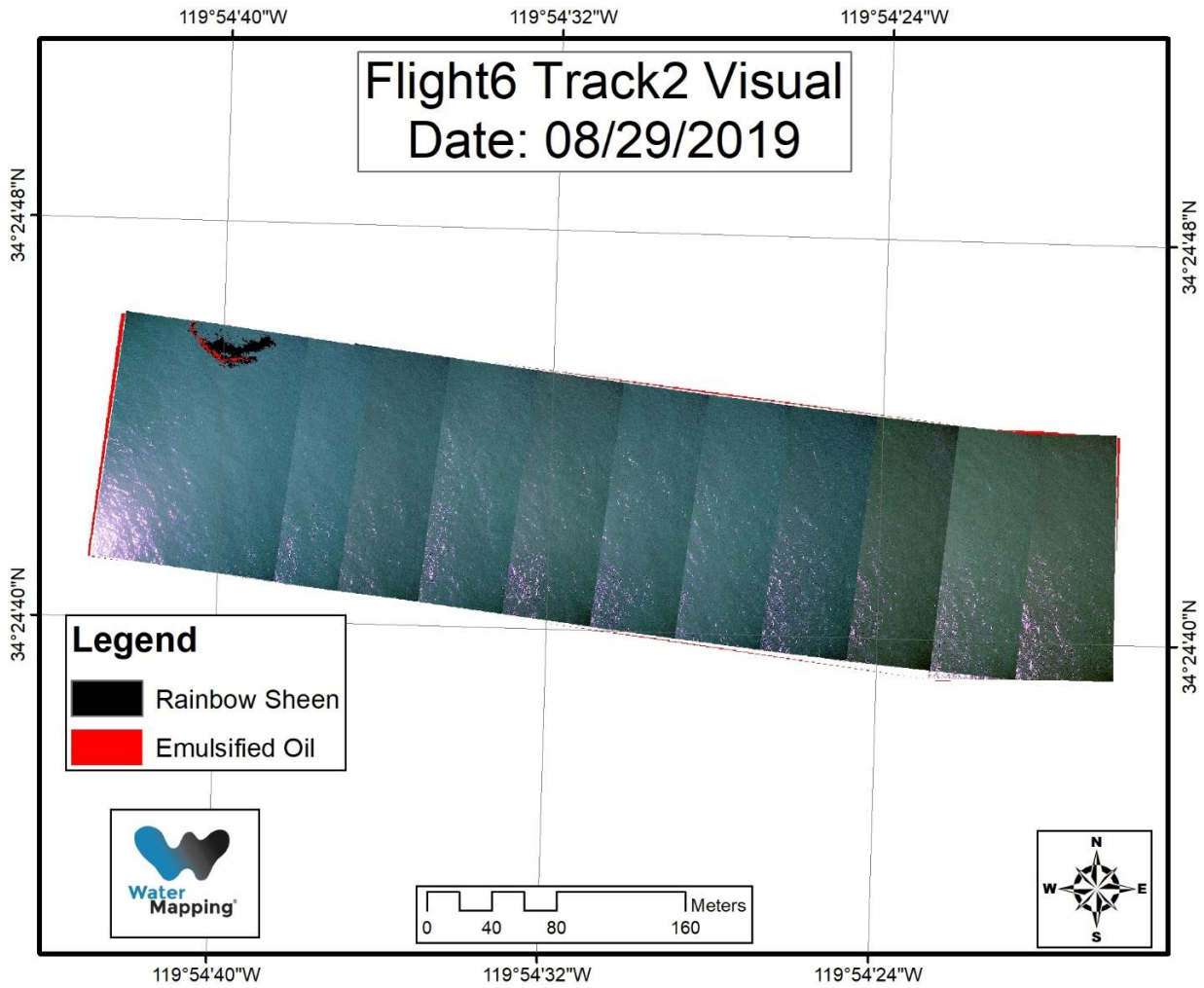**Figure D.21. Oil classifcation of the map generated during Flight 6 Track 2 on 8/29/2019.**

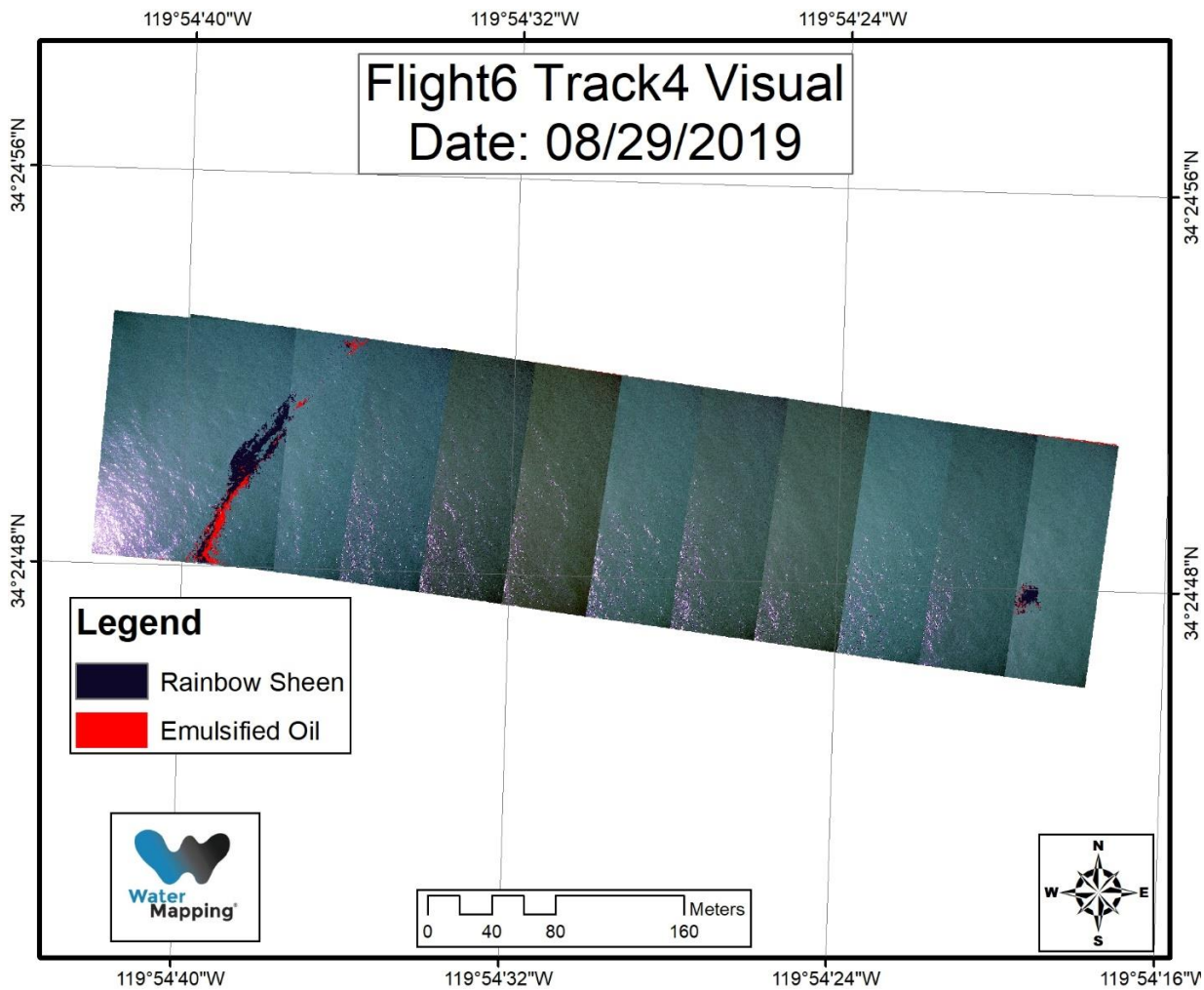**Figure D.22. Oil classifcation of the map generated during Flight 6 Track 4 on 8/29/2019.**

Figure D.23. Oil classifcation of the map generated during Flight 6 Track 6 on 8/29/2019.